NASA TECHNICAL REPORT

NASA TR R-322

NASA TR R-322

c. 1

DETERMINATION OF METEOROID ENVIRONMENTS FROM PHOTOGRAPHIC METEOR DATA

by Charles C. Dalton

George C. Marshall Space Flight Center
Marshall, Ala.

NATIONAL AERONAUTICS AND SPACE ADMINISTRATION • WASHINGTON, D. C. • OCTOBER 1969

1. Report No. NASA TR R-322	2. Government Accession No.	3. Recipient's Catalog No.
4. Title and Subtitle Determination of Meteoroid Environments from Photographic Meteor Data		5. Report Date October 1969 6. Performing Organization Code 7502-7500 0
7. Author(s) Charles C. Dalton		8. Performing Organization Report No. M146
9. Performing Organization Name and Address Aero-Astrodynamics Laboratory Marshall Space Flight Center Marshall Space Flight Center, Alabama 35812		10. Work Unit No. 124-091400 11. Contract or Grant No.
12. Sponsoring Agency Name and Address National Aeronautics and Space Administration Washington, D. C. 20546		13. Type of Report and Period Covered Technical Report December 1967-December 1968 14. Sponsoring Agency Code

15. Supplementary Notes

16. Abstract

A mathematical model is used to represent Öpik's 1958 physical theory of meteors in a form convenient for programming the computation of meteoroid photometric mass values. Sub-samples of 333 photographic meteors from McCrosky and Posen's sample are selected with respect to magnitude scaled for minimum velocity. A statistical comparison between the 1958 Öpik result and the 1933 Öpik provisional result, the Harvard-Meteor project basis for mass values, is given. Meteor and orbit parameter distributions and mean cumulative flux in absolute units for mass, momentum and energy are given separately for the terrestrial influx and for the lunar and interplanetary vehicle onfluxes.

17. Key Words	18. Distribution Statement
mathemetical model, meteor and orbit parameter distributions, mean cumulative flux, meteor luminous efficiency, cumulative flux	Unclassified - Unlimited

19. Security Classif. (of this report)	20. Security Classif. (of this page)	21. No. of Pages	22. Price *
Unclassified	Unclassified	123	$3.00

*For sale by the Clearinghouse for Federal Scientific and Technical Information Springfield, Virginia 22151

TABLE OF CONTENTS

LIST OF ILLUSTRATIONS

LIST OF ILLUSTRATIONS (Continued)

LIST OF ILLUSTRATIONS (Continued)

LIST OF ILLUSTRATIONS (Continued)

LIST OF ILLUSTRATIONS (Continued)

LIST OF ILLUSTRATIONS (Continued)

LIST OF ILLUSTRATIONS (Concluded)

LIST OF SYMBOLS

Symbol	Definition
"A"	Sub-sample for Öpik's [19] 1933 results
"B"	Sub-sample for Öpik's [2] 1958 results
C	Meteor color index, equation (39)
e	Heliocentric orbital eccentricity
H_B	Height at meteor beginning in kms
i	Inclination of meteoroid orbit to the ecliptic plane
K	Whipple's [42] (1954) empirical comet-asteroid criterion
k_2	Slope of M_{pg} or M_v as a linear function of log m, equation (36)
log	Common logarithm (base 10)
"Model A"	Öpik's [19] (1933) physics of meteors modeled by Whipple [25] (1938), equation (11)
"Model B"	Öpik's [2] (1958) physics of meteors modeled for stone dustballs by Dalton [49] (1967), equation (13)
"Model C"	Similar to "Model B" but presupposing compact stone particles, equation (14)
m_A	"Model A" mass value in grams
m_B	"Model B" mass value in grams
m_C	"Model C" mass value in grams
M_{pg}	Maximum absolute photographic magnitude
P	Öpik's [64] earth encounter probability per particle revolution

LIST OF SYMBOLS (Continued)

Symbol	Definition
p_q	Ionization probability for an evaporated meteor atom
q	Perihelion of orbit, AU
q'	Aphelion of heliocentric orbit in AU
r	Heliocentric distance, AU
$-s$	Mass exponent in meteor number derivative with respect to m, equation (37)
V_∞	Air-entry velocity of meteoroid, km/sec
V_G	Geocentric velocity of material in heliocentric orbit, km/sec
w	Whatever statistical weighting is used in equation (1)
w_l	Lunar weighting, a function for w appropriate for the lunar influx, equation (24)
w_s	Spatial weighting, for all meteoroids in space, equation (25)
w_t	Terrestrial weighting, a function for w appropriate for the terrestrial influx, equation (23)
w_w	Whipple's [42] cosmic weight as tabulated by McCrosky and Posen [18]
$\sum_L^x w/N$	Relative cumulative distribution of x weighted w
$\pm$	Probable error
β	Meteor luminous efficiency, radiation energy from 4500 to 5700 Å relative to the air-entry kinetic energy
β_A	"Model A" luminous efficiency, equation (11)

LIST OF SYMBOLS (Concluded)

Symbol	Definition
β_B	"Model B" luminous efficiency, equation (13)
β_b	Luminous efficiency of meteor black body radiation
β_C	"Model C" luminous efficiency, equation (14)
β_e	Celestial latitude of a meteor radiant
β_0	Luminous efficiency of meteor impact radiation
β_t	Luminous efficiency of meteor temperature radiation
β_z	Celestial latitude of the zenith
λ_λ	Longitudinal component of the elongation of the meteor radiant from the earth-way apex
τ_0	Luminosity coefficient
χ_{pg}	Factor by which the meteor cumulative flux with respect to M_{pg} increases per unit increase of M_{pg}, equation (35)
$\sim$	In proportion to

DETERMINATION OF METEOROID ENVIRONMENTS FROM PHOTOGRAPHIC METEOR DATA

SUMMARY

A mathematical model is used to represent Öpik's 1958 physical theory of meteors in a form convenient for programming the computation of meteoroid photometric mass values. Sub-samples of 333 photographic meteors from McCrosky and Posen's sample are selected with respect to magnitude scaled for minimum velocity. A statistical comparison between the 1958 Opik result and the 1933 Opik provisional result, the Harvard-Meteor-Project basis for mass values since 1938, is given. Meteor and orbit parameter distributions and mean cumulative flux in absolute units for mass, momentum, and energy are given separately for the terrestrial influx and for the lunar and interplanetary vehicle onfluxes.

INTRODUCTION

Scope

Way, Gove, and van Lieshout [1] gave a systems functional diagram and description of what might appear to be a succinct and sufficient delineation of scope category for scientific information. The present work will not seem to fit any of their four stages: reports or papers, compilations of data or tabulations of functions, review articles, and treatises. Some aspects of each of those categories will be evident. The work does not aspire to the level of a treatise in the sense of Opik's [2] or Levin's [3], since it is not so definitive as either; e.g., the physical theory of meteors is treated herein mostly indirectly by statistical plausibility arguments. Considerable literature is surveyed, but with only limited objectives as they bear on a vied point or on some incidental product of the analysis.

Any descriptions, explanations, derivations, etc., which are already available on the subject are not intended except insofar as they are warranted by the particular issue. Textbooks are available which approach the problem from a variety of special interests; e.g., for astronomy by Lovell [4], for engineering by McKinley [5], and for space science by Hawkins [6]. Broad general surveys of the subject are available which are relatively less involved in tedium than this one; e.g., those recent ones by Cosby and Lyle [7] and by Vedder [8], by Dalton [9] in 1962, and our 1963 review [10] and annotated bibliography [11]. The reader wanting a relatively short account of meteors, but more than just a descriptive treatment, will appreciate Whipple and Hawkins' [12] excellent 45-page paper. A very good and even shorter introduction to meteors is given in the first part of a paper by Opik [13]. Numerous works are available which relate to the hazard of meteoroid impact in space; e.g., contracted studies (as by Frost [14]), papers in engineering journals (as by Christman and McMillan [15], and astronautical symposia papers (as by Dalton [16]). But, toward hazard modeling, this report goes only so far as to show the particle flux and distributions of mass, velocity, momentum, and kinetic energy.

It must be understood that no inferences can be made from this analysis concerning the possibility of a flux of orbiting meteroids in cislunar space, the possibility for which has been studied theoretically by several authors, e.g., Katasev and Kulikova [17]. Any such particle flux would be in addition to that inferred from any meteor statistics, but would not be independent of satellite impact and puncture experiments. There is not sufficient information about this possibility to know confidently whether it may or may not exist.

Emphasis is placed on the more pertinent aspects of the study, rather than on all aspects equally. Some of the results are of little interest per se, but have been included primarily to broaden the perspective basis for deciding the relative plausibility of the alternative models for particle mass. Such results are passed over lightly. Some of the other results which are of interest per se, may not be of much direct interest for systems engineering. For example, the terrestrial influx, the lunar influx, and the onflux of particles impacting onto a vehicle in interplanetary space are of direct interest for systems engineering. But the concentration of particles in interplanetary space, independently of the probability of interaction with any space vehicle or other system of interest, is also helpful for tying the results in with other independent information, e.g., zodiacal light and solar F-corona.

Method

Instead of using weighting functions or a stratified analysis to reduce the bias from physical selectivity with respect to velocity, only those meteors are selected for further statistical analysis which should have had a reasonable chance of having been detected even if the same particle would have only the minimum infall (or escape) velocity. A sub-sample of such sporadic meteors is selected for each of two different models of luminous efficiency. Statistical analyses with respect to several parameters are made with means, correlations, scatter-diagrams, cumulative distributions, etc. The results are compared critically in relation to those reported for various efforts by others. Weighting functions are used in part of the analysis, for purposes other than to reduce the bias from physical selectivity with respect to velocity. However, methods to reduce their role, without loss of effectiveness, are used. For example, a slightly varying weighting of the arithmetic celestial latitude of the meteor radiant is substituted for the stronger weighting of algebraic values to reduce the bias from physical or geometrical selectivity due to the northern location of the data-collecting locale.

The extensive use of point-by-point cumulative distribution or relative cumulative distribution plots instead of the more conventional histograms of frequency distribution or probability density function for a variable of interest may seem strange, especially to those with backgrounds in engineering rather than physics, mathematics, etc. The historic practice of histograms was necessary to minimize computation and hand plotting before the prevalence of fast automatic digital computers and associated machine plotters. Most mathematicians and some physicists will prefer the cumulative distribution plots as used herein because they contain more than just the information necessary to construct the histograms. The most common histogram, with bars of equal width, can be constructed from a cumulative distribution plot by erecting ordinates at the boundaries of equally spaced intervals of the abscissa. The slope of the line segment or chord joining the points of intersection of the cumulative distribution plot and the adjacent ordinates is the height of the bar in the histogram. When the relative cumulative distribution plot of a continuously varying random variable is fitted with a smooth curve (usually not by algebraic computation but by judging the best fit of an adjustable curve marker), the slope of the curve at any abscissa value is the corresponding experimental value of the probability density function of the variable.

Mathematical Considerations

In addition to scatter diagrams, the programmed computations for this analysis are mostly for the means, standard deviations, and cumulative distributions of, and correlations between, several meteor parameters of interest. Comparable values are computed for each of the two partially overlapping selected sub-samples. These results are determined not only with uniform weighting, but also with other statistical weighting; e.g., the mean velocity for the lunar influx is computed from the same data as for the atmospheric influx, but with different statistical weighting.

The data used in these computations are from those of McCrosky and Posen [18] (1961): 2529 meteors, including 463 which were designated as belonging to showers, with mass and magnitude data missing from 26 of the remaining sporadics. This left 2040 sporadic meteors with values for absolute photographic magnitude. The latter were extrapolated to correspond with the minimum infall velocity before selecting the 333 brightest meteors as a sub-sample for statistical analysis. The extrapolation depends on the formulation for the meteor luminous efficiency. But it was intended that two alternative models for luminous efficiency should be compared. This selection gave two partially overlapping sub-samples, each of 333 meteors, one sub-sample for each of the two models of luminous efficiency.

Some of the meteors, which McCrosky and Posen [18] said were due to particles in heliocentric orbits of large aphelia, and which they called "hyperbolics," had no values tabulated for two of the twelve parameters considered in this analysis (aphelion q' and comet-asteroid criterion K). Sub-sample "A" (in consideration of Öpik's [19] 1933 meteor physical theory) includes two "hyperbolics." Sub-sample "B" (for Öpik's [2] 1958 results) includes 11 "hyperbolics." There are 274 members common to both "A" and "B," including the two "hyperbolics" of "A."

The errors which McCrosky and Posen [18] reported for the elements of the meteors by the graphical reduction (e.g., three percent rms deviation of velocity), and the errors in the reported

values of absolute photographic magnitude M_{pg} according to a subsequent study by Kresak [20] (0.25 probable error), are small enough to be ignored in this study. The uncertaintaies which play the main role in the propagation of confidence in the indicated calculations are those due to the finite size of the sample. The size of the sub-samples (333) is a compromise intended to foreshorten any physical selection effects and to avoid the complications of a stratified analysis.

For an analysis of two parameters x and y in a sample of N members, with parameter and weighting values x_i, y_i, and w_i, with w_i adjusted so that

$$N = \sum_{i=1}^{N} w_i , \qquad (1)$$

the mean $\bar{x}$ and standard deviation σ_x, for the parameter x, and the correlation r_{xy} between x and y are

$$\bar{x} = (1/N) \sum_{i=1}^{N} w_i x_i \qquad (2)$$

$$\sigma_x = \left[(1/N) \sum_{i=1}^{N} w_i (x_i - \bar{x})^2 \right]^{1/2} \qquad (3)$$

$$r_{xy} = (N \sigma_x \sigma_y)^{-1} \sum_{i=1}^{N} w_i (x_i - \bar{x}) (y_i - \bar{y}) , \qquad (4)$$

where, by equation (1), the weighting values w_i have been normalized so that N is both the number of elements and the total statistical weight. Here the number of elements N is 333, except in calculations involving either q' or K, where it is 333-2 and 333-11 in sub-samples "A" and "B," respectively. Equations (1) through (4) differ from textbook formulations (e.g., Reference 21) only for $w_i \neq 1$. The confidence intervals for the means and correlations are calculated in the usual manner, i.e., $\bar{x}$ is approximately normally distributed with standard deviation $\sigma_x/\sqrt{N}$, and the parameter $\frac{1}{2} \log [(1 + r_{xy})/(1 - r_{xy})]$ is approximately normally distributed with standard deviation $(N - 3)^{-\frac{1}{2}}$. For example, when N is 333 and the computed correlation is zero, the probable error of the correlation is 0.037. However, the textbook formulation for the confidence intervals in r_{xy}, although unavoidable if it were necessary to establish percentiles of very high order, can be further approximated for the present purposes. These results were checked for a matrix of representative values of N and r_{xy} over the intervals $59 \leq N \leq 333$ and $-1 \leq r_{xy} \leq 1$, and they have shown that r_{xy} is approximately normally distributed throughout the interquartile range, with standard deviation

$$\left.\begin{aligned} \sigma_{r_{xy}} &= 2 (1 - |r_{xy}|) (N - 3)^{-\frac{1}{2}} \\ &\quad \text{for} \quad |r_{xy}| \geq 0.9 \\ &= \left(\cos \frac{\pi r_{xy}}{2} \right)^{0.87} (N - 3)^{-\frac{1}{2}} \\ &\quad \text{for} \quad |r_{xy}| < 0.9 \quad . \end{aligned}\right\} \qquad (5)$$

For example, the semi-interquartile range (or probable error) of r_{xy} is found, by multiplying equation (5) by 0.6745, to be accurate to within 0.001 for $|r_{xy}| \leq 0.3$ and to within 0.002 for $|r_{xy}| > 0.3$, in comparison with the more tedious transformation.

Confidence intervals for the computed values of the cumulative distributions of the parameters of interest can be approximated by a formulation previously given by Dalton [22] for uniformly weighted data. The normal approximation, though expedient, is grossly inaccurate. The binomial formulation for the percentile p_s of order C ($0 \leq C \leq 1$) for the relative cumulative distribution (e.g., Reference 23) is implicit, rather than explicit, with the result that users' results are usually read from tabulations (e.g., reference 24), subject to the errors of interpolation. When the sub-sample "A" or "B" has been ranked with respect to a parameter of interest, and a value of that parameter has been chosen to divide the sample so that $n_f \leq N/2$ of the members are on a side of it, then the confidence C ($1/2 \leq C \leq 1$) that the fraction of the population on that side does not exceed p_s is related to p_s by

$$p_s = 1 - \left[(1 - C)/e^{\sum_{i=0}^{n_f} w_i} \right]^{[(3 + 2C)/4]^{\delta}} \left(N - \sum_{i=0}^{n_f} w_i/2 \right)^{-1} \quad (6)$$

where

$$\delta = 0 \quad \text{when} \quad \sum_{i=0}^{n_f} = 0$$

$$= 1 \quad \text{when} \quad \sum_{i=0}^{n_f} \neq 0 .$$

For example, with $N = 333$ and $n_f = 0$, the values of p_s corresponding to $C = \frac{1}{2}$ and $C = \frac{3}{4}$ are 0.0021 and 0.0042, respectively; or if $\sum_{i=1}^{n_f} w_i$ were 33.3, the median and third quartile of p_s would be 0.107 and 0.122, respectively.

When calculated values for sub-sample "A" are being compared with the corresponding results for "B," it is necessary to account for the 274 members common to both "A" and "B," and for their role in equations (1) through (6), before estimating the statistical significance of the differences between results. The variances of the parameters were not computed separately for the N_0 members which are common to both sub-samples "A" and "B." But in computing the confidence for the difference between corresponding values from the two sub-samples, the mean variance for the N_A members of "A" not in "B," and for the N_B members of "B" not in "A," can be approximated by the mean variance for the corresponding total sub-sample. Then the difference between the mean $\bar{x}_B$ of a parameter x_B in sub-sample "B" and the corresponding mean $\bar{x}_A$ from sub-sample "A" is approximately normally distributed, with standard deviation

$$\sigma_{(\bar{x}_B - \bar{x}_A)} = (1/N) \left(N_B \sigma^2_{x_B} + N_A \sigma^2_{x_A} \right)^{\frac{1}{2}} . \quad (7)$$

For example, with uniform weighting, the values for the mean air-entry velocity for "A" and "B" are 16.62 and 20.23 km/sec, respectively; and the corresponding values for the standard deviation of the air-entry velocity are 5.01 and 10.32 km/sec, respectively. In this case, since the data for the "hyperbolics" also enter the computation, N is 333 and both N_A and N_B are 59. Then the calculated value and standard deviation of the difference in uniformly weighted mean velocity are 3.61 and 0.27 km/sec. Similarly, in terms of the terrestrial statistical weighting and probable error, the mean air-entry velocity for "B" is 18.83 ± 0.31 km/sec, which is higher than that for "A" by 2.66 ± 0.15 km/sec.

With the same approximations which were used in deriving equation (7), the difference between the "A"- and "B"-calculations for a particular correlation can be expressed by

$$r_{xy_B} - r_{xy_A} \approx (1/N) \left[N_B (r_{xy})_{N_B} - N_A (r_{xy})_{N_A} \right] , \quad (8)$$

where $(r_{xy})_{N_B}$ is distinguished from r_{xy_B} in that the latter is the value of r_{xy} in "B" with all members N, whereas the former is that in "B" with only members N_B, and similarly for the subscript "A." Since, by equation (5), equation (8) is a linear function of approximately normally distributed variables, it is also approximately normally distributed, with standard deviation

$$\sigma_{(r_{xy_B} - r_{xy_A})} \approx \begin{cases} \frac{2}{N} \left[\frac{N_B^2 \left(1 - |r_{xy_B}|\right)^2}{N_B - 3} \cdot \frac{N_A^2 \left(1 - |r_{xy_A}|\right)^2}{N_A - 3} \right]^{\frac{1}{4}} & \text{for } r_{xy} \geq 0 \\ \frac{1}{N} \left[\frac{N_B^2 \left(\cos \frac{\pi r_{xy_B}}{2}\right)^{2(1 - |r_{xy_B}|)}}{N_B - 3} \cdot \frac{N_A^2 \left(\cos \frac{\pi r_{xy_A}}{2}\right)^{2(1 - |r_{xy_A}|)}}{N_A - 3} \right]^{\frac{1}{2}} & \text{for } r_{xy} < 0 \end{cases} \quad (9)$$

For example, with terrestrial statistical weighting, the correlation between air-entry velocity and "Model-A" mass m_A in sub-sample "A" is 0.020 ± 0.037 while the correlation between air-entry velocity and "Model-B" mass m_B in sub-sample "B" is 0.191 ± 0.035. In consideration of the overlap between "A" and "B," the difference between

these correlations is 0.171, and to the extent that one might neglect the fact that "Model-A" mass and "Model-B" mass are not really the same parameter and may play a somewhat different role in the common members N_0, the probable error of the difference between these correlations is 0.009. In other words, the "A" and "B" values of the correlation between mass and velocity differ quite significantly from a statistical point of view.

Not only is the same analysis for sub-sample "A" repeated for "B," but also, in addition to uniform weighting, the analysis is repeated three more times, each time with a different function for the statistical weighting w: terrestrial weighting w_t, lunar weighting w_l, and spatial weighting w_s. Just as the two sub-samples, "A" and "B," are not statistically independent, but, having some common members, must be interpreted with equations (7) through (9), so also do any two of the analyses with different functions for the statistical weighting w. The following summations play essentially the same role as N_A and N_B:

$$\sum_{i=1}^{333} |w_{t_i} - 1| = 60.5 \quad \text{for sub-sample "A"}$$

$$= 69.3 \quad \text{for sub-sample "B"}$$

$$\sum_{i=1}^{333} |w_{l_i} - w_{t_i}| = 120.3 \quad \text{for sub-sample "A"}$$

$$= 117.9 \quad \text{for sub-sample "B"}$$

$$\sum_{i=1}^{333} |w_{s_i} - w_{l_i}| = 193.5 \quad \text{for sub-sample "A"}$$

$$= 206.9 \quad \text{for sub-sample "B"}.$$

For example, with terrestrial weighting w_t, the mean and standard deviation of the geocentric velocities of the particles are 14.47 and 9.88 km/sec, respectively, for sub-sample "B," while with lunar weighting, w_l, they are 18.04 and 11.09 km/sec, respectively. These means could be reported as 14.47 ± 0.37 and 18.04 ± 0.41 km/sec; and, by substituting 117.9 for N_A and N_B in equation (7), the difference between these statistically dependent mean values would be 3.57 ± 0.33. The fact that these means for the geocentric velocities in the terrestrial and lunar influxes show any statistically significant differences is due to the velocity dependence of the gravitationally modified particle influx cross section of the earth.

The particle influx cross section which the earth would have without a gravitational field, relative to that which it actually has, is proportional to the square of the ratio of the geocentric and air-entry velocity, with a different value for each particle. But when this result is multiplied by the terrestrial weighting w_t and summed over all 333 particles, one gets the number of particles, within the same mass interval, which should have encountered the earth without gravitational focusing. When this result is divided by 333, the size of "A" or "B," one gets a good approximation to the mass-cumulative influx of the moon k_f (per unit area) relative to that of the earth (within the mass interval of the data); i.e.,

$$k_f = \left(\frac{1}{333}\right) \sum_{i=1}^{333} w_{t_i} \left(\frac{V_{G_i}}{V_{\infty_i}}\right)^2 \qquad (10)$$

$$= 0.470 \quad \text{for sub-sample "A"}$$

$$= 0.540 \quad \text{for sub-sample "B"}$$

ACKNOWLEDGMENT

Discussions with Dr. E. J. Opik at the University of Maryland, Dr. J. S. Dohnanyi at Bellcomm, Inc., Dr. B. S. Baldwin, Jr., at NASA-Ames Research Center, Mr. K. Baker from NASA-Manned Spacecraft Center, Mr. C. D. Miller from NASA-Lewis Research Center, Dr. B.-A. Lindblad from the Lund Observatory in Sweden, and Drs. F. Verniani, R. B. Southworth, L. G. Jacchia, and H. S. Hawkins at the Smithsonian Astrophysical Observatory were helpful in planning this effort.

DISCUSSION

Meteor Luminous Efficiency

A meteor particle (or meteoroid) enters the atmosphere with some initial (or air-entry) velocity,

V_∞, essentially corresponding with the meteor beginning height H_B. Some fraction of the air-entry kinetic energy is converted to meteor radiative energy. Following Öpik [19], who calculated this entity in 1933, the integrated meteor radiative energy in the wavelength interval 4500 to 5700 Å, relative to the air-entry kinetic energy, is called the meteor luminous efficiency β. Öpik [19] gave values for two components of β, a component β_0 for impact radiation, and a component β_t for temperature radiation. He concluded, "In most of the meteors visible to the naked eye, temperature radiation is insignificant compared with impact radiation." A plot of his tables of values for β_0 versus V_∞ is shown in Figure 1, separately for visual and telescopic (i.e., fainter) meteors. He suggested that the transition between these (quite different visual versus telescopic trends) might begin at the fainter visual meteors. In 1938, Whipple [25] used those results as the basis of his model for visual meteors, "Model-A" in this report:

$$\left.\begin{aligned} \beta_A &= \tau_{0_V} V_\infty \\ \tau_{0_V} &= 8.5 \times 10^{-5} \text{ sec/km} \quad , \end{aligned}\right\} \qquad (11)$$

where the constant τ_{0_V} is usually called the luminosity coefficient (e.g., by McCrosky and Posen [18]), visual, in contradistinction to τ_{0_p}, photographic (e.g., by Verniani [26]). This "Model-A" was also used by Whipple [27] in 1943 for his meteor studies relating to the properties of the upper atmosphere. Indeed, as Whipple [27] stated, the results reported in 1933 by Öpik [19] are well represented by "Model-A." But it is at considerable disparity to the more studied analysis published by Öpik [2] in 1958 and illustrated by tables of calculated values also by Öpik [28] in 1963.

When the product of the meteor luminous efficiency (visual or photographic) and air-entry kinetic energy is equated to the integrated intensity (visual or photographic), a mass value can be calculated which is called photometric mass. Such values were tabulated for the Super-Schmidt photographic meteors by McCrosky and Posen [18]. They used the "Model-A" luminous efficiency and derived the integrated intensities by Hawkins' [29] short-trail method. It must be understood that, in order for them to use "Model-A," they converted the photographic intensity to an equivalent visual intensity by means of a color index, as discussed by Verniani [26] (i.e., the relation between radiative energy and meteor intensity is somewhat different for visual intensity and photographic intensity). Another value for the mass of a meteoroid, called the dynamic mass, can be calculated by considering the measured deceleration of the particle during its interaction with the atmosphere. But Öpik [2] says that the photometric mass values are more reliable; and Verniani [26] states that all Harvard meteoric masses have been computed with the "Model-A" luminous efficiency (i.e., also photometric).

While claiming no high accuracy for "Model-A," some authors (e.g., McCrosky and Posen [18]) imply that the tabulated values can be corrected when the appropriate scaling factor becomes better established; i.e., as illustrated by Clough and Lieblein [30], the scaling factor is the ratio of the old and new values of the luminosity coefficient, τ_{0_V} in equation (11). This impression probably is encouraged unwittingly by the practice of expressing particle mass as twice the product of the integrated intensity divided by $\tau_{0_V} V_\infty^3$, where $\tau_{0_V} V_\infty^3$ might be better written as $\beta_A V_\infty^2$. Then, when an alternative "Model-B" gives a luminous efficiency β_B, the scaling factor is β_A/β_B, which one should not expect to be independent of either mass or velocity. Anyway, the product of luminous efficiency and photometric mass value is invariant between alternative mathematical models: i.e.,

$$\beta_A m_A = \beta_B m_B = \left(\frac{2}{V_\infty^2}\right) \int^T I \, dt \quad . \qquad (12)$$

Thus, what is actually known about any meteor is neither the luminous efficiency nor the mass, but the product of the two.

Papers by Kallmann [31] and Öpik [32] at the 1954 symposium in Liege suggested an interpretation of Öpik's [19] results quite different from Whipple's [25, 27] "Model-A." Noting the latter model, Kallmann [31] said that it must be assumed that the luminous efficiency is not only a function of the velocity but is also a function of the size or magnitude of the particle, and that the same must be true for the visible path length of the meteoroid. Öpik [32] noted some data for shower meteors which

seem to indicate that the luminous efficiency would vary inversely with the 0.87-power of the velocity.

Other papers by Kallmann [33] and Öpik [34] in the 1954 symposium at Jodrell Bank carried the disagreement with "Model-A" somewhat further. Kallmann [33] used Öpik's [19] relation between luminous intensity and magnitude to estimate the masses of meteors of different visual magnitudes greater than zero and of different velocities. He showed that the luminous efficiency is a function not only of the velocity of the meteor for all magnitudes, but also of the visual magnitude or physical size of the particle itself. This was done by showing that the duration of visibility of the particle is one function of the luminous efficiency and another function of the visual magnitude. Öpik [34] said that from his 1933 work [19], which he referred to as the provisional theory, with certain corrections, the most probable expression for the luminous efficiency was assumed to be $0.020/V_\infty$. This value would equal that given by "Model-A" at 24 km/sec. By 1957, Weiss [35] was led, by examination of the literature, to adopt "Model-A" for meteors with negative absolute visual magnitudes; but for positive magnitudes he chose to equate luminous efficiency to $0.021/V_\infty^{0.3}$.

A description and technical review of Öpik's [2] (1958) more definitive "Physics of Meteor Flight in the Atmosphere" were given by Eshleman [36]. The results remain rather involved and tedious to apply; but Öpik [28] (1963) mitigated that difficulty with tables of values of the luminous efficiency β and the components β_0 for impact radiation, β_t for temperature radiation, and β_b for black-body radiation -- each for an array of values for the air-entry velocity V_∞ and mass m. The values for β_0, the only component considered toward the construction of "Model-A," are somewhat different from the values which Öpik [19] tabulated in 1933, and some of the values of β_t (and even of β_b) are relatively quite appreciable. The tables are in three parts, separately for stone dustballs, compact iron, and compact stone particles.

Curves for the luminous efficiencies of compact iron and of stone meteoroids, relative to the luminous efficiency of a stone dustball of the same mass and velocity, are plotted from Öpik's [28] values in Figures 2 and 3. The curves for 7.4 km/sec are of more interest for re-entry of orbited debris than for infalling natural meteors. Otherwise, the effective similarity between Figures 2 and 3 is quite apparent, indicating that nearly the same mass would be inferred whether a particular meteor was considered to be compact iron or compact stone. Figure 3 shows further that, for a meteoroid of any mass and any velocity, a higher luminous efficiency and consequently lower mass is inferred by the assumption of a compact, rather than dustball, particle. Therefore, not only the mass-cumulative influx, but also, by the hypervelocity impact and puncture model which Dalton [37] gave in 1966 and presented again after some further refinement in 1967 [16], the puncture hazard which one infers from meteor data is higher when the particles are presumed to be dustballs.

Results reported by different authors back through 1954 are at variance concerning the structural integrity and density of the meteoroids responsible for the meteor phenomena. Öpik [13] presents a case for the rarity of compact iron versus compact stone meteoroids. Also Öpik [34, 32, 2] reports that the meteors of the visible range, as a rule, are not stony compact bodies, but some kind of loose aggregates of dust particles, "stone-flakes" or "dustballs." Smith [38] finds, by analysis of meteor flares, that such dustballs consist of thousands of fragments, each about 10^{-6} grams. Fragmentation, another observational evidence supporting the dustball concept, has been reported by Jacchia [39] and by McCrosky [40]. Meteor particle fragmentation is supported on theoretical grounds in consort by Whipple's [41] icy comet model and by analysis of meteoroid orbits with respect to Whipple's [42] comet-asteroid criterion. But some of the recent results are contrariwise. Ceplecha's [43, 44, 45] analysis of meteor height and orbit data indicates three distinct groups — A_C, B_C, and C_C — with material specific gravities 4.0, 2.2, and 1.4, respectively, with the A_C group and B_C group being most abundant and least abundant, respectively, in the mass interval from about 1 to 10^{-4} grams. Laboratory observations of the effects of high enthalpy electric arc jet winds over exposed rock samples at low ambient pressure by Allen and Baldwin [46, 47] suggest that frothing and sluffing of compact stone meteoroids may be a more general explanation for the anomalously low material density. Also, Lebedinets and Portnyagin [48] reported a theoretical analysis suggesting that the observed properties of faint photographic meteors can be interpreted on the basis of a dense-meteoroid

model, without invoking the hypothesis of an exceptionally friable structure. Therefore, to approximate Öpik's [2, 28] results, for programming purposes, a "Model-C" was constructed for compact stone meteoroids. This is in addition to the "Model-B" for Öpik's [2, 28] stone dustballs, a detailed derivation for which was published elsewhere by Dalton [49].

"Model-B" for stone dustballs, which is illustrated in Figure 4 with Öpik's [28] values superimposed, relates luminous efficiency β_B, air-entry mass m_B and velocity V_∞ as follows: β_B and m_B are functionally independent when either

$$V_\infty < 14.8$$

and

$$\log\log (m_B\beta_B)^{-1} \geq 0.0125\, V_\infty + 0.665$$

or

$$V_\infty \geq 14.8$$

and

$$\log\log (m_B\beta_B)^{-1} \geq -0.00304\, V_\infty + 0.895;$$

otherwise,

$$\log\log (\beta_B)^{-1} = a_0 + a_1 \log\log (m_B\beta_B)^{-1} \quad , \quad (13)$$

where

$$a_0 = 0.4042 + 0.193\ (\log\log V_\infty - 0.0682)$$

$$\text{for } V_\infty \geq 14.8$$

$$= 0.4042 + 0.33\ (0.0682 - \log\log V_\infty)$$

$$\text{for } V_\infty < 14.8$$

and

$$a_1 = 0.0840 + 0.00113\ |V_\infty - 14.8| \ .$$

Correspondingly, "Model-C" for compact stone meteoroids is illustrated in Figure 5 with Öpik's [28] compact stone values superimposed. All of the members of sub-sample "B" map into the region of functional interdependence of β_C and m_C:

$$\log\log (\beta_C)^{-1} = a_2 + a_3 \left[\log\log (m_C\beta_C)^{-1} - 0.364\right] \quad , \quad (14)$$

where

$$a_2 = 0.313 + 0.079 \log V_\infty \quad \text{when } V_\infty > 14.8$$

$$= 0.695 - 0.248 \log V_\infty \quad \text{when } V_\infty \leq 14.8$$

$$a_3 = 0.1527 + 0.001315\, V_\infty .$$

The computation of m_B and m_C by equations (12) and (13) is facilitated by the fact, as already noted, that the product of luminous efficiency β and mass m is invariant from one photometric mass model to another, and the values for "Model-A" have been tabulated by McCrosky and Posen [18]. After β_B is found, it is divided into $m_B\beta_B$ to find m_B, and similarly for β_C and m_C.

Compilation of Representative Statistics

As recently as 1967, Cook [50] concluded that the best research data concerning meteor physical theories comes from photographic meteors. The photographic Super-Schmidt meteor data of McCrosky and Posen [18] give the most extensive photographic observational material for 2040 sporadic meteors with tabulated values for "Model-A" mass and various other data. Their data have been used as the main observational material for statistical studies by Ceplecha [44], Dohnanyi [51], and Miller [52]. Ceplecha [44] noted that the limiting and maximum

magnitudes of the meteors have a statistical distribution that indicates a very good homogeneity of the McCrosky and Posen [18] material.

An analysis of the velocity dependence of luminous efficiency with Hawkins and Southworth's [53] reputedly more accurate data for 285 sporadic photographic meteors was reported in 1965-66 by Dalton [54, 55]. The results were given with different combinations of statistical weighting and luminous efficiency functions. The results now seem invalid. It is evident now that the sample size was too small. Ordinarily one should consider that a sample with 285 members would constitute fairly reliable statistics, but it is necessary to consider the role of the statistical weighting in reducing the effective size of the sample. Another uncertainty with Dalton's [54, 55] results is due to the role of velocity in the weighting function. The velocity dependence of the weighting function was adapted from Whipple's [42] cosmic weight. Both of these disadvantages are avoided in the present analysis by choosing sub-samples which do not necessitate a statistical weighting as a function of velocity.

If one is to avoid velocity-dependent statistical weighting, then legitimate statistics of meteors can be made only when one eliminates the data for those meteors which would have been too faint for reasonable detectability if they would have had only the minimum velocity of interest (e.g., infall or escape velocity, 11 km/sec). Such a procedure was outlined in 1967 by Dalton [49]. It is based on maximum effectively detectable absolute photographic magnitude M_{pgo} as a criterion, a velocity extrapolation of the actual absolute photographic magnitude M_{pg}. Jacchia, Verniani, and Briggs [56] found, by an analysis of data for 413 precisely reduced photographic meteors, that the integrated photographic intensity, and therefore also the product of luminous efficiency and kinetic energy, is proportional to $I_{pm}^{1.11}/V_\infty^{0.89} \cos^{2/3} Z_R$. The angle Z_R is the zenith-to-radiant deviation and I_{pm} is the maximum photographic luminous intensity, related to M_{pm} by

$$M_{pm} = -\left(\frac{5}{2}\right) \log I_{pm} .$$

Therefore, the criterion for selecting sub-samples relatively free of bias due to physical selectivity with respect to velocity is

$$M_{pgo} = M_{pg} + 2.25 \log \left(\frac{\beta}{\beta_{11}}\right) + 6.50 \log \left(\frac{V_\infty}{11}\right) , \qquad (15)$$

where β and β_{11} are the luminous efficiency at velocity V_∞ and the luminous efficiency at 11 km/sec, respectively.

The order or rank with respect to M_{pgo} for McCrosky and Posen's [18] 2040 sporadic meteors depends on whether β/β_{11} in equation (15) is evaluated with "Model-A," equation (11), or with "Model-B," equation (13). Sub-sample "A" contains the 333 meteors for which $M_{pgo} < 2.3$ by "Model-A," and sub-sample "B" contains the 333 meteors for which $M_{pgo} < 2.0$ by "Model-B."

The most obvious comparisons between the two selected sub-samples are illustrated by the scatter-diagrams. Figure 6 shows "Model-A" versus "Model-B" mass values, and Figure 7 shows mass versus velocity. For example, considerably more of the high velocity meteors are represented in sub-sample "B."

Statistical Weighting

According to formulas for the transformation of coordinates, given by Lovell [4] and Ericke [57], a meteor radiant with right ascension α and declination δ has celestial latitude β_e, where

$$\sin \beta_e = 0.91741 \sin \delta - 0.39795 \cos \delta \sin \alpha . \qquad (16)$$

In Figure 8, where the values of β_e for both sub-samples are plotted, the values of β_e are predominately positive.

Kells, Kern, and Bland [58] state that the zenith right ascension α_z of a place is the sidereal time at that place; and Russell, Dugan, and Stewart

[59] state that sidereal time is usually correct within four or five minutes when approximated from civil time by assuming that on September 22 the two times agree and that sidereal time gains two hours each month, and proportionately for each day and hour. For the Harvard stations in New Mexico, the locale of the meteor data, Hawkins and Southworth [53] state that, to obtain the time of appearance in local mean time at the Dona Ana station, 0.29667 must be subtracted from the date given in universal time. Also Hawkins [29] gave for that station the zenith declination δ_z as

$$\delta_z = \sin^{-1} 0.8433343 = \cos^{-1} 0.5373893. \qquad (17)$$

With this information, together with equation (16), the zenith celestial latitude β_z can be formulated.

Local (Dona Ana station) sidereal day t_{ds} is

$$t_{ds} = t_{du} + (t_{mu} - 9)\left(\frac{2}{24}\right) + \frac{\left(t_{du} - 22\right)}{365.26} - 0.29667\left(\frac{366.26}{365.26}\right), \qquad (18)$$

where t_{mu} and t_{du} are the numbers of the month and day universal time, respectively. The zenith right ascension α_z is given in radians by

$$\alpha_z = 2\pi t_s, \qquad (19)$$

where t_s is the local sidereal time expressed as a decimal fraction of a day; i.e., t_s is the decimal residue which is left after subtracting the next lower integral value (postive, nil, or negative) from the local sidereal day t_{ds}, equation (18). By equations (16), (17), and (19), the zenith celestial latitude β_z is related to the local sidereal time t_s by

$$\left.\begin{aligned} \sin\beta_z &= 0.77368 - 0.21385 \sin 2\pi t_s \\ 34.0^\circ &\le \beta_z \le 80.9^\circ \end{aligned}\right\}. \qquad (20)$$

The values of β_z versus β_e for the two sub-samples are plotted as scatter diagrams in Figure 8.

One should expect the reason the distribution of β_e is not symmetric with respect to zero (the ecliptic) is related to the fact that the distribution of β_z also is not symmetric with respect to zero. These data give no basis for supposing that any more than random deviation from a distribution of β_e symmetric about zero should be found from data for which the time and locale would have been chosen for the ecliptic to be through the zenith. Contrariwise, radio meteor data give some evidence for the essentially symmetric distribution of radiants with respect to celestial latitude. Correspondingly weighted radio meteor results, from the northern hemisphere by Davies and Gill [60] and from the southern hemisphere by Keay [61], showed that correction for observational selection reduced the earth-way apex mode of radiant density well below two accentuated broad modes at about 60 degrees on either side of the apex to the earth's way. Davies and Gill [60] found that correcting their radio meteor data for observational selection essentially produced symmetry in the distribution of radiants in ecliptic latitude, and they considered it as evidence for the correctness of the statistical weighting.

The radiant density per square degree of the celestial hemisphere is proportional to the probability density function for $\sin \beta_e$.[1] The cumulative distribution of the positive values of β_e, with weighting inversely proportional to the square of the beginning height H_B and relative to their total statistical weight, is plotted in Figure 9. The weighting is intended to correct for differences in the effective area of surveillance of the cameras. Also in Figure 9, with the same ordinate scale, is the corresponding distribution of the negative values. The fact that the number of positive values of β_e exceeds the number of negative values by a factor of nearly 3 for both sub-samples "A" and "B" was already apparent in Figure 8. But Figure 9 suggests more clearly how a further weighting function might be used to minimize bias with respect to β_e.

The data show that most of the meteors have radiants above the horizon. Then, as a tentative step, it seems appropriate that meteors which have radiants on circles of celestial latitude with not more than 90 percent occlusion (by the horizon) should be weighted by a factor w_c in near inverse proportion to the apparent (above the horizon) fraction. The weighting factor w_c is related to the difference $2\lambda_e$ between the celestial longitudes of the horizon points on the circle of celestial latitude β_e through the meteor radiant.

The pole of the ecliptic, the zenith, and either one of the horizon points, on the circle of celestial latitude β_e, form a spherical triangle such that the angle at the pole of the ecliptic is $180° - \lambda_e$, with opposite side $90°$, and with adjacent sides $90° - \beta_e$ and $90° - \beta_z$, where β_z is the celestial latitude of the zenith. The solution to the spherical triangle gives

$$\begin{aligned} \lambda_e &= 0 && \text{when } \beta_e \geq 90° - \beta_z \\ \cos \lambda_e &= \tan \beta_e \tan \beta_z && \text{when } \beta_e < 90° - \beta_z \\ & && \text{and } \tan \beta_e \tan \beta_z > -1 \\ &= -1 && \text{when } \tan \beta_e \tan \beta_z < -1 \ . \end{aligned}$$

At the Dona Ana station, $\tan \beta_z$ is always positive, $0 \leq \lambda_e \leq 90°$ when $\beta_e > 0$, $90° \leq \lambda_e \leq 180°$ when $\beta_e < 0$, and the circles of celestial latitude with $\beta_e > 90° - \beta_z$ are entirely above the horizon. Then

$$\begin{aligned} w_c &= 180°/(180° - \lambda_e) && \text{when } \beta_e < 90° - \beta_z \\ & && \text{and } 180°/(180° - \lambda_e) \leq 10 \\ &= 10 && \text{when } \beta_e < 90° - \beta_z \\ & && \text{and } 180°/(180° - \lambda_e) > 10 \ . \end{aligned} \qquad (21)$$

---

1. Let y be some function of β_e with probability density function $f(y)$ proportional to the radiant density per square degree of the celestial sphere, i.e.,

$$f(y) \sim \frac{dN}{dA} \sim \frac{f(y)\, dy}{\cos \beta_e \, d\beta_e} \ ,$$

where dA is the measure of square degrees in the differential element of width $d\beta_e$ along the $2\pi \cos \beta_e$ length of the circle of celestial latitude through the radiant, and dN is the differential number of radiants in dA and equals $f(y)\, dy$. Therefore,

$$dy \sim \cos \beta_e \, d\beta_e$$

$$y \sim \sin \beta_e \ .$$

The effect of weighting $\sim w_c H_B^{-2}$, instead of $\sim H_B^{-2}$, is to transform the results of Figure 9 into those of Figure 10. The results show that the extra weighting w_c from equation (21) is quite effective in reducing the disparity between the positive and negative branches of the parameter of interest. Actually, there is a slight over-correction, which could be avoided by choosing a lower limiting value for w_c in equation (21), say 8 instead of 10.

From Figure 10 one gets the impression that weighting $\sim H_B^{-2} w_c$ should be quite appropriate for each member of the sub-samples. But when the positive and negative branches of β_e are combined with that weighting in Figure 11, the undesirability of the result is more obvious. Too much of the statistical weight was shifted to too few members, leaving a very jagged distribution. But, by looking back at Figure 10, one sees that the positive branch remains quite uniform even with the weighting $\sim H_B^{-2} w_c$. So, one would accept the positive branch of Figure 10 as being sufficiently free of bias with respect to β_e. But instead of using the weighting w_c, a milder weighting w_f is used to correct the bias in $|\beta_e|$ rather than in β_e. By dropping the weighting w_c from Figure 11, and using only $\sim H_B^{-2}$, one gets the results shown in Figure 12. Then, because only $|\beta_e|$ and not β_e is considered in the rest of the analysis, the milder weighting w_f which can replace w_c is the ratio of the slopes of the corresponding curves in Figures 10 and 12, plotted in Figure 13. The values of the ratios for w_f plotted in Figure 13 indicate an inappreciable difference between sub-samples "A" and "B"; therefore, the following mean result can be used for both:

$$\left.\begin{aligned} w_f &= 1.10 \quad \text{for } 0 \le \sin|\beta_e| < 0.32 \\ &= 0.61 \quad \text{for } 0.32 \le \sin|\beta_e| < 0.45 \\ &= 0.94 \quad \text{for } 0.45 \le \sin|\beta_e| < 0.80 \\ &= 1.22 \quad \text{for } 0.80 \le \sin|\beta_e| \le 1 \quad . \end{aligned}\right\} \qquad (22)$$

The equation (21) weighting w_c for β_e, the role of which is accomplished by the weighting w_f for $|\beta_e|$, implicitly involves no weighting with respect to the radiant zenith angle Z_R. However, the weighting $\sim H_B^{-2}$ involves Z_R because the beginning height H_B equals the product of the range and cos Z_R. But McKinley [62] stated in 1951, and Öpik [32, 63] found also in 1955 by the data from the Arizona Expedition, that the meteor detection probability function for a visual observer is cos Z_R, not cos^2 Z_R. This means that if the observer sees n meteors per hour from a radiant overhead, he would see n cos Z_R meteors per hour from the same radiant if it were at a zenith angle Z_R. This suggests that weighting $\sim H_B^{-2}$ may over-correct for Z_R, and that such an over-correction would have to be adjusted by letting the weighting w_c depend on Z_R. For example, one would not have been surprised if, instead of calculating the length of the apparent segment of the circle of celestial latitude, one might have needed to integrate some function of Z_R along that segment. But the weighting in Figure 10 seems to have been sufficiently effective in restoring the essential symmetry of the radiant distribution with respect to the ecliptic.

The statistical analysis in the next part of this section was done first with uniform weighting. Then it was repeated, once with w_t for the (world-wide) terrestrial influx, again with w_l for the lunar influx, and with w_s for the population of particles in interplanetary space regardless of the probability of collision with the earth, the moon or an interplanetary vehicle. The weighting functions, with coefficients adjusted so that the sum of the weights equals the sub-sample size 333 in accordance with equation (1), are

$$w_t = \left(\frac{333}{\sum_1^{333} H_B^{-2} w_f} \right) H_B^{-2} w_f \qquad (23)$$

$$w_l = \left(\frac{333}{\sum_1^{333} (V_G/V_\infty)^2 w_t} \right) (V_G/V_\infty)^2 w_t \qquad (24)$$

$$w_s = \left(\frac{333}{\sum_1^{333} w_t/P} \right) w_t/P \ , \qquad (25)$$

where P is proportional to Öpik's [64] earth encounter probability, and is normalized from the values which McCrosky and Posen [18] tabulated for Whipple's [42] cosmic weight w_w by

$$P = \left(\frac{333}{\sum_1^{333} V_\infty^2 \, w_w} \right) V_\infty^2 \, w_w \ . \qquad (26)$$

The lunar weighting w_l from equation (24) is applicable at least for the back side of the moon. The extent to which it may be applicable for the front side is not certain. Several authors have reported that the decrease in flux due to the moon's lower gravitational field, i.e., to about 50 percent by equation (10), is somewhat compensated on the earthward side by an increase in flux due to the focusing effect of the earth. In 1959 Beard [65] gave a factor of 2 as the maximum increase in impact frequency on the earthward side. Shoemaker, Hackman, and Eggleton [66] reported in 1962 that the maximum local increase in the lunar influx may be greater than a factor 2 but must be less than a factor 3. In 1964 Hale and Wright [67] reported considerable theoretical analysis of the problem. More recently Hartmann [68] wrote that "... the net effect on the earthward side of the decrease in flux due to the moon's lower gravitational field and the increase due to the focusing effect of the earth is a decrease in flux by 0.8, consistent with Öpik [69]..." But Öpik's [69] value 0.80 is just the reciprocal of his value 1.3 for the factor by which the influx of meteoroids into the atmosphere would be gravitationally enhanced if the geocentric velocity V_G were uniformly 20 km/sec. Convenient formulation for this calculation was shown by Shoemaker, Hackman, and Eggleton [66]. It may very well be that the lunar weighting w_l is just as applicable for the earthward side as for the back side.

Further familiarity with the role of the three weighting functions w_t, w_l, and w_s is gained by considering their extreme values. By equations (23) through (25) which define the functions, each function has a unit mean value for either of the two sub-samples "A" or "B." Consequently, those meteors which are common to both sub-samples have relative weighting values somewhat different in "A" than they have in "B." In sub-sample "A": $0.4 \le w_t \le 2.4$, with 6 values $w_t < 0.6$ and 8 values $w_t > 1.3$; $0 \le w_l \le 2.3$, with 6 values $w_l < 0.2$ and 7 values $w_l > 1.7$; and $0 \le w_s \le 7.0$, with 28 values $w_s < 0.1$ and 8 values $w_s > 3.5$. Thus, as should be expected, the terrestrial weighting w_t departs from uniformity only mildly, while the lunar weighting w_l is rather more pronounced, and the spatial weighting w_s is severe enough to reduce appreciably the effective size of the sub-samples.

Statistical, Comparative, and Analytical Results

The numerical results of statistical analysis with mass values from "Model-C" versus "Model-B" for Öpik's [2, 28] compact stone versus stone dustball meteoroids are tabulated for comparison in Figure 14. The compared values are in very near agreement, except that the mass values by the dustball "Model-B" have a larger standard deviation. No basis is evident for any suspicion that the results from the further statistical analysis could be invalidated by using only the dustball "Model-B" mass values to represent Öpik's [2, 28] results in comparison to those from "Model-A."

The quantitative results of the statistical analysis with sub-samples "A" and "B" are tabulated for ready reference and comparison in Figures 15 through 17. For example, Figure 15 gives the weighted mean velocity of air-entering and lunar (primary) meteoroids as 16.17 ± 0.17 and 13.66 km/sec, respectively, for sub-sample "A," and 18.83 ± 0.32 and 18.04 km/sec, respectively, for sub-sample "B." In Figure 16, for example, air-entry velocity V_∞ has the correlations 0.020 and 0.191 with the "Model-A" mass m_A in sub-sample "A" and with the "Model-B" mass m_B in sub-sample "B," respectively. The corresponding correlations with the lunar impact velocity, as approximated by the weighted geocentric velocity V_G in Figure 17, are 0.035 and 0.228, respectively.

The various numbers tabulated in Figures 15 through 17 are quite intricately interrelated. As a typical example of these intricacies, consider the meteor beginning height H_B. Hawkins and Southworth [53] showed how H_B, for meteors photographed like those in the present sample, is related to velocity V_∞. Meteors for which V_∞ is about 40 km/sec have values of H_B about 100 km, the standardized reference height in the specification of absolute magnitudes, e.g., M_{pg}. The mean values for H_B from Figure 15, 82.99 ± 0.23 and 85.14 ± 0.31 km with the terrestrial weighting w_t for sub-samples "A" and "B," respectively, are a reflection of the lower mean values for velocity V_∞, already cited. The same explanation accounts for the higher mean values of H_B with the lunar weighting w_l, 84.84 and 87.78 km for sub-samples "A" and "B," respectively; i.e., the air-entry velocity V_∞ would tend to be distributed more toward higher values, except for the gravitational enhancement of the influx of slower meteoroids. Similarly for the even higher mean values of H_B with the spatial weighting w_s, i.e., particles with higher closing velocity V_G, are less favored for interaction with the earth, for more reasons than just gravitational attraction; otherwise, the air-entry velocity V_∞ would tend toward even higher values. Higher V_∞ is also the explanation of higher H_B for "B" versus "A" with each of the four weighting functions (Fig. 15). In Figures 16 and 17, the correlations between H_B and most of the other parameters are due primarily to the correlations between those same parameters and velocity V_∞.

Instead of the elongation λ of the meteor radiant from the earth-way apex, its longitudinal projection (along the ecliptic) λ_λ is used as one of the 12 main parameters in this study. It is related to λ and the radiant celestial latitude β_e by

$$\cos \lambda_\lambda = (\cos \lambda) / \cos \beta_e \ , \qquad (27)$$

wherein it must be noted that λ_λ and λ are always in the same quadrant because $\cos \beta_e$ never changes sign.

Figures 16 and 17 show that the longitude interval λ_λ is correlated directly with perihelion q and inversely with the velocities V_∞ and V_G. But q is inversely correlated with V_∞ and V_G. The mean values of V_∞ and V_G from Figure 15 are lower for sub-sample "A" than for "B," and lower for the weighting functions w_t than for w_l, which are lower than for w_s. These velocity changes are the basis for some trends in the distribution of λ_λ in Figures 18 through 20. Those figures show that, for either of the two sub-samples with either of the three weighting functions, λ_λ has only one mode (point of steepest ascent of the relative cumulative distribution), always near the median (point where the relative cumulative distribution is 0.5). In the respective Figures (18 through 20), by progressing from w_t to w_l to w_s in parts "A" or parts "B," or from part "A" to part "B" in either figure, the mode shifts progressively toward lower values, becoming very nearly 90 degrees for the sub-sample "B" with spatial weighting w_s. The combination "B" with w_s, giving λ_λ the mode near 90 degrees (Fig. 20b), is seen, in Figure 15, to represent a hypothetical sample with 26.39 km/sec average V_∞. But the combination "A" with w_t, giving λ_λ the mode near 105 degrees (Fig. 18a), corresponds to 16.62 km/sec average V_∞ (Fig. 15). It could be expected that, by extrapolation to a sample with even higher values of V_∞, the mode of λ_λ might be shifted downward from 90, perhaps to as low as 60 degrees. Davies and Gill [60] found a λ_λ mode of about 60 degrees with radio meteor data.

The weighted means of meteor heliocentric orbit eccentricity e, tabulated in Figure 15, are within 0.02 of the corresponding median values, which are determined to about that accuracy by smoothing the cumulative distribution plots in Figures 21 through 23. Because e is strongly correlated with velocity (Figs. 16 and 17), a progression of changes, from sub-sample to sub-sample and from weighting function to weighting function, is evident in Figures 21 through 23. For example, with either "A" or "B," the proportion of meteoroids in the total influx with $e \leq 0.25$ is about twice as large for the earth (Fig. 21) as for the moon (Fig. 22).

The medians of the weighted values of the perihelions q of the heliocentric orbits of the meteoroids are appreciably different from the corresponding mean values from Figure 15. With the terrestrial weighting w_t, the medians of q for sub-samples "A" and "B" in Figure 24 are 0.909 and 0.881 AU, respectively, while the corresponding means in Figure 15 are 0.8606 ± 0.0054 and 0.8161 ± 0.0071 AU, respectively. With the lunar weighting w_l, the medians of q for "A" and "B" in Figure 25 are 0.886 and 0.838 AU, respectively, while the corresponding means in Figure 15 are 0.8427 and 0.7804 AU, respectively. And, with the spatial weighting w_s, the medians of q for "A" and "B" in Figure 26 are 0.844 and 0.775 AU, respectively, while the corresponding means in Figure 15 are 0.8184 and 0.7103 AU, respectively. The inverse correlation between perihelion q and the velocities V_∞ and V_G is evident both by visual inspection of Figures 24 through 26 and by comparison of the figures just mentioned for the means or the medians of q from "A" to "B" and from w_t to w_l to w_s.

The distributions of meteoroid perihelion q and aphelion q' with lunar weighting w_l and with spatial weighting w_s are of particular interest. They concern the variation of particle concentration with heliocentric distance and the corresponding impact flux against a moving interplanetary vehicle. In the data for "A" and "B," q is given to only the nearest hundredth AU, and q' to only the nearest tenth. This grouping results in some irregularity of the cumulative distributions when several members have the same indicated values. Histograms of the probability density function corresponding to these 0.01 increments as q approaches unity in Figures 25 and 26 are plotted in Figure 27. The histograms for the four largest abscissa values ($0.96 \leq q \leq 1.00$ AU) are fitted in Figure 27 with dotted lines rising appreciably as q increases. This effect is more accentuated with "A" rather than "B" and with w_l rather than w_s; i.e.,

$$\left.\begin{aligned} f(q) &= 145.5\,q - 137.5 \quad \text{for "A" and } w_l \\ &= 64.5\,q - 59.5 \quad \text{for "A" and } w_s \\ &= 90.0\,q - 83.8 \quad \text{for "B" and } w_l \\ &= 21.5\,q - 18.3 \quad \text{for "B" and } w_s \end{aligned}\right\} \quad (28)$$

Nevertheless, at lower values of q the cumulative distributions in Figures 25 and 26 are nearly linear over a wide range, indicating a constant value of f(q). Over the linear segments in Figures 25 and 26, the relative cumulative distribution spans from 0.25 to 0.62 sloping 2.00 for "A" with w_l, from 0.36 to 0.70 sloping 1.86 for "B" with w_l, from 0.25 to 0.75 sloping 2.38 for "A" with w_s, and from 0.30 to 0.75 sloping 1.72 for "B" with w_s. The nearly constant slope of these segments, which may measure f(q) more nearly free from selection effects, are extended by dashed horizontal lines into the plots in Figure 27.

The distribution of meteoroid aphelion q' for different sub-samples "A" and "B" and different weighting functions w_t, w_l, and w_s are plotted in Figures 28 through 30. In each case the distribution is highly skewed toward the lower values of q', the most prominent mode is at 1 AU, and there is a slight secondary mode near 4 AU. With the spatial weighting w_s in Figure 30, there is another mode near 5 AU (Jupiter's heliocentric distance). This mode near 5 AU in Figure 30 is barely evident for "A," but for "B" it is accentuated about the same as the mode at 1 AU. Only values of q' less than 10 AU are plotted, but the off-scale values and the "hyperbolics" (those known to have large but maybe finite q') were also used in the computation of the relative cumulative distribution. This is why the plotted values do not span the entire ordinate from 0 to 1. Due to skewness, the mean values of q' from Figure 15 are all much larger than the corresponding medians from Figures 28 through 30. Nevertheless, the trend toward larger q' is quite evident for both means and percentiles in the aforementioned transition, "A" to "B" or w_t to w_l to w_s.

A histogram of the probability density function of meteoroid aphelion q', corresponding to the 0.1 increments of q' near unity in Figures 29 and 30, is plotted in Figure 31. The same analysis is given for q' in Figure 31 as was given for q in Figure 27. The histograms for the four smallest abscissa values ($1.0 \leq q' \leq 1.4$ AU) are fitted by linear segments; i.e.,

$$
\left.
\begin{aligned}
f(q') &= -0.48\,q' + 1.02 \quad \text{for "A" and } w_l \\
&= 0.14\,q' + 0.22 \quad \text{for "A" and } w_s \\
&= -0.34\,q' + 0.75 \quad \text{for "B" and } w_l \\
&= 0.30\,q' - 0.06 \quad \text{for "B" and } w_s .
\end{aligned}
\right\} \quad (29)
$$

For values of q beyond 2.0 AU in Figures 29 and 30, there are nearly linear segments of the relative cumulative distribution, with "A" in the interval $2 \le q' \le 4$ AU, sloping 0.19 and 0.17 for w_l and w_s, respectively, and with "B" in the interval $2 \le q' \le 5$ AU, sloping 0.15 and 0.12 for w_l and w_s, respectively. It is not clear whether the slopes of these segments (which are extended with dashed horizontal lines into Figure 31) may represent f(q') as accurately as equation (29) in the interval $1.0 \le q' \le 1.4$ AU. It seems likely that equation (29) for f(q') should be a more substantial result than equation (28) for f(q) because the data spanned an increment of 0.4 instead of 0.04 AU.

Rejecting equation (28) and using the dashed lines for f(q) in Figure 27 while using equation (29) for f(q') gives the expected values for differences between the probability density functions of perihelion q and aphelion q' when both q and q' are in the vicinity of 1 AU; i.e.,

$$
\left.
\begin{aligned}
f(q) - f(q') &= 1.46 \quad \text{for "A" with } w_l \\
&= 1.45 \quad \text{for "B" with } w_l
\end{aligned}
\right\} \quad (30)
$$

$$
\left.
\begin{aligned}
&= 2.03 \quad \text{for "A" with } w_s \\
&= 1.48 \quad \text{for "B" with } w_s .
\end{aligned}
\right\} \quad (31)
$$

Equation (30) represents the derivative at 1 AU, with respect to heliocentric distance r in AU, of the relative number of meteoroids available with orbits appropriate for the constitution of a flux of particles in the vicinity of a vehicle which has an approximately circular heliocentric orbit. This is the reason for the lunar weighting w_l, the moon is such a moving target with a practically circular heliocentric orbit which remains always approximately at 1 AU. The corresponding impact flux varies as the product of the closing velocity V_G and the volume concentration. The velocity and volume vary as $r^{-\frac{1}{2}}$ and r^3, respectively, (e.g., Öpik [70] formulated the closing velocity V_G as the product of the earth's orbital velocity, proportional to $r^{-\frac{1}{2}}$, and a function of the meteoroid orbit parameters). In interpreting the zodiacal light, it is usually assumed (e.g., by Fesenkov [71], Ingham [72], and Beard [73]) that the concentration of light-scattering dust particles varies with r^{-n}, where n is a constant. In this study a similar assumption is made for the flux F of particles in the vicinity of an interplanetary vehicle at heliocentric distance r. Then, the value of $-n_l$ in the corresponding exponential r^{-n_l} is found by subtracting 3 for volume and $\frac{1}{2}$ for velocity from equation (30); i.e.,

$$F \sim r^{f(q) - f(q') - 3.5} = r^{-n_l}$$

$$(1/F)\,\frac{dF}{dr} = -n_l\, r^{-1} = -n_l \quad @\ 1 \text{ AU}$$

$$
\left.
\begin{aligned}
-n_l &= f(q) - f(q') - 3.5 \quad \text{with } w_l \\
&= -2.04 \quad \text{for "A"} \\
&= -2.05 \quad \text{for "B"} .
\end{aligned}
\right\} \quad (32)
$$

A corresponding exponential $\sim r^{-n_s}$ is assumed for the concentration of meteoroids in space, except that there is no component for velocity variation and equation (31) with w_s is used instead of equation (30) with w_l, i.e.,

$$
\left.
\begin{aligned}
-n_s &= f(q) - f(q') - 3 \quad \text{with } w_s \\
&= -0.97 \quad \text{for "A"} \\
&= -1.52 \quad \text{for "B"} .
\end{aligned}
\right\} \quad (33)
$$

It may not be particularly significant that, in comparison to zodiacal light and solar F-corona results, "A" in equation (33) agrees with Fesenkov's [71] result that particle concentration varies with r^{-1}, while "B" agrees with Ingham [72], and Beard

[73], that concentration varies with $r^{-3/2}$. The linear dimensions of the meteoroids in "A" and "B" are perhaps two orders of magnitude larger than those most representative of the optical effects. Still, the dissipative optical effects are reported (e.g., by Briggs [74]) to be quite pertinent to the distribution of meteor particles in space.

In 1954 Whipple [42] noted that the orbits of comets can be distinguished from those of asteroids by the value of a parameter K,

$$K = \log\left(\frac{q'}{1-e}\right) - 1 ,$$

where, as Jacchia and Whipple [75] noted subsequently, the term in parentheses is inversely proportional to the square of the velocity at aphelion. In suggesting the criterion, Whipple noted that K is positive for 96 percent of the known comet orbits and negative for all but 3 asteroid orbits. Jacchia and Whipple [75] cautioned that the values of K are not well known for asteroids of perihelion $q < 1$ AU. The practice by some authors (e.g., Whipple [42], Hawkins and Southworth [76], Jacchia and Whipple [75], Whipple and Hawkins [12], and McCrosky and Posen [18]) of applying the criterion to the orbits of meteor particles has been criticized (e.g., by Dycus and Bradford [77] and by Ceplecha [44]) as an inappropriate extrapolation (with respect to perihelion distance) from the data on which it was based. Still it is an interesting parameter; and the present analysis gives results quite different from others. Whipple [42] analyzed 144 meteors "from double-station photographs by cameras equipped with rotating shutters ... presenting a fairly representative sampling of meteors to about 0 to 1 magnitude visually." His results, illustrated graphically by Whipple and Hawkins [12] and further discussed by McCrosky and Posen [18], showed only 5.6 percent with $K < 0$. In their own analysis of the 2529 photographic meteors, from which sub-samples "A" and "B" were taken for the present analysis, McCrosky and Posen [18] found 25.5 percent with $K < 0$. But in the present analysis with terrestrial weighting w_t, the meteors with $K < 0$ in sub-samples "A" and "B" are 77 percent and 67 percent, respectively. That (essentially) meteors with lower than a limiting mass were not included in "A" and "B" does not explain the preponderance of members with $K < 0$, because Figure 16 shows significant (albeit small) positive correlation with respect to mass. With probable error less than 0.037, the correlations between K and m_A in "A" and between K and m_B in "B" are 0.084 and 0.160, respectively, with terrestrial weighting w_t. If one would interpret $K < 0$ as some indication for asteroidal origin of meteor particles, then the positive correlation with mass, especially in "B," would support Kresak's [20] finding that the ratio of asteroidal to cometary meteors increases with decreasing brightness. And, except for Öpik's [78] cautioning that not only dustballs but also meteoroids of compact iron and of compact stone may originate from comet nuclei, the positive correlation between the K parameter and mass also supports Ceplecha's [44] finding "that weaker meteors photographed by Super-Schmidt cameras contain more observed dense particles than the small camera meteors" (i.e., the brighter meteors). But a further confirmation that the smaller meteoroids actually do have more structural integrity is given through the appreciable positive correlation between meteor beginning height H_B and mass. From Figure 16, the correlations between H_B and mass m_A in "A" and mass m_B in "B" are 0.131 and 0.249, respectively (with weighting w_t). This tends to imply that the smaller meteoroids are more likely to have the higher structural integrity to remain optically quiescent by delaying breakup down to the lower meteor beginning heights H_B. Jacchia, Verniani, and Briggs [79] found, by analysis of 413 precisely reduced Super-Schmidt photographic meteors, that on the average, meteors in short-period orbits appear to be about 1.4 times as dense as meteors in long-period orbits, and also, for short-period meteors, that the density increases as the aphelion q' decreases. Their results are supplemented by those of other authors (e.g., Babadzhanov and Kramer [80]) who find that the proportion of short-period orbits is higher among the faint meteors than can be explained by observational selection. Thus, the smaller orbits tend to have the smaller meteoroids, tending also to have the higher densities and (whether coincidentally or significantly) the lower (most asteroid-like) values of the criterion K. The cumulative distributions of K with the weightings w_t, w_1, and w_s are shown in Figures 32 through 34, respectively. In each case not only the correlation with mass but also the median of K is higher (more comet-like) for "B" than for "A," for w_1 than for w_t, and for w_s than for w_1.

The density of meteor radiants per square degree of the celestial hemisphere is proportional to the slope of the relative cumulative distribution of $\sin \beta_e$, as has been mentioned. Using $|\beta_e|$ instead of β_e, some attention was given to the distribution of this parameter in the development of the weighting functions. The weighting function w_t gives a distribution of $\sin |\beta_e|$ which approximates that of $\sin \beta_e$ when only positive values of β_e are counted and they are weighted as a function of the apparent fraction of the circle of celestial latitude through the meteor radiant. The results, plotted in Figure 10, show that half of the meteor radiants in the atmosphere are within $\pm \sin^{-1} 0.44$ or 26° and $\pm \sin^{-1} 0.39$ or 23° of the ecliptic for sub-samples "A" and "B," respectively. Also, from the slope of the plot in Figure 10, one sees that between $\pm \sin^{-1} 0.32$ or 19° and $\pm \sin^{-1} 0.90$ or 64° the density of radiants per square degree is much less than elsewhere. It is of some interest to check these results with those with the lunar weighting w_l. Figure 35 shows that the intermediate values of $|\beta_e|$ are still associated with the low values of radiant density per square degree. The median values of $|\beta_e|$ are shifted to somewhat higher values with the lunar weighting w_l, being $\sin^{-1} 0.47$ or 28° and $\sin^{-1} 0.45$ or 27° for "A" and "B," respectively. The density of meteor radiants per square degree, as they enter the atmosphere or as they approach the moon or an interplanetary vehicle, is of interest for impact hazard considerations. Figures 10 and 36 show that the prospect for shielding a vehicle against an enhanced meteoroid flux from regions in the vicinity of the ecliptic are of little practical merit because even within angular distance from the celestial poles up to 26 degrees the radiant density per square degree is just as high as it is within ± 19° of the ecliptic. Anticipation of such practical shielding possibilities undoubtedly results from information about the distribution of sin i, where i is the inclination of the meteoroid orbit to the ecliptic. This distribution is plotted in Figure 36, where the spatial weighting w_s is used to approximate the characteristics of the meteoroids in space. The median values of sin i in Figure 36 are 0.24 or sin 14° and 0.29 or sin 17° for "A" and "B," respectively. The mean values of sin i in Figure 15 show a pronounced and consistent tendency to increase from "A" to "B" and from w_t to w_l to w_s.

The cumulative distributions of meteoroid air-entry velocity V_∞ (with terrestrial weighting w_t) and lunar impact velocity V_G (with lunar weighting w_l) are plotted in Figures 37 and 38, respectively. The medians for sub-samples "A" and "B," practically coincident with the single distinct modes, are 15.3 and 16.5 km/sec, respectively, for V_∞ in Figure 37, and 12.6 and 14.8 km/sec, respectively, for V_G in Figure 38. These medians are consistently lower than the corresponding means, tabulated in Figure 15, because the distributions are skewed toward the low velocity ends of the ranges of values. By multiplying the abscissa by $r^{-1/2}$, Figure 38 would approximate the cumulative distribution of meteoroid closing velocity V_v with respect to an interplanetary vehicle in a (practically) circular orbit at heliocentric distance r AU,

$$V_v = V_G \, r^{-1/2} \quad . \tag{34}$$

Because the vehicle orbital velocity varies with $r^{-1/2}$, equation (34) follows from Öpik's [70] formulation for closing velocity proportional to the product of orbital velocity and a function of the meteoroid orbit parameters, together with the assumption that the particular function of meteoroid orbit parameters does not depend strongly on r.

In addition to the correlations between the air-entry velocity V_∞ and the mass evaluations m_A (in sub-sample "A") and m_B (in "B"), further information about the relations between these parameters and the differing constitutions of "A" and "B" is plotted in Figure 39. Each of the two sub-samples "A" and "B" was ordered with respect to its characteristic mass parameter (m_A for "A" and m_B for "B"). Each of "A" and "B" was partitioned (by an intermediate value of its mass parameter) into larger-mass and smaller-mass sets giving the most nearly balancing sums of the terrestrial weighting w_t. The relative cumulative distributions of V_∞ for the different mass regimes are shown in Figure 39 to be significantly different for "B," but not for "A." This checks with the corresponding correlation values from Figure 16; i.e., 0.020 with m_A in "A" (less than the probable

error of 0.037) and 0.191 with m_B in "B." The meteors in Figure 39 with small values of the mass m_B (dot points) tend to have the lower values of velocity V_∞ in "B" than the meteors with large values of m_B (asterisk points).

In making statistical studies with meteor data, most investigators (e.g., Hawkins and Upton [81], Öpik [32], Lindblad [82], Watson [83], Lovell [4, 84], McCrosky [85], Whipple [86], Dohnanyi [87], and Erickson [88]) use the distribution of absolute magnitude in a random sample of meteors for the determination of the mass distribution. Their results are based on the experimental finding that the "luminosity function" $N_{>M}(M)$, the number of meteors equal to or brighter than a given absolute magnitude M (photographic M_{pg} or visual M_v), is of the form

$$N_{>M}(M) = N_{>M}(O)\ \chi^{M} \qquad (35)$$

in a random sample of meteors, where the parameter χ (photographic χ_{pg} or visual χ_v) is considered to be constant over a fairly wide range of magnitudes M. Then, by representing magnitude M as a linear function of log mass m (e.g., m_A or m_B) at constant velocity, etc.,

$$M(m) = k_0 + k_1 \log V_\infty + k_2 \log m + k_3 \log \cos Z_R \quad , \qquad (36)$$

where k_1, k_2, and k_3 are constants, it follows (as Lindblad [82] shows) that the "mass function" $N_{>m}(m)$, the number of meteors of mass equal to or greater than m, is

$$\left.\begin{aligned} N_{>m}(m) &= N_{>m}(1)\ m^{k_2 \log \chi} \\ &= N_{>m}(1)\ m^{-(s-1)} \quad , \end{aligned}\right\} \qquad (37)$$

where s, following the convention of some authors (e.g., Divari [89]), is a constant over a fairly wide range of m. Except Dohnanyi [87], all of the investigators who have followed that procedure have taken the theoretical value -5/2 for k_2 (i.e., "5" and "2" because when magnitude is increased by an increment "5" the luminous intensity is increased by a factor $10^{"2"}$). In an evaluation of χ_{pg} in equation (35) for McCrosky and Posen's [18] entire sample of 2530 meteors, Dohnanyi [87] used the empirical value -2.25 for k_2 in equation (36) which Jacchia, Verniani, and Briggs [56] found by statistical analysis of photographic meteor data. Also, corrections which Dohnyani [87] made for the photographic magnitude scale discrepancy, noted by Kresak [20] for the 300 meteors tabulated by Hawkins and Southworth [53] and also, with somewhat different magnitudes M_{pg}, by McCrosky and Posen [18], have the effect of reducing the value of $-k_2$ by a factor 0.79 for use with McCrosky and Posen's [18] data. Then the effective value of k_2 in equation (36) should be -1.78 in the luminosity function for present analysis with sub-samples "A" and "B."

The present analysis, with data selected by a criterion for absolute magnitude M_{pg} extrapolated for a definite limit of velocity V_∞, is effectively more nearly selected down to a definite limit of mass. Consequently, the distribution of mass is determined directly, instead of from the luminosity function. The distribution of meteoroid mass in the terrestrial and lunar influxes and in the concentration of particles in interplanetary space are plotted in Figures 40 through 42, respectively. The straight lines approximating the respective plots were not fitted by least squares, but were determined by the points for which the ordinate, the log relative cumulative distribution, has the values -0.25 and -1.00. These two points are appropriate for sub-samples with 333 members because the upper point is near the region beyond which the log cumulative distribution has what must be a spurious curvature, and the lower point is near the region where the slope is unduly influenced by the randomness of the individual data points.

That the indicated lines in Figures 40 through 42 must be the best models for the populations of meteoroids, which are represented by the sub-samples "A" and "B" statistically weighted with w_t, w_l, or w_s, is not evident beyond a reasonable doubt. But no process or procedure is evident by which the results could be interpreted better when any one of the plots is considered, whether individually or in comparison with another. The slopes of

the plots in Figures 40 through 42 (involving the respective weighting functions w_t, w_l, and w_s), are -1.48, -1.42, and -1.42, respectively, with sub-sample "A" and are -1.31, -1.21, and -1.37, respectively, with "B." The slopes from Figure 40, -1.48 and -1.31 for "A" and "B," respectively, can be equated to the exponent $k_2 \log \chi_{pg}$ in equation (37) to find the values of the parameter χ_{pg}. By using the empirical value 2.25 for k_2 in order to compare results on the same basis with most reported results, one finds

$$\left.\begin{aligned} \chi_{pg} &= 4.55 \quad \text{inferred from "A"} \\ &= 3.82 \quad \text{inferred from "B"} \ . \end{aligned}\right\} \tag{38}$$

It must be understood that the values of χ_{pg} *in* equation (38) are inferred for a random sample of meteors, like McCrosky and Posen's [18] entire sample of sporadic meteors instead of the selected sub-samples "A" and "B," and that they presuppose the statistical independence of the mass and velocity of meteor particles. Due to the correlation between mass and velocity (tabulated in Figure 16) it should be expected that the values of χ_{pg} determined directly from photographic meteor data may be somewhat different from those in equation (38). Nevertheless, the value 3.82 for "B" in equation (38) should be considered a fairly close agreement with the value 3.44 which Hawkins and Upton [81] found *directly for* χ_{pg} *in an analysis of the distribution* of magnitude for 2123 sporadic photographic meteors. The agreement would be even almost perfect if the theoretical value -5/2 were used for k_2.

In 1941, and in a revised edition in 1956, Watson [83] gave visual meteor data showing that in the interval $-3 \leq M_v \leq 2$ the number of meteors seems to increase approximately 2.5 times with each fainter magnitude. Watson [83] interpreted that result to indicate that $\log \chi_v$ is exactly the reciprocal of $-k_2$ in equation (37), so that the value of the corresponding parameter s is 2. Many authors (e.g., Divari [89]) have quoted Watson's [83] results in that sense. But the same value of k_2 cannot be applied to both visual and photographic meteor data. The visual data are complicated by the Purkinje effect (transition from phototopic to scotopic visual sensitivity, i.e., from cone to rod sensors) and other differences between visual and photographic spectral sensitivity which are corrected collectively by a color index C,

$$C = M_{pg} - M_v \ . \tag{39}$$

Verniani [26] suggests that, in the interval $-2 \leq M_{pg} \leq 1.5$, Jacchia's [90] results for color index C can be approximately described by

$$C = 0.28\, M_{pg} - 1.34 \ . \tag{40}$$

By equations (39) and (40) the derivative of M_v with respect to M_{pg} is 0.72. Therefore, by equation (35),[2]

---

2. For meteors sufficiently bright to be effectively free of both visual and photographic selection effects, equation (35) gives the same number of meteors with subscripts for visual or with subscripts for photographic meteors. Then the relative derivatives of these numbers N_v and N_{pg} with respect to M_{pg} are also equal; i.e.,

$$\left(\frac{1}{N_{pg}}\right)\frac{dN_{pg}}{dM_{pg}} = \log_e \chi_{pg}$$

$$\left(\frac{1}{N_v}\right)\frac{dN_v}{dM_{pg}} = (\log_e \chi_v)\frac{dM_v}{dM_{pg}} = 0.72 \log_e \chi_v = \log_e \chi_v^{0.72}$$

$$\chi_{pg} = \chi_v^{0.72} \ .$$

$$\chi_{pg} = \chi_v^{0.72} \quad \text{for } -0.1 \leq M_v \leq 2.4 . \qquad (41)$$

Watson's [83] value 0.4 for log χ_v in equation (41) would give 0.288 for log χ_{pg}; and, with Jaccia, Verniani, and Briggs' [56] value -2.25 for k_2 from equation (36), the corresponding value of the mass distribution parameter s in equation (37) would be 1.65 instead of 2 over part of the range M_v in Watson's [83] data. This reduces considerably the basis for Watson's [83] inference about the mass distribution. The somewhat higher value 3.7 for χ_v was reported in 1957 by Millman and Burland (see Millman [91]) for a larger sample of visual sporadic and shower meteors. In 1965 Lindblad [82] reported an observational program and analysis of visual meteors directed toward the identification and elimination of the major sources of bias in visual meteor data. From a total of 4000 meteors, 859 were determined to be sporadic and 255 of those sporadic were brighter than the faintest absolute magnitude at which the survey was judged to be complete; i.e., free of selection effects. The value of the parameter χ_v was reported to depend on the arbitrary width of that part of the observers' field of view within which an observed meteor would be counted. Extrapolation of the sporadic meteor data to zero angular distance from the center of the field of view gave 4.3 for the parameter χ_v. The difference between Lindblad's [82] value 4.3 for χ_v and Hawkins and Upton's [81] value 3.44 for χ_{pg} is probably essentially explainable by the varying role of the color index over part of the involved range of visual magnitude.

It was noted above that the value 3.82 for χ_{pg}, which by sub-sample "B" one would infer for a random sample of meteors, agrees well with the value 3.44 found directly by Hawkins and Upton [81], and that the theoretical value -5/2 for k_2 would give 3.34 for χ_{pg}. This does not seem to be a sufficient basis to question the merit of Jacchia, Verniani, and Briggs' [56] statistical determination -2.25 for k_2. On the contrary, if one takes, as Erickson [88] did, the (above) experimental value -2.25 for k_2, then the Hawkins and Upton [81] value 3.44 for χ_{pg} would imply a value of 2.21 instead of 2.34 for the mass distribution parameter s in equation (37) if mass and velocity could be assumed independent. Actually, the value 2.21 is not s but the corresponding parameter s_e in the distribution of kinetic energy for meteor particles; i.e.,

$$N_{>\frac{1}{2}mV_\infty^2}\left(\tfrac{1}{2}mV_\infty^2\right) = N_{>\frac{1}{2}mV_\infty^2}(1)\left(\tfrac{1}{2}mV_\infty^2\right)^{-(s_e - 1)}. \qquad (42)$$

The distribution of meteor particle kinetic energy, unlike either mass or momentum, is practically well represented by a random sample of meteors.

Fialko [92] showed that the distribution parameters s for mass m in equation (37) and s_e for energy in equation (42) would be identical except for any statistical dependence between the air-entry mass and velocity. The English translation of Fialko's [92] paper from Russian appeared in the September-October 1965 issue of Soviet Astronomy-AJ. Being unaware of Fialko's [92] analysis, the author had distributed a Trip Report in August 1965 with a short proof of the more general result that, in equation (37) for the distribution of particle mass, the parameter s is invariant with respect to the replacement of mass by the product of mass and any exponential function of velocity, provided only that mass and velocity were statistically independent. The same proof was also published by Dalton [93] in a NASA Technical Memorandum in November 1965. Marcus' [94] boundary-effect criticism of Fialko's [92] analysis would apply equally to Dalton's [93] more general result, but Fialko [95] showed that those boundary effects are not practically significant for meteoroids in the terrestrial influx. Subsequently, in an analysis of 184 radio meteors, Fialko [96] found a value ≈ 2.3 for the energy distribution parameter s_e in equation (42). But, as Fialko [96] noted, "quite apart from the complexity of this method, one should realize that so far an accurate dependence of the meteor ionization 'probability' p_q on V_∞ has not been obtained." The value 2.21 for s_e inferred from the Hawkins and Upton [81] value 3.44 for χ_{pg} is probably the most substantial result for the energy distribution, at least for sub-sample "A."

With sub-sample "B" the correlation 0.191 between mass m_B and velocity V_∞ with terrestrial weighting w_t might be sufficient to account for the difference between the value 2.31 for the parameter s in the mass distribution and the value 2.21 for the

corresponding parameter s_e in the energy distribution. But the corresponding results for "A," with the value 2.48 for s and only 0.020 for the mass-velocity correlation, are somewhat less plausible. But in either case "A" or "B," as long as one has not yet made a choice between "A" and "B," the best basis at hand for the computation of the meteoroid impact hazard in space is the value 2.21 for the parameter s_e in the energy distribution, equation (42), for both the terrestrial influx and the lunar influx. Near the end of the last part of this section a choice is made between "Model-A" and "Model-B." There some further discussion of the role of k_2 and its effect on s_e is given. In constructing the models for the distributions of energy, it is noted that the lines representing the distributions of mass in Figures 40 and 41 were fitted through the points for which the ordinates were -0.25 and -1.00. The region of best fit tends to be centered approximately around the quartile, where the ordinate is -0.60. Through the point with this ordinate -0.60 on the fitted line, with abscissa m_e, a line with slope -1.21 for $-(s_e - 1)$ has the ordinate intercept

$$y_{m_e} = -0.60 + 1.21 \log m_e \, . \qquad (43)$$

This is the line for the mass distribution which would be inferred from the energy distribution if one could assume that mass and velocity were statistically independent. By representing the corresponding ordinate for the (similarly plotted) energy distribution by y_e, Fialko's [92] formulation gives

$$y_e = y_{m_e} + \log E\left[(V^2/2)^{s_e - 1}\right] , \qquad (44)$$

where E[ ] designates expected value; i.e.,

$$y_e = y_{m_e} - 0.36 + \log \left[\frac{\sum_1^{333} V^{2.42} w}{\sum_1^{333} w} \right] . \qquad (45)$$

With the terrestrial weighting w_t the expected values of $V_\infty^{2.42}$ in equation (45) are $(17.65)^{2.42}$ and $(23.91)^{2.42}$ for sub-samples "A" and "B," respectively; and with the lunar weighting w_l the expected values of $V_G^{2.42}$ are $(14.72)^{2.42}$ and $(22.08)^{2.42}$ for "A" and "B," respectively.

For "A" and "B" in Figures 40 and 41, the mean of the four values of s for mass is 2.35. The effect of the correlation between mass and velocity is that the value of s_e for energy is reduced to 2.21. By linear interpolation (with respect to n in mV^n) the corresponding parameter s_m for momentum is 2.28, and the ordinates y_{m_m} and y_m corresponding to y_{m_e} and y_e, respectively, in equations (43) and (45), respectively, are

$$y_{m_m} = -0.60 + 1.28 \log m_e \qquad (46)$$

$$y_m = y_{m_m} + \log \left[\frac{\sum_1^{333} V^{1.28} w}{\sum_1^{333} w} \right] . \qquad (47)$$

With the terrestrial weighting w_t the expected values of $V_\infty^{1.28}$ in equation (47) are $(16.69)^{1.28}$ and $(20.71)^{1.28}$ for sub-samples "A" and "B," respectively; and with the lunar weighting w_l the expected valuesof $V_G^{1.28}$ are $(12.55)^{1.28}$ and $(17.38)^{1.28}$, respectively.

In the same paper in which he introduced his comet-asteroid criterion K in 1954, Whipple [42] suggested that a weighting factor, V_∞^{-2} for $V_\infty > 19$ km/sec and $3\,V_\infty^{-2}$ for $V_\infty < 19$ km/sec should reduce the distribution of observed velocities in a random sample of meteors roughly to a distribution applying to meteoroids of a constant mass. He defined his "cosmic weight" w_w as

$$w_w \sim P^{-1} V_\infty^{-2} \, , \qquad (48)$$

where P is the meteoroid's earth-encounter probability which was formulated by Öpik [64]. This weighting w_w is often tabulated (e.g., by Hawkins and Southworth [76], Jacchia and Whipple [75], and

McCrosky and Posen [18]) and is of some interest to check with the present analysis. The weighting w_w was formed as the product of several factors, one being $V_\infty^{-\frac{1}{2}}$ because the effective surveillance area is considered to vary with the square of the meteor beginning height H_B, which in turn was considered to vary with $V_\infty^{\frac{1}{4}}$. Thus, when meteor height is accounted for by a separate weighting, and one is concerned with the terrestrial influx instead of the total population of particles in interplanetary space, the weighting with respect to velocity would be $\sim V_\infty^{-3/2}$. Recently, Miller [51] derived a corresponding exponential velocity weighting for random photographic meteors. He found that the most appropriate velocity exponent is $-2.87\ (s - 1)$, where s is the parameter in the mass distribution, equation (37). The values of s corresponding to Figure 40 are 2.48 and 2.31 for sub-samples "A" and "B," respectively, and the corresponding values of the velocity exponent for Miller's [57] weighting are -4.25 and -3.76, respectively. An independent check on the exponent for velocity weighting of random meteors is afforded by assuming different values for the exponent and calculating the weighted mean of V_∞ with a random sample. Then by interpolation one can find the value of the exponent which gives the same mean value of V_∞ as is found in the present analysis with the selected sub-samples "A" and "B." This was done by hand computation with Hawkins and Southworth's [53] histogram of velocity values classified in 5 km/sec intervals for a random sample of 285 sporadic photographic meteors. With uniform weighting except for velocity, and with velocity weighting exponents -2, -3, and -4 the mean values of velocity V_∞ are 20.42, 17.48, and 15.77 km/sec, respectively. From Figure 15 the means of V_∞ with uniform weighting are 16.62 and 20.23 km/sec for "A" and "B," respectively. By interpolation one finds that the equivalent velocity weightings, without any adjustment for effective surveillance area, are $\sim V_\infty^{-3.50}$ and $\sim V_\infty^{-2.06}$ for sub-samples "A" and "B," respectively.

Metric of Cumulative Flux for Particle Parameters

One can calculate the mean flux (or the expected future flux for the year-around average exposure) instead of just the relative rate. The 333 meteors in each of the sub-samples "A" and "B" were, in each case, all of the sporadic meteors in McCrosky and Posen's [18] tabulation which were bright enough for selection with respect to a criterion function of magnitude and velocity roughly corresponding to meteoroid mass. McCrosky and Posen [18] noted that the 2529 meteors they tabulated were 70.4 percent of all meteors photographed during 1125 hours of exposure, that 13.8 percent had been rejected because the correspondence of points in the photographs from the two separated stations was uncertain, that 0.6 percent were rejected due to an ambiguity of radiant, that 4.8 percent could not be reduced for random technical reasons, and that 10.4 percent were just too faint. The 10.4 percent of too faint meteors are of no consequence to the present analysis because they would not have passed the selection criterion; but the other 19.2 percent must be accounted for by reducing the 1125 hours of exposure time. Of the 2529 meteors which they tabulated, they designated 2066 sporadic and 463 stream meteors. But only 2040 of the sporadics had values tabulated for M_{pg} and m_A, i.e., could be considered for selection. Then, the effective total exposure t was

$$t = \left[1 - \left(\frac{19.2}{70.4 + 19.2}\right)\right]\left(\frac{2040}{2066}\right) 1125 \text{ hrs} = 873 \text{ hrs.}$$

The effective surveillance area of equipment was given by Hawkins and Upton [81] as 5980 km^2 at the 90-km height for which the cameras are adjusted to overlap. The means $\overline{H}_B$ of the beginning heights H_B (from Figure 15) for sub-sample "A" are 82.99 and 84.84 km for terrestrial weighting w_t and lunar weighting w_l, respectively, and for "B" are 85.14 and 87.78 km for w_t and w_l, respectively. The effective area A is considered to be $(\overline{H}_B/90)^2\ 2980$ km^2. For both "A" and "B" the effective number N_e of sporadic meteors, with respect to which the

indicated relative cumulative distributions must relate, is 333 with the terrestrial weighting w_t; but with the lunar weighting w_l the number of sporadic meteors which relate to the indicated area A and time interval t must be reduced by the factor k_f from equation (10), 0.47 for "A" and 0.54 for "B." But, in showing the cumulative flux with respect to mass, momentum, and energy, in specific units, the interests of most readers is probably served best by increasing the sporadic flux by the factor 2529/2066 by which the total sample exceeds the sporadic component in the data shown by McCrosky and Posen [18]. Therefore, the increment Δy which must be added to the log relative cumulative distribution of sporadic meteors to get the log mean total flux per square meter per second is

$$\Delta y = \log \left\{ \left(\frac{2529}{2066}\right) (333\, k_f^{\delta}) \left[10^6 (2950) \left(\frac{\bar{H}_B}{90}\right)^2 (3600)(873) \right]^{-1} \right\} \quad (49)$$

$$= -9.453 + \log k_f^{\delta} - 2 \log \bar{H}_B \quad .$$

where δ has the values 0 and 1 with w_t and w_l, respectively. The results for Δy in equation (49) are -13.30 and -13.62 with weighting w_t and w_l, respectively. The results for "A" and "B" are averaged and do not differ from their mean result by more than ±0.015 with either w_t or w_l.

The mass cumulative influx $F_{>m}$, found by adding Δy from equation (49) to the equations indicated on the plots in Figures 40 and 41, is

$$\left.\begin{aligned} \log F_{>m} &= -1.48 \log m_A - 15.05 \\ &\quad \text{for "A" with } w_t \\ &= -1.42 \log m_A - 15.29 \\ &\quad \text{for "A" with } w_l \\ &= -1.31 \log m_B - 14.77 \\ &\quad \text{for "B" with } w_t \end{aligned}\right\} \quad (50)$$

$$= -1.21 \log m_B - 14.93$$

$$\text{for "B" with } w_l \quad . \qquad (50)\ (\text{cont'd})$$

Also, in each case, the equation indicated on the plot in Figures 40 and 41 can be solved for the value $\log m_e$ of the abscissa corresponding to the ordinate value -0.60. By substituting the results for $\log m_e$ into equation (46) one gets, for the mass reference intercept y_{m_m} for momentum, the values -1.59 and -1.56 with w_t and w_l, respectively, for "A," and the values -1.45 and -1.35 with w_t and w_l, respectively, for "B." Then, by equations (47) and (49), the momentum cumulative influx $F_{>mv}$ is

$$\left.\begin{aligned} \log F_{>mv} &= -1.28 \log m_A V_\infty - 13.33 \\ &\quad \text{for "A" with } w_t \\ &= -1.28 \log m_A V_G - 13.78 \\ &\quad \text{for "A" with } w_l \\ &= -1.28 \log m_B V_\infty - 13.07 \\ &\quad \text{for "B" with } w_t \\ &= -1.28 \log m_B V_G - 13.38 \\ &\quad \text{for "B" with } w_l \quad . \end{aligned}\right\} \quad (51)$$

Similarly with the mass reference intercept y_{m_e} in equation (43), one gets the energy intercept y_e in equation (45), and adds Δy from equation (49) to get the energy cumulative influx $F_{>\frac{1}{2}mv^2}$; i.e.,

$$
\log F_{>\frac{1}{2}mV^2} = \begin{cases} -1.21 \log (\tfrac{1}{2} m_A V_\infty^2) - 12.18 \\ \quad \text{for "A" with } w_t \\ -1.21 \log (\tfrac{1}{2} m_A V_G^2) - 12.66 \\ \quad \text{for "A" with } w_l \\ -1.21 \log (\tfrac{1}{2} m_B V_\infty^2) - 11.72 \\ \quad \text{for "B" with } w_t \\ -1.21 \log (\tfrac{1}{2} m_B V_G^2) - 12.04 \\ \quad \text{for "B" with } w_l \end{cases} \qquad (52)
$$

It is of some interest to compare the mass cumulative terrestrial influx in equation (50) with the results of the meteoroid-puncture experiments in near-earth-orbit space from Explorers XVI and XXIII and the three Pegasus flights. Dalton [16] showed that the product $m^{19/54} V^{2/3}$ must be constant for just-puncturing meteoroids when the other impact circumstances are fixed. By taking 26.7 km/sec for the mean impact velocity, Dalton [16] showed that the combined puncture data for the Explorers XVI and XXIII would indicate $10^{-5.374}$ impacts per square meter per second of particles of mass down to $10^{-6.17}$ gram, and that the corresponding values implicated by the Pegasus' thickest target would be $10^{-7.164}$ and $10^{-6.03}$, respectively, in the same units. With the mean values 16.17 and 18.83 km/sec for "A" and "B," respectively, (for $\overline{V}_\infty$ weighted w_t from Figure 15) the indicated just-puncture mass values should be increased by factors $10^{0.413}$ and $10^{0.287}$ for "A" and "B," respectively. Actually, this explanation is overly simplified because the $E[V_\infty^{2.42}]$ rather than $E[V_\infty]$ is pertinent here, as in equations (44) and (45), but these values are not known for the minuscule particles. The results are plotted in Figure 43 with an extrapolation of the equation (50) mass cumulative terrestrial influx for comparison. But the mass values for the just-puncturing meteoroids plotted in Figure 43 presuppose the velocity distributions from the meteor sub-samples "A" and "B" to be applicable for particles of nearly eight orders of magnitude smaller mass. This presupposition is more nearly a valid representation of the results from "A" than from "B." With "A" the 0.020 correlation between mass m_A and velocity V_∞ is negligible in comparison with the probable error of ± 0.037, but with "B" the 0.191 correlation between mass m_B and velocity V_∞ is unmistakably significant. This would imply from "A" a lower velocity, and consequently higher mass for the satellite-puncturing particles. One can show that the Explorer puncture data most probably concerns typical zodiacal light particles.

According to Takaknbo (see Ericke [57]) the radius of the dust particles most effective in the zodiacal light and the solar F-corona is about 20 microns. With Öpik's [2] value 3.4 g cm^{-3} for the average density of meteoritic stone, the mass of such a particle is 1.14×10^{-7} g. Other authors (e.g., Briggs [74]) adopt density values as low as 0.2 g cm^{-3} for zodiacal light particles of 20 micron radius. So the mass probably is between 10^{-8} and 10^{-7} g. According to Öpik [97] the velocities of the zodiacal light particles relative to the moving earth, the moon, or an interplanetary vehicle (i.e., V_G) are small, the average being about one-fifth of the Earth's orbital velocity, or 6 km/sec. If all of the particles with that mass value would have that same velocity, the air-entry velocity would be 12 km/sec, i.e., $(6^2 + 11^2)^{\frac{1}{2}}$. But, as is likely, if V_G has a distribution with lower and higher values, the lower values are favored by the larger effective interaction cross section of the earth. The resulting air-entry velocity is then likely more nearly 11 than 12 km/sec. Then, when one takes 11 km/sec for the average air-entry velocity and combines it vectorially with that of a low-flying satellite (of about 7.5 km/sec), the average velocity of impact is 13.3 km/sec, i.e., $(11^2 + 7.5^2)^{\frac{1}{2}}$. Then Dalton's [16] value for the meteoroid mass corresponding to the centroid of the Explorers XVI and XXIII puncture data should have been increased by a factor $10^{0.570}$ instead of $10^{0.283}$. The resulting estimate of the mass of the just-puncturing meteoroids for the centroid of the Explorer data would be $10^{-7.60}$ g, most probably a typical zodiacal light particle.

It is difficult to judge for "B" whether or not the change in average air-entry velocity $\overline{V}_\infty$ from 18.83 to 11 km/sec corresponds correctly with the correlation 0.191 between mass m_B and velocity

V_∞ with terrestrial weighting, or whether or not the change in average geocentric velocity $\overline{V}_G$ from 18.04 to 6 km/sec corresponds with the correlation 0.188 between mass m_B and velocity V_G with lunar weighting, when mass is extrapolated down seven orders of magnitude. But the explanation is probably correct. This means that the Explorer point marked for sub-sample "B" in Figure 43 should be shifted 0.283 units further to the right, bringing it into even closer agreement with the model extrapolated from the photographic meteor results. The Pegasus point would also be shifted somewhat to the right, but by a smaller increment due to the smaller difference in velocity from that of the photographic meteors. The point is sufficiently important that the satellite puncture data are compared in Figure 44 with the model for the energy-cumulative influx extrapolated from the photographic meteor results in equation (52). Again the agreement between the satellite puncture data and the model extrapolated from the meteor data is considerably closer with sub-sample "B" than with "A." Furthermore, for either "A" or "B," the agreement with the satellite puncture results is considerably better when the extrapolation is with respect to energy in Figure 44 than when it is with respect to mass in Figure 43. This tends to confirm the suspicion that the lack of closer agreement with the model extrapolated with respect to mass is due to the fact that the velocity distribution of the meteor particles was erroneously presupposed for the satellite puncturing meteoroids in Figure 43. By shifting the satellite points in part (b) for "B" in Figure 43 to the right for the increment 0.283 in log m_B corresponding to a change in mean impact velocity from 18.83 to 13.3 km/sec, the satellite points acquire the same configuration with respect to the mass model as they have in Figure 44 with respect to the energy model.

Without the supporting evidence from the satellite puncture experiments, the extrapolation of the photographic meteor models into the mass and energy regions characteristic of the zodiacal light particles would have been quite eclectic. Nevertheless, one can consider the extrapolations well substantiated down to about 10^{-6} g (which, according to Smith [38], is the mass of a typical individual grain in a dustball meteoroid) and a further extrapolation down to about $10^{-7.6}$ g reasonably corporeal. Regardless of whether the large dustballs are derived from the smaller ones by accretion, or the small ones are derived from the larger ones by disruption, the mass-cumulative distribution should begin to "level off" toward the vicinity of the minuscule particles. The process of "leveling off" should be quite gradual due to the natural distribution of grain size. A suggestion of this effect is evident in Figure 44 in that the slope of the line joining the Pegasus and Explorer points is arithmetically less than that of the extrapolated model. The same trend was evident in the Explorer data which is represented in Figure 44 by its centroid. Further confirmation of this suspicion is given by the reported results of analysis of the zodiacal light and solar F-corona. In 1947 van de Hulst [98] found, by assuming that the log cumulative space density of zodiacal light particles is a linear function of log particle radius with slope $-(p-1)$, that p has the value 2.6. In 1963 Ingham [72] reported the higher values 4 or 5 for p derived by extrapolation from meteor data. But in 1967 Blackwell, Dewhirst and Ingham [99] reported "... it seems likely that the van de Hulst [98] density [concentration of particles] is the more representative of the optical determination of interplanetary space density." Not enough is known about the relation between particle material density and mass over the range of zodiacal light particles to support an accurate formulation of the relation between the parameter p in the radius distribution and the parameter s in the mass distribution, equation (37). But ignoring any dependence between radius and material density would give the value 3 for $(p-1)/(s-1)$. Then, with the spatial weighting w_s in Figure 42, the values 2.42 and 2.37 for the parameter s from "A" and "B," respectively, would give the values 5.26 and 5.11 for p from "A" and "B," respectively. The value for p from either "A" or "B" is somewhat high in comparison with the zodiacal light results, especially van de Hulst's [98]; but there is somewhat closer agreement from "B" than from "A."

Figure 43 illustrates models for the mass-cumulative terrestrial influx extrapolated by equation (50) to mass values below the range of meteor data. It is also of interest to assess the validity of a similar extrapolation of the results in equation (50) with lunar weighting w_l. By equation (50), at $10^{-7.6}$ g in the models from sub-sample "A," the terrestrial influx exceeds the lunar influx by the factor $10^{-0.70}$ or 5; and the corresponding factor for "B" is $10^{-0.92}$ or 8. As already noted, Öpik's [97] value for the mean geocentric velocity $\overline{V}_G$ of these small particles is 6 km/sec. If all of the particles had the same velocity, then the factor by which the

terrestrial influx is increased by gravitational attraction would be $1 + (11/6)^2$ or 4.36. But one must expect that the particle velocities are distributed about their mean, with some values sufficiently small to increase the gravitational enhancement factor considerably. For example, any particles with a value 3 km/sec for V_G would have a gravitational enhancement factor of 14.44 but a particle with velocity higher than the mean by the same amount would have a gravitational enhancement factor of only 2.49. The average of the enhancement factors for 3 and 9 km/sec is 8.47, which is nearly twice as large as that for the 6 km/sec particles. Thus, both values for the gravitational enhancement factor, 5 for the extrapolation from sub-sample "A" to $10^{-7.6}$ g and 8 for the extrapolation from "B," are plausible; but the value 8 from "B" is more probable than the value 5 from "A." Anyway, nearly the same conclusions as for the mass-extrapolation of the terrestrial influx also apply in the extrapolation of equation (50) for the lunar influx; i.e., one can consider the extrapolation fairly well substantiated down to about 10^{-6} g, with the further extrapolation down to about $10^{-7.6}$ g somewhat more diaphanous.

The extrapolation of equation (52) for the energy-cumulative terrestrial influx is supported in Figure 44 by the satellite puncture results. The corresponding extrapolation of the energy-cumulative lunar influx in equation (52) is similarly supportable, but needs some explanation. By extrapolation of equation (52), the lunar and terrestrial energy-cumulative flux values are in the fixed ratios $10^{0.48}$ or 3 and $10^{0.32}$ or 2 from sub-samples "A" and "B," respectively, independently of the extrapolation. It was already mentioned that meteoroids of $10^{-7.6}$ g and average low-earth-orbit-satellite-impact velocity 13.3 km/sec should be 5 to 8 times less abundant in the lunar influx and with a mean geocentric or lunar-orbiter-vehicle-impact velocity $\overline{V}_G$ about 6 km/sec. Because the particle energy is reduced by a factor 5, and the influx is reduced by a factor 5 to 8, one might suppose the energy-cumulative influx to be reduced by a factor 25 to 40. But the low velocity particles, which have the high gravitational flux enhancement factors, have little effect on the cumulative distribution of energy. The punctures are made not so much by particles with average velocity and just-sufficient mass, but more by smaller particles with above-average velocity. What is significant is not the expected value of V_G, but the expected value of $V_G^{2.42}$ as in equations (44) and (45). This explanation and the extrapolation of the results from sub-sample "B" by equation (52) agree exactly with Gurtler and Grew's [100] results for the Lunar Orbiter puncture experiments. They (Gurtler and Grew [100]) reported that data collected between lunar altitudes 30 and 6200 km "... continuously for 17 months indicate (by 22 punctures) that the rate of penetration in the lunar environment is approximately half the rate in the near-earth environment as measured by detectors of the same type aboard Explorers XVI and XXIII." The agreement with the corresponding extrapolated results from sub-sample "A" is somewhat poorer in that the "A" results indicate that the puncture flux reduction should have been by a factor 1/3 instead of 1/2.

Comparisons to Other Reported Results

As noted in 1966 by Nilsson [101], for several years there has been a considerable volume of literature concerning the alleged existence of a concentration of dust in the vicinity of the earth, as inferred primarily from the satellite piezoelectric microphone measurement reported by Dubin and McCracken [102] and by Alexander, McCracken, Secretan, and Berg [103]. They had reported that the mass-cumulative impact rate, in particles per square meter per second for mass m in grams in the interval 10^{-10} g $\lesssim$ m $\leq 10^{-6}$ g, were $10^{-17.0}$ $m^{-1.70}$. Nilsson's [101] paper in 1966 cast considerable doubt on the validity of those measurements by reporting satellite and laboratory evidence that the microphone crystals emit noise when subject to slowly varying temperatures. In 1968 Konstantinov, Bredov, and Mazets [104] reported experiments from the Soviet artificial earth satellite Kosmos-135 which verified Nilsson's [101] contention. They reported using piezoelectric sensors, analogous to the others which had given the anomalously high readings, but specially developed and applied with careful precautions so as to protect the system from interferences of acoustic, thermal, or electrical origin. They reported good agreement with the puncture data from Explorers XVI and XXIII and Pegasus 1 and 2. Somewhat later, Koptev [105] wrote further about those experiments, which he said, although producing readings several thousand times smaller than anticipated, were in conformity with the American satellite puncture experiments with gas-filled pressure cells on Explorers XVI and XXIII and with electrical condensers on Pegasus. It has already been indicated that those puncture

results agree well with the energy-cumulative distribution extrapolated by equation (52) from the photographic meteor results, the agreement being somewhat closer with sub-sample "B" than with "A."

In the present analysis the total flux (cumulative with respect to mass, momentum, or energy) was found by multiplying the sporadic flux by the factor 2529/2066 (or 1.22) by which the total exceeds the sporadics in McCrosky and Posen's [18] sample of photographic meteors. This may have constituted a slight over-correction, because the proportion of stream meteors which could have qualified by the selection criteria for the sub-samples "A" and "B" might have been lower than the proportion of sporadic meteors which qualified. This aspect of the relative frequency of sporadic versus stream meteors was treated recently in an interesting analysis by Erickson [106]. He found that the total luminous flux of known streams is about 30 percent of the sporadic flux, that the total mass influx of known streams is of the order of one percent of that from sporadic meteors, and that the target puncture peak rates of the most active streams are no larger than the average puncture rate from sporadic meteoroids.

The distribution of meteor-forming, vehicle puncturing, and zodiacal-light-distributing particles in interplanetary space may be quite different from the distribution of the bodies responsible for the craters apparent in the telescopic or Lunar Orbiter pictures of the lunar surface and the Mariner IV pictures of Mars. According to an analysis by Anders and Arnold [107], at least 75 percent of lunar craters down to a diameter of 20 km are caused by impact of bodies of asteroidal rather than of cometary origin, and the rate of crater formation on Mars by these asteroidal bodies is about 25 times higher than that on the moon.

With respect to heliocentric distance r, by equation (33) the concentration in interplanetary space of the meteoroids (spatially weighted) from sub-samples "A" and "B" varies with $r^{-0.97}$ and $r^{-1.52}$, respectively. Briggs [74] computed the spatial variation of particle concentration which would support the measured values of the zodiacal light under steady-state conditions of Poynting-Robertson retardation of debris continuously ensuing by the disintegration of comets, but exemplified by the appropriately weighted distribution of photographic meteor particles. Briggs [74] found that concentration should vary with a power of r which would change from -0.97 through -1.09 to -1.27 as r changes from 0.5 through 1.0 to 1.5 AU. His result for the exponent agrees well with the value -0.97 from "A" in equation (33) for 1 AU. This result gives some support to the methods of the present analysis; but Briggs [74] used Hawkins and Southworth's [76] random sample of 359 photographic meteors as an input with the mass values which were computed from "Model-A" rather than from "Model-B." In 1967 papers by Southworth [108] and Divari [109] analyzed the space concentration of radio meteor particles. Divari [109] used the bivariate distribution of orbit inclination and semi-major axis from 7511 radio meteors by Kashcheev, Lebedenets, and Lagutin (see Divari [109]), statistically weighted to correct for the probability of earth encounter. He found that, for heliocentric distance r in the interval $0.5 \leq r \leq 1.5$ AU space concentration in the ecliptic plane varies nearly as r^{-1}. Southworth [108] used data for 13 672 meteors observed from 1962 to 1965 by the six-station radar network in Havana, Illinois. The meteors with negative celestial latitude of radiant β_e were discarded and the remaining ones were carefully weighted for probability of earth encounter and other physical selective effects. The mass values in Southworth's [108] sample ranged from about 10^{-5} to 10^{-3} g with optimum representation from $10^{-3.5}$ to 10^{-4} g. He plotted the logarithm of the relative space density versus the logarithm of the heliocentric distance r in the vicinity of the ecliptic by a series of connected line segments, evidently representing the 20 discrete stratifications made in r. Between Mercury and Earth the plot can be closely represented by a line with slope -0.77, and between Earth and the middle of the asteroid belt at 2.7 AU by a line with slope -1.56. In addition to this "dog-leg" at 1 AU in the plot, there are also "dog-legs" seeming to hinge at the points for Mercury and Jupiter. These three appreciable bends in the plot at Mercury, Earth, and Jupiter may be spurious. The value -1.56 for the slope between Earth and Jupiter agrees well with the value -1.52 for sub-sample "B" in equation (33); but the mean (-1.17) of the two values -1.56 and -0.77 at the Earth agrees somewhat better with the value -0.97 for "A" from equation (33).

In an editorial reporting on the mission of the Mariner IV voyage to Mars in the 10 September 1965 issue of "Science," Abelson [110] noted that the micrometeorite study shows that interplanetary dust was more abundant in the vicinity of Mars than near Earth. In the same copy of "Science" with

Abelson's [110] editorial were a report by Anderson [111], describing the Mariner IV spacecraft, and a report by Alexander, McCracken, and Bohn [112] on the dust experiment. Impact measurements of cosmic dust were made on the Mariner IV spacecraft throughout the nearly eight months of flight from Earth in November 1964 to Mars in 1965. Alexander, McCracken, and Bohn [112] reported an analysis of the 215 impacts of particles for which momenta were larger than 1.96×10^{-3} dyne-sec. The detector was described as an acoustical transducer bonded to an aluminum sensor plate with a viewing solid angle of about π steradians. They reported an enhancement of the flux by a factor 5 as the heliocentric distance r from the sun increased, and a change in the mass-cumulative impact flux from $\sim m^{-0.55}$ near both planets to $\sim m^{-0.9}$ over the interval $1.25 \leq r \leq 1.36$ AU. But the reports did not mention any consideration of possibly changing orientation of the impact detector during the mission. Anderson [111] noted that the impact detector was on the body of the spacecraft, with the microphone plate approximately perpendicular to the plane of the orbit when the axis of the guide-star Canopus was approximately perpendicular to the roll axis aligned with the heliocentric radial vector. But the reports did not mention the orientation of the detector with respect to the Sun, nor whether or not the same guide-star was used throughout the flight. An analysis with respect to the detector plate orientation, similar to Dalton's [113] method for the interpretation of the orientation information in the puncture data from the Pegasus spacecraft, might account for the impact flux variations during the flight. More likely, however, the results are not valid if the sensor was of the type which Nilsson [101], Konstantinov, Bredov, and Mazets [104], and Koptev [105] have shown to give spurious signals.

Notwithstanding the difference between "Model-A" and "Model-B" for photographic meteors, the bias and factors of physical selectivity in radio meteor data are less accurately known. The results are often quite disparate. For example, Figure 10 illustrates that half of the meteoroids have radiants within ● 26 degrees or ± 23 degrees of the ecliptic by sub-samples "A" and "B," respectively; but Davies and Gill [60] noted in 1960 that half of the statistically weighted radio meteors have radiants within ± 15 degrees of the ecliptic. In 1963 Greenhow [114] discussed the peculiar difficulties of interpretation of radar meteor data in some detail and stressed the general lack of substance in prior results and the need for caution in future experiments and analysis. The most obvious difference between sporadic radio and photographic meteor data is in the velocity distributions. By the differences between the velocity distributions of sporadic meteors from photographic versus radio measurements, one does not imply that the velocity of an individual meteor would be assessed with such different results by the two methods, but that the samples are differently constituted by physical selectivity. This was illustrated in 1955 by Whipple [115] by tabulating radio and photographic measurements of the velocity of meteors in several distinct streams. A thoughtful paper by Furman [116], translated from the 1966 Russian publication, facilitates a realistic perspective for the difficulties remaining in the interpretation of radio meteor phenomena and for the uncertainty extant after careful analysis. Even more recently (in 1967) Fialko [96] has noted that so far an accurate dependence of meteor ionization probability p_q on velocity V_∞ has not been obtained (where ionization probability p_q means the probability that a single evaporated meteor atom will produce a free electron). The hope of getting a more accurate determination of the velocity dependence of the luminous efficiency β through a determination of the velocity dependence of p_q and of the ratio β/p_q does not seem to be very helpful so far. For example, in 1956 Hawkins [117] reported that β/p_q were $\sim V_\infty^{-4.56}$, and in 1964 Hawkins [6] noted that a detailed calculation gives approximately $p_q \sim V_\infty^{3.4}$. Solving for β between Hawkins [117, 6] 1956 and 1964 results would give approximately $\beta \sim V_\infty^{-1.16}$, in better agreement with "Model-B" than with "Model-A." But in both papers Hawkins [117, 6] gave the relation $\beta \sim V_\infty$, as in "Model-A," and likely intended it to be understood as a more substantial result. On analysis of the 1956 data on meteor echoes and magnitudes by Millmann and McKinley [118], Delcourt [119] deduced in 1963 that the ionization coefficient β_q (or ionization efficiency in the conversion of meteoroid kinetic energy into the freeing of electrons) is approximately related to β by $\beta_q/\beta \sim V_\infty^2$. But in 1968 Derbeneva [120] gave an analysis of experimental ionization and excitation cross sections for collisions of meteoroid atoms with nitrogen molecules and concluded that β_q/β is independent of V_∞. The onus,

evidently, is that Fialko's [96] notion in 1967, that so far an accurate dependence of p_q on V_∞ has not been established, is correct. In 1967 Slattery and Friichtenicht [121] measured p_q for micron-size iron particles injected at from 20 to 45 km/sec into air targets, getting $p_q \sim V^{3.12}$. Their result is even more difficult to reconcile with "Model-A" than was Hawkins' [6] $\beta \sim V_\infty^{3.4}$. In comparing results from photographic and radio meteors, it should be noted that the photographic meteors span a transition region for radio meteors. The median mass for both sub-samples "A" and "B" is near the value 0.1 g, which McIntosh [122] shows is the value below which, for a single non-fragmenting meteoroid, it is expected that log echo duration of radio meteors is a linear function of log mass with slope (but not intercept) independent of velocity.

The papers concerning the statistical dependence of meteoroid mass and velocity offer a clearer choice between "Model-A," with mass m_A in sub-sample "A" correlated only 0.020 with velocity V_∞, and "Model-B," with mass m_B in sub-sample "B" correlated 0.191 with V_∞. Some of these papers, mentioned below, give a basis for a choice between "A_r" with a low velocity distribution averaging 16.17 ± 0.17 km/sec, and "B_r" with a higher distribution averaging 18.83 ± 0.32 km/sec.

In 1955 Whipple and Hughes [123] noted that the average velocity of photographic meteors must be higher than the value 16.5 km/sec which they adopted for the air-entry velocity of meteorites. This condition is satisfied by "B_r" with average velocity 18.83 km/sec, but not by "A" with average velocity 16.17 km/sec.

In two papers presented in 1957, Whipple [124, 125] noted that "...a velocity of 28 km/sec is average for photographic meteors. Undoubtedly the velocity falls off for smaller meteoroids as we deal more and more with particles whose orbital eccentricities and dimensions have been reduced by physical effects... A mean value of 15 km/sec has been arbitrarily chosen for the smallest meteoroids and an arbitrary gradation of velocity with magnitude adopted." The value 28 km/sec is near the geometric mean velocity for a random sample of photographic meteors, whereas the mean values 16.17 and 18.83 km/sec for "A" and "B_r," respectively, are for random samples of meteoroids in the terrestrial influx. Those results favor "B" over "A" both in the higher mean value (18.83 for "B" versus 16.17 km/sec for "A") and in the higher correlation (0.191 for "B" versus 0.020 for "A") necessary to account for the change in mean velocity from 28 to 15 km/sec as mass decreases.

In 1964 Hawkins, Lindblad, and Southworth [126] described a controlled experiment in which the velocity distribution of radio meteors was measured at several different limiting magnitudes, with minimization of various selection effects. Mean air-entry velocity of all meteors brighter than visual magnitude +9 was found to be only 87 percent of that for all meteors brighter than visual magnitude +6; i.e., 33.3 versus 38.3 km/sec. The velocity measurements were considered preliminary. They are subject to the continuing disparity between photographic and radio assessments of the statistical distribution of meteor velocity. Baker [127] had considered the average velocity decrement in that experiment to be only 3.9 instead of 5.0 km/sec, but concluded that the data still indicate a decrease in average meteor velocity with fainter meteors. The effect was attributed to the difference in orbits within the various meteor populations, in agreement with results attributed by McKinley [5] to Öpik. Also Hawkins [128] suggested that Eshleman and Gallagher [129], who found in 1962 that the average velocity of sporadic meteors decreased by 2 km/sec between magnitudes +7 and +12, would probably have noted a larger decrement in mean velocity if they could have included values below 35 km/sec. Although the disparity in the velocity distribution of radio versus photographic meteors makes one apprehensive about the integrity of these results to the extent that they might be overlooked except that they do agree with other results, they support choosing "B" for its significant correlation 0.191 between mass m_B and velocity V_∞.

In 1964 Öpik [97] noted that the average geocentric velocity $\overline{V}_G$ for dustballs and zodiacal light particles can be assumed equal to 18 and 6 km/sec. From Figures 15 and 16 with lunar weighting, the values for the mean velocity and correlation between mass and velocity in the lunar influx are 13.66 km/sec and 0.024, respectively, for "A" and 18.04 km/sec and 0.188, respectively, for "B." Öpik's [97] values give a clear support for choosing the "B" results.

In summary of his extensive literature survey and study of meteors in 1966, Vedder [8] noted that "... the fainter meteors seem to have lower velocities, possibly a results of the Poynting-Robertson effect..." and that the calculation of the masses and flux is complicated by the effects of fragmentation and radiative cooling. This supports choosing "B" for its significant correlation between mass m_B and velocity V_∞.

In 1967 Lebedinets and Kashcheev [130] reported statistical results for radar measurements of velocities and radiants and corresponding orbit computations for 12 500 meteors brighter than magnitude +7. The results, which they said were corrected for physical selectivity with respect to velocity and radiant position, were reported in comparison with corresponding results by McCrosky and Posen [18] for Super-Schmidt photographic meteors brighter than magnitude +3. They (Lebedinets and Kashcheev [130]) found that the radio meteor sample, with a threshold four magnitudes fainter (or about 1/60 lower mass threshold) than the photographic meteor sample, gave substantially different distributions of orbital elements. It was found that by considering meteoroids of smaller and smaller mass there is a systematic decrease in the mean dimensions of the orbits. The mean perihelion distance q for the radio meteor particles was found to be approximately half as great as for the photographic meteors. No comment was offered that these results imply a lower mean air-entry velocity V_∞ for the smaller particles. Velocity V_∞ (e.g., as is shown by Öpik [70]) depends also on eccentricity e and the inclination i of the orbit to the ecliptic, and the authors showed that the distribution of i, too, changes with particle mass. But the results lead one to suspect that the smaller particles may have a lower mean air-entry velocity V_∞. This interpretation is substantiated by Kresak's [20] carefully weighted analysis also of the data of McCrosky and Posen [18]. By these results, by Lebedinets and Kascheev [130] and Kresak [20], one expects some positive correlation between mass and velocity, as in "B," rather than "A." Further basis for that expectation is given by Ceplecha's [45] 1968 analysis of McCrosky and Posen's [18] photographic meteor sample. He found that the proportions of meteors in four distinct groups vary with brightness and velocity, and that the characteristics of the orbits vary from group to group. McCrosky and Posen [18] noted also that the orbital characteristics of photographic meteor particles vary considerably with meteoroid size.

A number of published works treating the distribution of meteor particle velocity and its dependence on mass have been mentioned. Their interest with respect to a choice between "Model-A" with sub-sample "A" and "Model-B" with "B" is quite indirect and not fully satisfying. Beginning in 1956 with Levin's [3] comprehensive treatise, a number of works have appeared which offer studied opinion, creative insight, unusual perspective, or accidental involvement in the ambit of meteor luminous efficiency. Some of these works will be mentioned further. The "Model-A" tends to be regarded as a truism after three decades from its first use by Whipple [25] in the determinations of the density of the upper atmosphere with an accuracy which has been supported subsequently fairly well from the behavior of orbiting satellites and re-entry bodies. But, as Levin [3] noted specifically and as Lovell [84], Babadzhanov [131], and Katasev [132] formulated also in mathematical detail, the calculated atmospheric density ρ_a is inversely proportional to the (1/3)-power of the meteor luminous efficiency β (and a function of other parameters). Therefore, the low accuracy of β is only slightly reflected in ρ_a; but the meteoroid mass $m \sim \rho_a^3$ has no gain in accuracy. Both Delcourt [119] in 1963 and especially Kovshun [133] in 1966 considered "Model-A" to be only an approximation and expedient to the detailed and thorough theory of meteor luminosity which in the present analysis is approximated by "Model-B." Kovshun [133] noted that for direct determination of β in each specific case the formulation approximated by "Model-B" "... is extremely inconvenient ... For this reason, meteor mass is computed to this day from the simplified theory of meteor luminosity [i.e., "Model-A"] which does not allow for the dependence of β on the mass, structure, and composition of meteoroids."

In 1967 Jacchia, Verniani, and Briggs [56] reported a statistical analysis of the in-atmosphere characteristics of 413 precisely reduced photographic meteors. They compared theoretical and empirical relations presupposing the "Model-A" luminous efficiency $\beta_A = \tau_0 V_\infty$ and corresponding mass value m_A. It is of interest to note how some of the empirical results would seem to be brought into

closer agreement with the theory if the "Model-B" luminous efficiency β_B and corresponding mass m_B were replacing β_A and m_A, respectively. Theoretically the meteor beginning height for meteoroids of a given mass should depend on the constant value of $\beta \rho V_\infty^5$, but the empirical criterion is $\rho V_\infty^{3.5}$, where ρ is the atmospheric density. The velocity exponent is unduly reduced by using β_A instead of β_B for β. The maximum photographic luminous intensity I_{pm} was found to be $\sim V_\infty^{3.5}$ (i.e., 8.75/2.5) instead of the theoretical value $\sim \beta V_\infty^3$. Thus, the velocity dependence of β would be more nearly $\sim V^{0.5}$ than in "Model-A" with $\sim V_\infty$. On the average this result would agree somewhat more closely with "Model-B." The empirical beginning height criterion $\rho V_\infty^{3.5}$ found by Jacchia, Verniani, and Briggs [56] agrees quite closely with Levin's [134] velocity dependence of the ratio of apparent radiant density of visual meteors and true radiant density, $\sim V_\infty^{3.6}$.

In one of the Smithsonian contributions to astrophysics in 1965, Verniani [26] equated the dynamic and photometric mass values in the data subsequently reported as "An Analysis of the Atmospheric Trajectories of 413 Precisely Reduced Photographic Meteors," by Jacchia, Verniani, and Briggs [79]. In his analysis presupposing an exponential velocity dependence of luminous efficiency β, Verniani [26] concluded that he had demonstrated the verity of $\beta \sim V_\infty$ per se in "Model-A," independently of its original basis and limitations (bright meteors only) in accordance with the model adapted by Whipple [25] in 1938 from Öpik's [19] 1933 "Atomic Collisions and Radiation of Meteors." Verniani [26] implies that Jacchia's [90] finding (confirmed by Jacchia, Verniani, and Briggs [56]), that meteor color index at constant magnitude is independent of velocity, should support the assumption that luminous efficiency is proportional to an exponential function of velocity. He showed that the independence of velocity and color index, which is proportional to the logarithm of the ratio of the photographic and visual luminous efficiencies, establishes that the photographic and visual luminous efficiencies can differ only in their coefficients (the luminous efficiency factors) and not in their velocity exponents. Actually Jacchia's [90] discovery has a broader implication, i.e., that the photographic and visual luminous efficiencies (for meteors of nearly the same magnitude) are proportional to the same function of velocity, whether exponential or not. It does not appear that Verniani's [26] discussion on this point has any bearing on the question of whether or not luminous efficiency might be adequately approximated as an exponential function of velocity. By equating the dynamic and photometric mass formulations, Verniani [26] got an explicit expression for β/ρ_m^2, the ratio of the luminous efficiency and the square of the meteoroid material density. He attributed all of the variation in β/ρ_m^2 to the variation of β with velocity V_∞ and discarded the 10 percent of the sample with the largest deviations of β/ρ_m^2 from its mean. In 1967 Verniani [135] repeated his analysis of β/ρ_m^2 with the same sample he had used in 1965 [26]; but this time he discarded 22 percent of the 247 sporadic meteors which he had not already discarded before (leaving only 189 for his new analysis). This was done by presupposing $\beta \sim V_\infty$ and discarding the meteors with β/ρ_m^2 differing most from its consequent mean. Thus, the result which Verniani got, $\beta \sim V_\infty^{1.0 \pm 0.15}$ in 1965 [26] and $\beta \sim V_\infty^{1.0 \pm 0.1}$ in 1967 [135], is probably mostly a reflection of his two presuppositions that $\beta \sim V_\infty^n$ and that n is unity.

Verniani's works [26, 135] have been widely referenced as evidence of the essential verity of "Model-A" with respect to the velocity variation of meteor luminous efficiency $\beta = \tau_0 V_\infty$ and as an authoritative refinement of the value of the constant luminous efficiency factor τ_0; i.e., $10^{-0.09}$ or 81 percent of the value of τ_0 in "Model-A." For example, Verniani [26] stated that in 1963 Whipple [136] used Verniani's value -18.91 for log τ_{0_p} (subtract 0.72 to convert to visual units, add 9.72 to convert from Jacchia's magnitude units to CGS units, and add 5.00 to convert from cm/sec to km/sec velocity units) in the construction of the mass-cumulative influx model for meteors, based on Hawkins and Upton's [81] magnitude cumulative influx model. The value -18.91 was based on an interpretation of the Trailblazer I artificial meteor rocket experiment by McCrosky and Soberman [137]. Verniani [26] stated that the reliability of that value based on Trailblazer I has to be considered higher

than that obtained with three "asteroidal" meteors by Cook, Jacchia, and McCrosky [138] in 1963. The value from Trailblazer I was $10^{-0.42}$, or 38 percent of the geometric mean of those by the three natural meteors studied by Cook, Jacchia and McCrosky [138]. Whipple adopted the geometric mean of those two separately reported sets of values, getting a visual luminous efficiency factor 31 percent of the value in "Model-A." The value advocated by Verniani [135] in 1967 for τ_0 is 81 percent of that in "Model-A." But in three recent papers Ceplecha [44, 43, 45] has spoken out increasingly more critically of Verniani's [26, 135] presupposition that a formula for β/ρ_m^2 could be derived by equating the expressions for dynamic and photometric mass values. In 1956 Levin [3] had criticized Whipple's earlier practice of equating the dynamic and photometric mass values to get inordinately low values for the meteoroid material density ρ_m. Levin [3] offered the explanation that "... the minuteness of the dynamic masses of meteoroids is a result of their partial fragmentation, not of the minuteness of their densities. In the case of fragmentation, the mass determined by deceleration is the mean mass of the individual fragments, while the photometric data give their total mass."

In 1967 Allen and Baldwin [46] reported observations, in ground laboratory facilities, showing that rock will froth during ablation, and that the froth may be sloughed as a result of aerodynamic pressure forces. Their results offer an alternative to the very low material densities usually reported for meteors; but, of more pertinent relation to the present analysis, their experiments also checked the velocity dependence of luminous efficiency. They found, when luminous efficiency β is considered to be the product of a luminous efficiency factor τ_0 and velocity V_∞, that their experimental results showed that τ_0 must decrease with increasing V_∞. This result is contrary to "Model-A," which has τ_0 constant, but the variation of τ_0 with V_∞ is in the sense that would tend toward agreement with "Model-B," which on the average has a weaker velocity dependence than "Model-A," i.e., the results by Allen and Baldwin [46] indicate that the velocity dependence of luminous efficiency is not as strong as in "Model-A." A later study by Baldwin and Allen [139] confirmed that photographic meteor data are consistent with their compact stone particle hypothesis, and that luminous efficiency β depends less strongly on velocity V_∞ than that indicated for "Model-A." Two other NASA-sponsored laboratory measurements of the luminous efficiency of hypervelocity particles are pertinent to a choice between "Model-A" and "Model-B." In 1965 the Utah Research and Development Company [140] reported on their contracted research with sub-micron hypervelocity spray particles generated by the hypervelocity impact of aluminum and steel balls into similar targets. With successful measurements under controlled conditions, the spray particles with radii between 0.005 and 0.1 micron and speeds between 3 and 18.4 km/sec, but with most of the data between 6 and 16 km/sec, the luminous efficiency proved to be independent of speed. This result is contrary to "Model-A" but would agree considerably better with "Model-B" on the average. In 1968 Friichtenicht, Slattery, and Tagliaferri [141] reported luminous efficiency measurements in the spectral band 3400 to 6300 Å for sub-micron diameter iron particles injected from an electrostatic particle accelerator into air targets. The luminous efficiency β was reported to be nearly constant over the velocity interval from 20 to 40 km/sec. They stated further that "... within the limits of the experimental errors, β actually appears to decrease slightly with increasing velocity." The results of Friichtenich, Slattery, and Tagliaferri [141] also tend to be compatible with "Model-B," but not with "Model-A."

In 1962 Levin [142] noted that the presumption of meteor luminous efficiency β proportional to velocity V_∞ independently of meteoroid mass m would have special implications for fragmenting meteors. For a meteoroid with given mass and velocity, the integrated luminous intensity would be independent of the meteor path-length L. The increase of the mean light intensity would have to be directly proportional to the decrease of the path-length. Detailed implications of that result, in effecting the parameter s in the mass distribution function, equation (37), were given in 1965 by Kruchinenko [143]. But in the same issue of the journal with Kruchinenko's [143] paper, Kramer [144] gave data showing that the theoretical predictions presupposing meteor luminous efficiency independent of mass, as in "Model-A," do not conform to reality in that the integrated radiation from a fragmenting meteoroid is always less than that which would be inferred by Levin's [142] rule. The "Model-B" agrees with Kramer's [144] results better than "Model-A" in that luminous efficiency β_B is a monotonically increasing function of particle mass m_B over a wide range of values of m_B.

By the results of the present analysis, comparison of consequences, and sampling of seemingly relevant material coming to the author's attention, the undeniably oversimplified "Model-A" must be rejected in preference for "Model-B" on grounds of relative plausibility of consequent implications. The undobtedly extreme complexity of the meteor luminous efficiency is substantiated by recent papers on meteor spectra, e.g., by Hoffman and Longmire [145] and by Smirnov [146]. In context with such investigations, it becomes clear that one must not interpret the present analysis as any proof of the validity of Öpik's [2] physical theory of meteors (approximated in the present analysis by "Model-B"), but only recognize that the inherent consequences led to no discernible contradiction or disagreement with other established fact so far as the analysis was pursued. On the other hand, the author feels that the case against any formulation of luminous efficiency proportional to velocity independently of mass, such as "Model-A," has been presented so sufficiently that it could be mollified only by legerdemain.

Now that "Model-A" has been eliminated in favor of "Model-B," it is of interest to return to equations (36) and (37) and reconsider the role of the parameter k_2 with the value -2.25 which Jacchia, Verniani, and Briggs [56] found by least-squares statistical analysis of photographic meteor data. In equation (36) the values for mass m used by Jacchia, Verniani, and Briggs [56] were the "Model-A" values m_A for photometric mass. Therefore, the same value -2.25 for the coefficient k_2 would have been found if mass m_A in equation (36) had been replaced by $\beta_B m_B$, the model-invariant product of luminous efficiency and photometric mass. This follows because $\beta_B m_B$ is the same product as $\beta_A m_A$, and β_A is independent of m_A. But β_B is not independent of m_B. The definition of magnitude M, as introduced in 1856 by Pogson (see Jones [147]) for stars, is sufficient for the proof[3] that mass m_B in the right side of equation (37) can be replaced by $\beta_B m_B$; i.e.,

$$N_{>m}(m) = N_{>m}(1)\ m^{(1+k_2')(\ k_2 \log \chi)} \quad , \qquad (53)$$

where k_2' is a constant in the exponential approximation of β_B as a function of m_B,

$$\beta_B \sim m_B^{k_2'} \quad . \qquad (54)$$

A check on the relation in equation (54) was made with a constant value for V_∞ of 19 km/sec, near the mean value 18.83 ± 0.32 km/sec for the terrestrial influx (Fig. 15). A plot of log $(\beta_B m_B)$ versus

---

3. $2.512^{-M} = \dfrac{I_M(M)}{I_M(O)}$ $\quad \therefore M = (-\log 2.512)^{-1}\ [\log I_M(M) - \log I_M(O)]$

$$= k_0 + k_1' \log V_\infty + k_2 \log (\beta m) + k_3 \log \cos Z_R$$

$$\therefore I_M(M) \sim (\beta m)_M(M)^{-k_2 \log 2.512} \text{ @ const. } V_\infty, \text{ etc.}$$

$$\therefore M_{\beta m}(\beta m) = k_2 \log \left[\frac{(\beta m)_M(M)}{(\beta m)_M(O)}\right], \quad F_M\left[M_{\beta m}(\beta m)\right] = F_M(O)\ \chi^{M_{\beta m}(\beta m)}$$

$$\int_m^\infty f_m(m)\ dm = \int_{\beta m}^\infty f_M\left[M(\beta m)\right]\ dM_{\beta m}(\beta m) \sim \left[(\beta m)_M(M)\right]^{k_2 \log \chi}$$

$$\sim m^{(1+k_2')(\ k_2 \log \chi)} \quad \text{where } \beta \sim m^{k_2'} \ .$$

log m_B over the interval 10^{-4} g $\leq$ m $\leq$ 10 g showed no graphically discernible deviation from linearity. The value of the exponent k_2' in equation (54) was found to be 0.069 when V_∞ is 19 km/sec. This means that the value of the mass exponent - (s - 1) deduced from Hawkins and Upton's [81] analysis of meteor data is changed from -1.21 to -1.29. This value -1.29 compares very favorably with the value -1.31 found directly from the cumulative distribution of mass values in Figure 40. Although the value of k_2' in equation (54) was evaluated only for 19 km/sec, it is probable that the resulting value 0.069 for k_2' is somewhat lower than the effective mean value averaged over the range of velocity V_∞. This is evident from Figure 4, which shows that the mass dependence of the luminous efficiency β_B is stronger for the higher values of velocity V_∞. It is not unreasonable to expect that the effective value of $\overline{k_2'}$ might be as high as 0.10. If so, then, by equation (53), the entire discrepancy between the theoretical value -5/2 for k_2 and the empirical value -2.25 found by Jacchia, Verniani, and Briggs [56] would be accounted for through the factor $(1 + \overline{k_2'})$ due to the dependence of meteor luminous efficiency β_B on meteoroid mass m_B from "Model-B." But the author's opinion is that the correlation 0.191 $\pm$ 0.037 between mass m_B and velocity V_∞ may play some part in the role of k_2. Therefore, the value -1.21 for the exponent - $(s_e - 1)$ in the energy-cumulative distribution of meteoroids in the terrestrial influx is retained as in equation (52) and Figure 44b.

CONCLUSIONS

The greater merit of Öpik's [2] 1958 physical theory of meteors, approximated in the present analysis by "Model-B" [equation (13) and Fig. 4], relative to Öpik's [19] 1933 provisional theory [approximated by "Model-A," equation (11)], or any theory for luminous efficiency β proportional to velocity V_∞ independently of photometric mass m, is demonstrated by the present analysis.

The meteoroid natural environment for the earth is, as expressed by $F_{>m_B}$, $F_{>m_B V_\infty}$, and $F_{>\frac{1}{2}m_B V_\infty^2}$, the mean cumulative influx per square meter per second with respect to mass, momentum, and kinetic energy, respectively,

$$\log F_{>m_B} = -1.31 \log m_B - 14.77 \quad \text{(Terrestrial)} \tag{50}$$

$$\log F_{>m_B V_\infty} = -1.28 \log m_B V_\infty - 13.07 \quad \text{(Terrestrial)} \tag{51}$$

$$\log F_{>\frac{1}{2}m_B V_\infty^2} = -1.21 \log \left(\tfrac{1}{2}m_B V_\infty^2\right) - 11.72 \quad \text{(Terrestrial)}, \tag{52}$$

where mass m_B is in grams and velocity V_∞ is in km/sec.

The corresponding meteoroid natural environment for the moon is:

$$\log F_{>m_B} = -1.21 \log m_B - 14.93 \quad \text{(Lunar)} \tag{50}$$

$$\log F_{>m_B V_G} = -1.28 \log m_B V_G - 13.38 \quad \text{(Lunar)} \tag{51}$$

$$\log F_{>\frac{1}{2}m_B V_G^2} = -1.21 \log \left(\tfrac{1}{2}m_B V_G^2\right) - 12.04 \quad \text{(Lunar)} \tag{52}$$

The meteoroid natural environment for an interplanetary vehicle at heliocentric distance r in AU differs from that for the moon only in that the particle mass-cumulative impact flux varies with $r^{-2.05}$, by equation (32), and the mean impact velocity varies with $r^{-0.50}$. The concentration of particles in space varies as $r^{-1.52}$, equation (33).

George C. Marshall Space Flight Center
National Aeronautics and Space Administration
Marshall Space Flight Center, Alabama 35812
September 3, 1969 124-091400

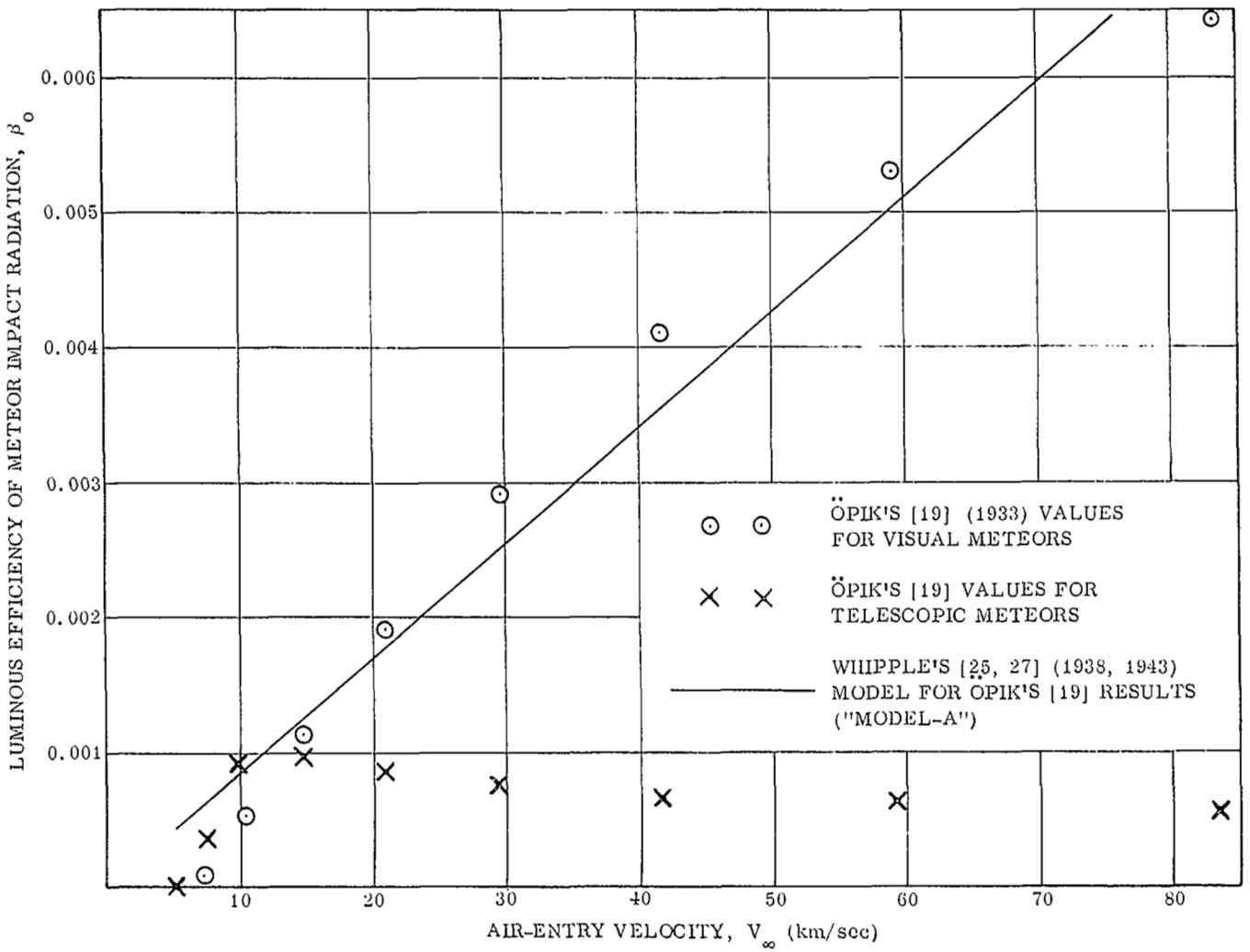

FIGURE 1. ORIGINAL BASIS FOR THE HARVARD LUMINOUS EFFICIENCY OF METEORS

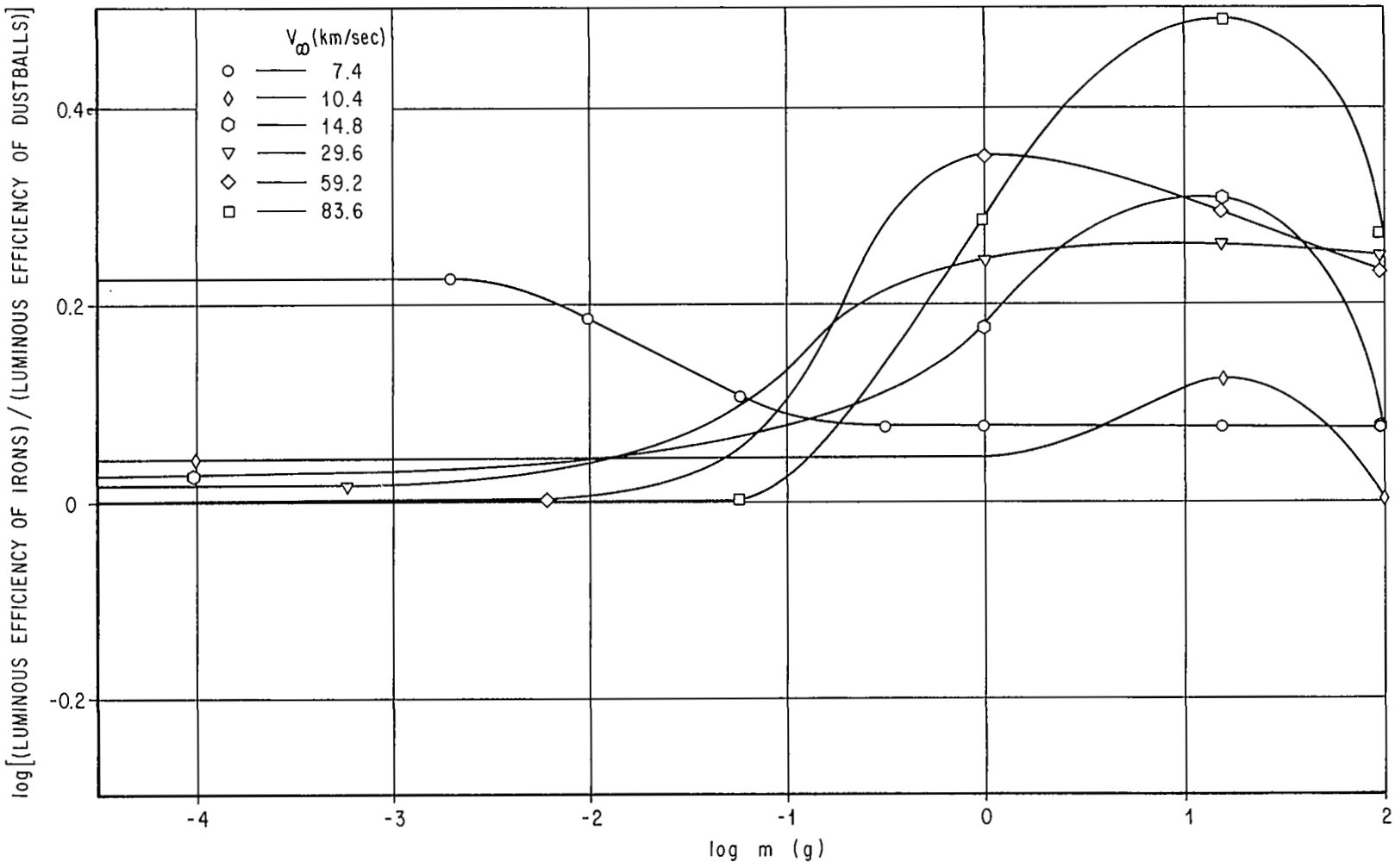

FIGURE 2. RELATION BETWEEN THE ÖPIK [2, 28] (1958, 1963) LUMINOUS EFFICIENCIES OF COMPACT IRON AND STONY DUSTBALL METEOROIDS

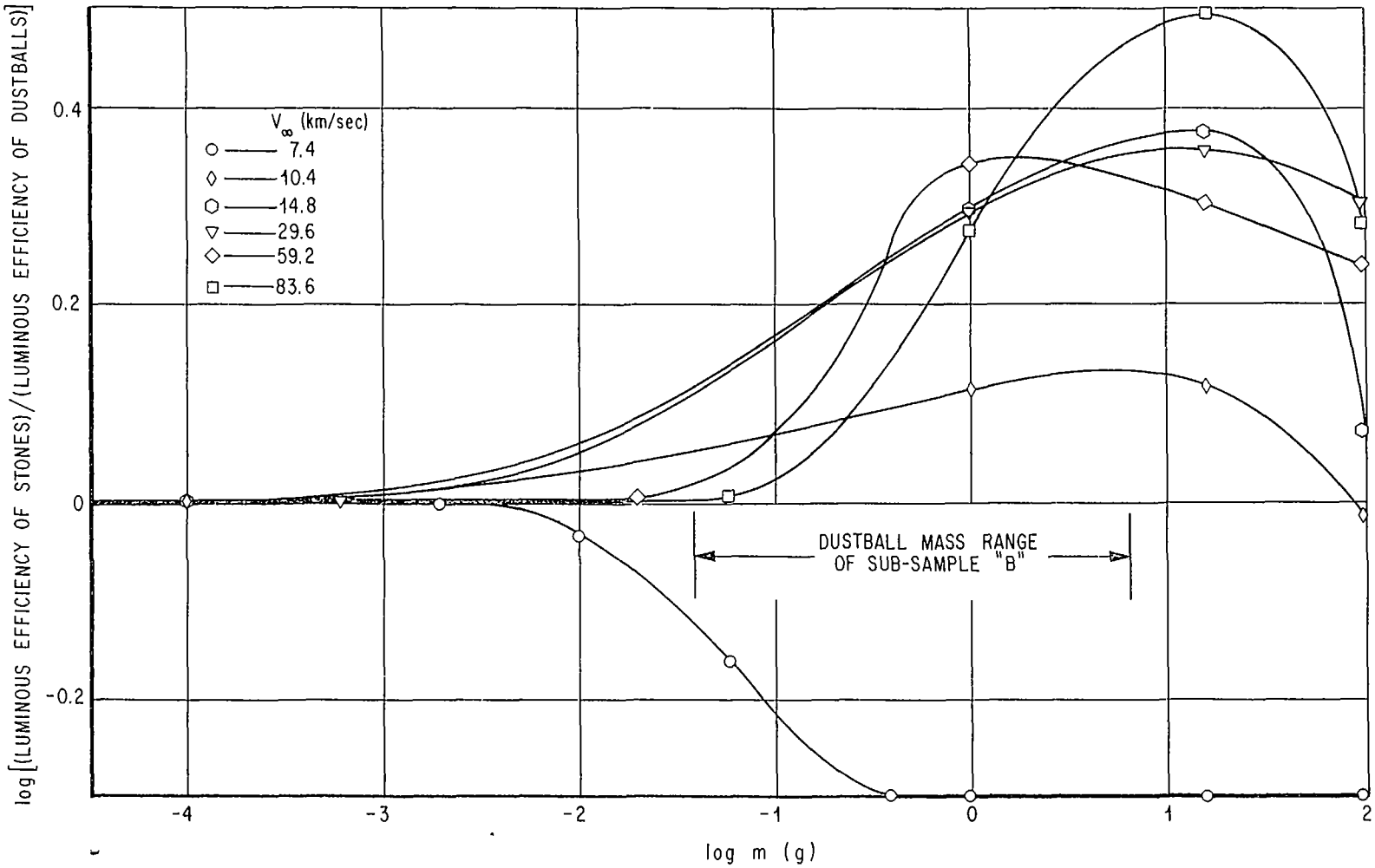

FIGURE 3. RELATION BETWEEN THE ÖPIK [2, 28] (1958, 1963) LUMINOUS EFFICIENCIES OF COMPACT STONY AND STONE DUSTBALL METEOROIDS

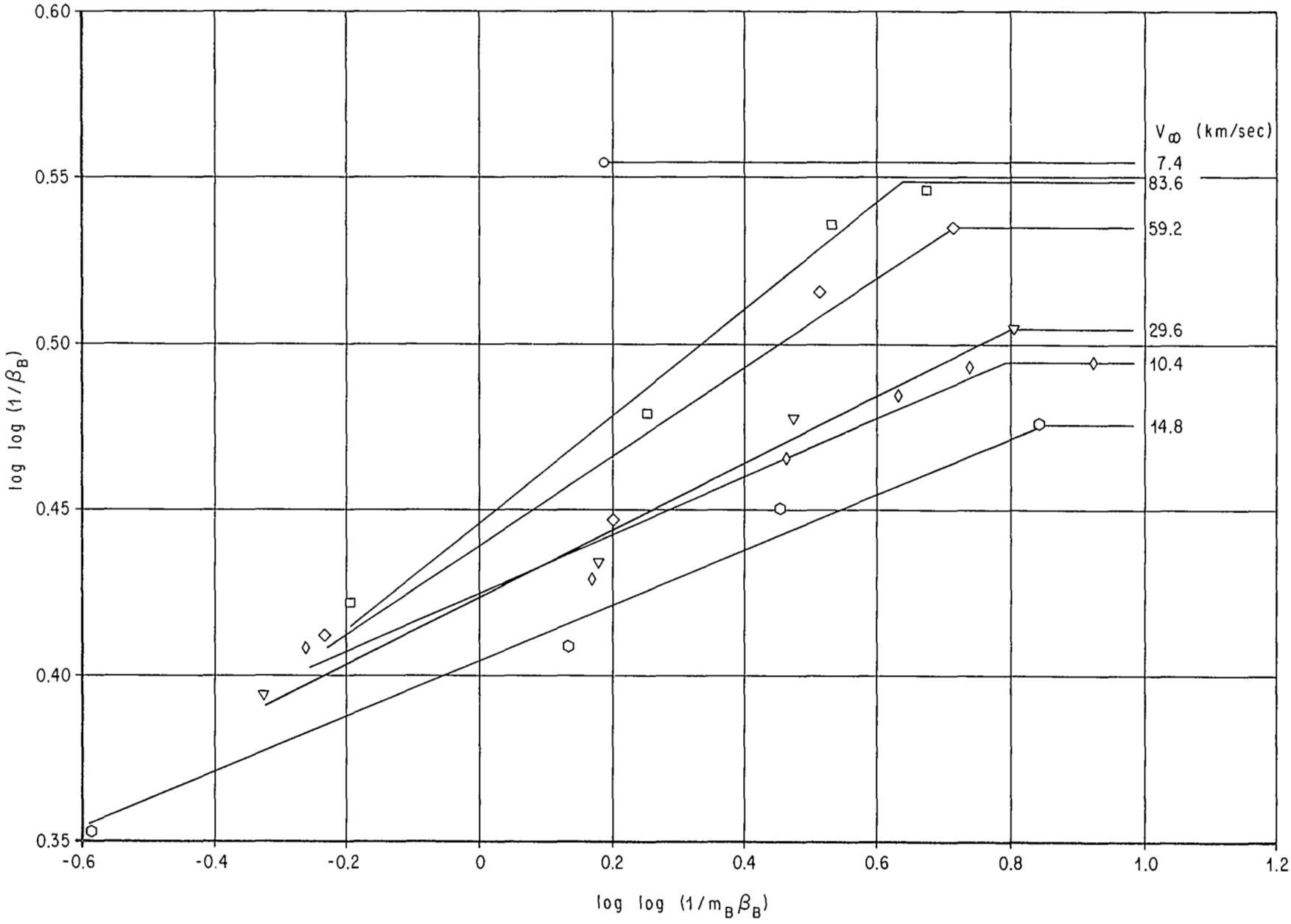

FIGURE 4. "MODEL-B" APPROXIMATING ÖPIK'S [2, 28] (1958, 1963) LUMINOUS EFFICIENCY β_B FOR DUSTBALL METEOROIDS $\leq 10^2$ g

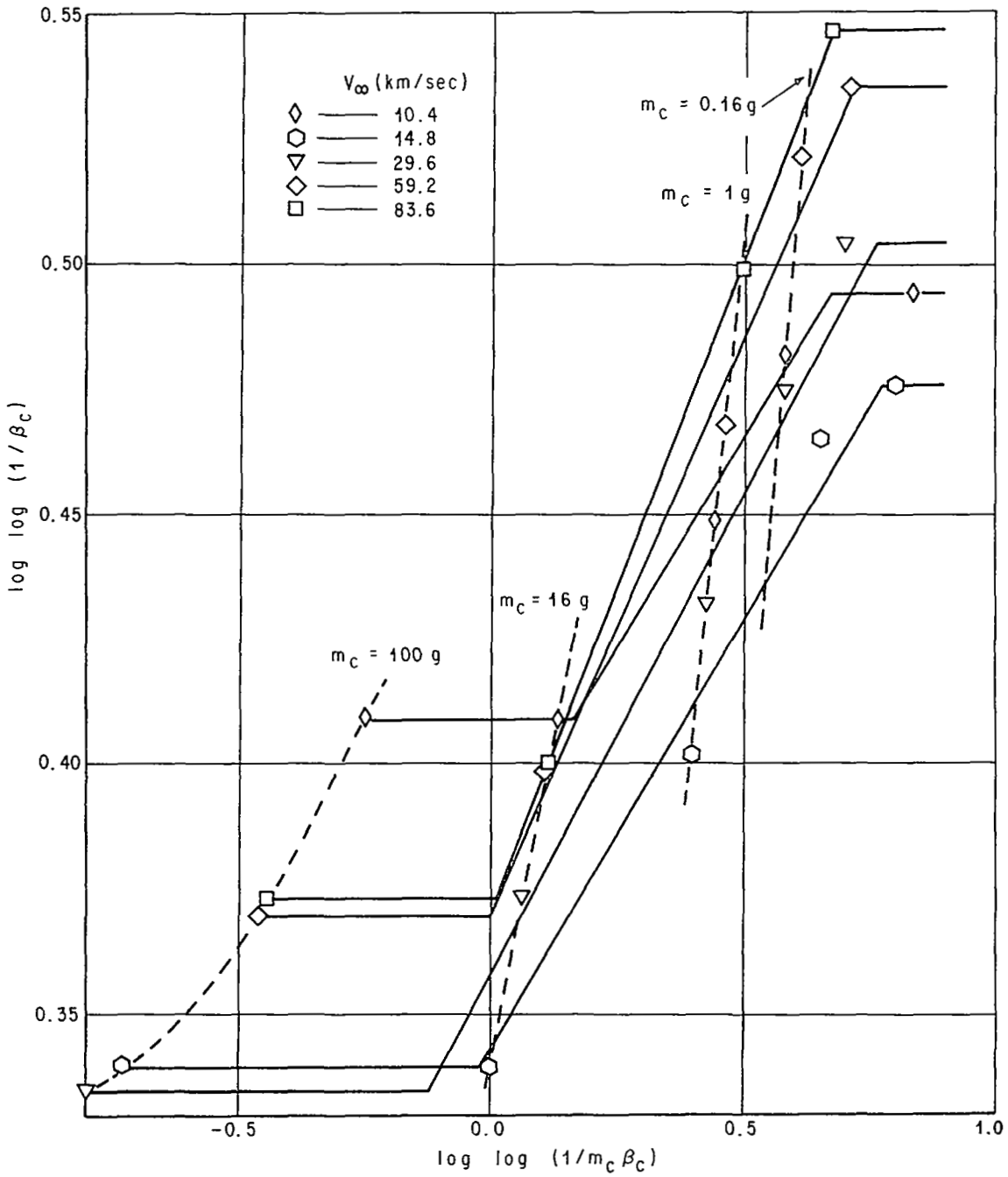

FIGURE 5. "MODEL-C" APPROXIMATING ÖPIK'S [2, 28] (1958, 1963) LUMINOUS EFFICIENCY β_C FOR COMPACT STONE METEOROIDS $\leq 10^2$ g

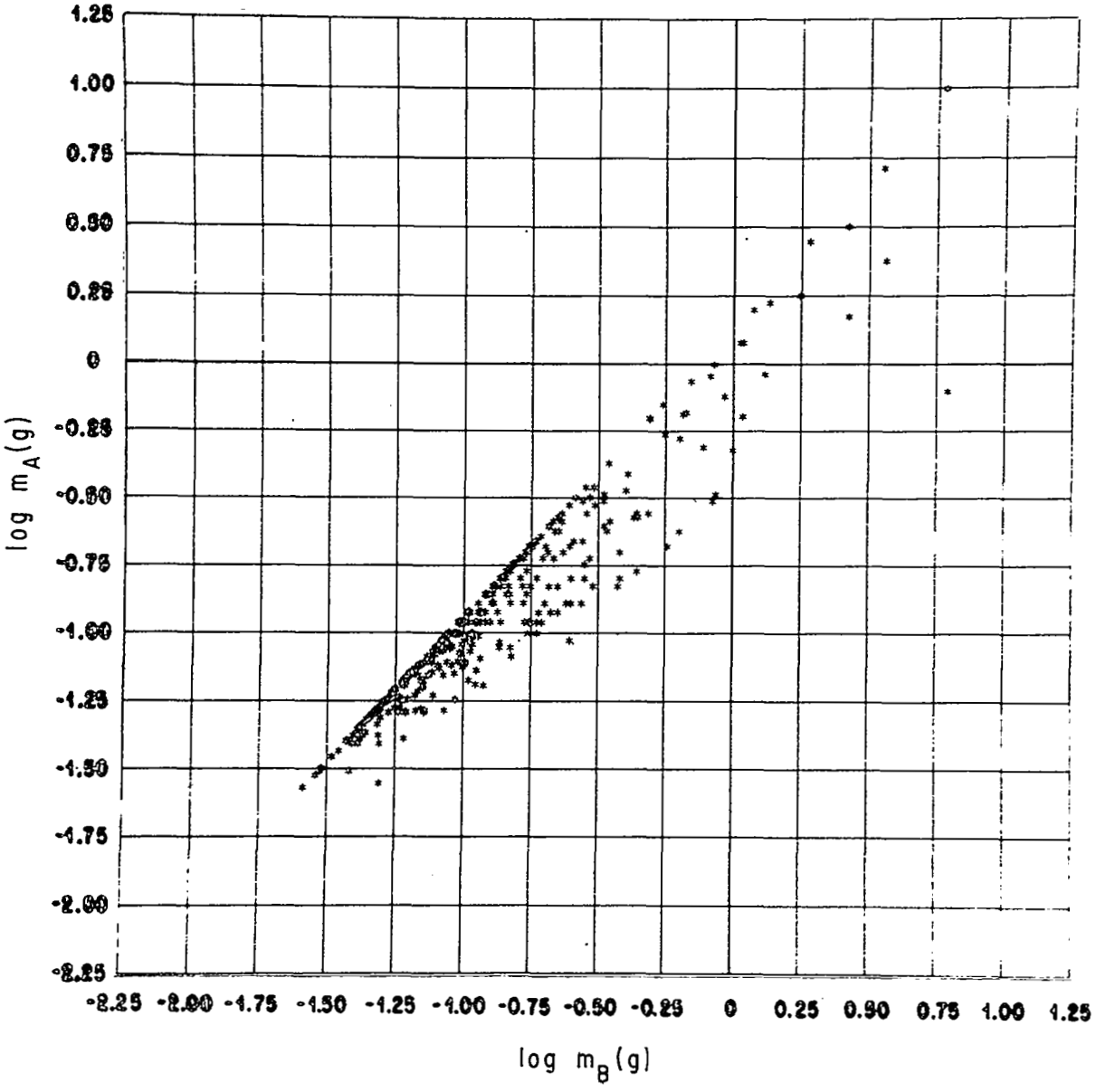

FIGURE 6a. MASS VALUES BY "MODEL-A" VERSUS "MODEL-B," SUB-SAMPLE "A"

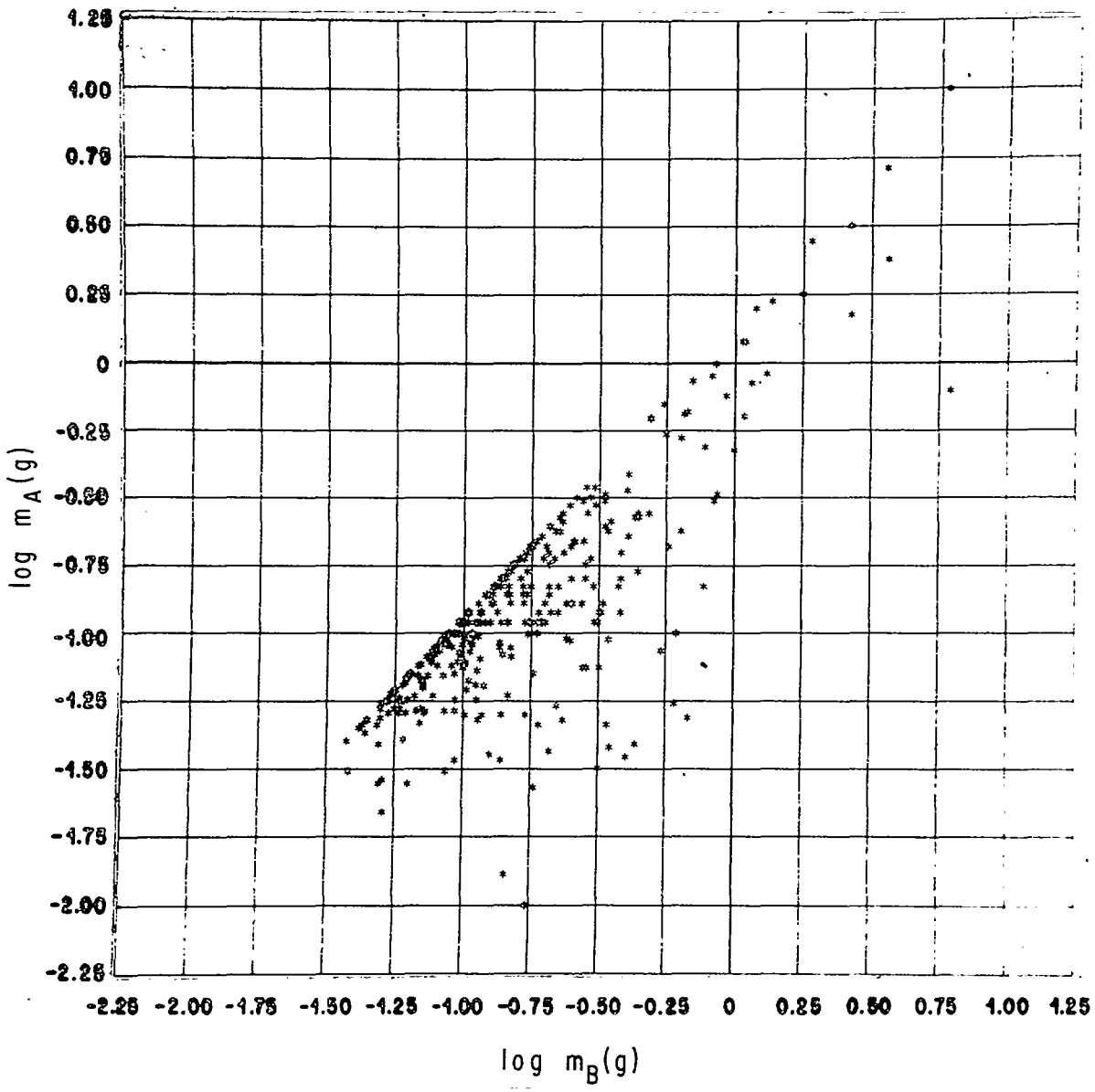

FIGURE 6b. MASS VALUES BY "MODEL-A" VERSUS "MODEL-B," SUB-SAMPLE "B"

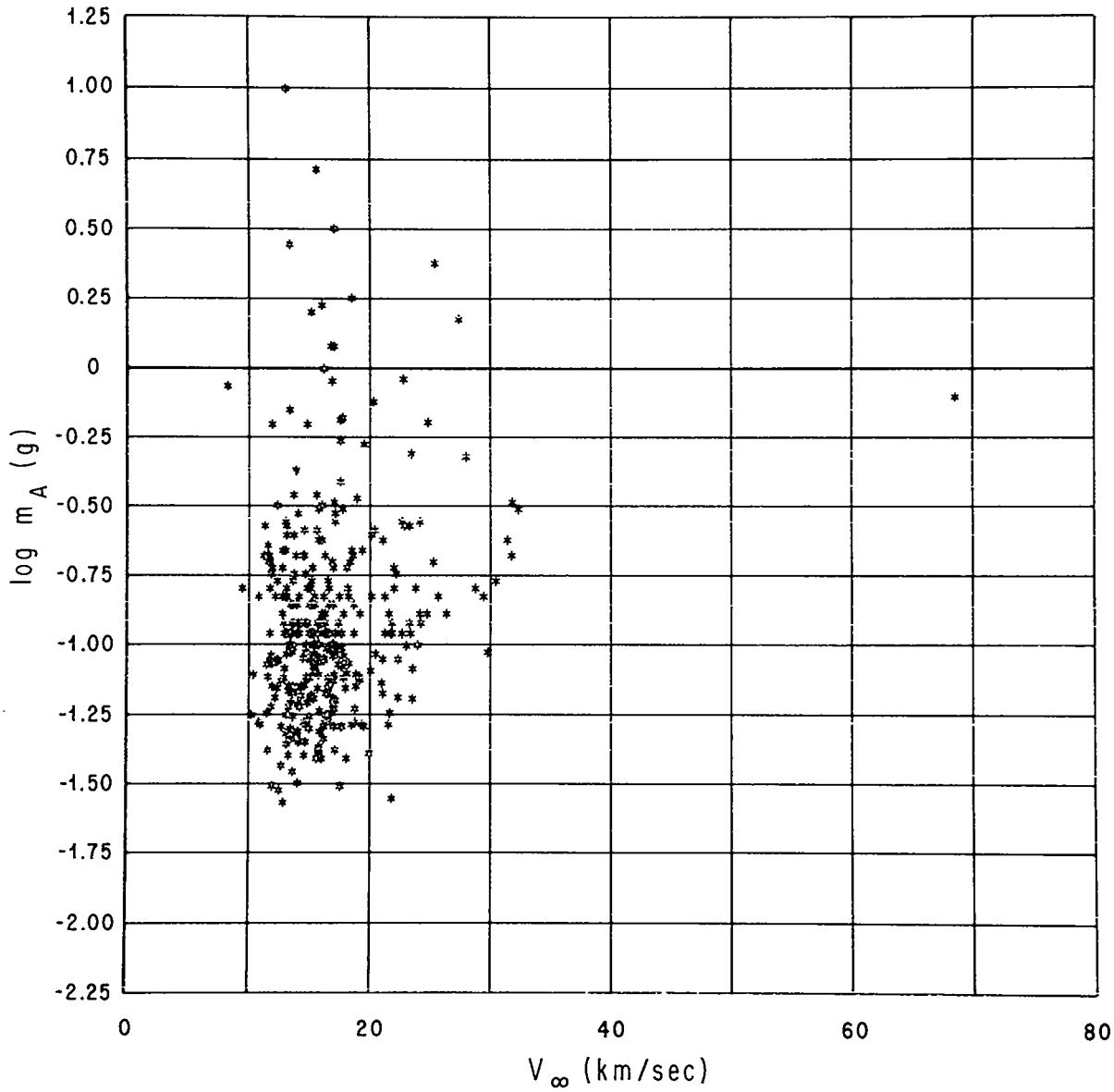

FIGURE 7a. MASS VALUES VERSUS AIR-ENTRY VELOCITY, SUB-SAMPLE "A"

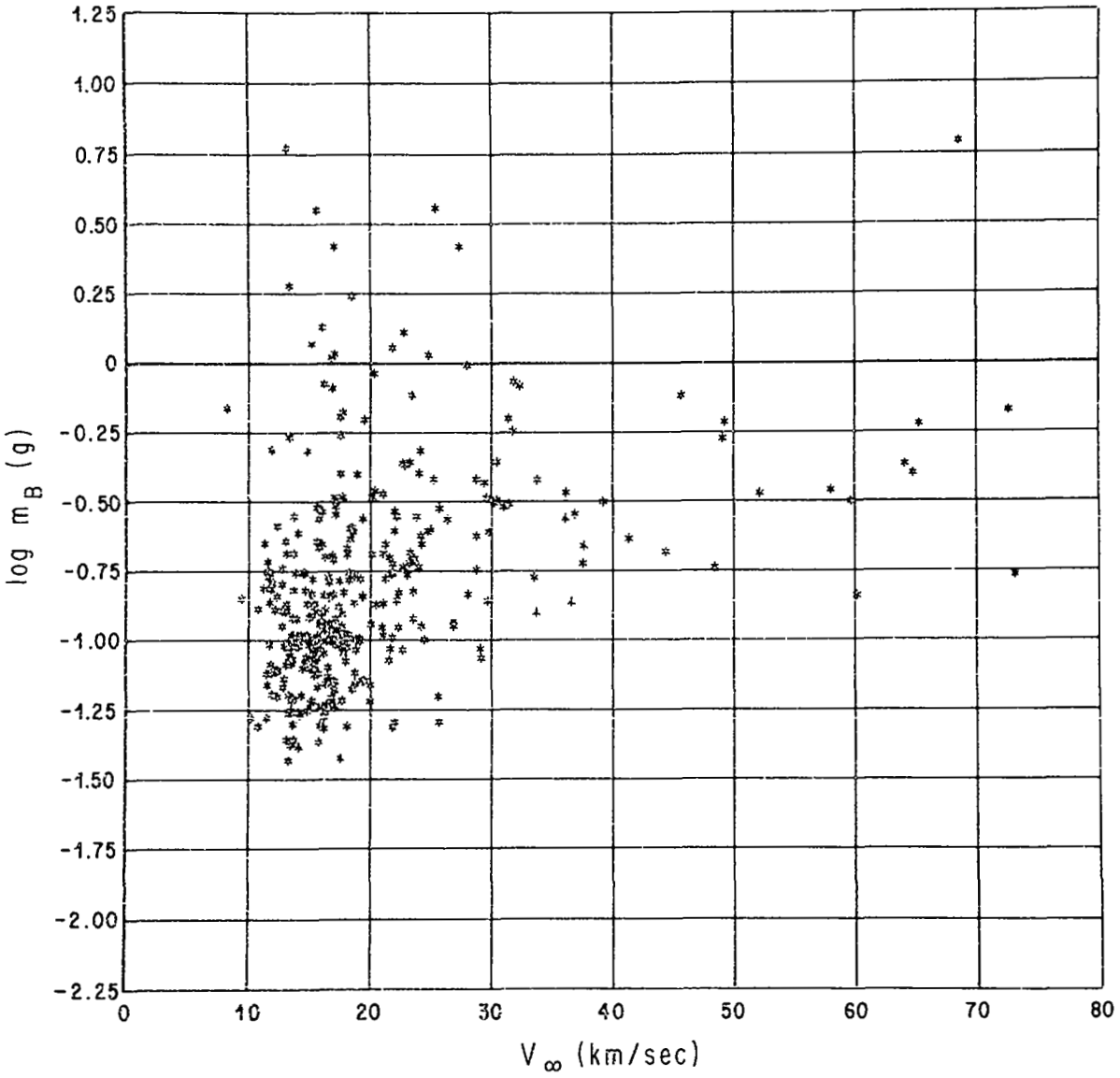

FIGURE 7b. MASS VALUES VERSUS AIR-ENTRY VELOCITY, SUB-SAMPLE "B"

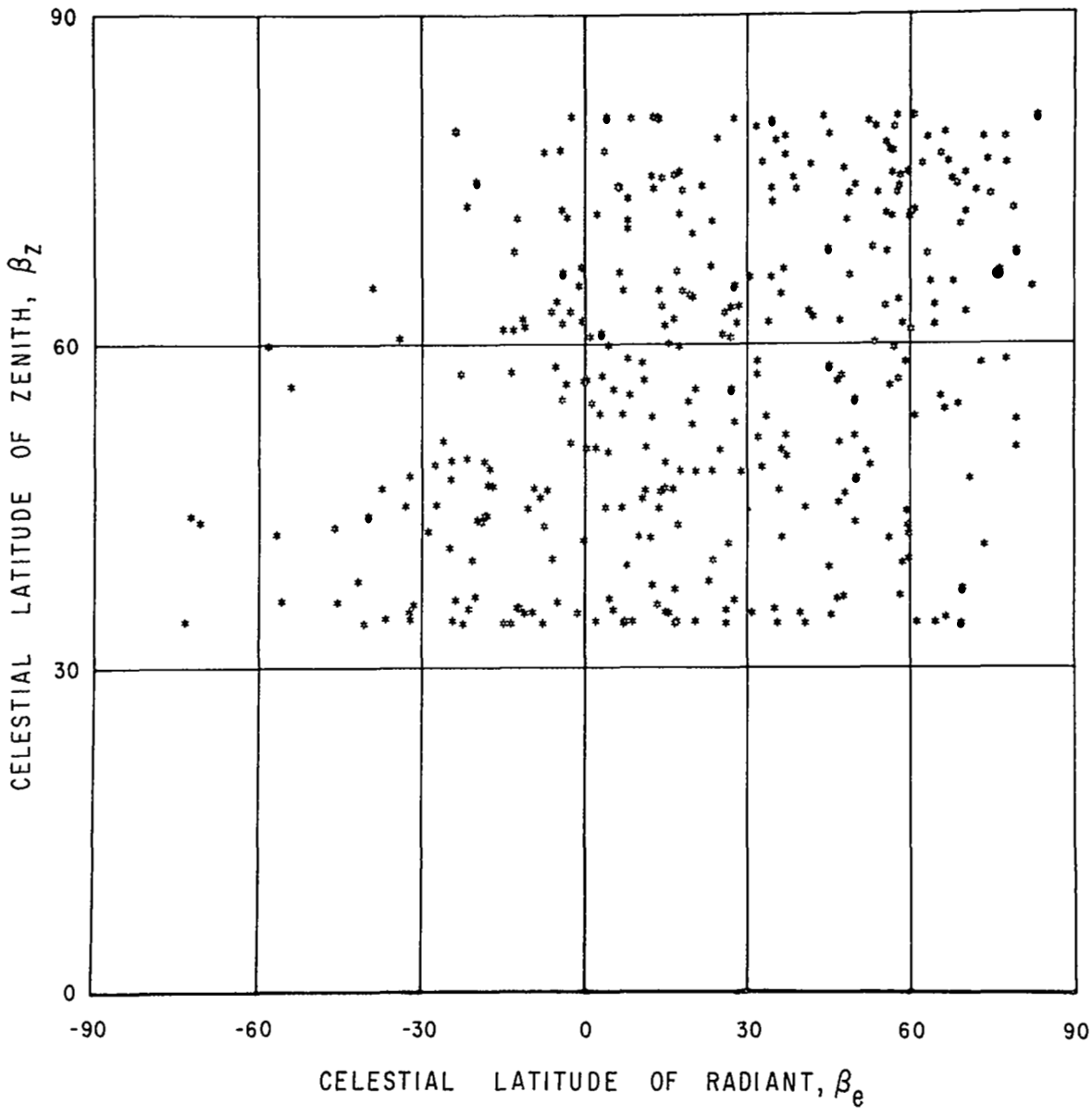

FIGURE 8a. ZENITH VERSUS RADIANT DEVIATIONS FROM THE ECLIPTIC, SUB-SAMPLE "A"

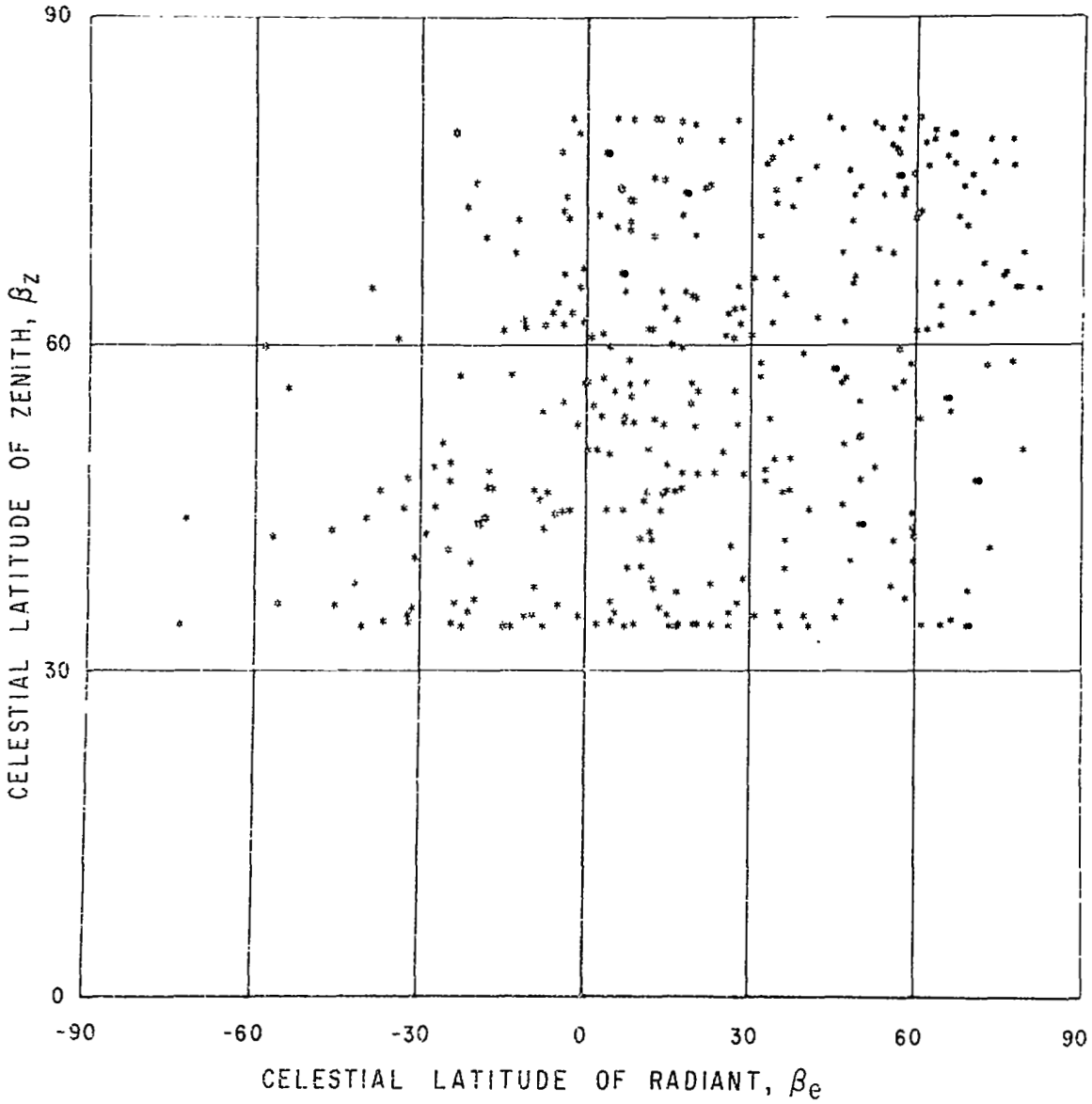

FIGURE 8b. ZENITH VERSUS RADIANT DEVIATIONS FROM THE ECLIPTIC, SUB-SAMPLE "B"

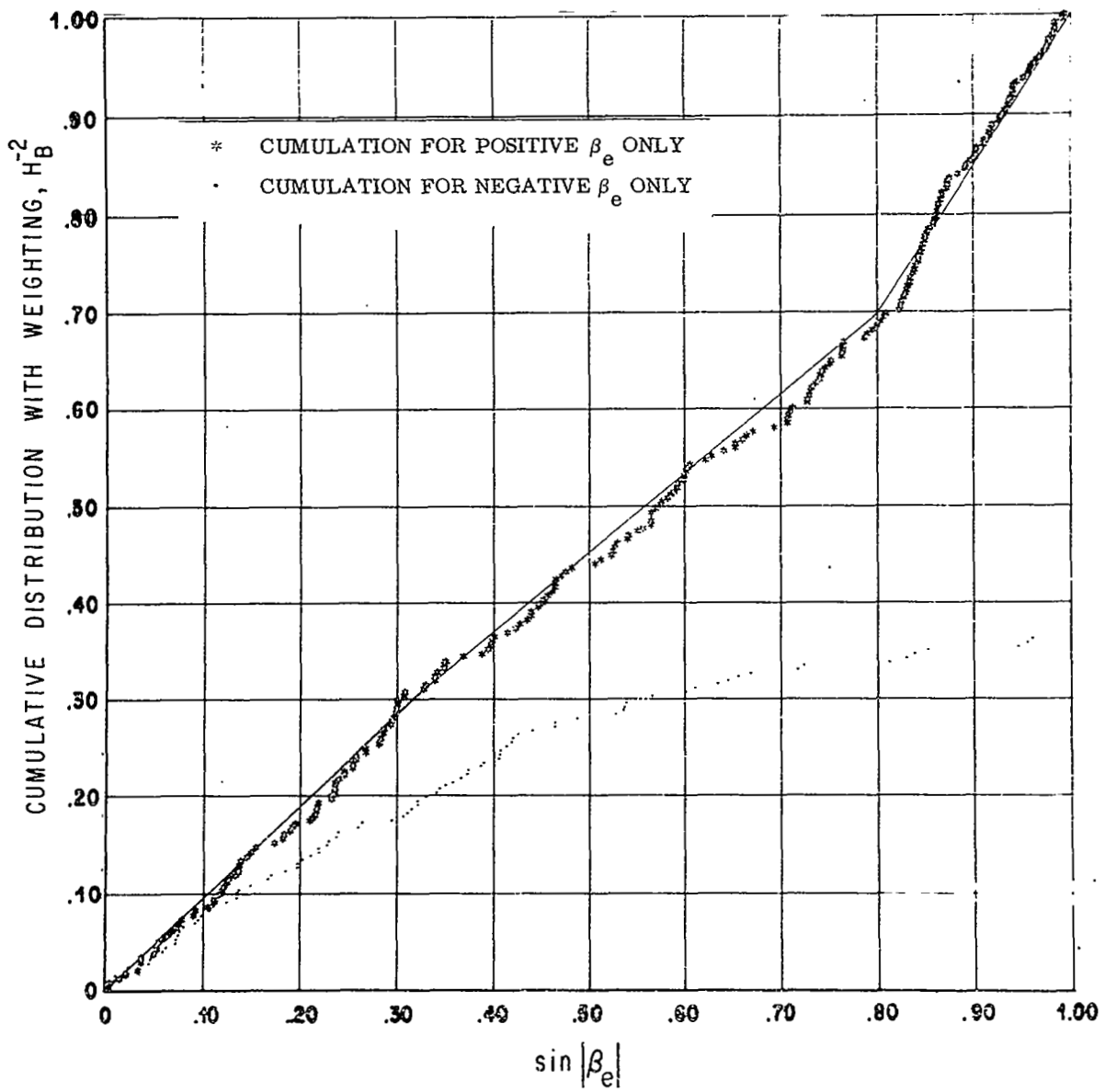

FIGURE 9a. DISTRIBUTIONS OF NEGATIVE VERSUS POSITIVE CELESTIAL LATITUDE WEIGHTED FOR SURVEILLANCE AREA, SUB-SAMPLE "A"

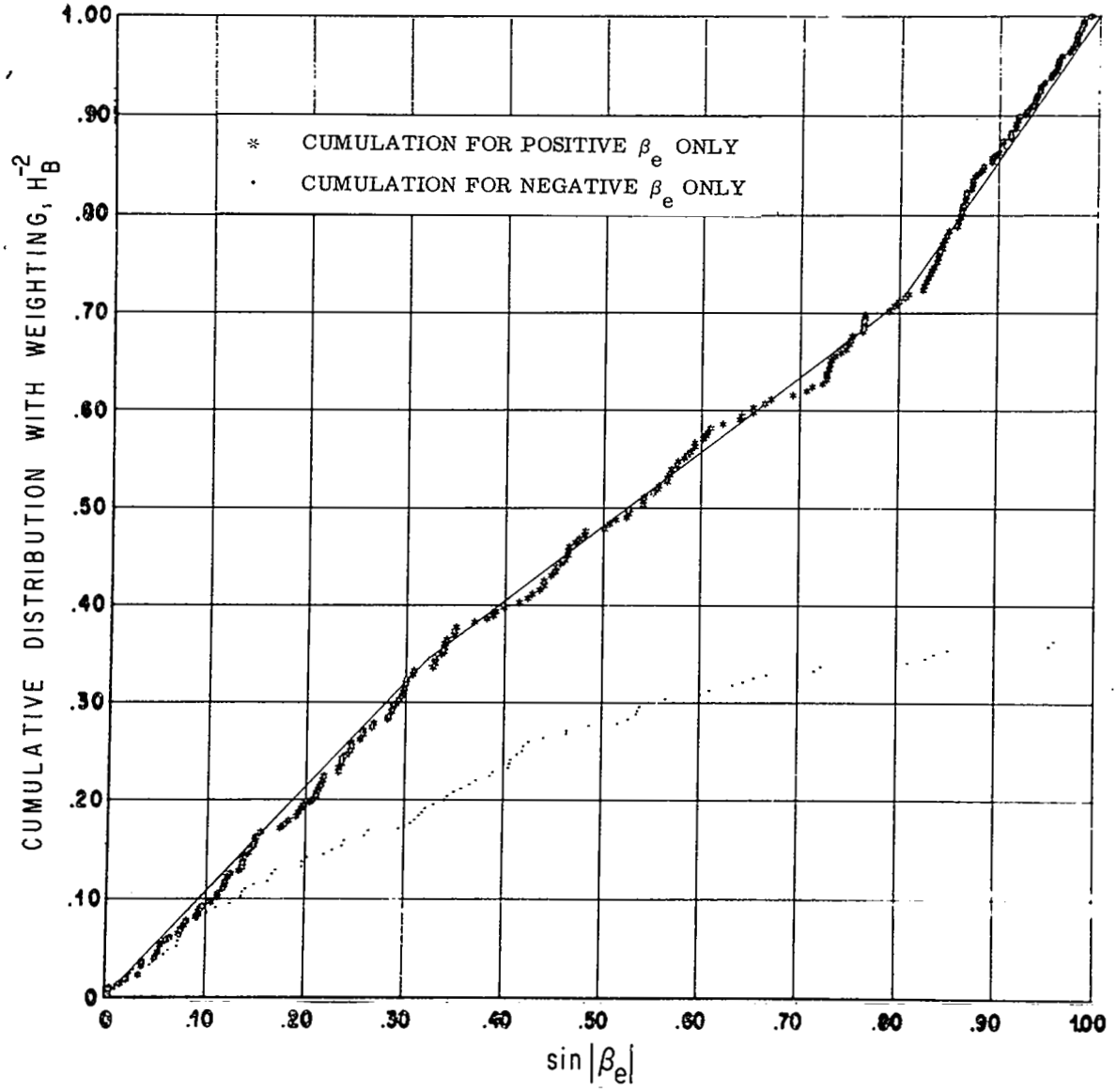

FIGURE 9b. DISTRIBUTIONS OF NEGATIVE VERSUS POSITIVE CELESTIAL LATITUDE WEIGHTED FOR SURVEILLANCE AREA, SUB-SAMPLE "B"

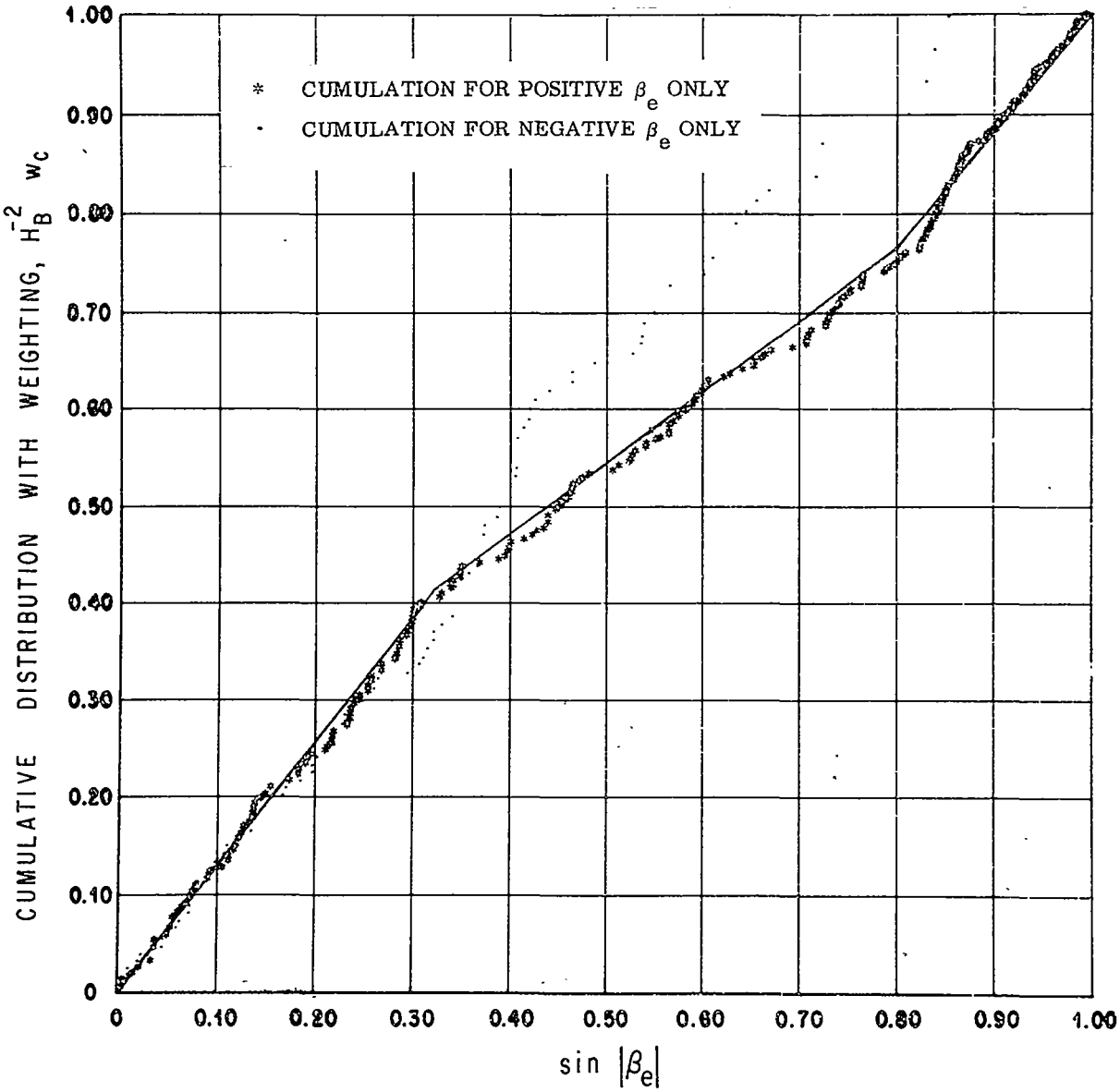

FIGURE 10a. DISTRIBUTION OF NEGATIVE VERSUS POSITIVE CELESTIAL LATITUDE WEIGHTED FOR SURVEILLANCE AREA AND APPARENT FRACTION OF CIRCLE OF CELESTIAL LATITUDE, SUB-SAMPLE "A"

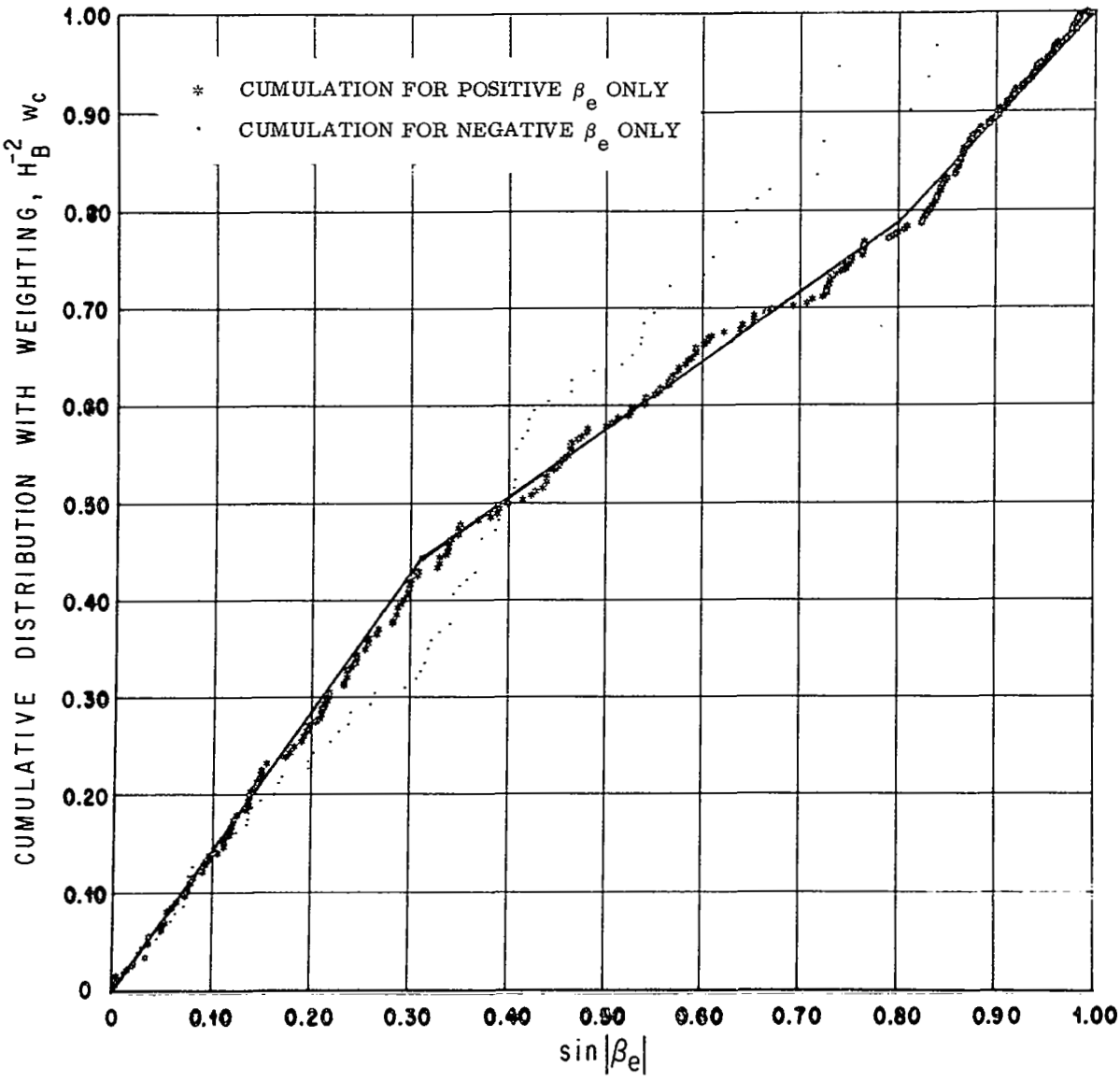

FIGURE 10b. DISTRIBUTION OF NEGATIVE VERSUS POSITIVE CELESTIAL LATITUDE WEIGHTED FOR SURVEILLANCE AREA AND APPARENT FRACTION OF CIRCLE OF CELESTIAL LATITUDE, SUB-SAMPLE "B"

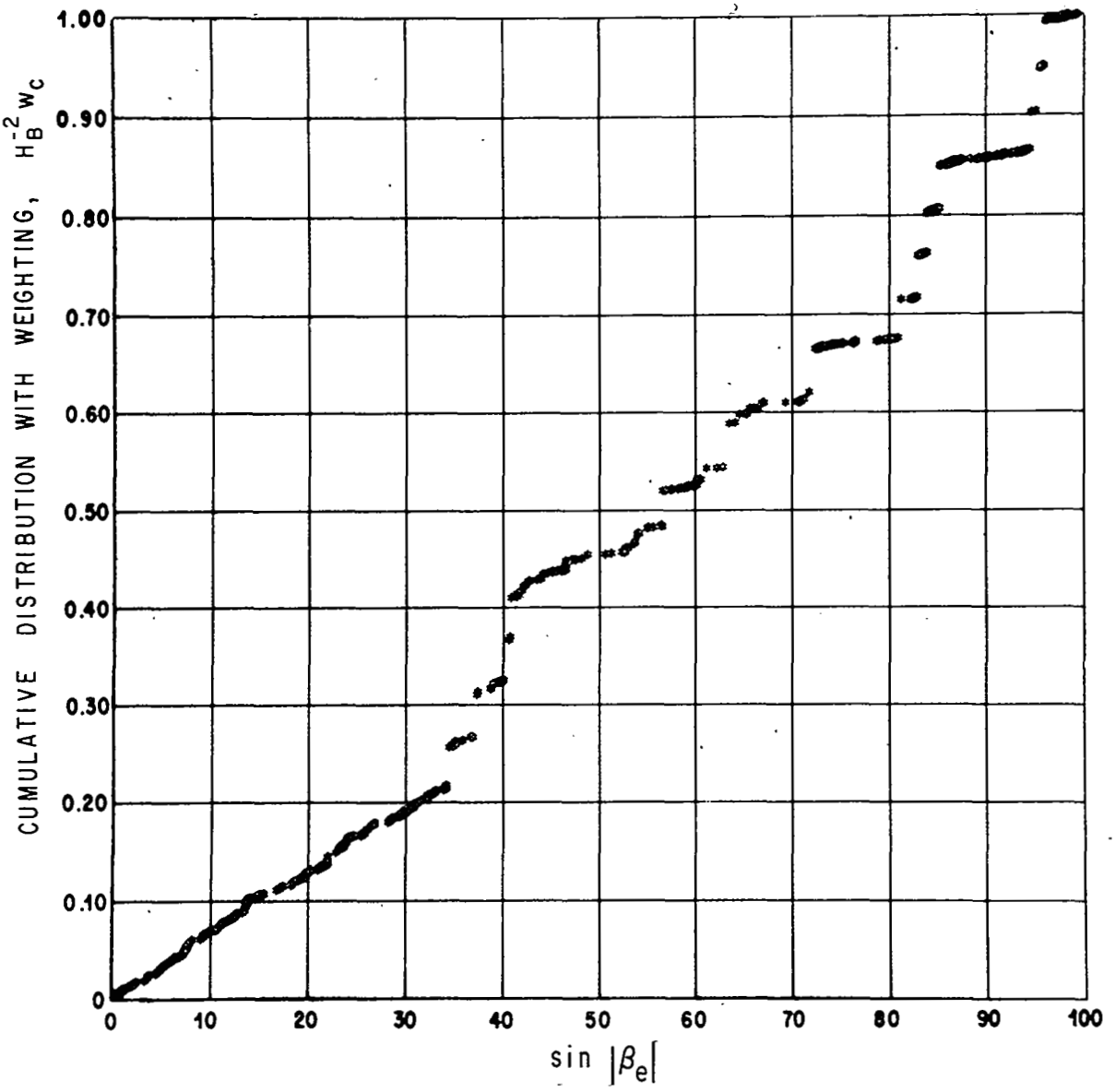

FIGURE 11a. DISTRIBUTION OF ARITHMETIC CELESTIAL LATITUDE WEIGHTED FOR SURVEILLANCE AREA AND APPARENT FRACTION OF CIRCLE OF CELESTIAL LATITUDE, SUB-SAMPLE "A"

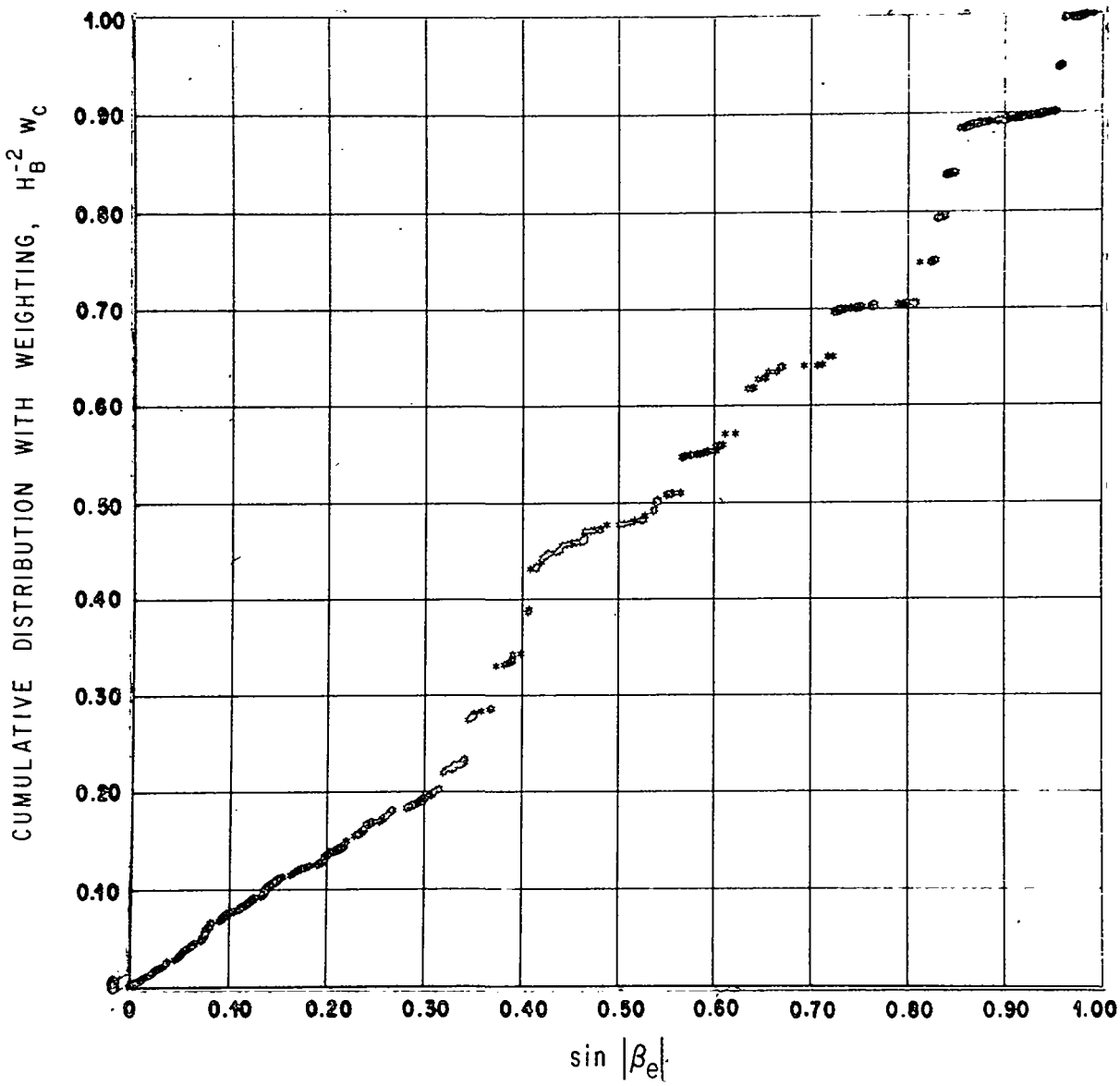

FIGURE 11b. DISTRIBUTION OF ARITHMETIC CELESTIAL LATITUDE WEIGHTED FOR SURVEILLANCE AREA AND APPARENT FRACTION OF CIRCLE OF CELESTIAL LATITUDE, SUB-SAMPLE "B"

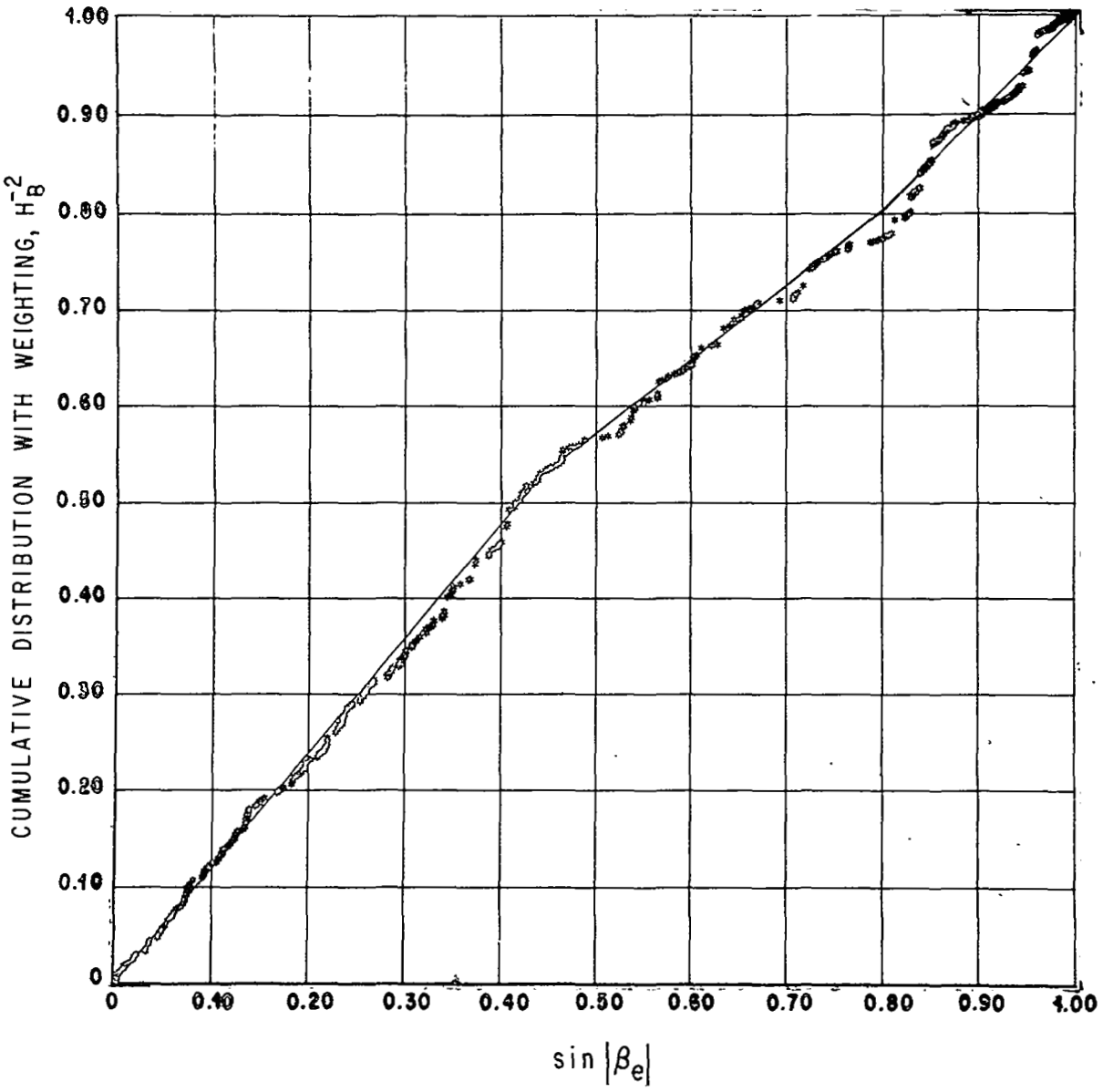

FIGURE 12a. DISTRIBUTION OF ARITHMETIC CELESTIAL LATITUDE WEIGHTED FOR SURVEILLANCE AREA, SUB-SAMPLE "A"

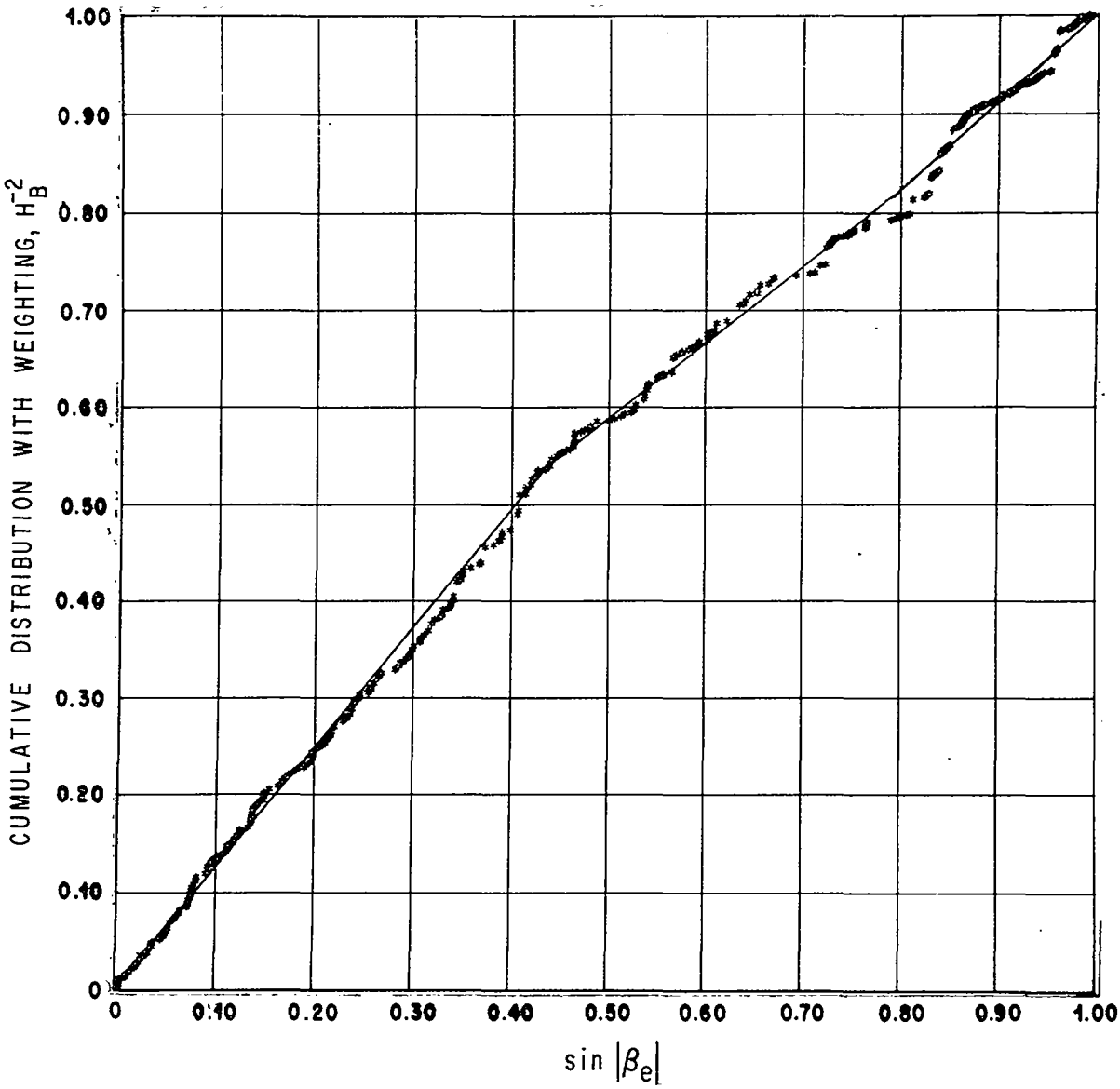

FIGURE 12b. DISTRIBUTION OF ARITHMETIC CELESTIAL LATITUDE WEIGHTED FOR SURVEILLANCE AREA, SUB-SAMPLE "B"

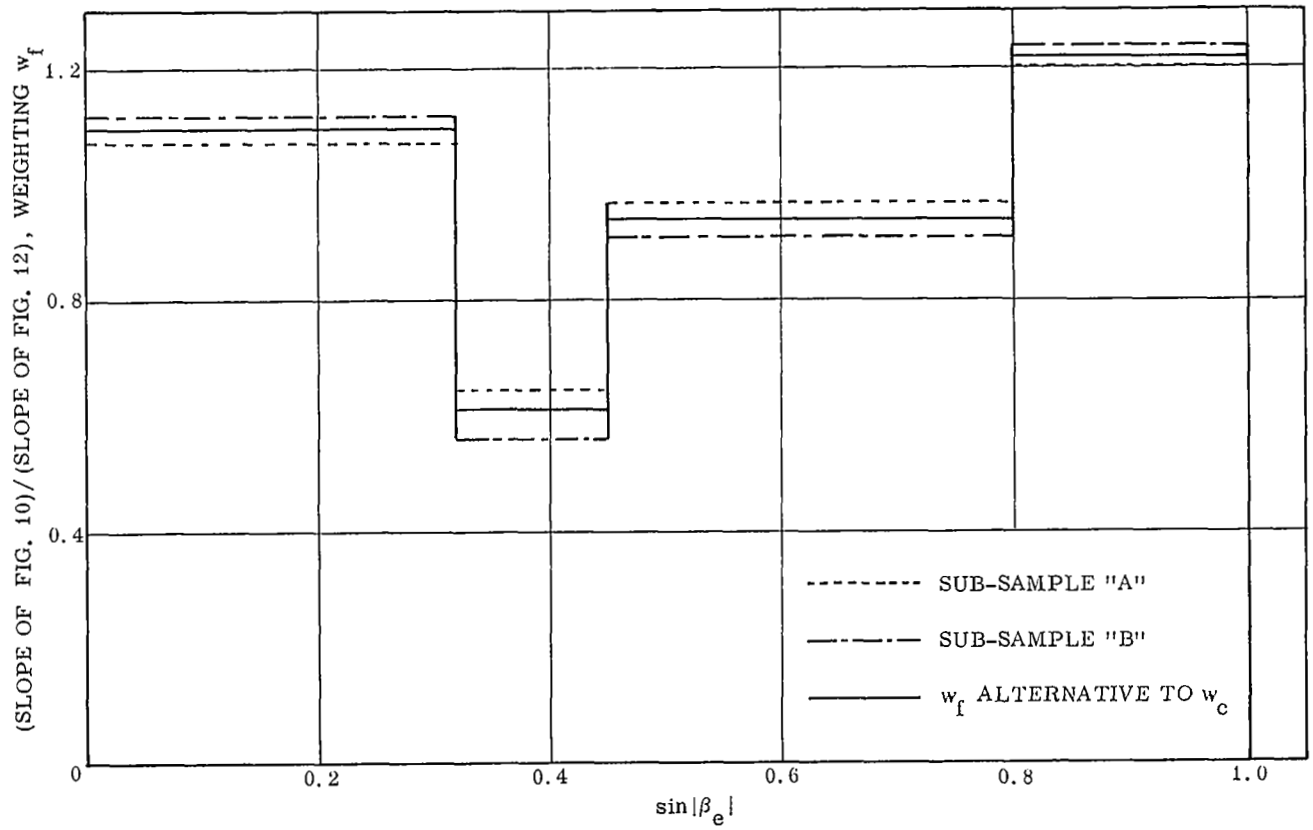

FIGURE 13. WEIGHTING FOR ARITHMETIC CELESTIAL LATITUDE

Weighting	Uniform	Terrestrial	Lunar	Spatial
Mean Mass	0.293 0.223	0.267 0.207	0.298 0.225	0.299 0.230
Standard Deviation of Mass	0.604 0.383	0.564 0.362	0.583 0.366	0.441 0.288
Other Parameters	Correlation Between Mass and Other Parameters, Times 10^3			
V_∞	221 212	191 180	232 227	167 184
V_G	219 211	188 177	228 225	169 186
e	202 210	186 188	205 222	222 247
q	079 077	072 073	081 076	019 008
q'	038 044	033 037	034 040	074 086
sin i	116 016	097 094	101 104	104 121
m_B m_C	1000 1000	1000 1000	1000 1000	1000 1000
λ_λ	020 032	054 062	010 024	013 009
K	182 193	160 168	160 177	208 233
M_{pg}	-495 -499	-471 -474	-506 -518	-455 -481
m_A	805 833	856 875	776 807	821 823
H_B	277 282	249 248	283 291	262 285

NOTE: Upper and lower entries in each table-block involve "Model-B" and "Model-C" mass values, respectively.

FIGURE 14. STATISTICAL ROLE OF MATERIAL CONSISTENCY, PRESUPPOSING STONE DUSTBALL VERSUS COMPACT STONE PARTICLES, BY MODELS FOR ÖPIK'S [2, 28] (1958, 1963) RESULTS WITH SUB-SAMPLE "B"

Parameter	Means				Standard Deviations			
Weighting	Uniform	Terrestrial	Lunar	Spatial	Uniform	Terrestrial	Lunar	Spatial
V_∞	16.62 20.23	16.17 ± 0.17 18.83 ± 0.32	17.83 21.66	19.34 26.39	5.01 10.32	4.47 8.52	5.14 9.99	5.07 12.28
V_G	11.95 16.13	11.33 ± 0.21 14.47 ± 0.37	13.66 18.04	15.59 23.39	6.25 11.64	5.79 9.88	6.16 11.09	6.06 13.34
e	0.4528 0.5422	0.4262 ± 0.0085 0.4989 ± 0.0099	0.5060 0.5969	0.5380 0.6802	0.232 0.277	0.230 0.267	0.220 0.252	0.225 0.263
q	0.8524 0.8032	0.8606 ± 0.0054 0.8161 ± 0.0071	0.8427 0.7804	0.8184 0.7103	0.149 0.199	0.145 0.193	0.154 0.216	0.157 0.248
q'	6.3 9.0	5.6 ± 1.7 7.5 ± 1.9	8.0 10.5	17.0 21.1	50.5 55.0	46.6 50.9	60.7 62.3	105.0 95.4
sin i	0.1817 0.2306	0.1776 ± 0.0049 0.2118 ± 0.0067	0.2071 0.2544	0.2707 0.3837	0.132 0.200	0.133 0.180	0.147 0.207	0.152 0.261
m_B	0.261 0.293	0.235 ± 0.020 0.267 ± 0.021	0.276 0.298	0.286 0.299	0.604 0.606	0.549 0.564	0.606 0.583	0.516 0.441
λ_λ	106.7 99.6	106.8 ± 1.4 101.2 ± 1.4	107.4 99.8	101.4 89.3	36.9 36.8	37.8 36.7	35.0 35.1	27.7 30.5
K	-0.297 -0.094	-0.354 ± 0.021 -0.193 ± 0.027	-0.189 0.029	-0.067 0.334	0.604 0.784	0.570 0.724	0.628 0.786	0.825 1.059
M_{pg}	0.142 -0.314	0.230 ± 0.038 -0.181 ± 0.039	-0.138 -0.551	-0.436 -0.951	1.08 1.11	1.04 1.05	1.05 1.02	1.03 1.02
m_A	0.244 0.245	0.234 ± 0.026 0.244 ± 0.026	0.239 0.228	0.227 0.181	0.692 0.693	0.694 0.714	0.630 0.609	0.588 0.495
H_B	83.92 86.81	82.99 ± 0.23 85.14 ± 0.31	84.84 87.78	86.43 91.39	6.40 9.27	6.34 8.41	6.19 8.71	6.52 9.92

NOTE: Upper and lower entries in each table-block are for sub-samples "A" and "B," respectively.

FIGURE 15. WEIGHTED MEANS AND STANDARD DEVIATIONS OF SELECTED PARAMETERS

Parameter / Symbol	Air-Entry Velocity	Geo-centric Velocity	Helio. Orb. Eccent.	Peri-helion of Orb.	Ap-helion of Orb.	Sine of Inc. of Orb. to Ec.	Mass by "Model-B"	Long. of Elong. Apex. E. W.	W. Comet-Asteroid Criter.	Absol. Photo. Mag.	Mass by "Model-A"	Height at Begin.
V_∞		987 993	679 724	-305 -444	142 157	452 599	353 191	-104 -327	601 643	-810 -774	020 -065	664 762
V_G	989 995		735 772	-301 -453	139 158	463 600	319 188	-059 -291	636 675	-828 -807	024 -062	693 785
e	657 728	718 769		-088 -303	186 197	109 319	236 186	385 150	872 833	-652 -729	092 016	594 710
q	-291 -377	-294 -392	-088 -280		051 021	145 008	065 072	688 593	064 -210	241 340	105 132	-115 -244
q'	135 169	136 171	191 205	055 018		131 185	027 033	059 027	535 529	-129 -163	002 -006	158 184
sin i	463 661	479 663	144 407	118 -025	146 217		122 097	-079 -201	150 368	-393 -475	021 -027	348 519
m_B	453 221	415 219	271 202	069 079	029 038	167 116		048 054	205 160	-519 -471	862 856	312 249
λ_λ	-150 -442	-105 -413	365 036	690 567	062 005	-094 -300	020 020		387 150	057 156	098 134	031 -143
K	589 613	627 643	866 791	051 -215	540 550	189 436	244 182	356 059		-564 -642	084 015	551 628
M_{pg}	-822 -789	-844 -817	-669 -740	240 321	-132 -181	-416 -528	-562 -495	075 246	-580 -644		-329 -247	-573 -654
m_A	040 -071	043 -069	115 015	114 142	004 -008	034 -038	813 805	112 155	104 017	-332 -225		131 049
H_B	702 804	726 820	642 748	-114 -215	167 201	384 602	396 277	023 -251	603 637	-619 -690	162 040	

NOTE: Upper and lower entries in each array-block, times 0.001, are for sub-samples "A" and "B," respectively.

FIGURE 16. CORRELATION ARRAY - BLOCKS WITH TERRESTRIAL WEIGHTING (ABOVE THE DIAGONAL) AND WITH UNIFORM WEIGHTING (BELOW)

Symbol \ Parameter	Air-Entry Velocity	Geo-centric Velocity	Helio. Orb. Eccent.	Peri-helion of Orb.	Ap-helion of Orb.	Sine of Inc. of Orb. to Ec.	Mass by "Model-B"	Long. of Elong. Apex E. W.	W. Comet-Asteroid Criter.	Absol. Photo. Mag.	Mass by "Model-A"	Height at Begin.
V_∞		993 997	614 706	-291 -418	128 144	394 588	484 232	-226 -501	529 601	-823 -781	036 -084	688 781
V_G	996 999		663 738	-299 -431	130 146	402 587	451 228	-197 -484	560 623	-841 -801	035 -085	700 791
e	719 768	746 789		-089 -307	205 205	030 301	287 205	350 000	840 787	-635 -693	129 015	600 707
q	-370 -504	-366 -513	-184 -412		069 038	224 057	064 081	684 580	058 -220	242 324	116 150	-109 -214
q'	163 160	164 161	283 250	131 061		139 191	025 034	071 021	598 569	-129 -164	001 -008	179 191
sin i	499 760	504 759	130 496	178 -121	190 224		143 101	-107 -292	108 368	-340 -453	015 -047	344 551
m_B	360 167	344 169	311 222	-012 019	035 074	093 104		007 010	220 160	-572 -506	783 776	414 283
λ_λ	-206 -662	-182 -651	311 -238	660 575	160 039	-163 -532	065 013		330 016	128 304	130 175	-028 -302
K	583 649	594 659	812 750	004 -308	724 626	210 534	242 208	304 -180		-527 -598	094 003	554 603
M_{pg}	-832 -796	-841 -809	-683 -732	269 408	-163 -214	-415 -608	-535 -455	098 453	-543 -655		-315 -208	-580 -631
m_A	015 -130	014 -132	098 -052	091 143	-001 -010	-016 -110	847 821	138 194	072 -038	-284 -126		160 032
H_B	715 789	717 795	687 767	-191 -267	247 228	340 643	402 262	009 -441	635 612	-573 -631	157 -018	

NOTE: Upper and lower entries in each array-block, times 0.001, are for sub-samples "A" and "B," respectively.

FIGURE 17. CORRELATION ARRAY - BLOCKS WITH LUNAR WEIGHTING (ABOVE THE DIAGONAL) AND WITH SPATIAL WEIGHTING (BELOW)

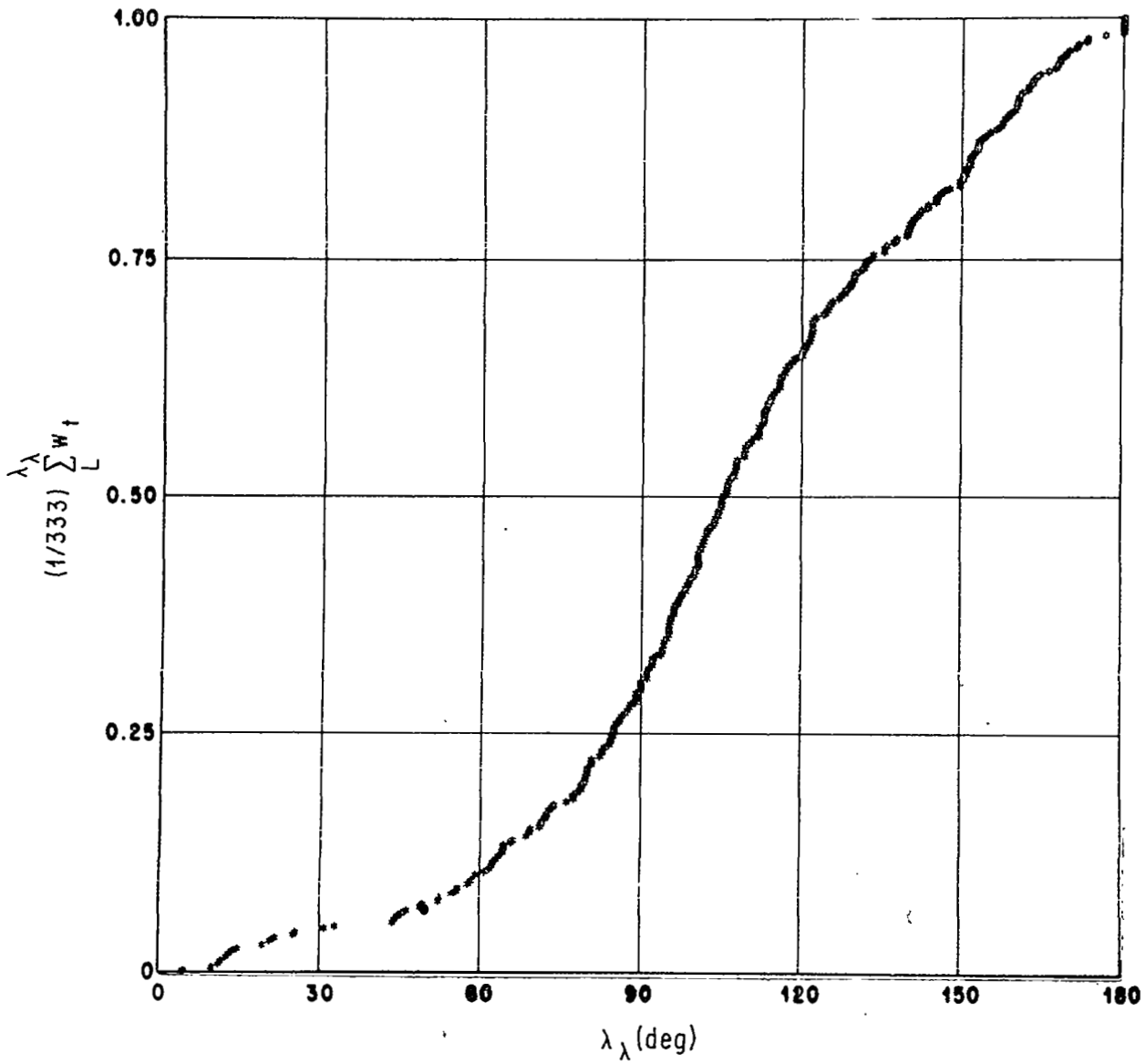

FIGURE 18a. APEX-RADIANT LONGITUDE DISTRIBUTION, TERRESTRIAL WEIGHTING, SUB-SAMPLE "A"

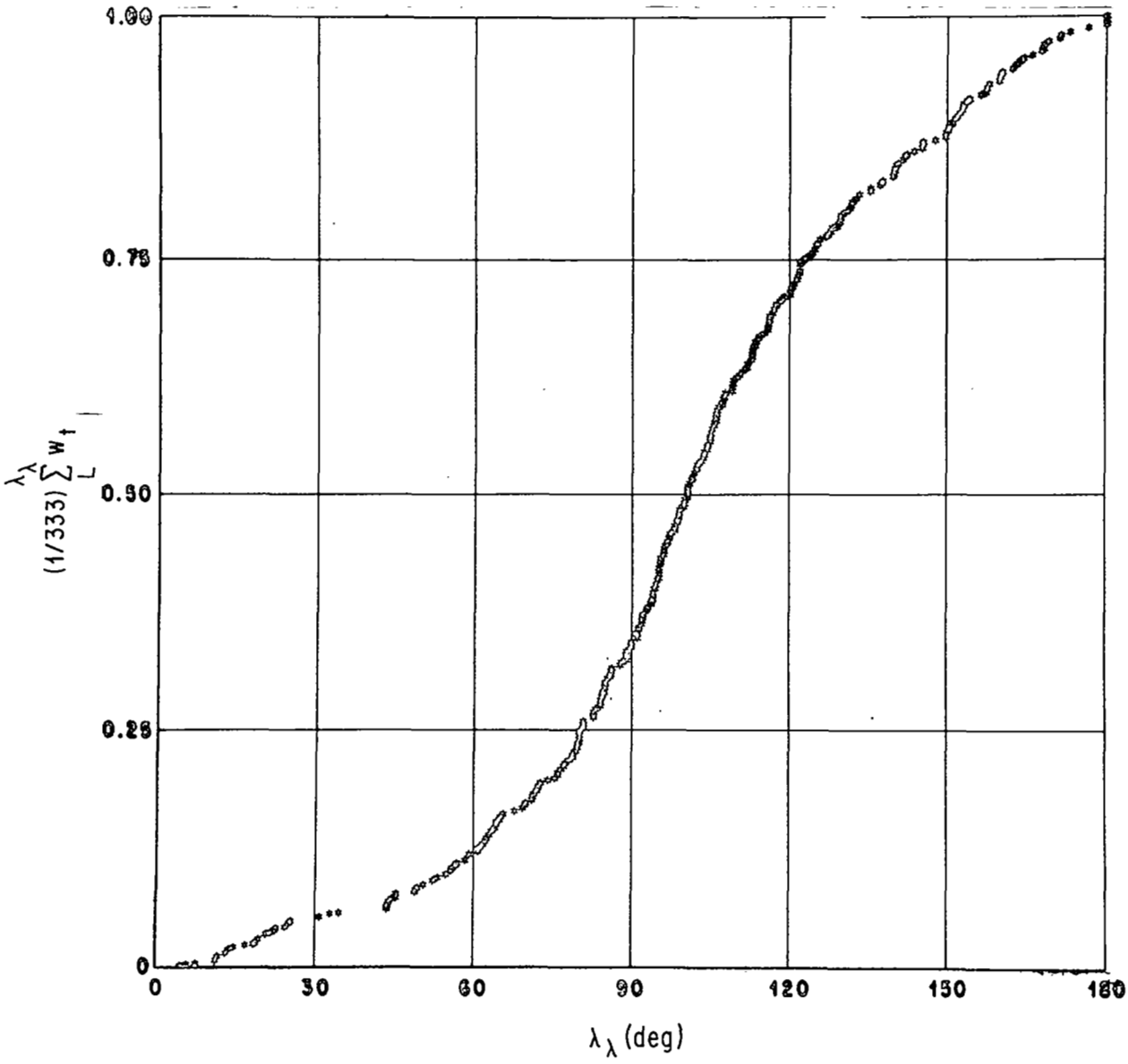

FIGURE 18b. APEX-RADIANT LONGITUDE DISTRIBUTION, TERRESTRIAL WEIGHTING, SUB-SAMPLE "B"

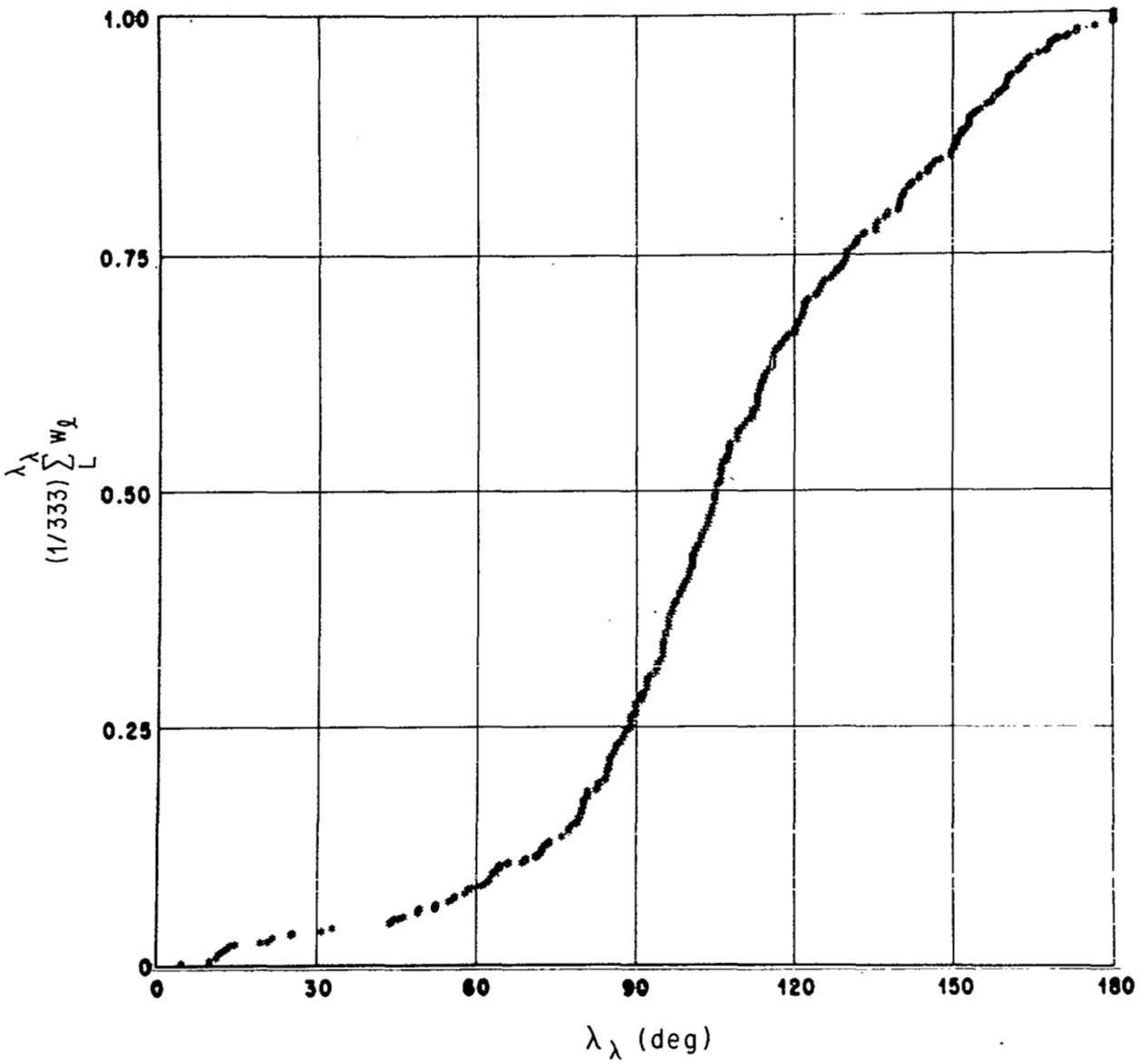

FIGURE 19a. APEX-RADIANT LONGITUDE DISTRIBUTION, LUNAR WEIGHTING, SUB-SAMPLE "A"

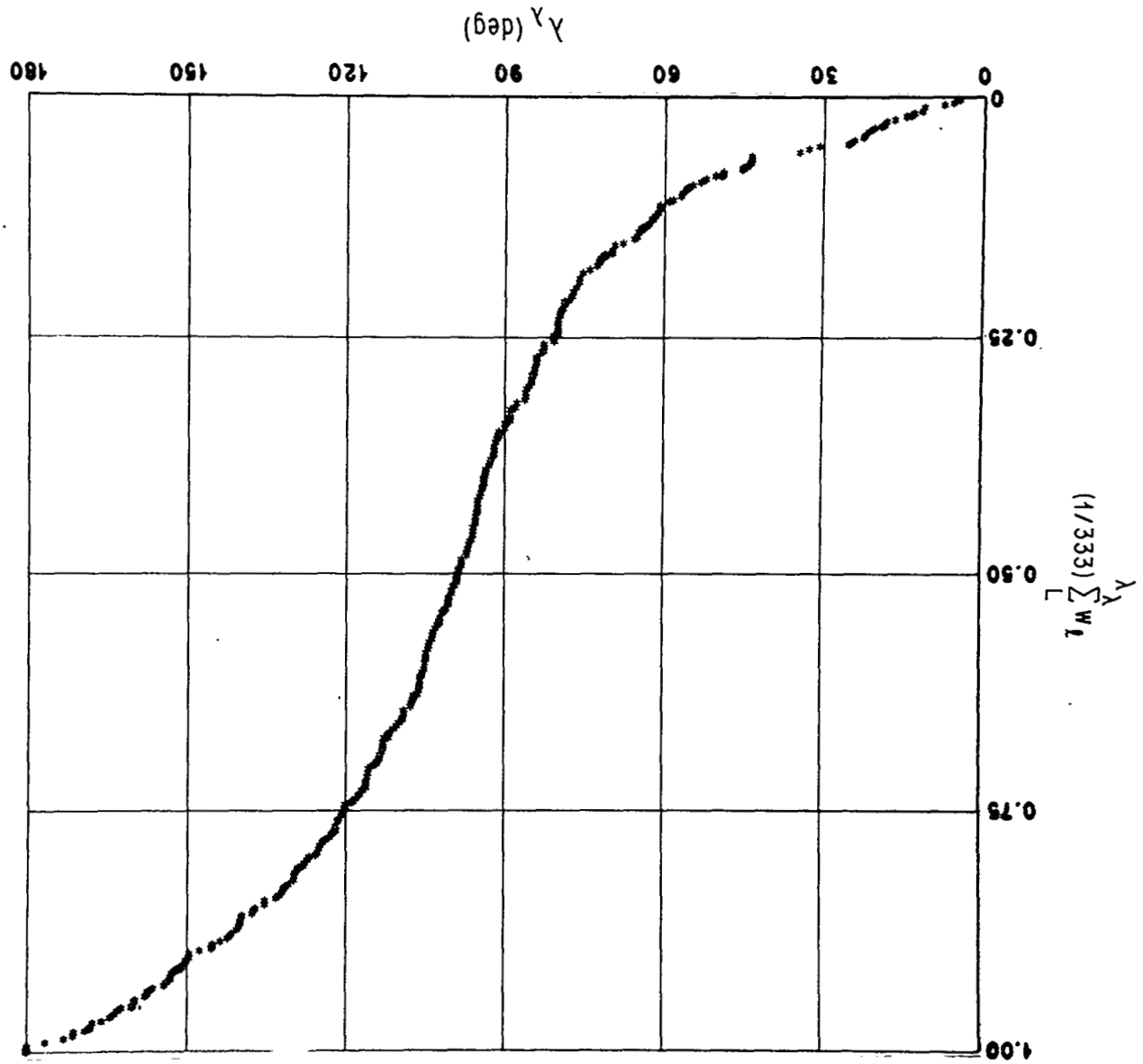

FIGURE 19b. APEX-RADIANT LONGITUDE DISTRIBUTION, LUNAR WEIGHTING, SUB-SAMPLE "B"

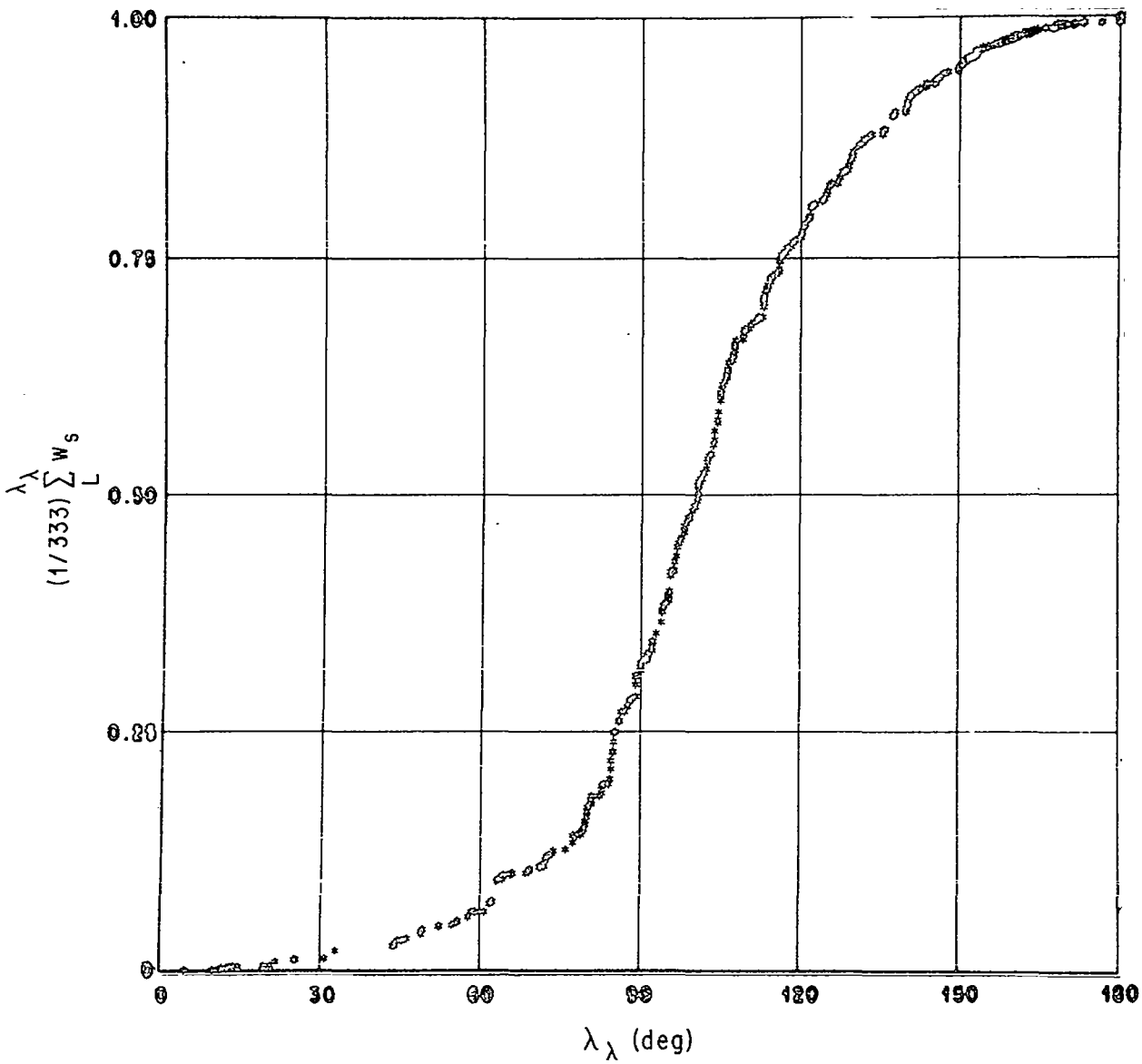

FIGURE 20a. APEX-RADIANT LONGITUDE DISTRIBUTION, SPATIAL WEIGHTING, SUB-SAMPLE "A"

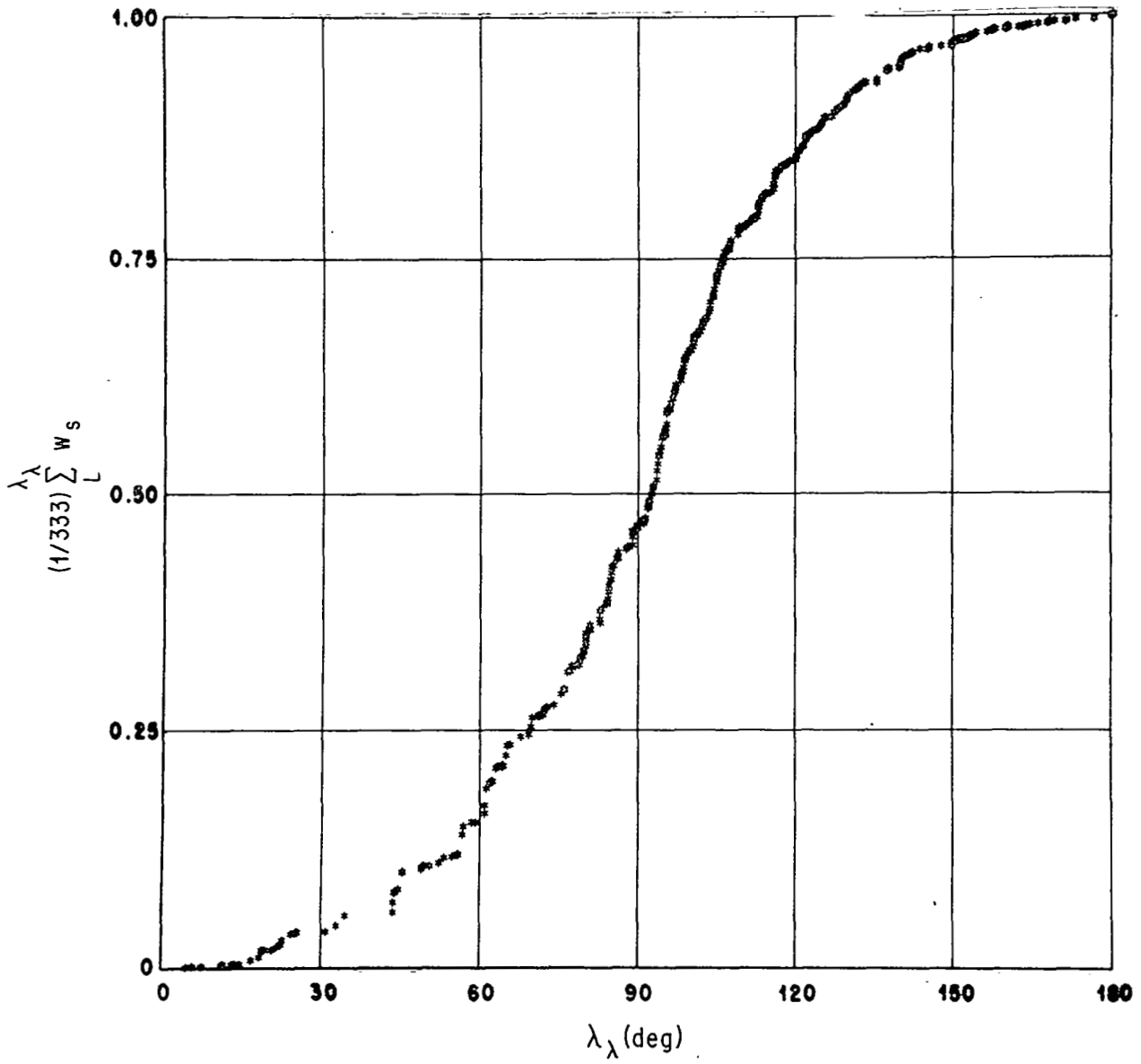

FIGURE 20b. APEX-RADIANT LONGITUDE DISTRIBUTION, SPATIAL WEIGHTING, SUB-SAMPLE "B"

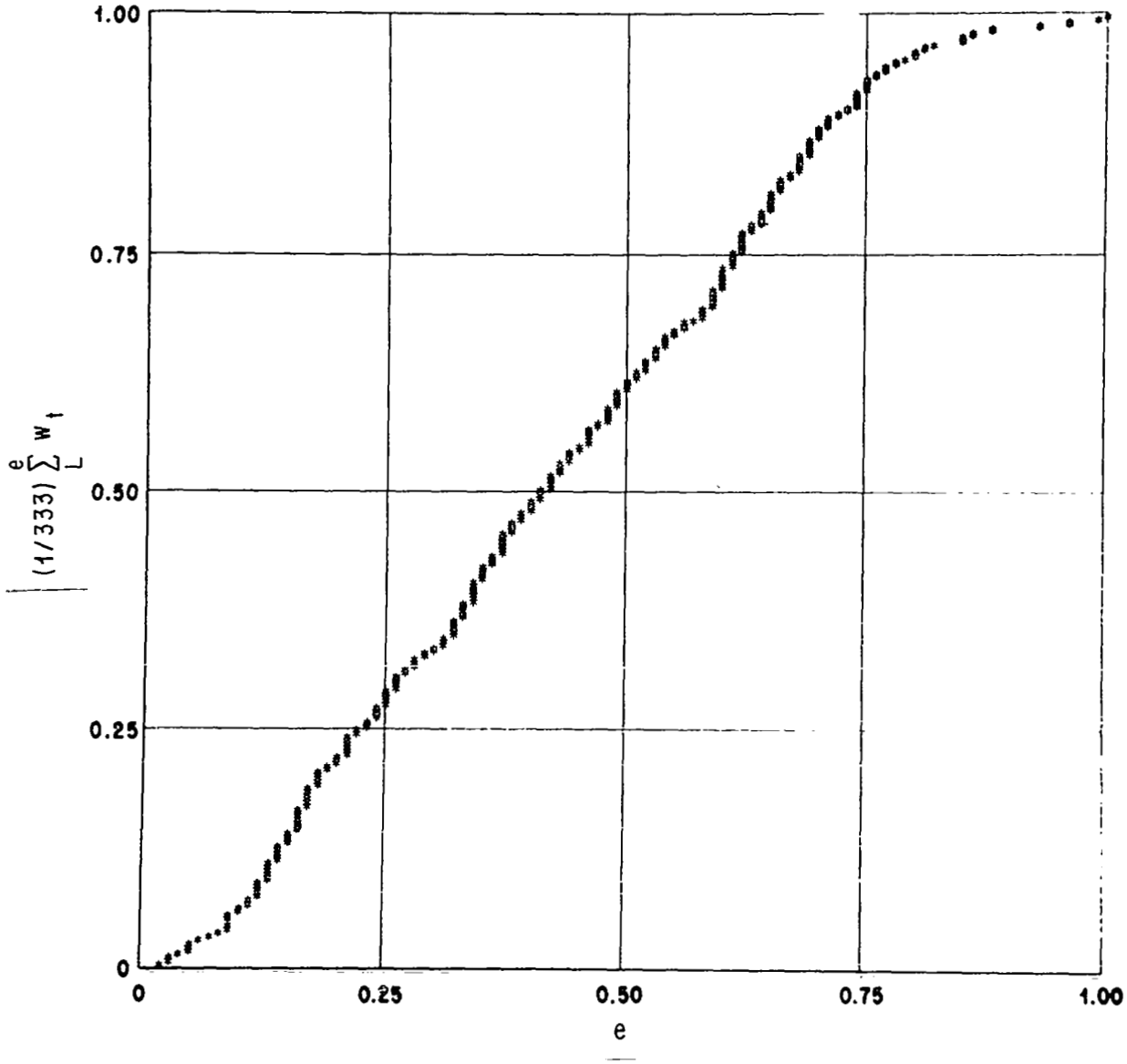

FIGURE 21a. DISTRIBUTION OF ORBIT ECCENTRICITY, TERRESTRIAL WEIGHTING, SUB-SAMPLE "A"

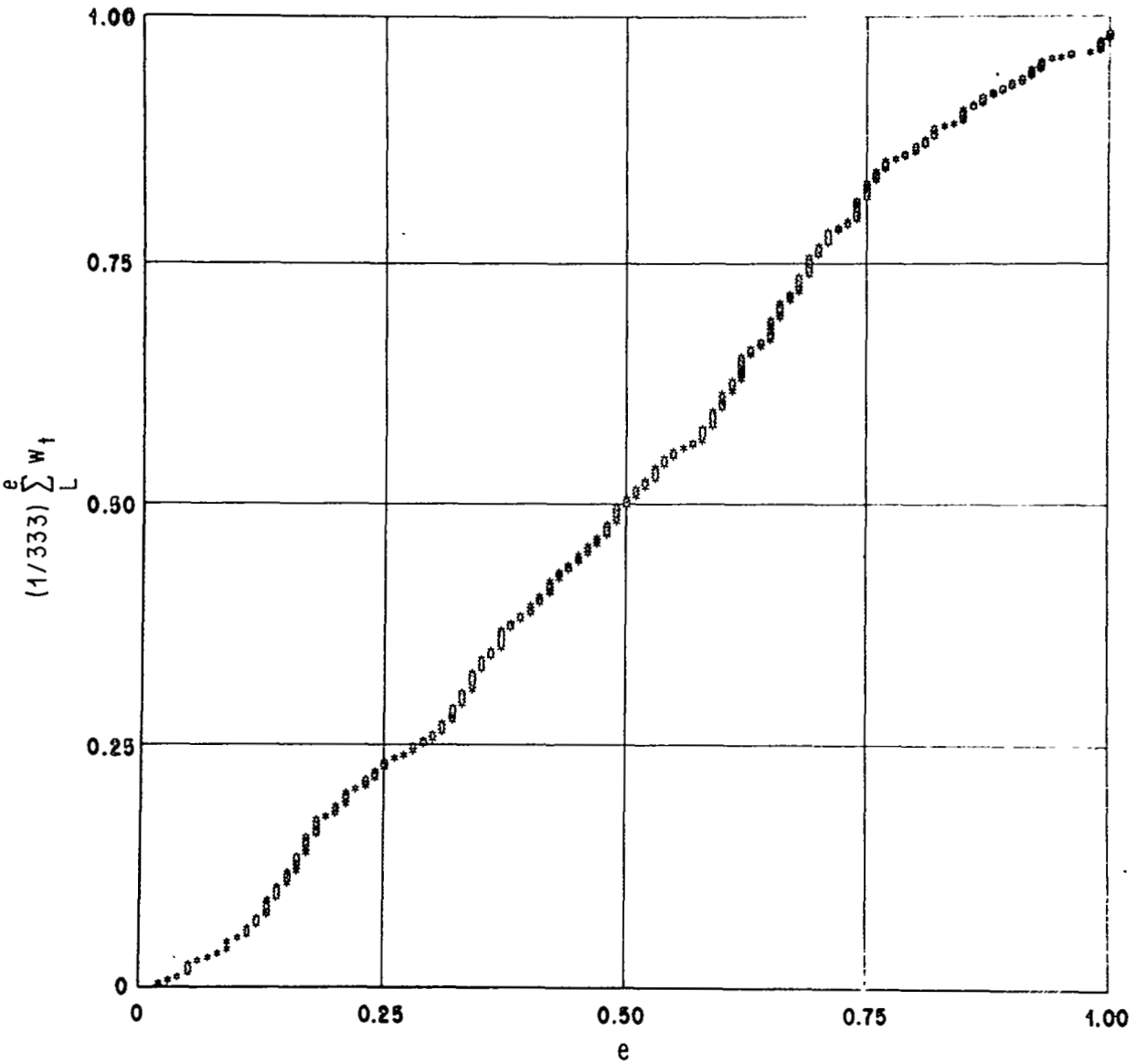

FIGURE 21b. DISTRIBUTION OF ORBIT ECCENTRICITY, TERRESTRIAL WEIGHTING, SUB-SAMPLE "B"

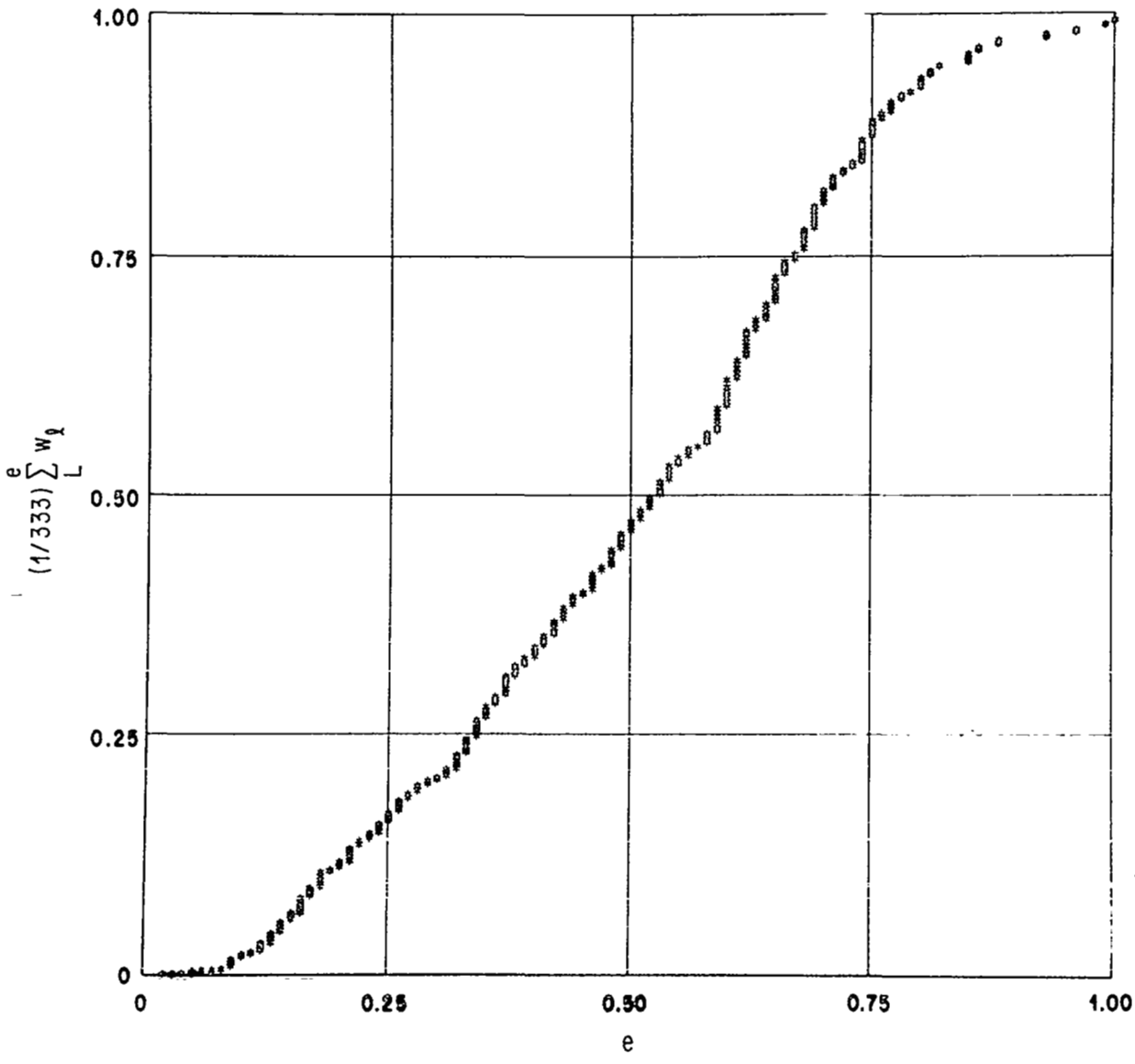

FIGURE 22a. DISTRIBUTION OF ORBIT ECCENTRICITY, LUNAR WEIGHTING, SUB-SAMPLE "A"

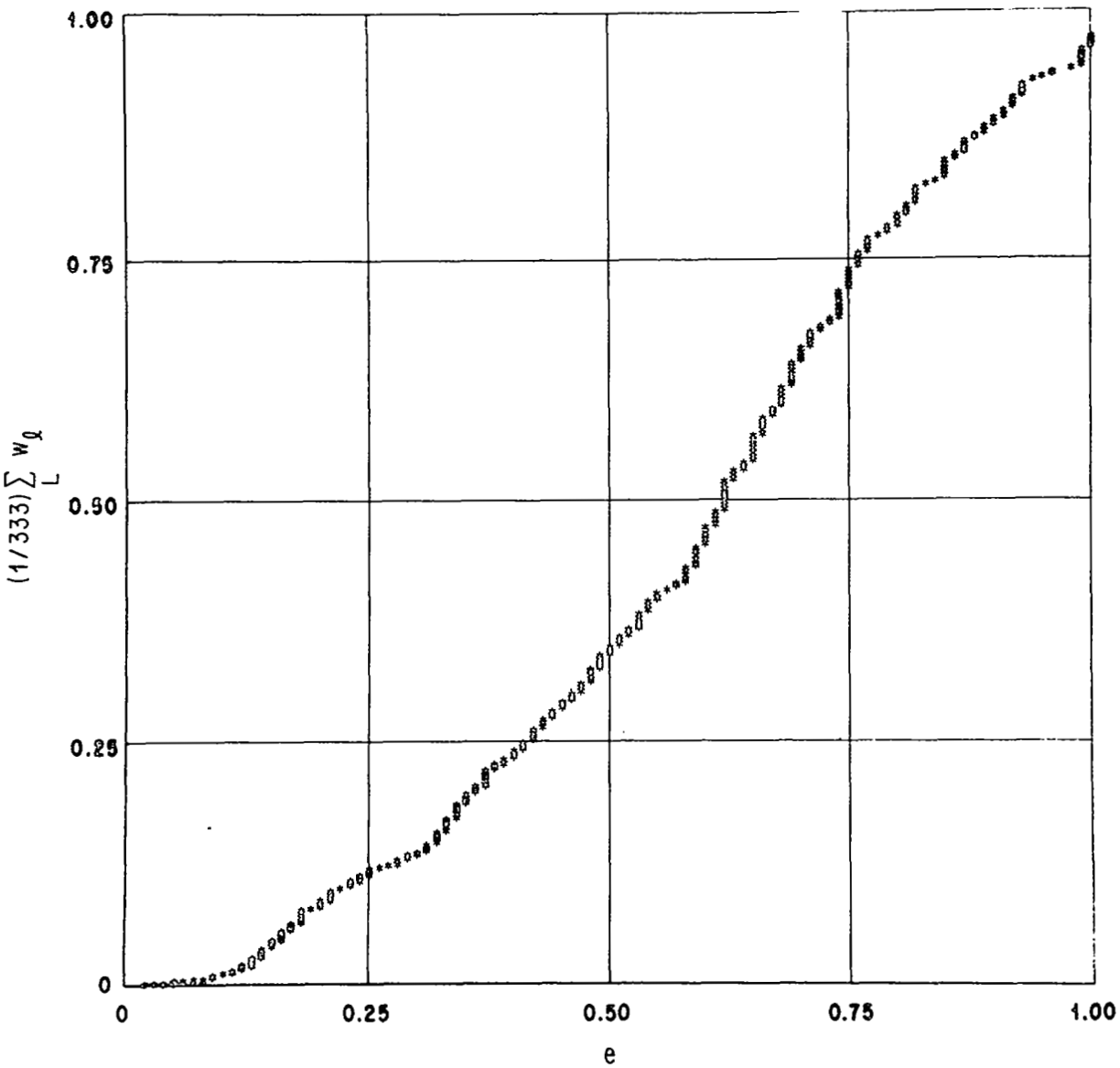

FIGURE 22b. DISTRIBUTION OF ORBIT ECCENTRICITY, LUNAR WEIGHTING, SUB-SAMPLE "B"

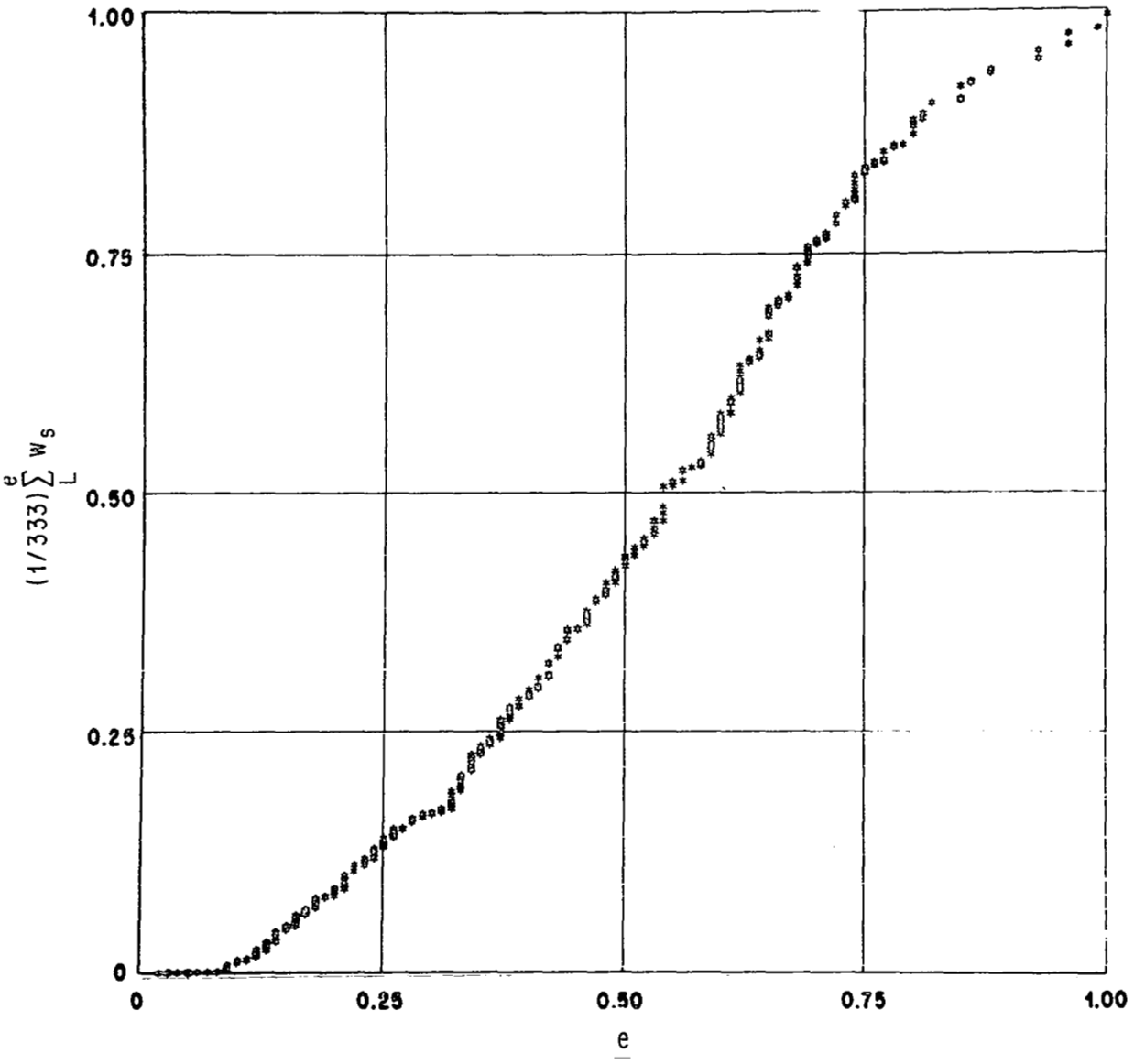

FIGURE 23a. DISTRIBUTION OF ORBIT ECCENTRICITY, SPATIAL WEIGHTING, SUB-SAMPLE "A"

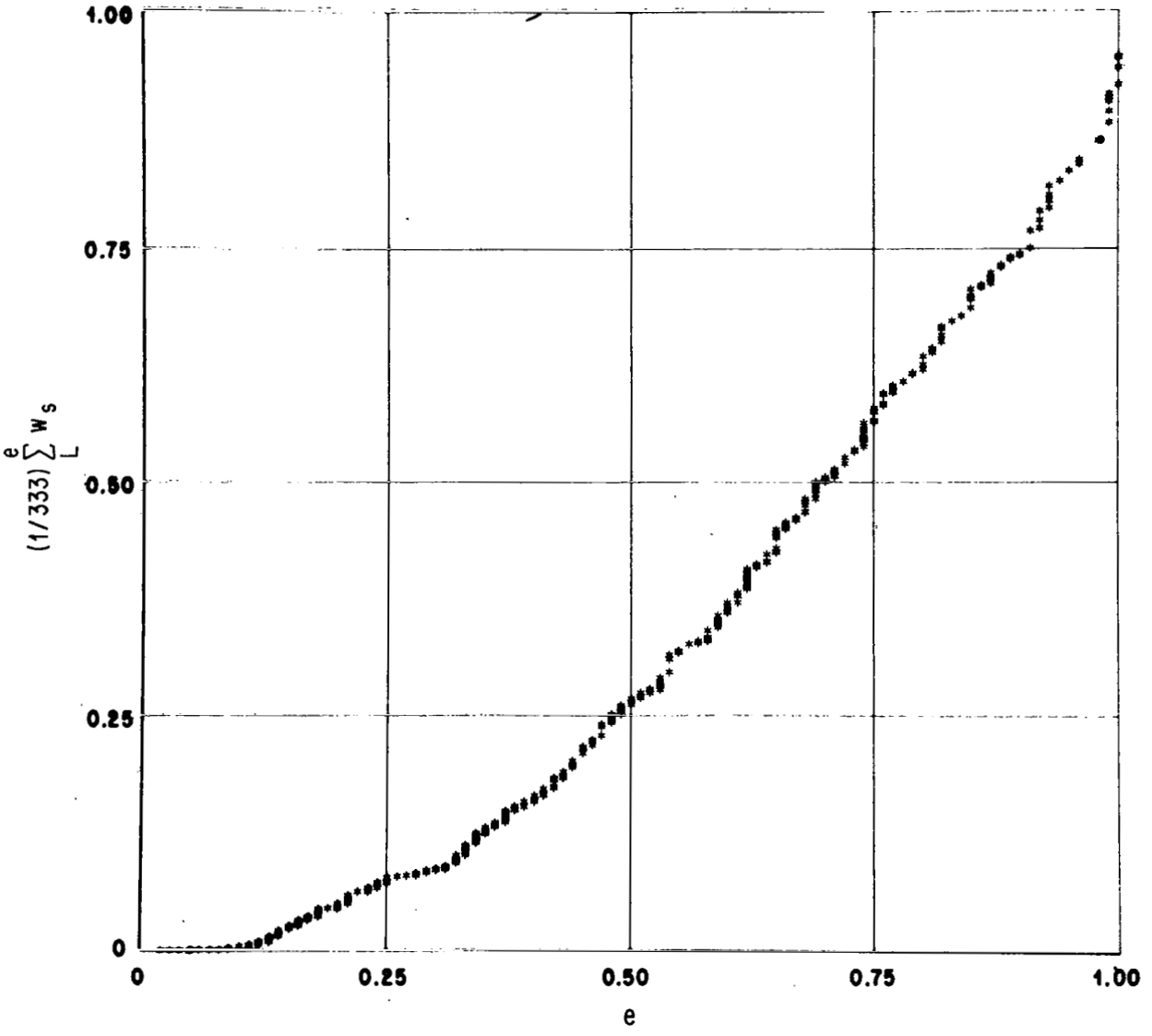

FIGURE 23b. DISTRIBUTION OF ORBIT ECCENTRICITY, SPATIAL WEIGHTING, SUB-SAMPLE "B"

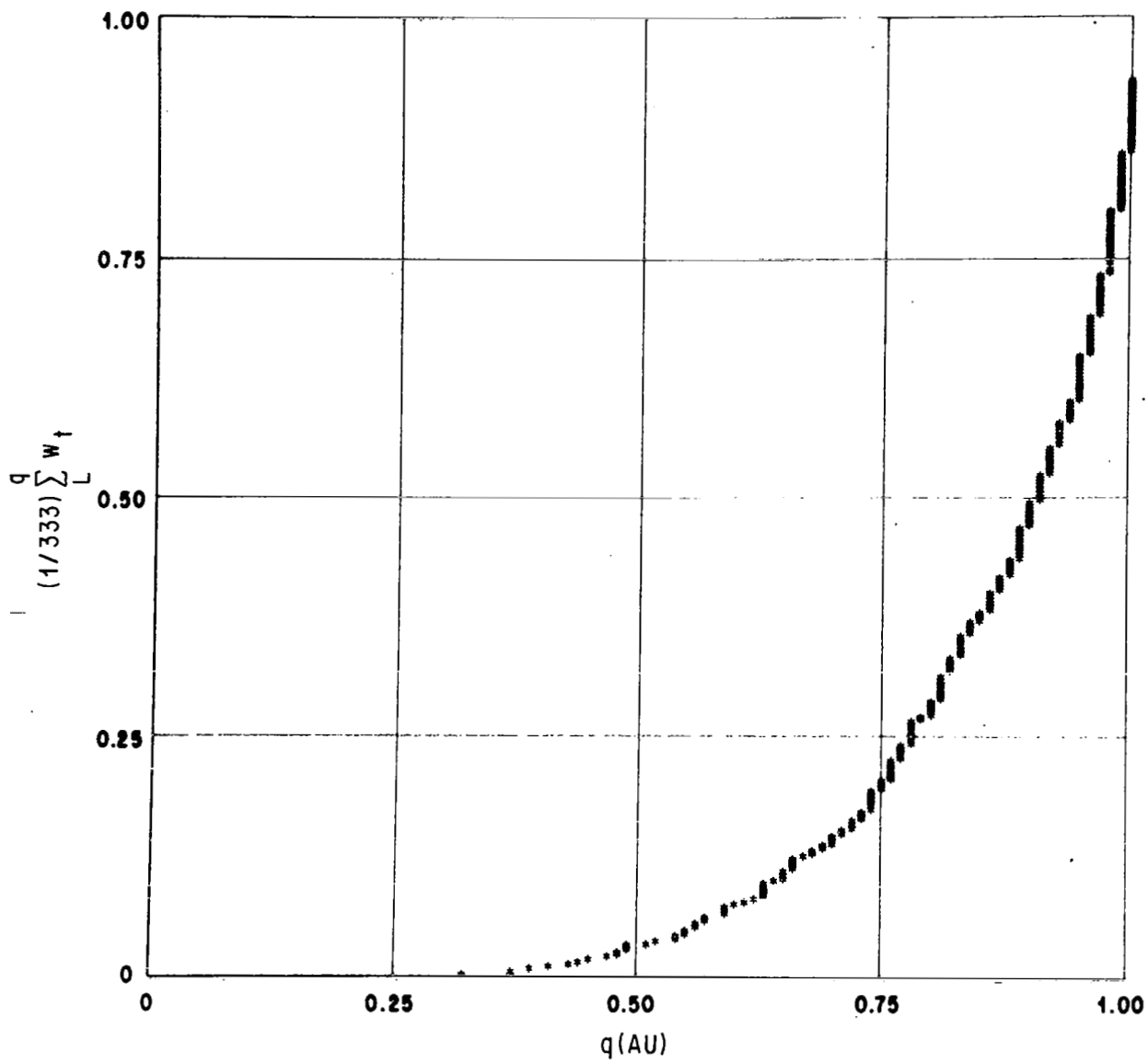

FIGURE 24a. PERIHELION DISTRIBUTION IN THE TERRESTRIAL INFLUX, SUB-SAMPLE "A"

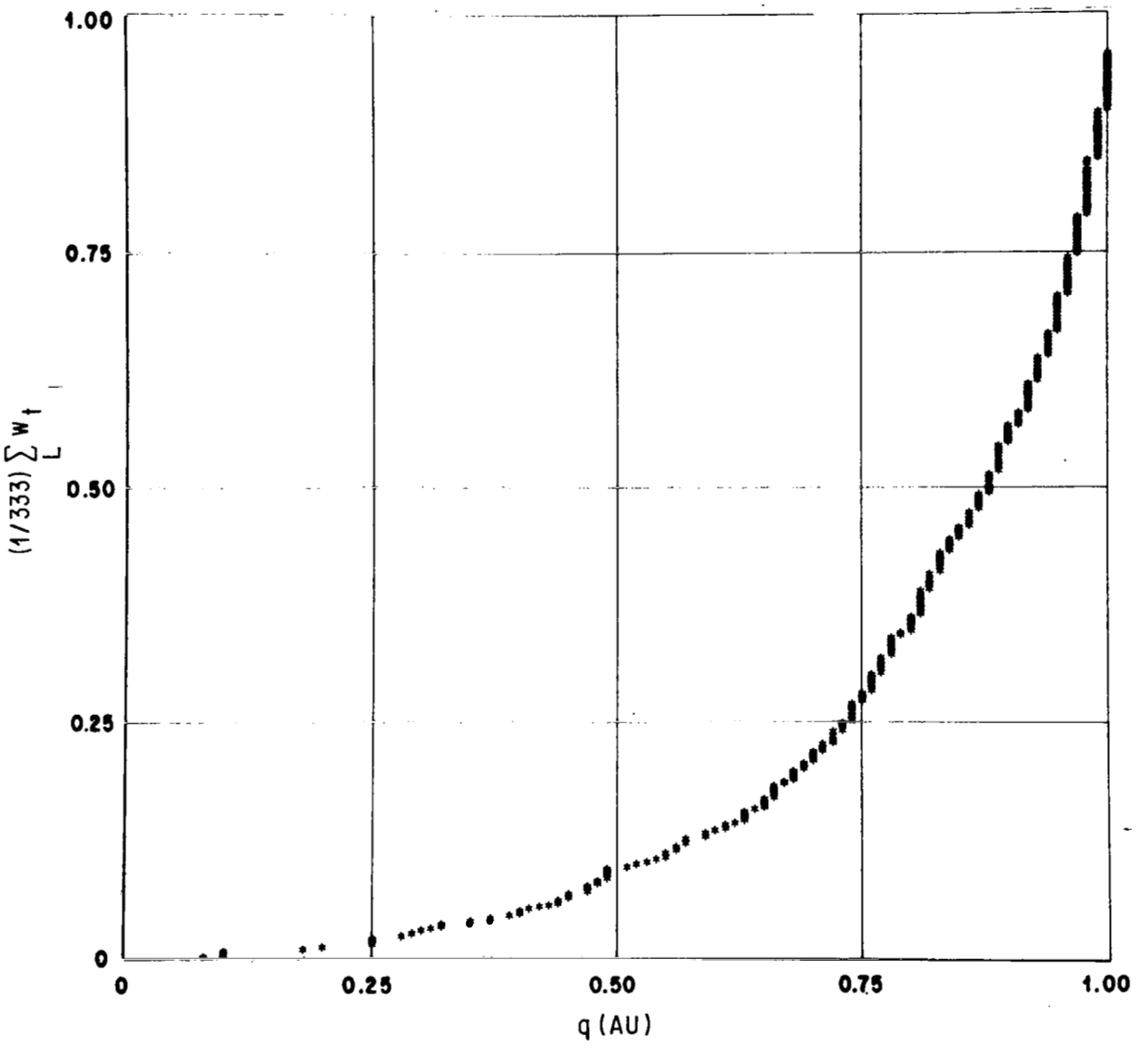

FIGURE 24b. PERIHELION DISTRIBUTION IN THE TERRESTRIAL INFLUX, SUB-SAMPLE "B"

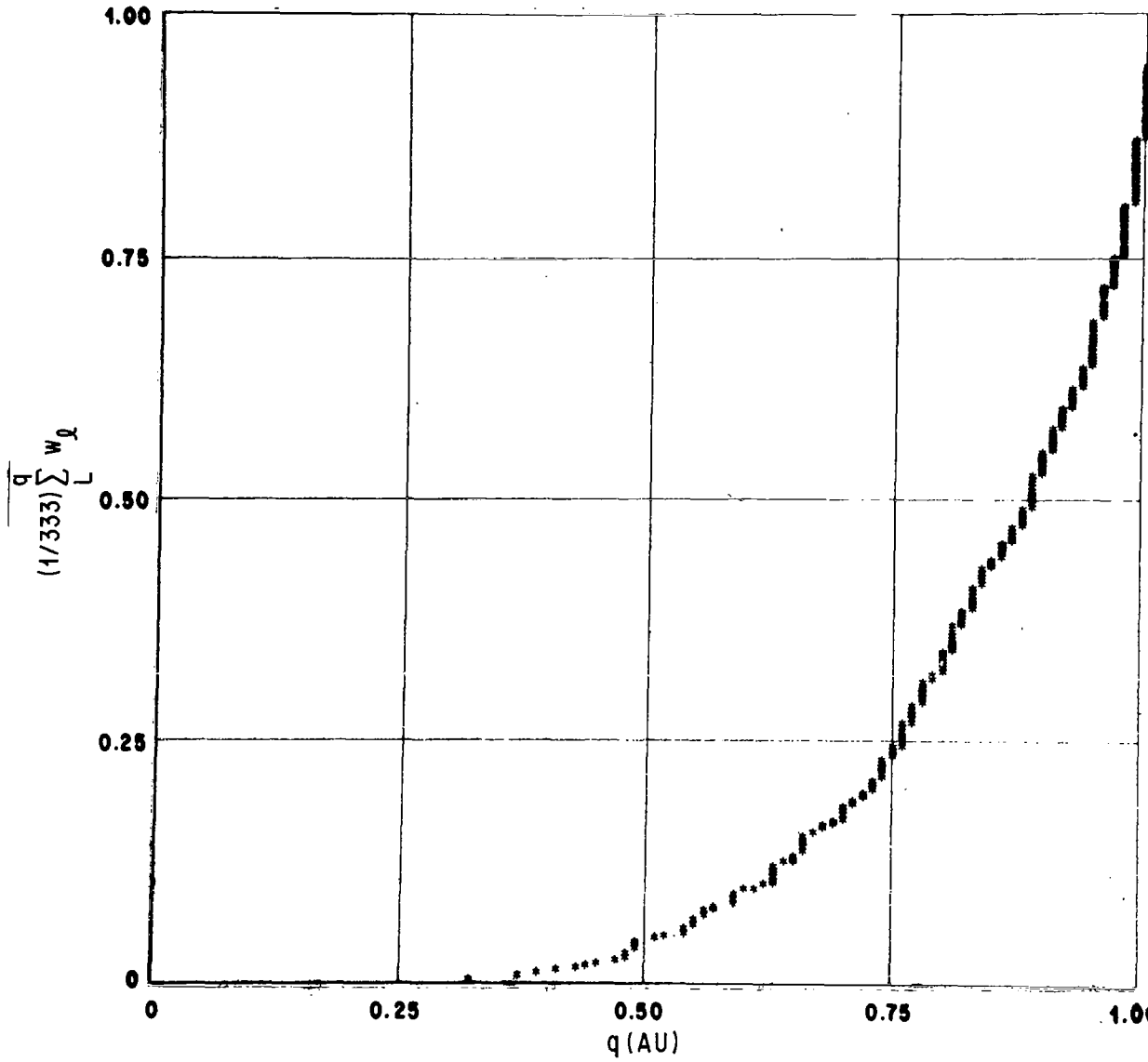

FIGURE 25a. PERIHELION DISTRIBUTION IN THE LUNAR INFLUX, SUB-SAMPLE "A"

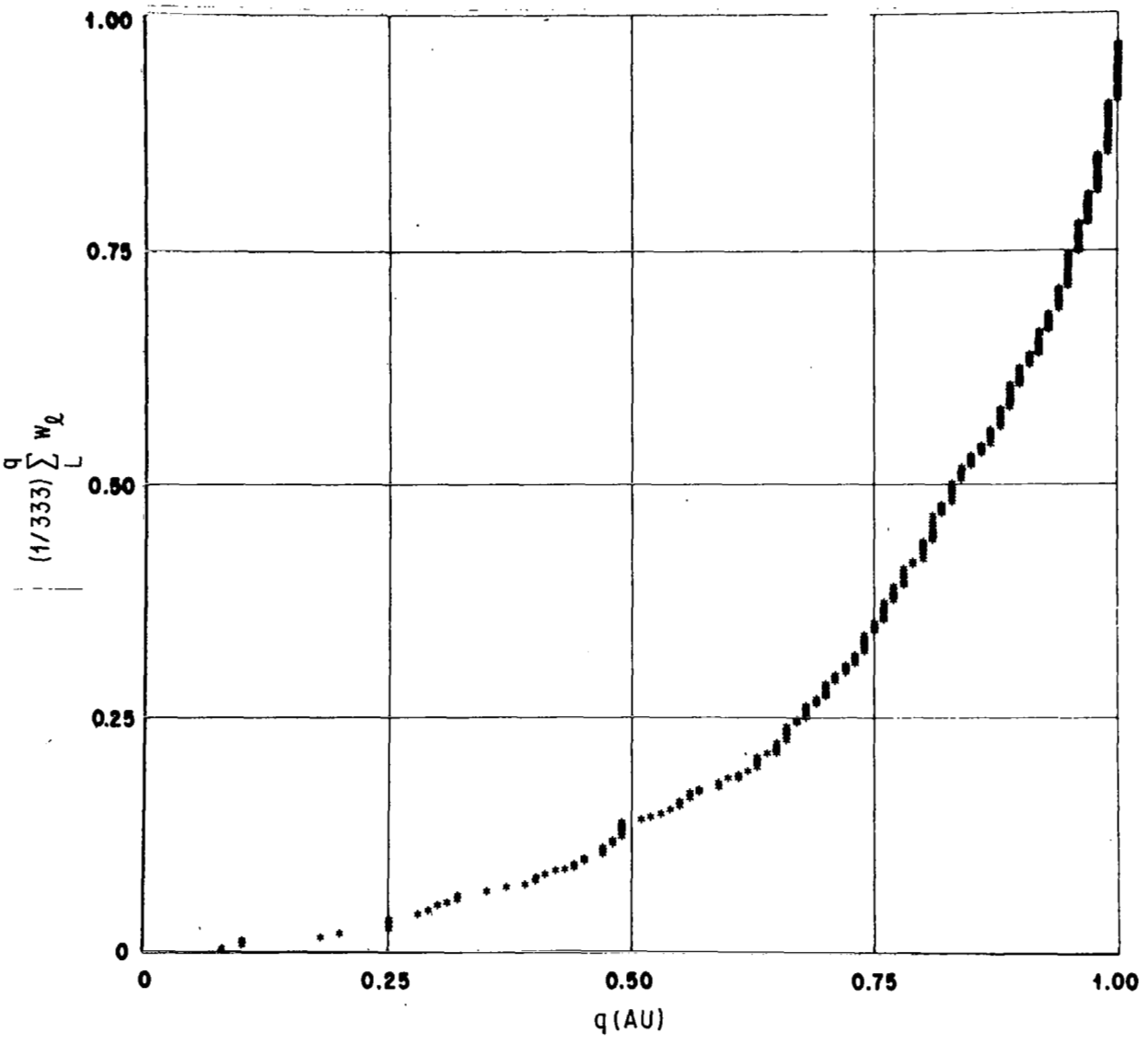

FIGURE 25b. PERIHELION DISTRIBUTION IN THE LUNAR INFLUX, SUB-SAMPLE "B"

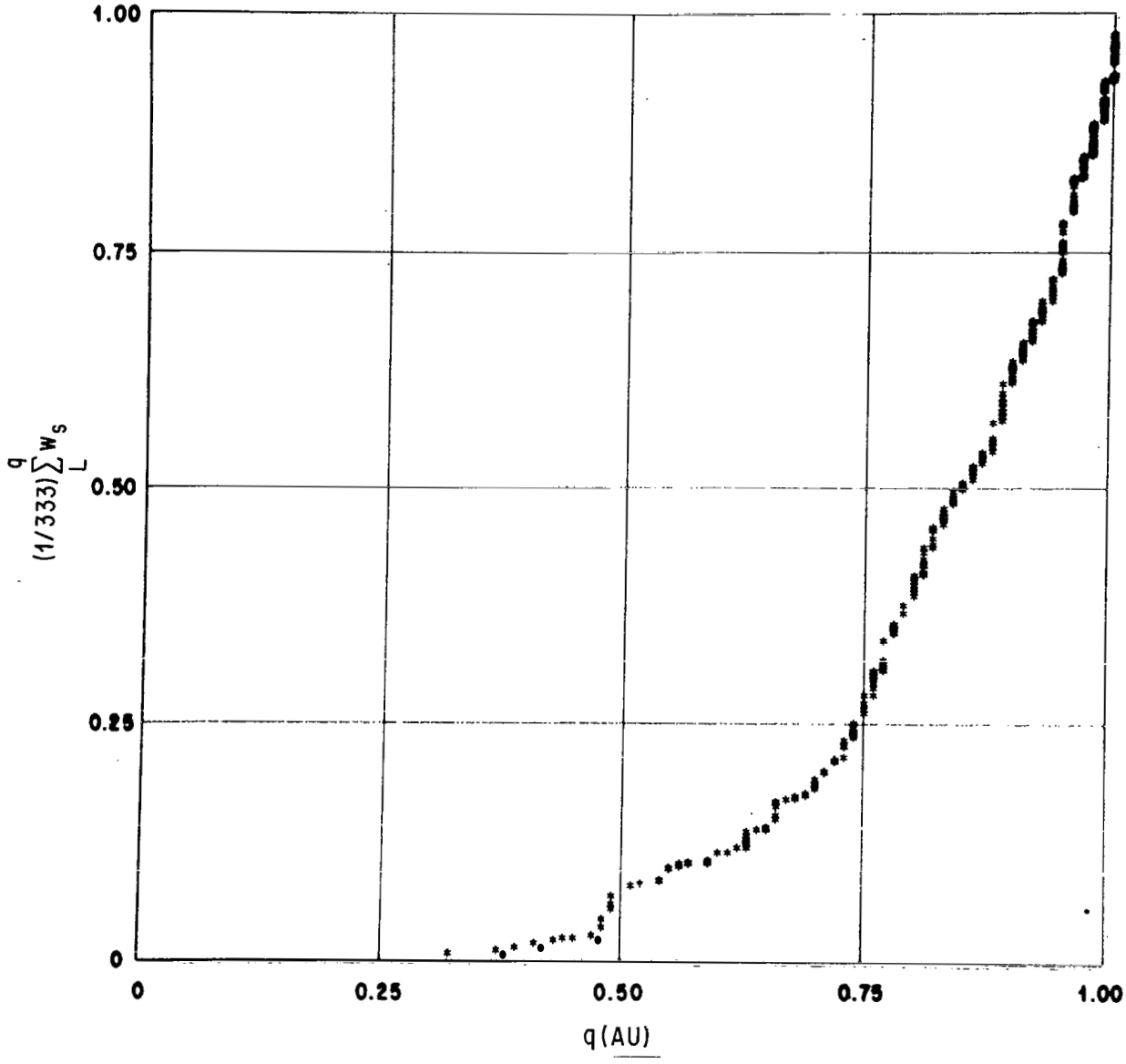

FIGURE 26a. PERIHELION DISTRIBUTION FOR METEOROIDS IN SPACE, SUB-SAMPLE "A"

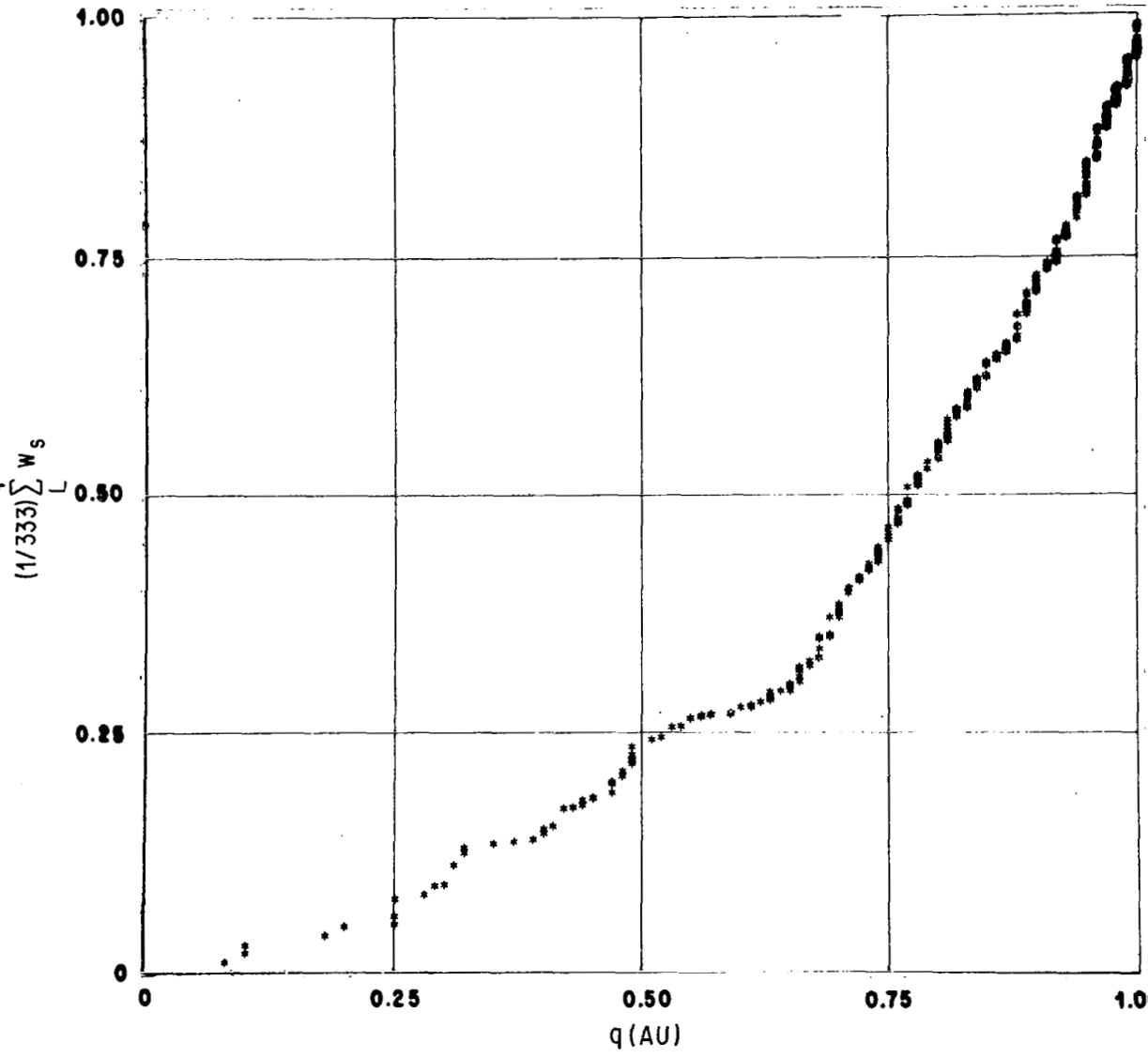

FIGURE 26b. PERIHELION DISTRIBUTION FOR METEOROIDS IN SPACE, SUB-SAMPLE "B"

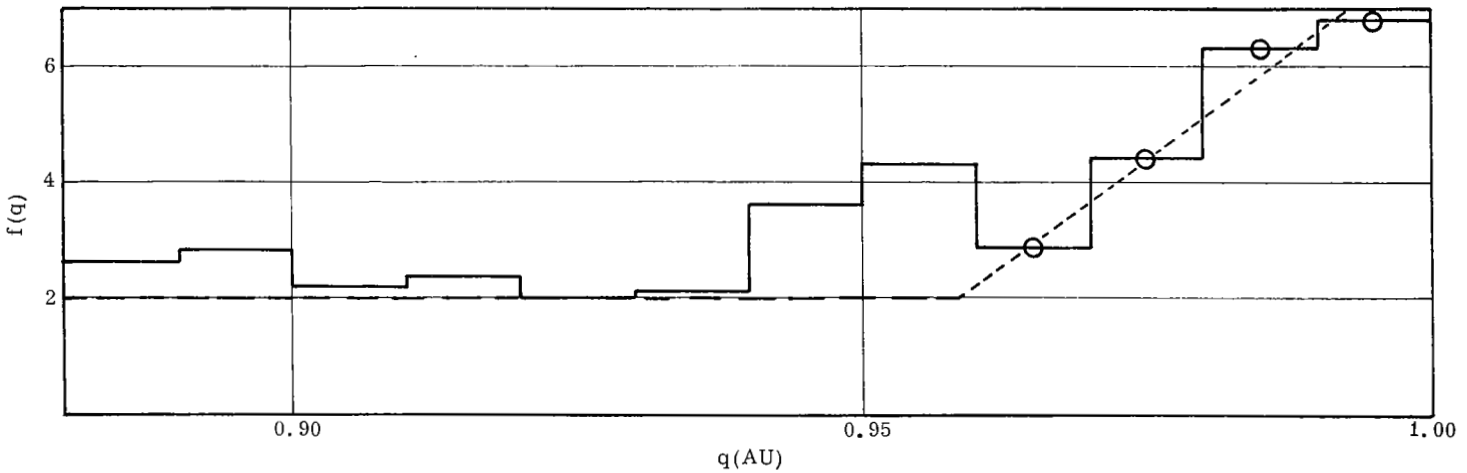

LUNAR WEIGHTING w_l

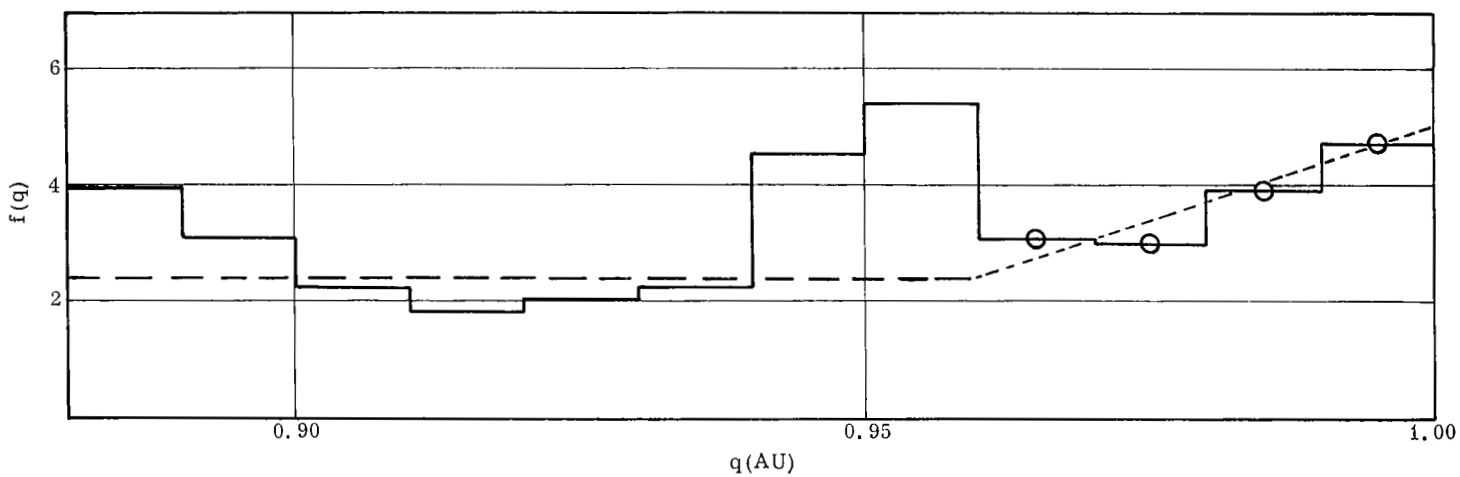

SPATIAL WEIGHTING w_s

FIGURE 27a. PERIHELION PROBABILITY DENSITY FUNCTION. SUB-SAMPLE "A" WITH LUNAR WEIGHTING w_l, AND SPATIAL WEIGHTING w_s

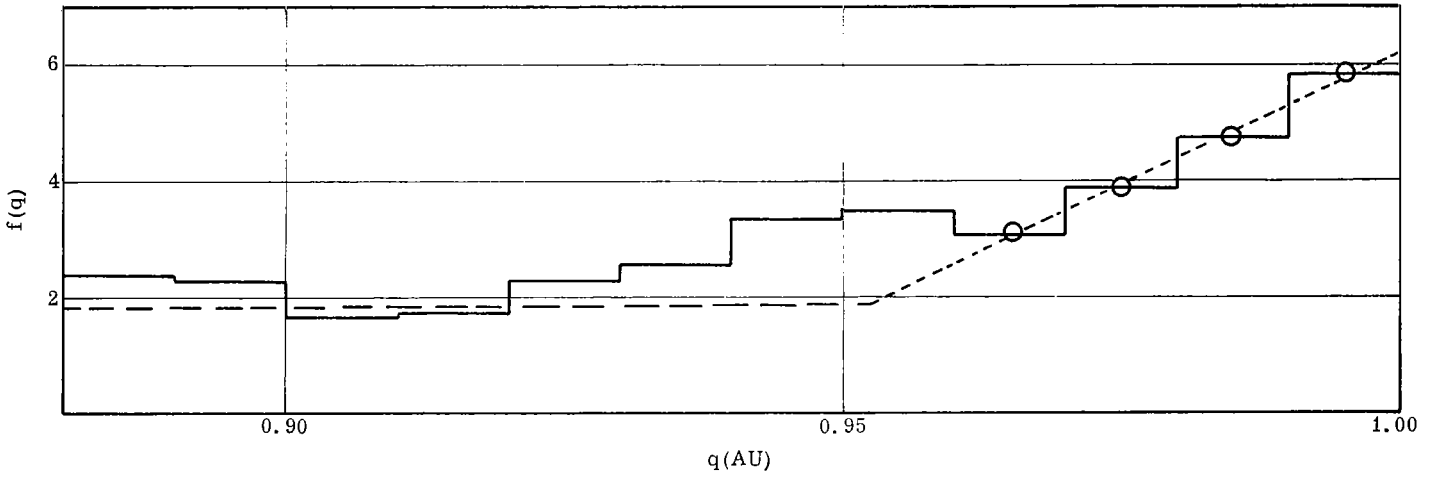

LUNAR WEIGHTING w_l

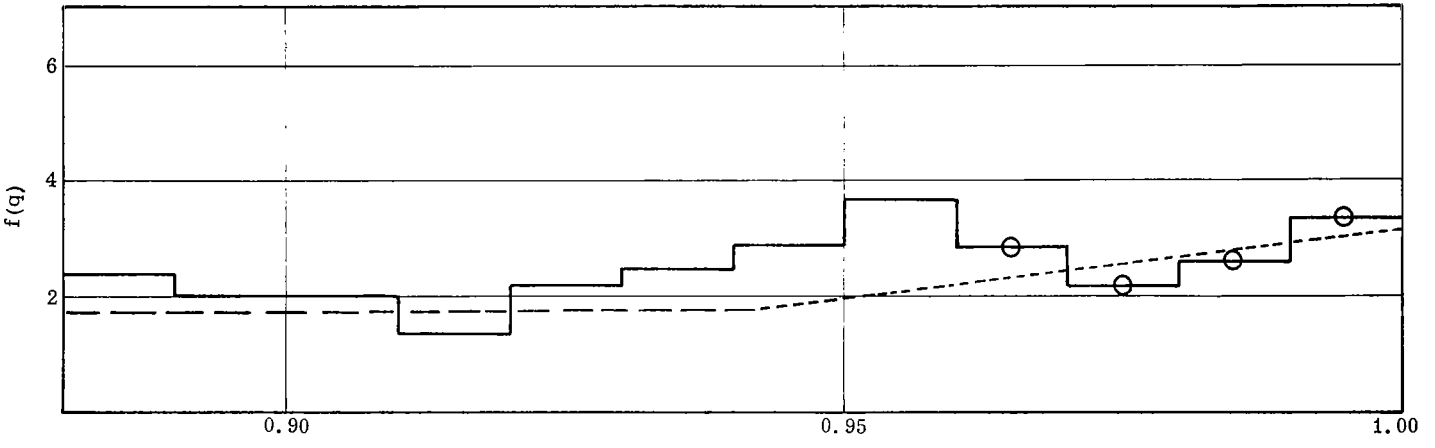

SPATIAL WEIGHTING w_s

FIGURE 27b. PERIHELION PROBABILITY DENSITY FUNCTION, SUB-SAMPLE "B" WITH LUNAR WEIGHTING w_l, AND SPATIAL WEIGHTING w_s

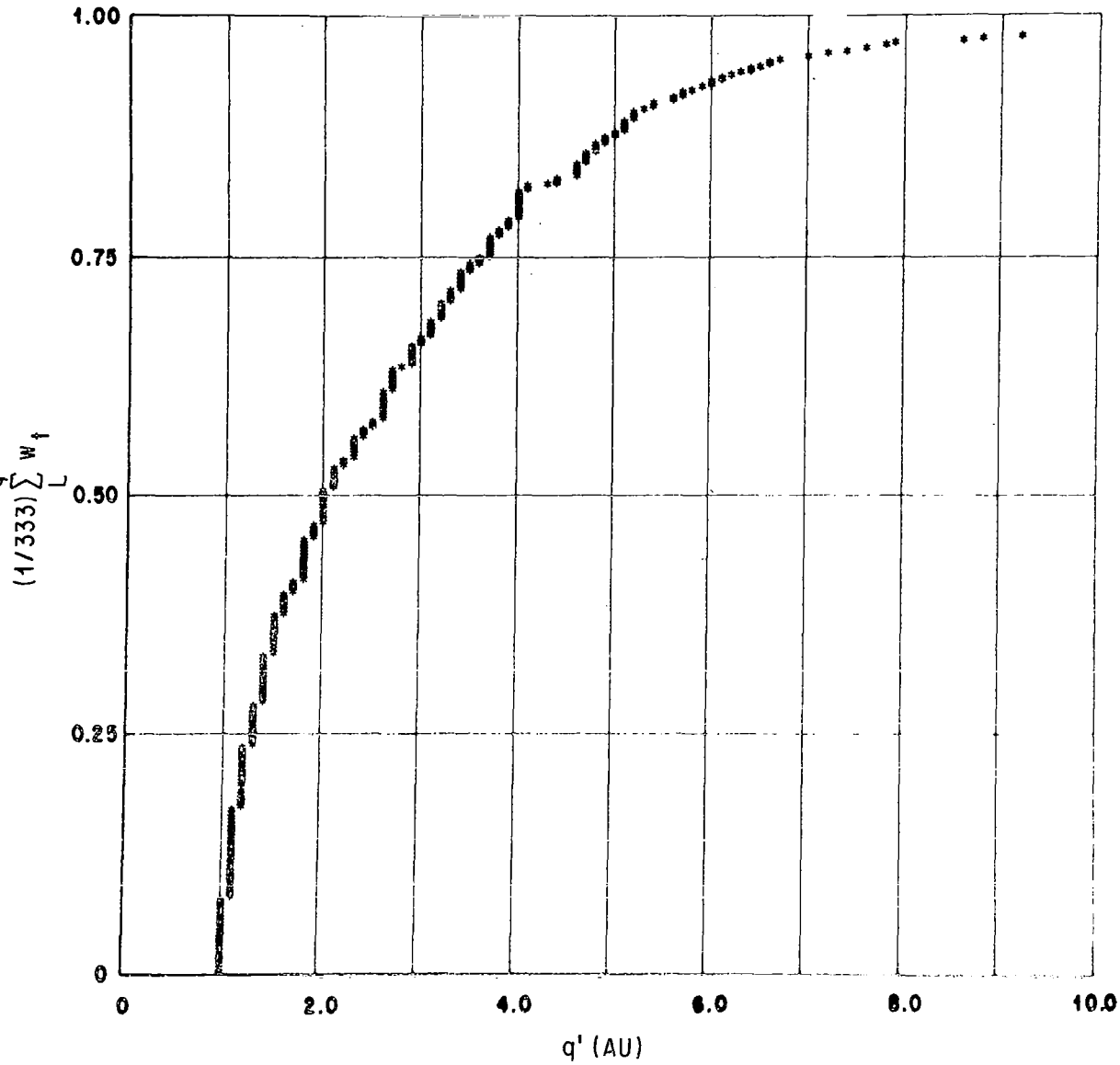

FIGURE 28a. APHELION DISTRIBUTION IN THE TERRESTRIAL INFLUX, SUB-SAMPLE "A"

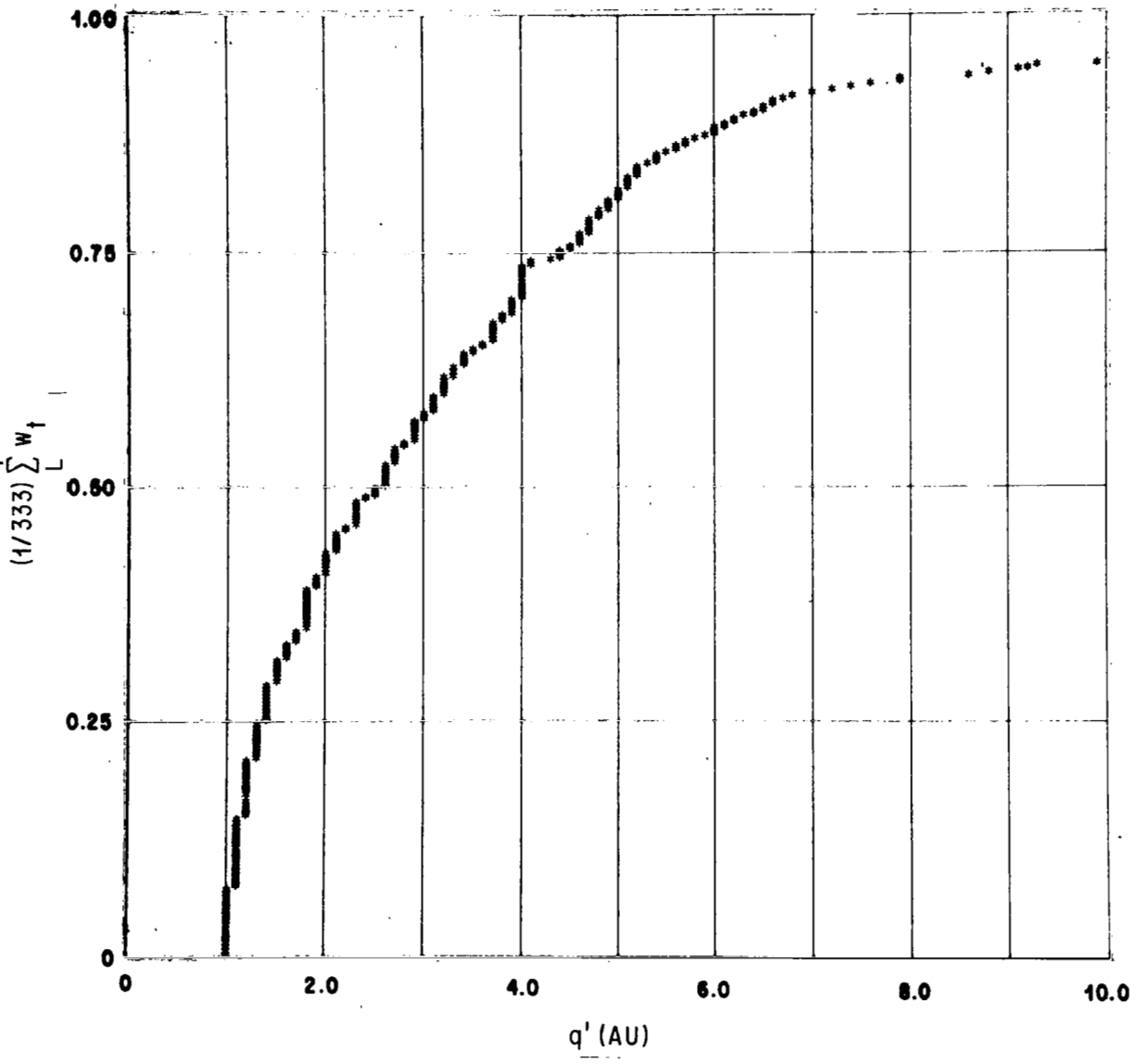

FIGURE 28b. APHELION DISTRIBUTION IN THE TERRESTRIAL INFLUX, SUB-SAMPLE "B"

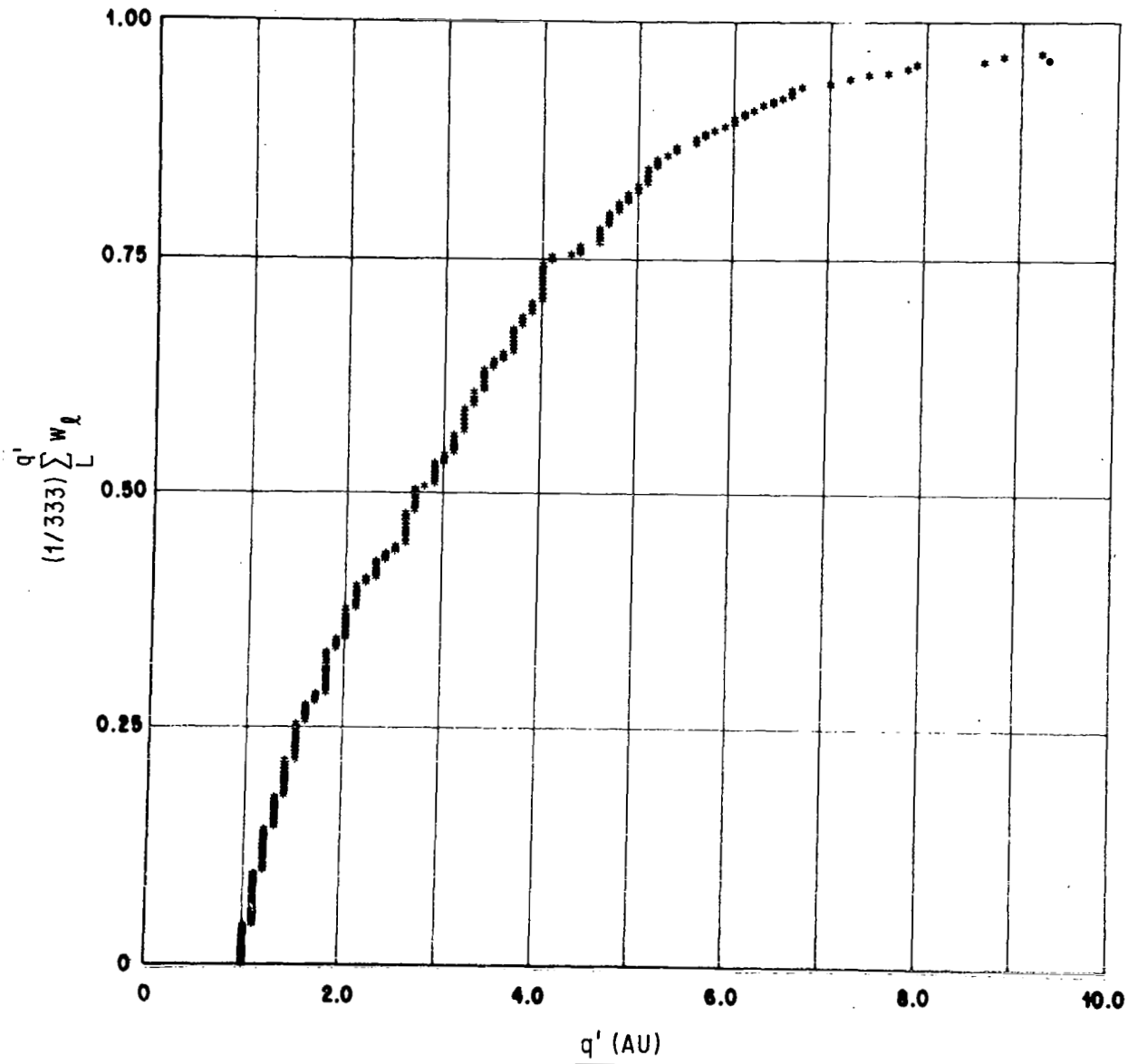

FIGURE 29a. APHELION DISTRIBUTION IN THE LUNAR INFLUX, SUB-SAMPLE "A"

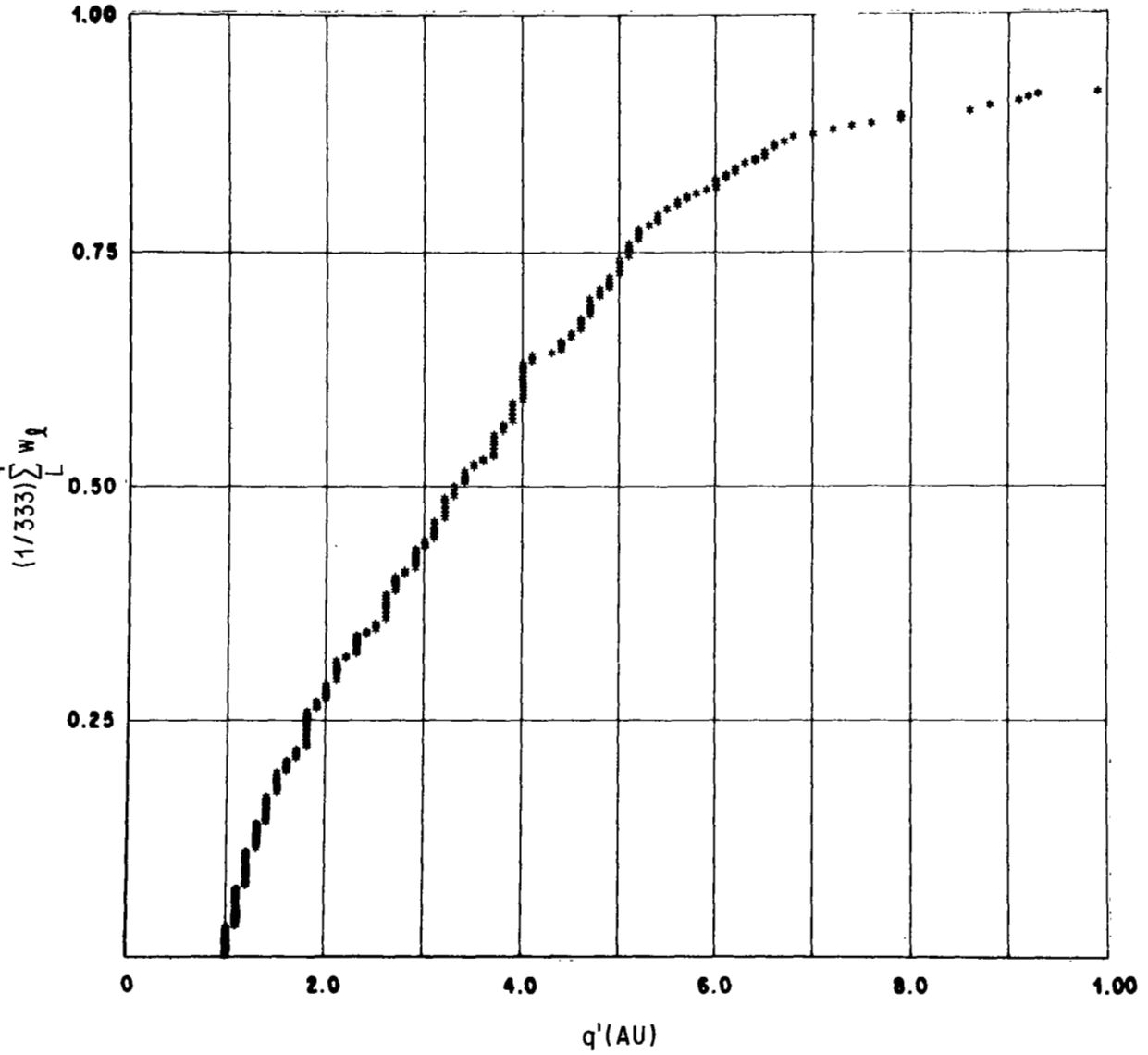

FIGURE 29b. APHELION DISTRIBUTION IN THE LUNAR INFLUX, SUB-SAMPLE "B"

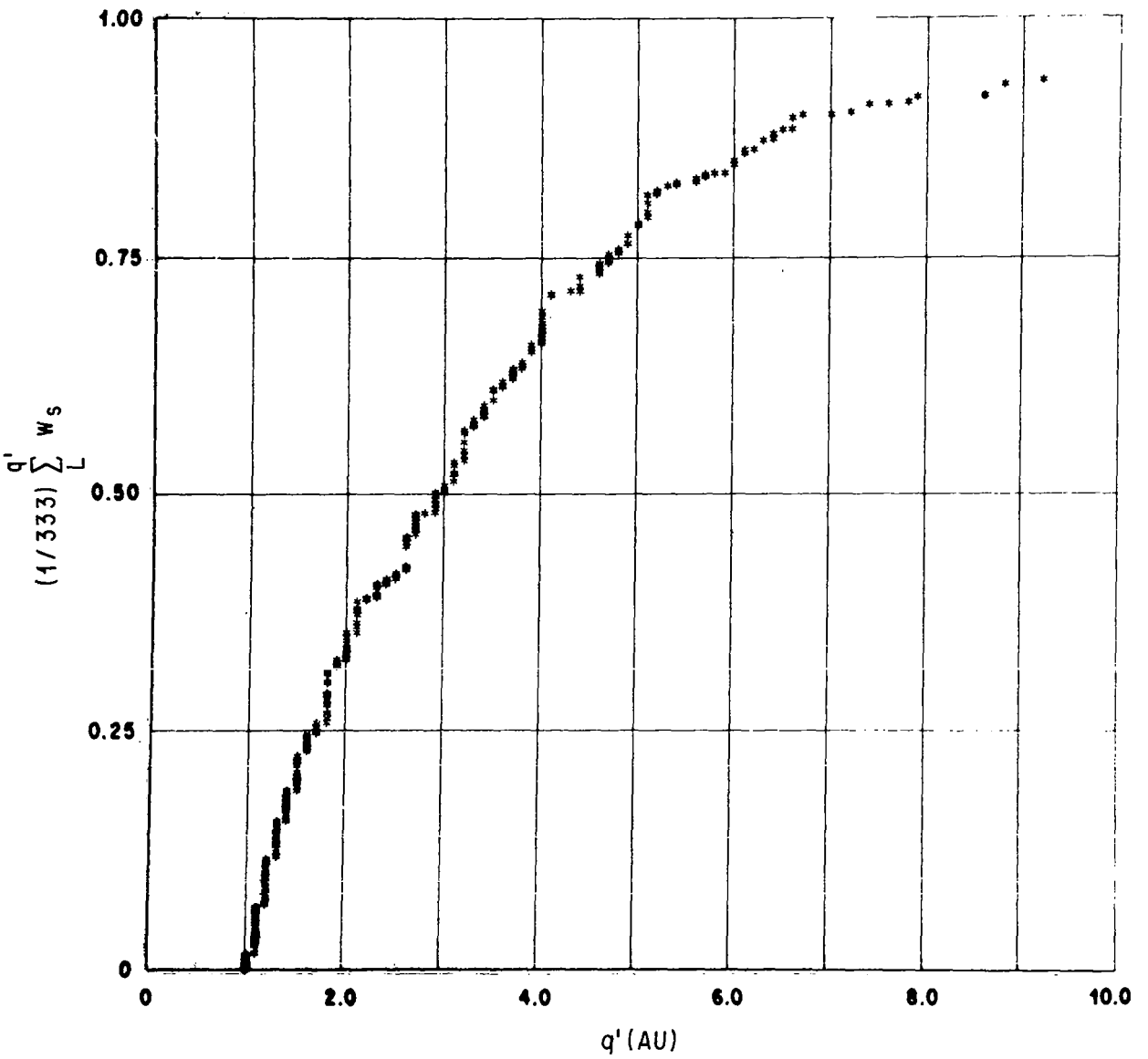

FIGURE 30a. APHELION DISTRIBUTION FOR METEOROIDS IN SPACE, SUB-SAMPLE "A"

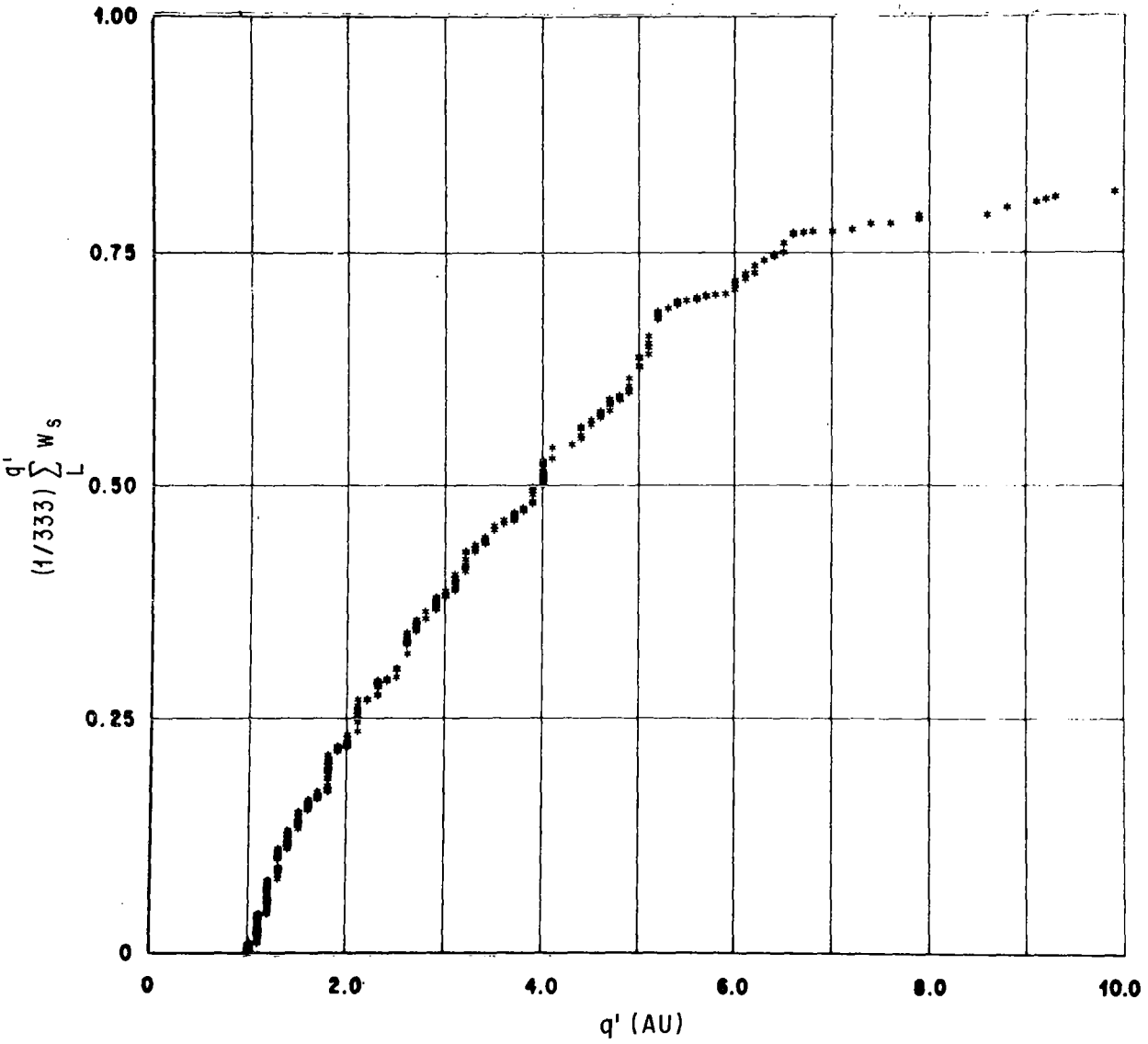

FIGURE 30b. APHELION DISTRIBUTION FOR METEOROIDS IN SPACE, SUB-SAMPLE "B"

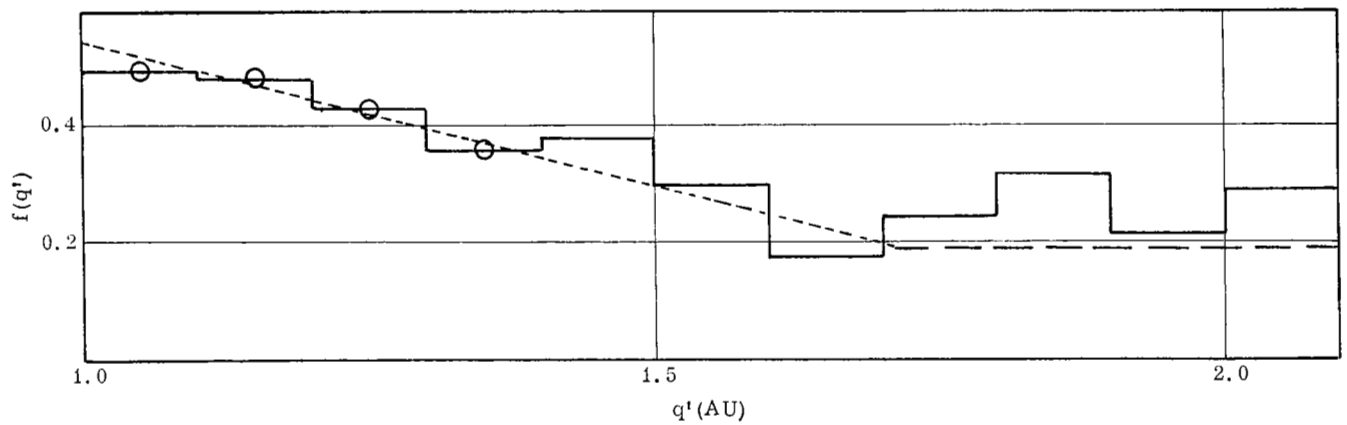

LUNAR WEIGHTING w_l

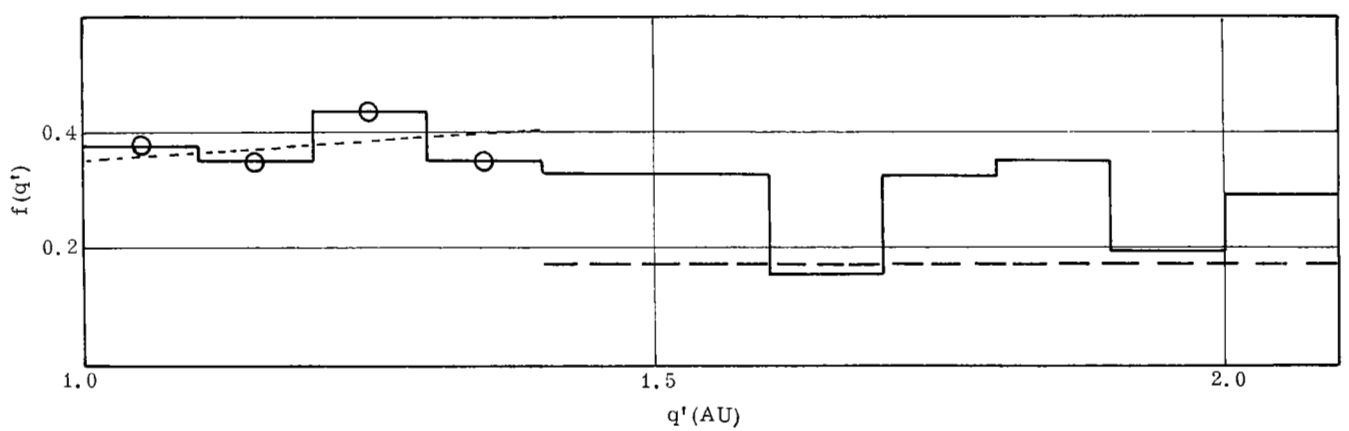

SPATIAL WEIGHTING w_s

FIGURE 31a. APHELION PROBABILITY DENSITY FUNCTION. SUB-SAMPLE "A" WITH LUNAR WEIGHTING w_l, AND SPATIAL WEIGHTING w_s

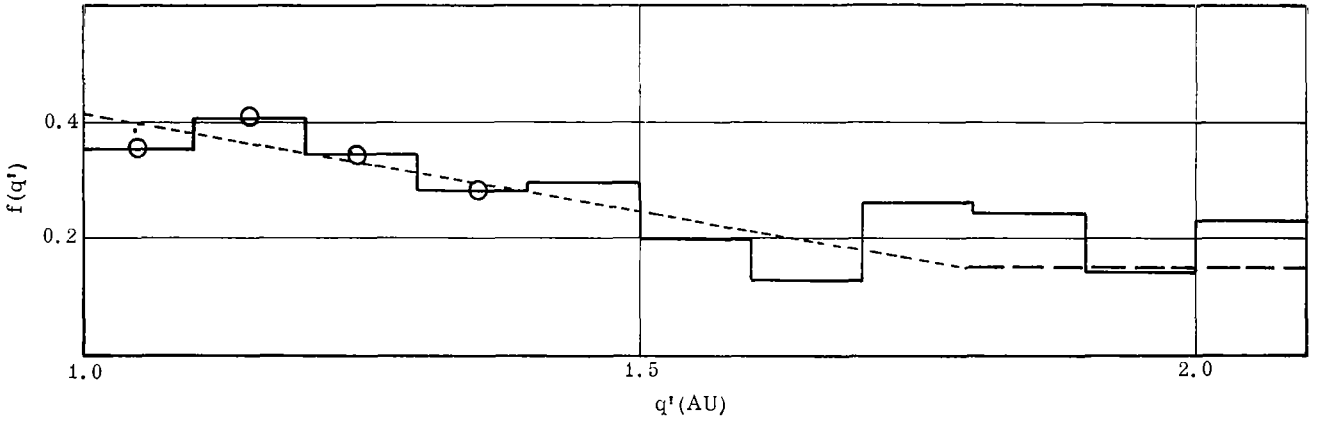

LUNAR WEIGHTING w_l

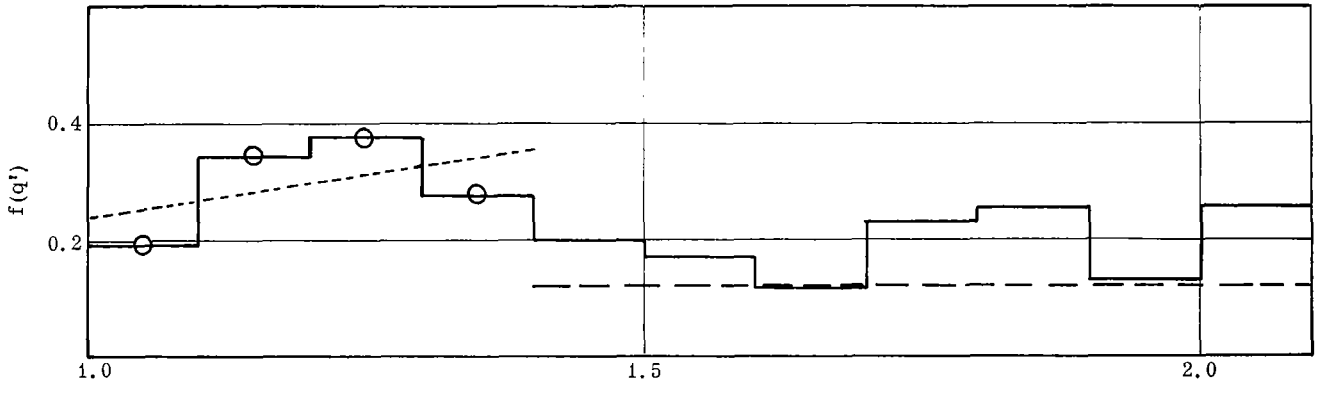

SPATIAL WEIGHTING w_s

FIGURE 31b. APHELION PROBABILITY DENSITY FUNCTION. SUB-SAMPLE "B" WITH LUNAR WEIGHTING w_l, AND SPATIAL WEIGHTING w_s

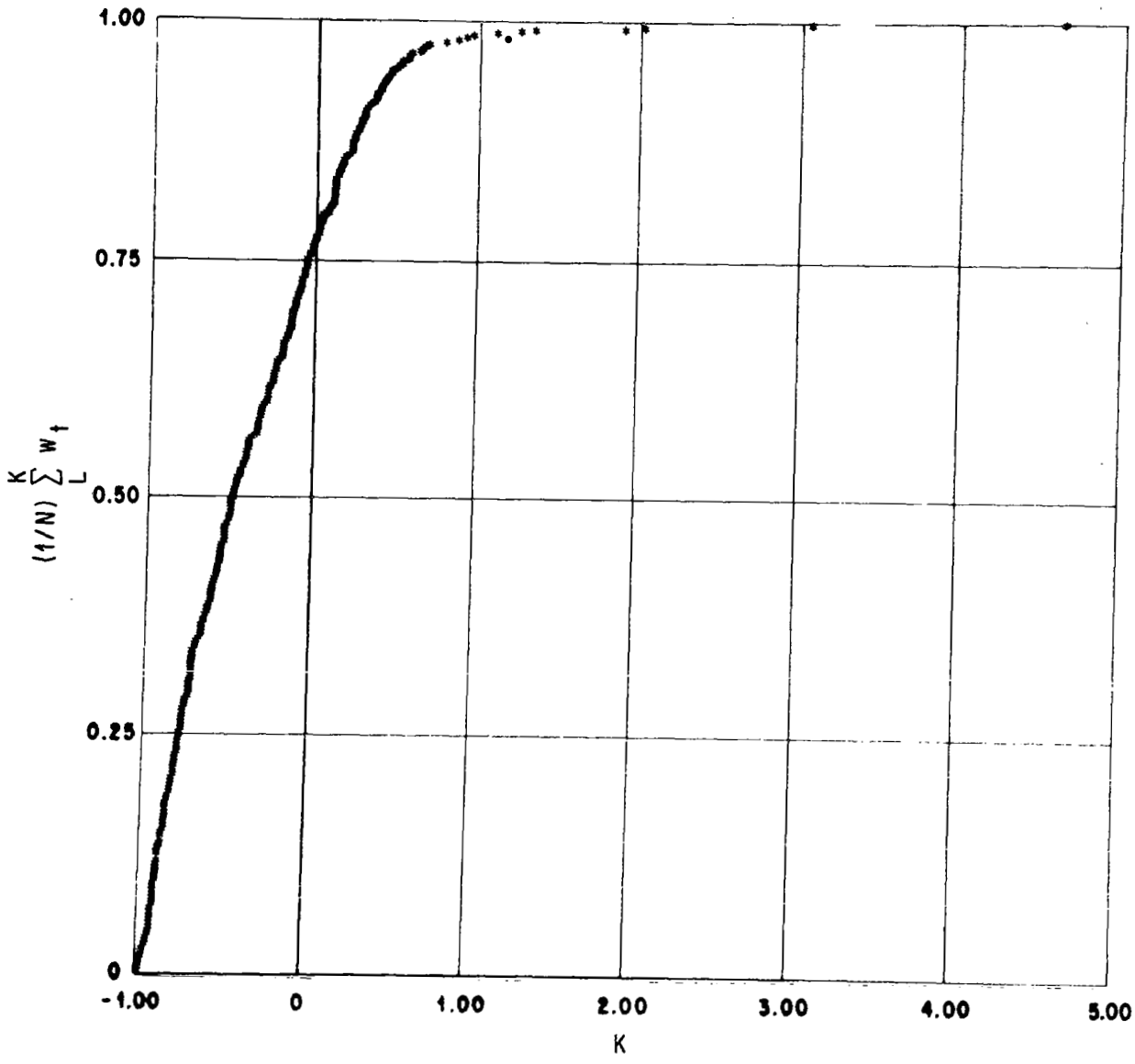

FIGURE 32a. DISTRIBUTION OF WHIPPLE'S COMET-ASTEROID CRITERION, TERRESTRIAL WEIGHTING, SUB-SAMPLE "A"

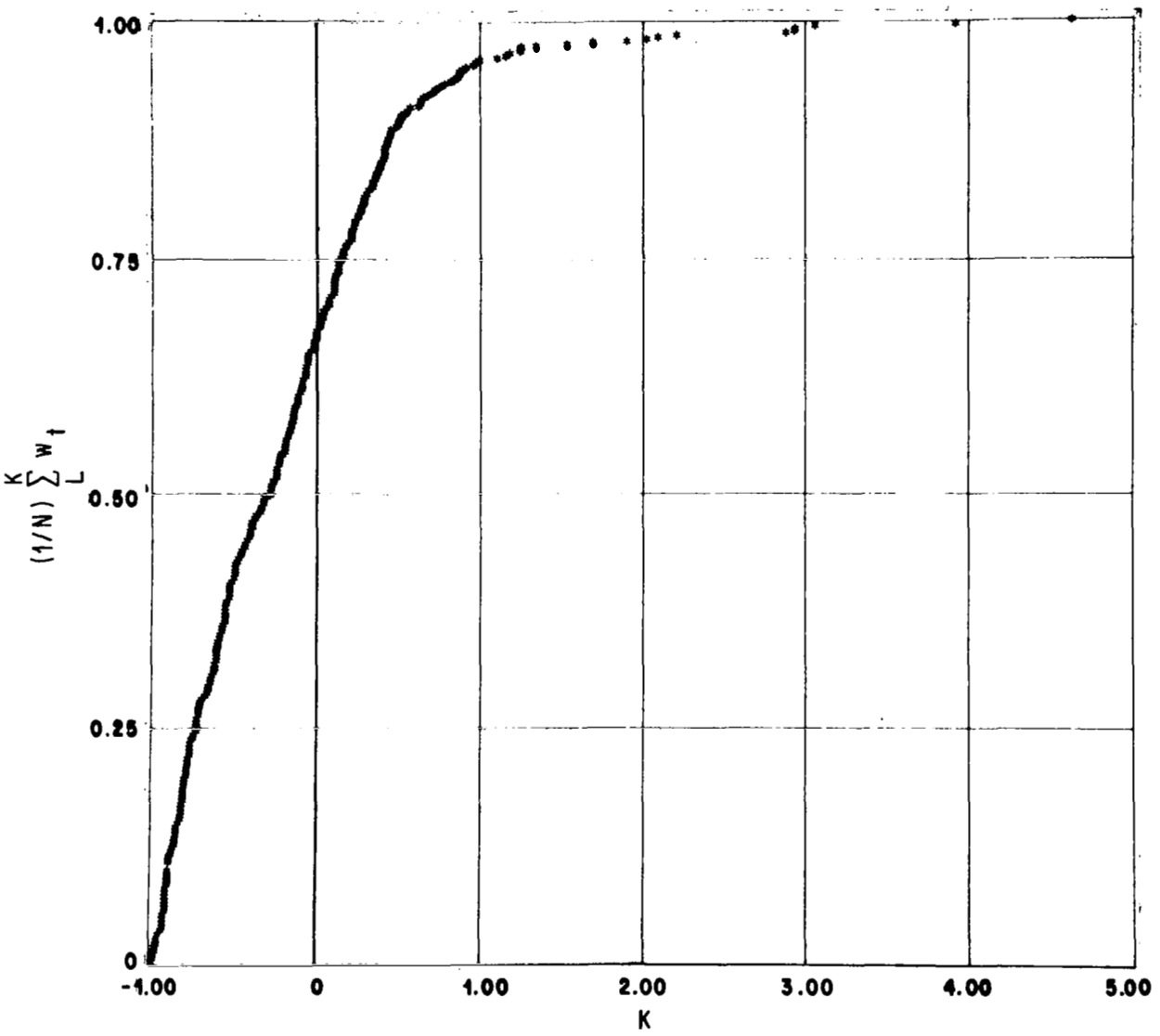

FIGURE 32b. DISTRIBUTION OF WHIPPLE'S COMET-ASTEROID CRITERION, TERRESTRIAL WEIGHTING, SUB-SAMPLE "B"

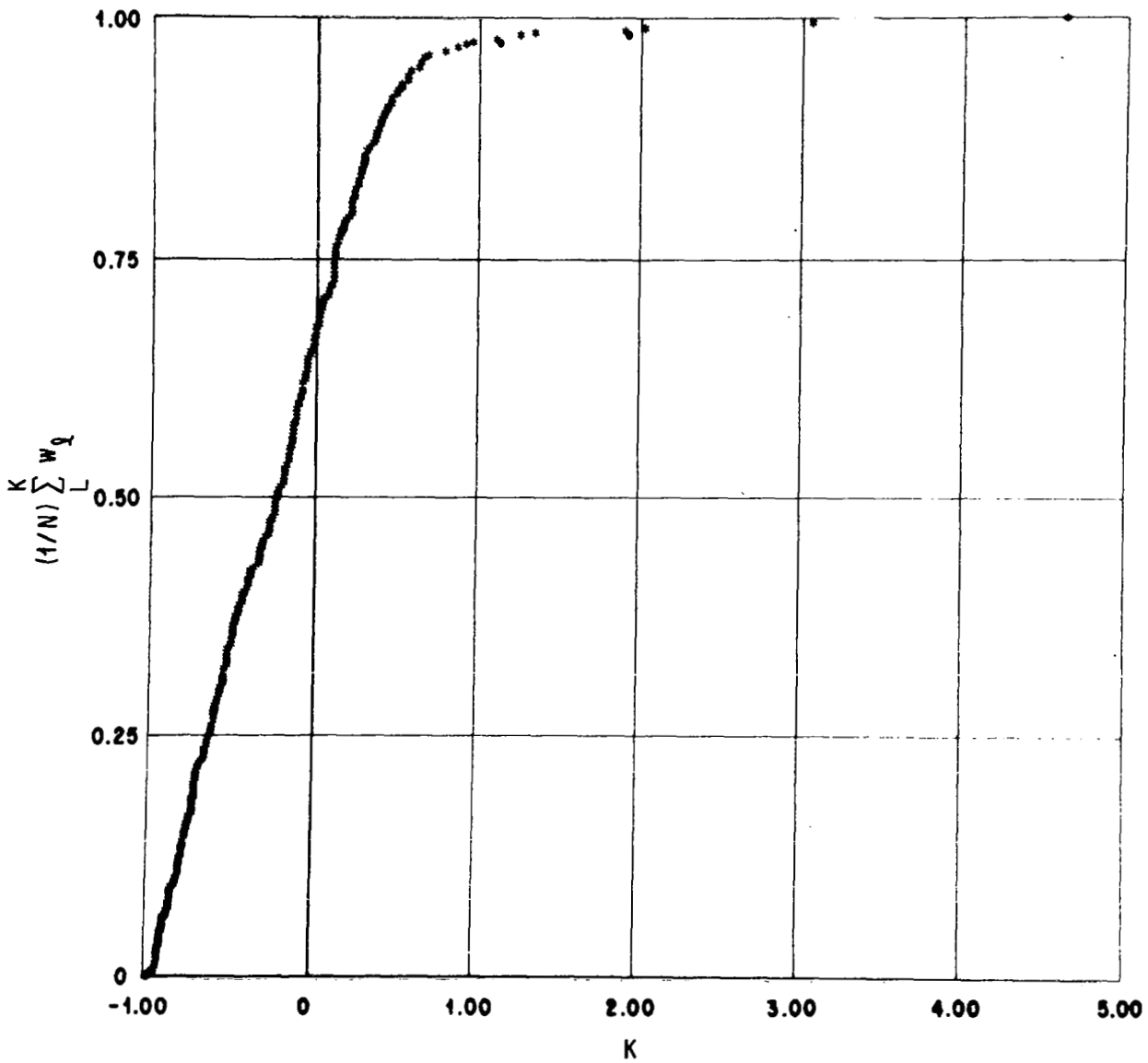

FIGURE 33a. DISTRIBUTION OF WHIPPLE'S COMET-ASTEROID CRITERION, LUNAR WEIGHTING, SUB-SAMPLE "A"

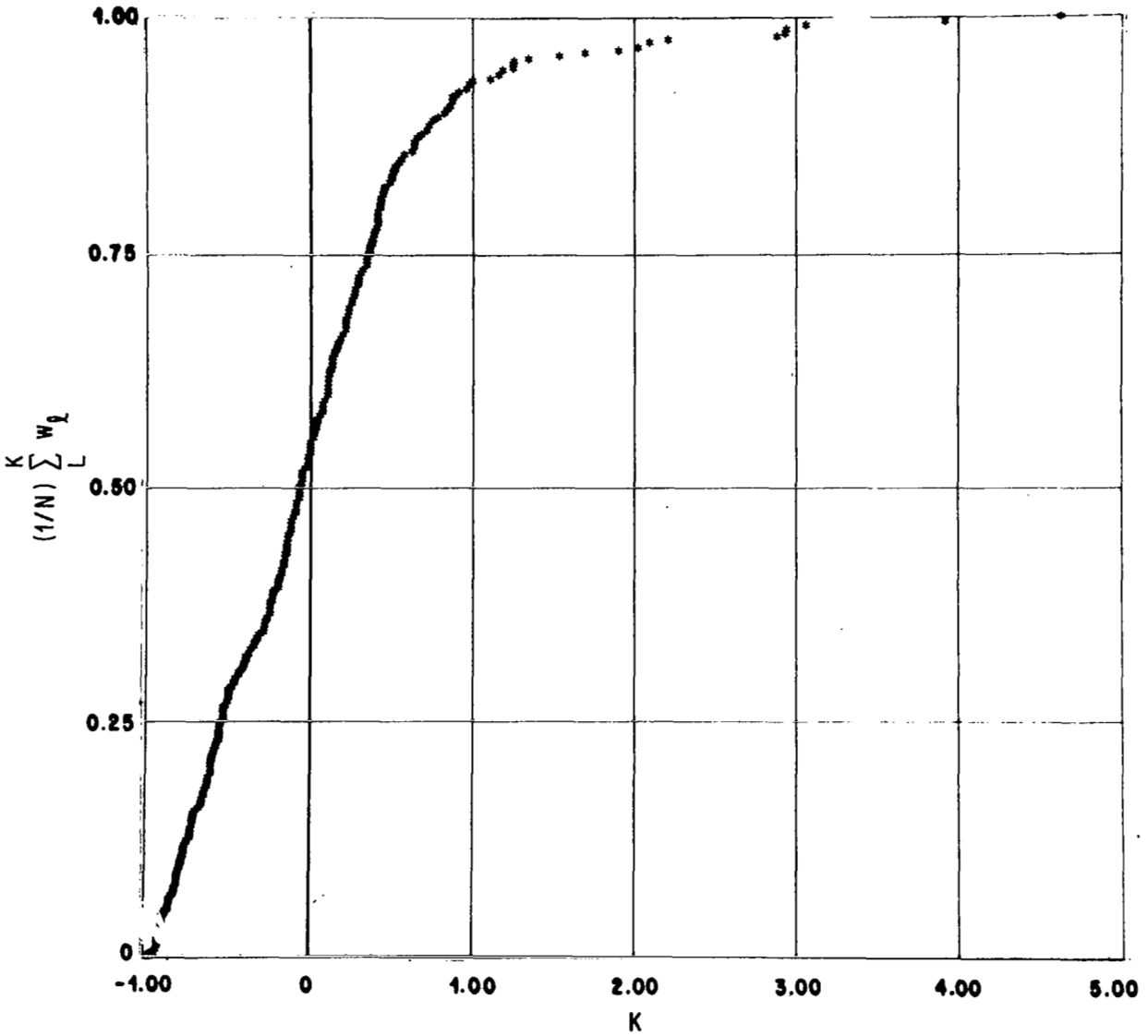

FIGURE 33b. DISTRIBUTION OF WHIPPLE'S COMET-ASTEROID CRITERION, LUNAR WEIGHTING, SUB-SAMPLE "B"

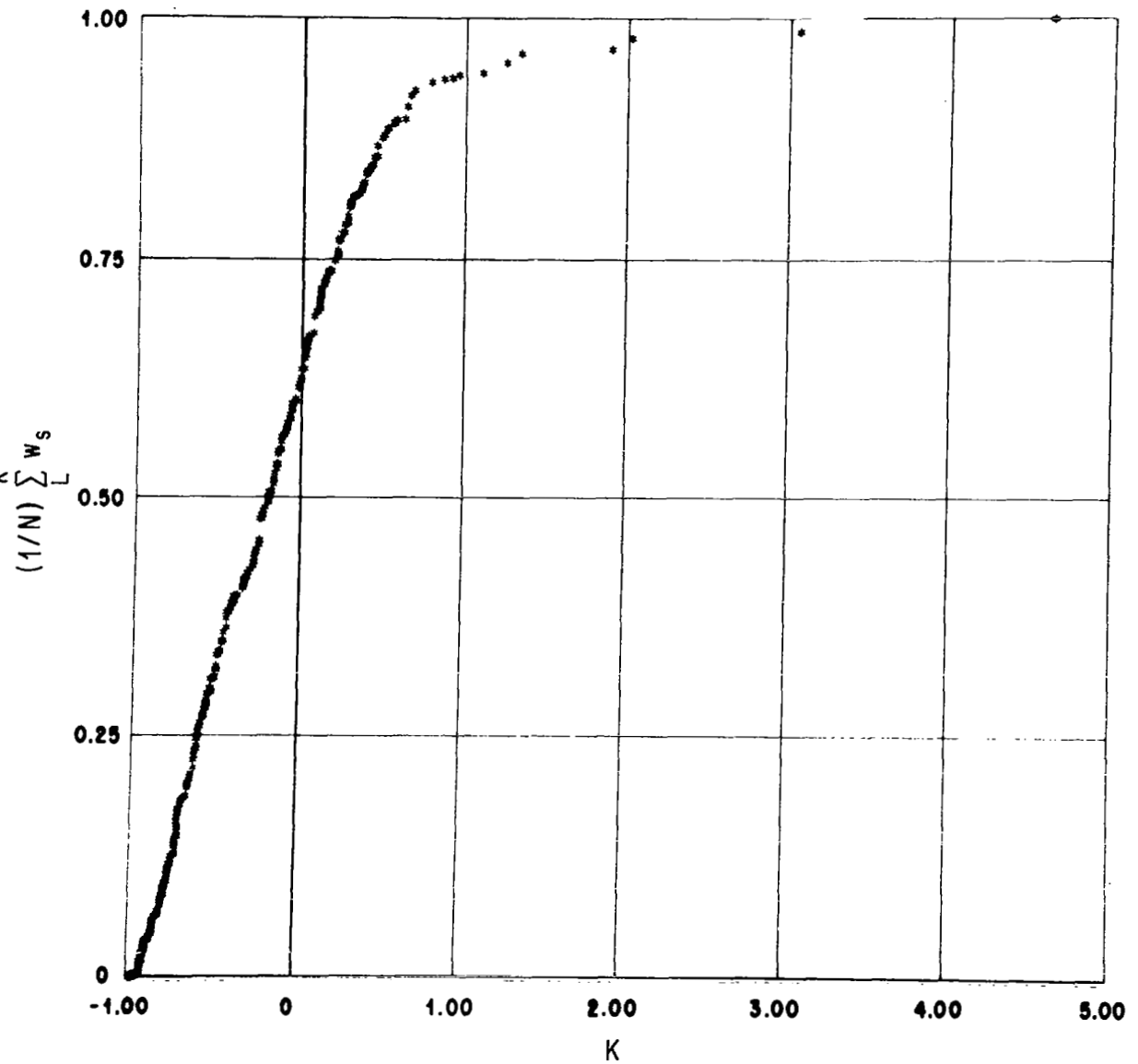

FIGURE 34a. DISTRIBUTION OF WHIPPLE'S COMET-ASTEROID CRITERION, SPATIAL WEIGHTING, SUB-SAMPLE "A"

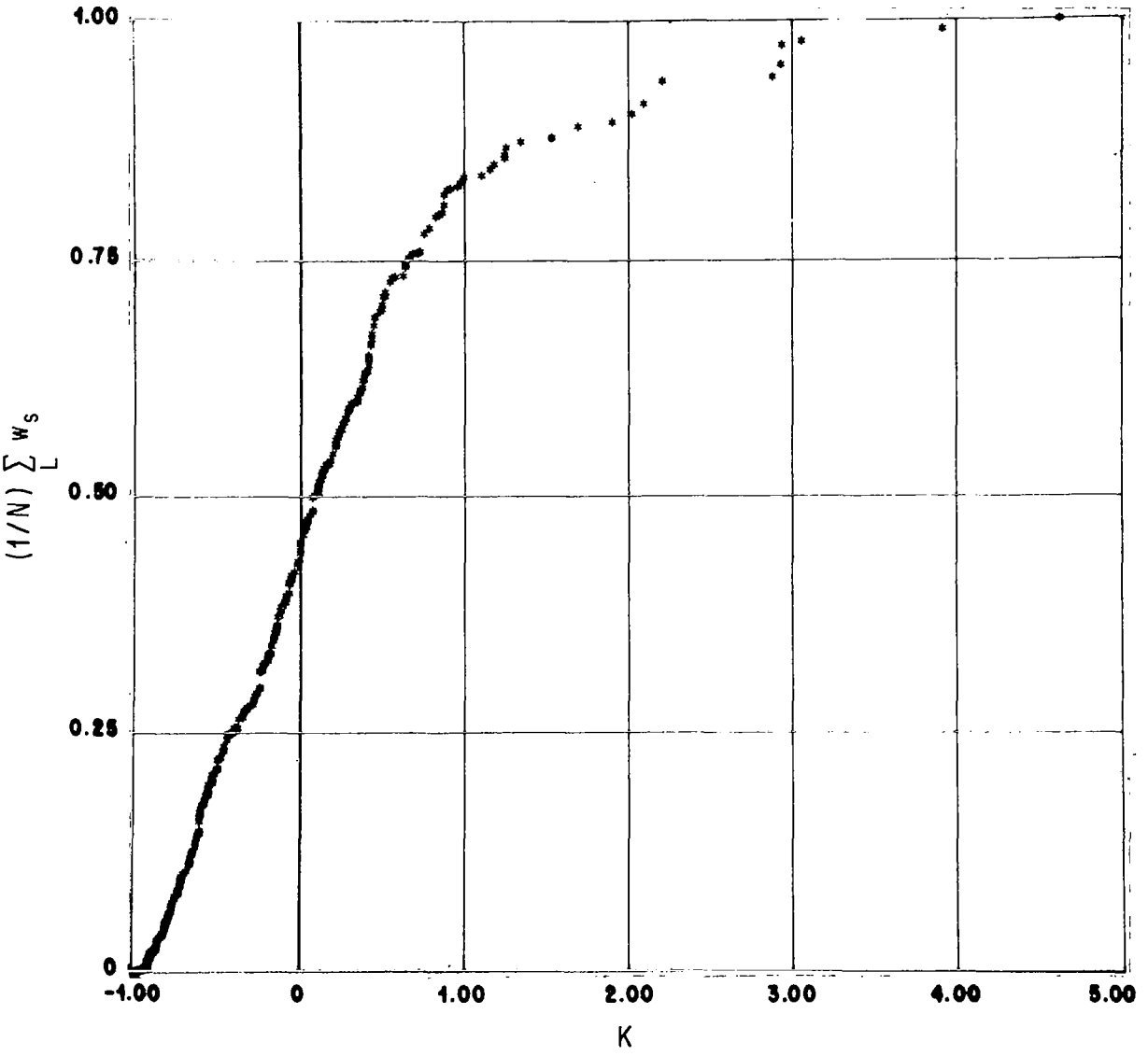

FIGURE 34b. DISTRIBUTION OF WHIPPLE'S COMET-ASTEROID CRITERION, SPATIAL WEIGHTING, SUB-SAMPLE "B"

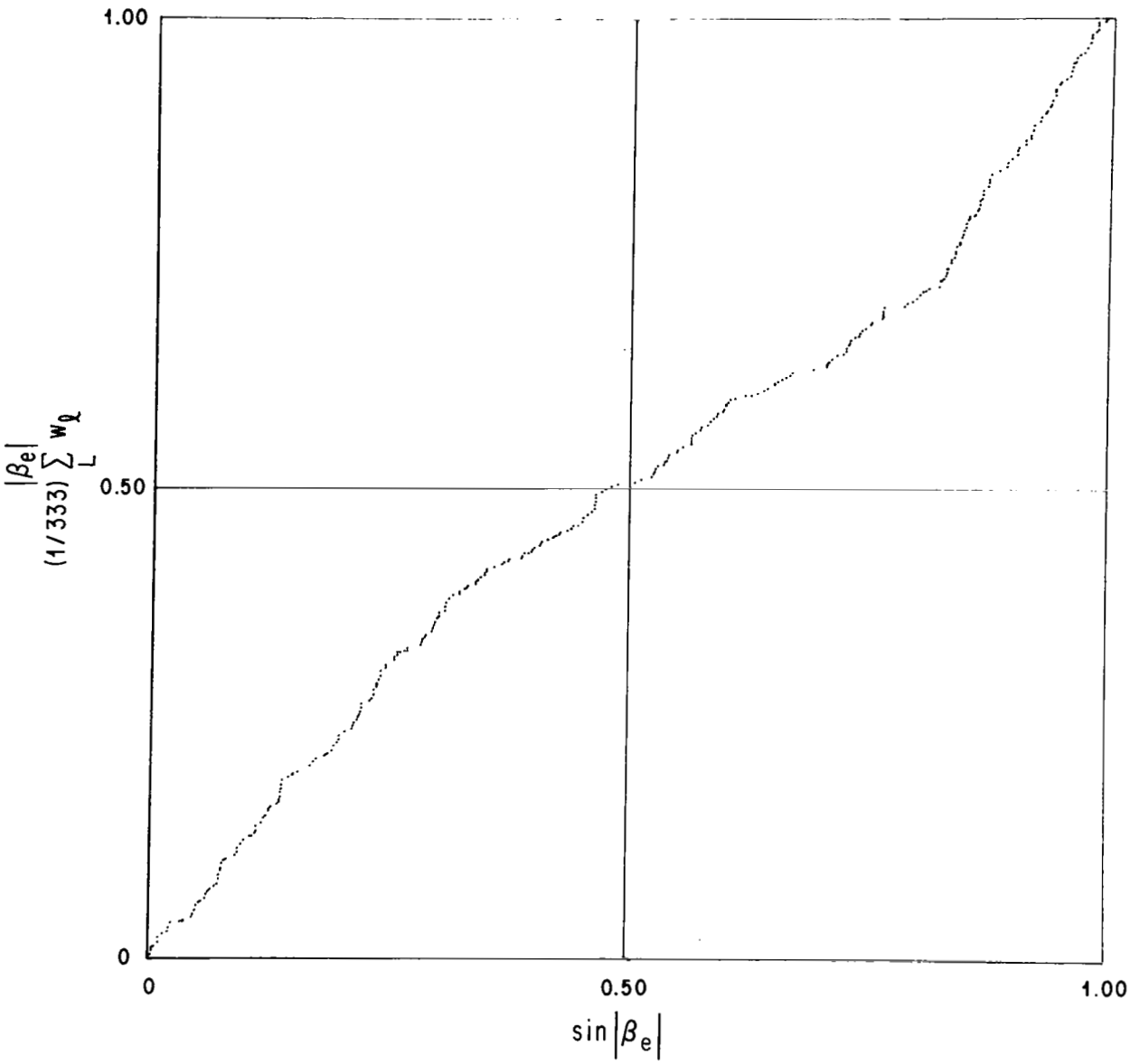

FIGURE 35a. DISTRIBUTION OF ARITHMETIC CELESTIAL LATITUDE OF RADIANT, LUNAR WEIGHTING, SUB-SAMPLE "A"

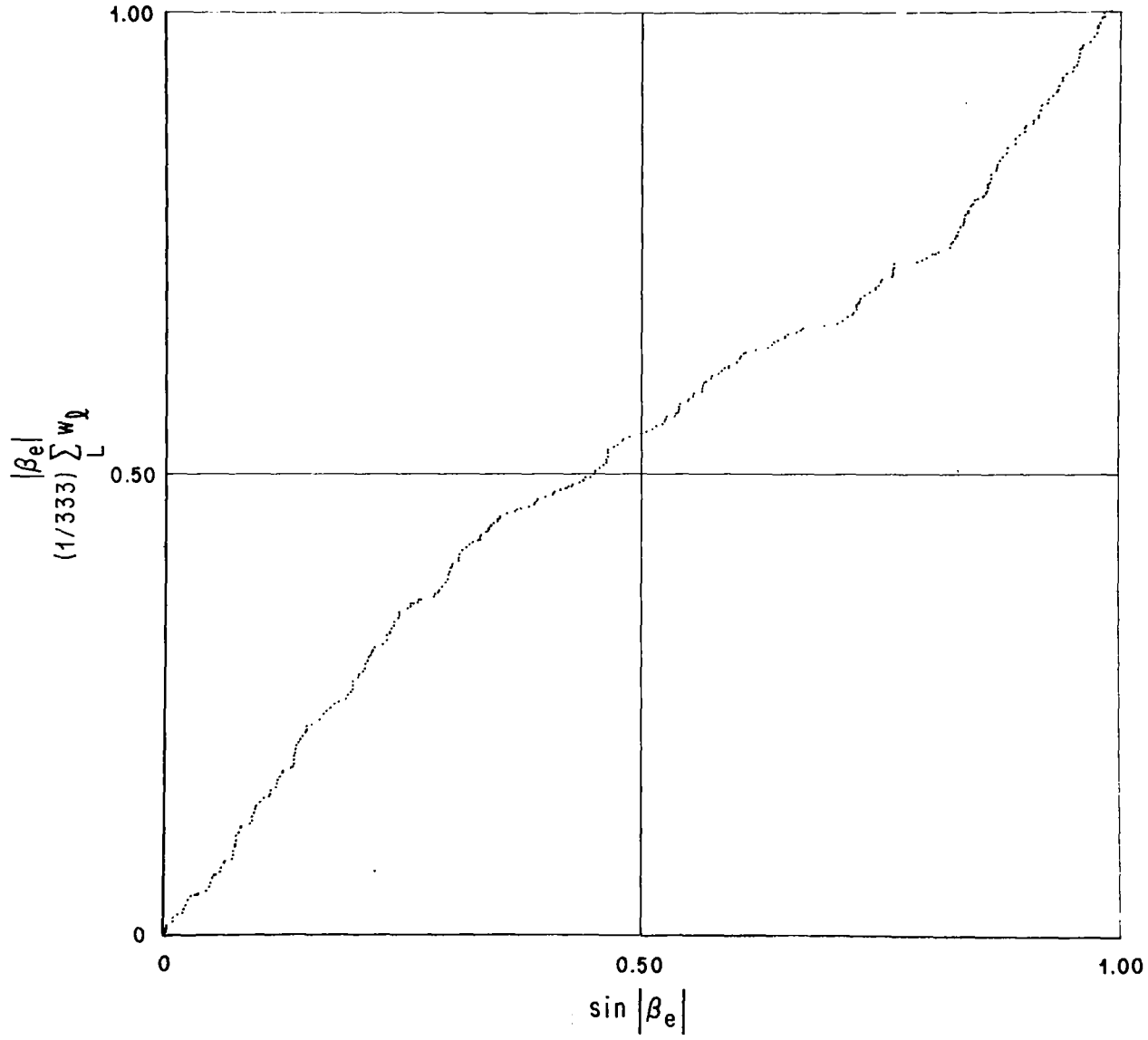

FIGURE 35b. DISTRIBUTION OF ARITHMETIC CELESTIAL LATITUDE OF RADIANT, LUNAR WEIGHTING, SUB-SAMPLE "B"

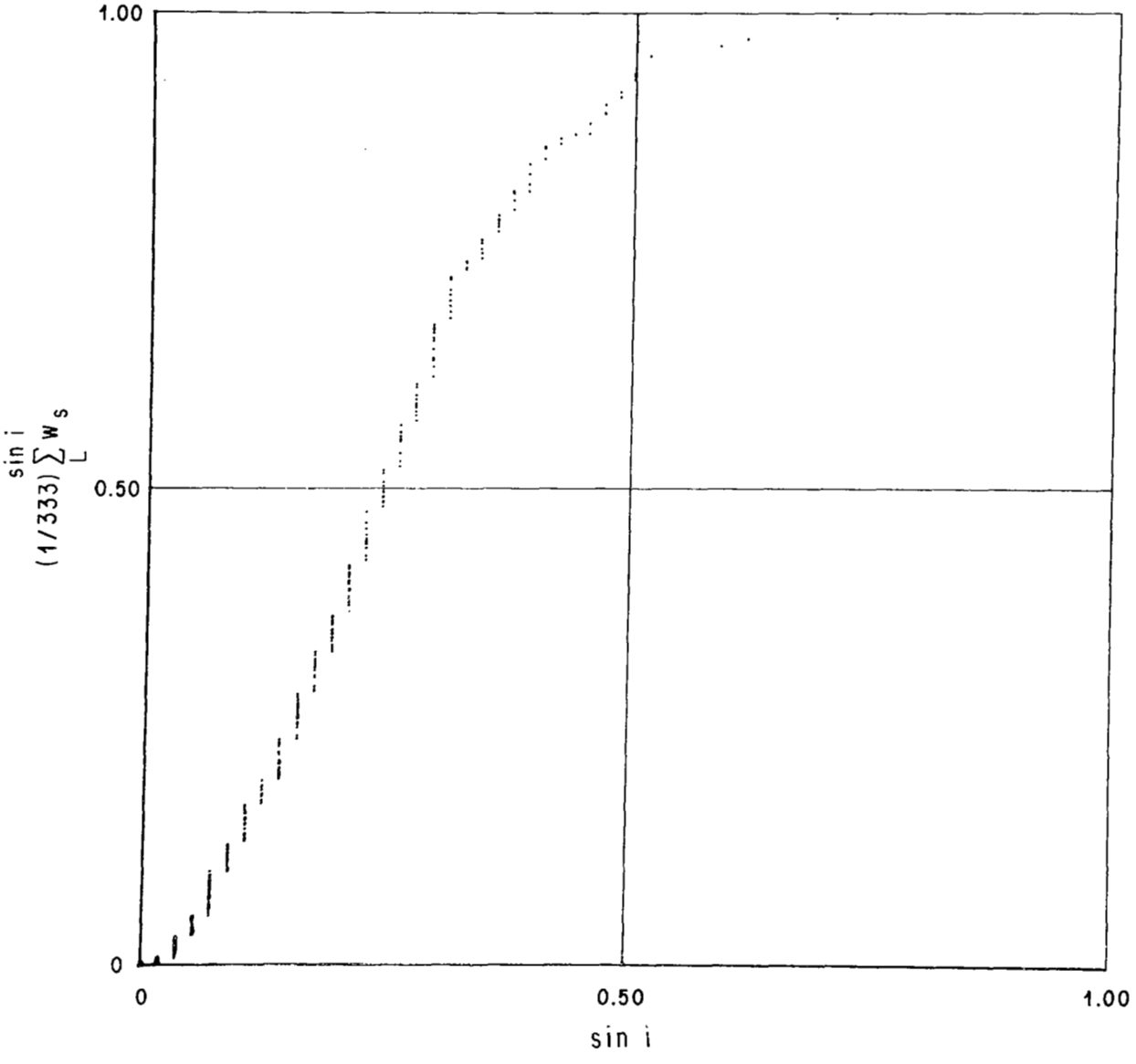

FIGURE 36a. DISTRIBUTION OF SINE INCLINATION OF ORBIT TO ECLIPTIC, SPATIAL WEIGHTING, SUB-SAMPLE "A"

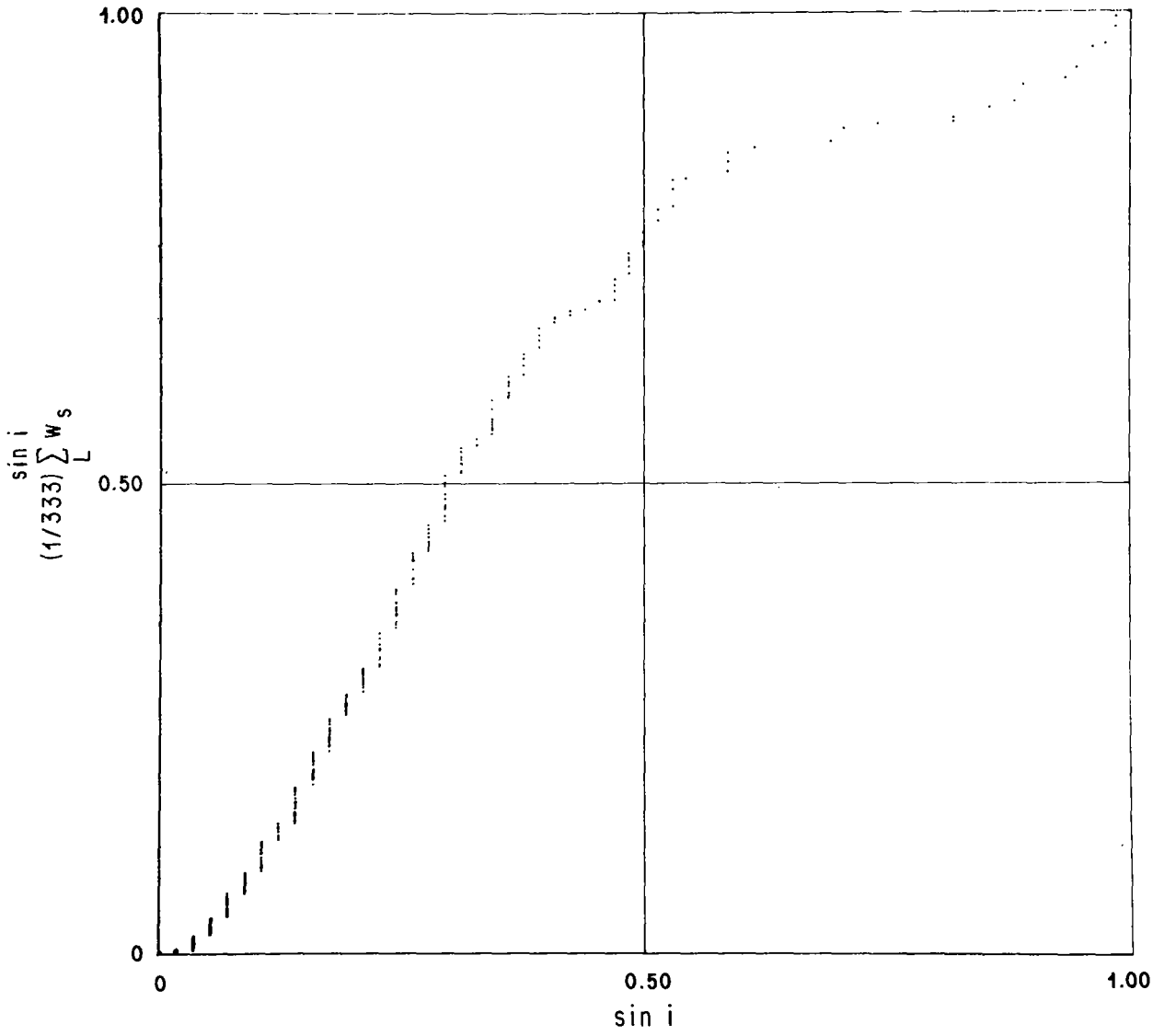

FIGURE 36b. DISTRIBUTION OF SINE INCLINATION OF ORBIT TO ECLIPTIC, SPATIAL WEIGHTING, SUB-SAMPLE "B"

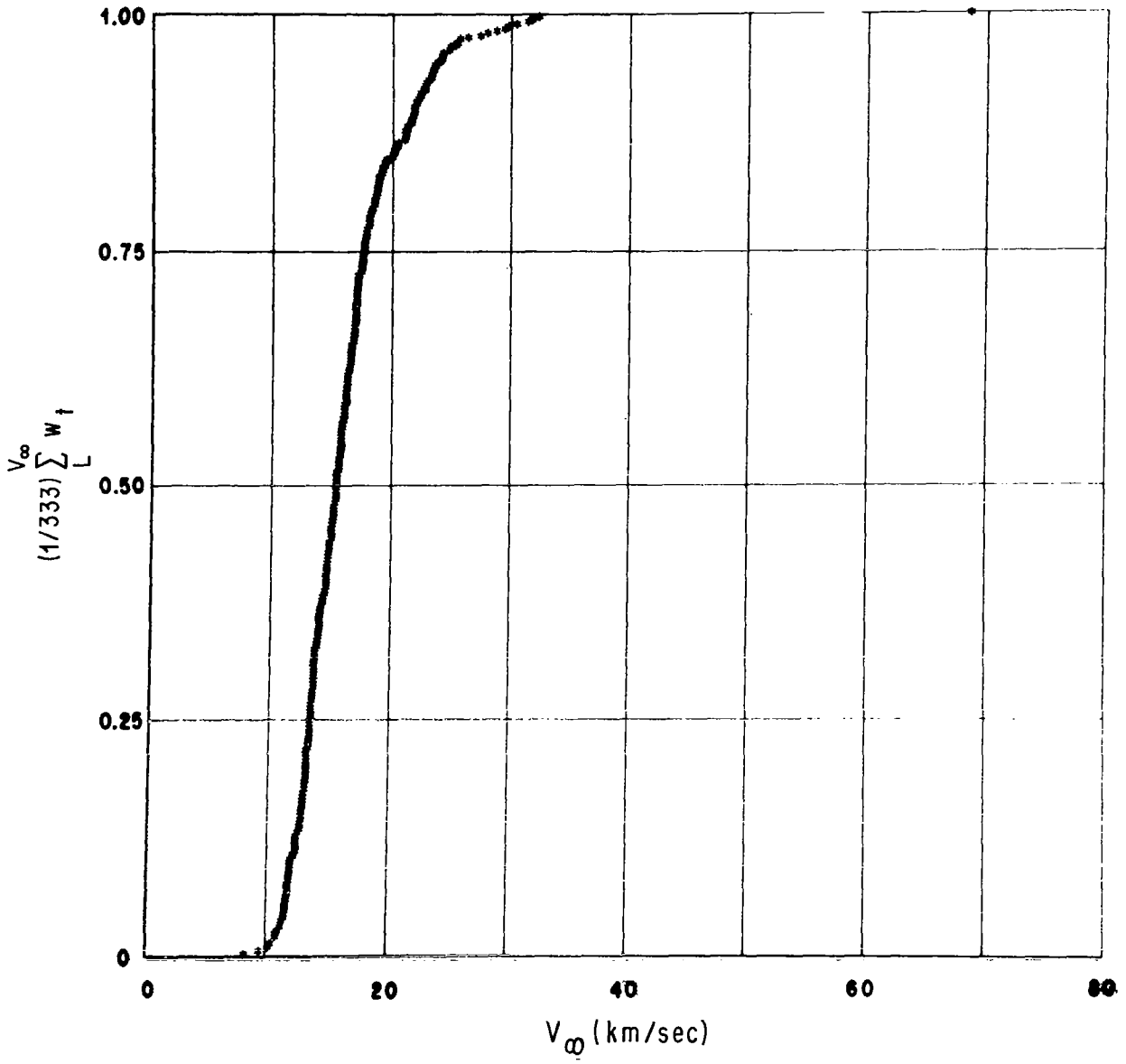

FIGURE 37a. DISTRIBUTION OF AIR-ENTRY VELOCITY, TERRESTRIAL WEIGHTING, SUB-SAMPLE "A"

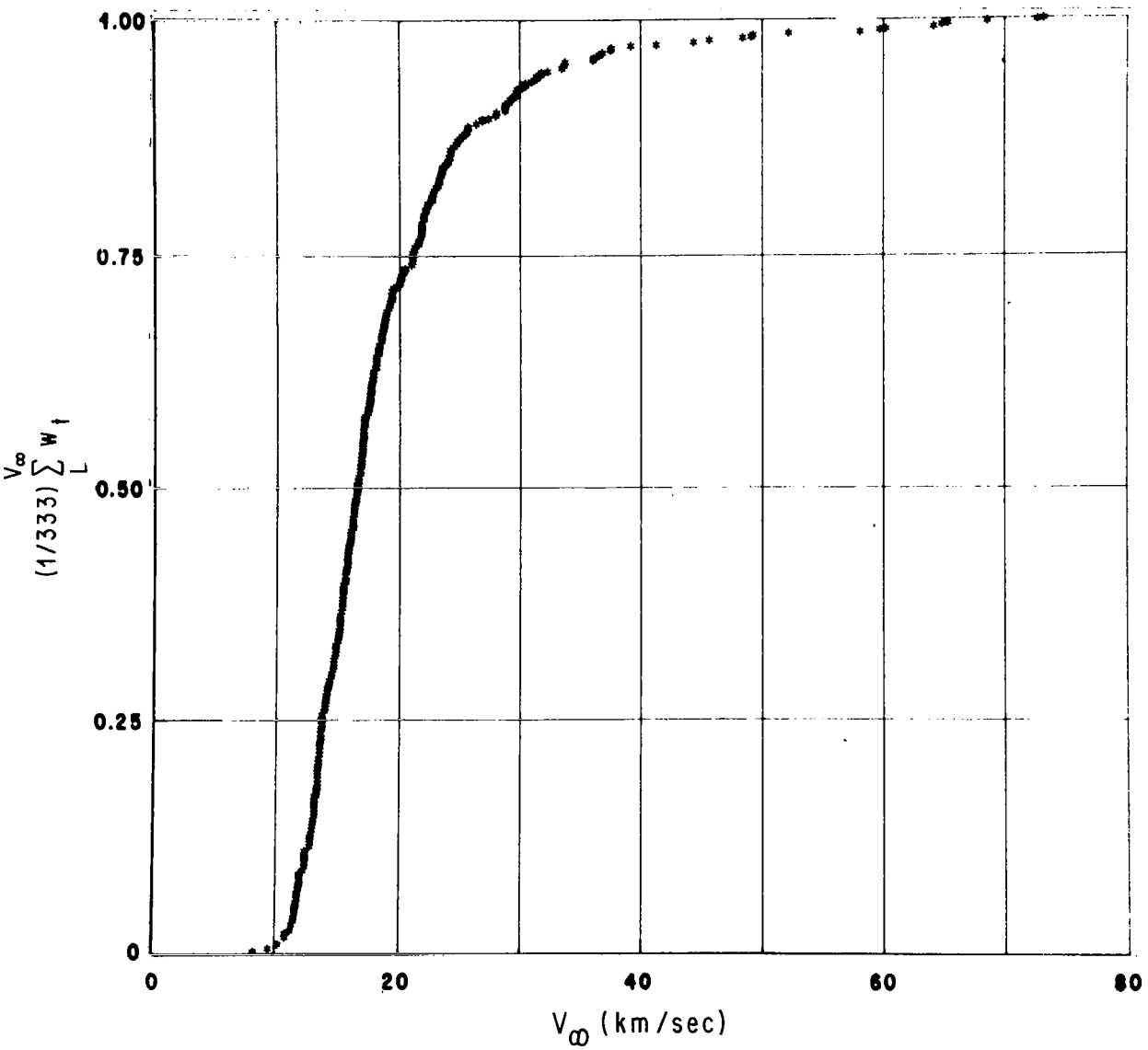

FIGURE 37b. DISTRIBUTION OF AIR-ENTRY VELOCITY, TERRESTRIAL WEIGHTING, SUB-SAMPLE "B"

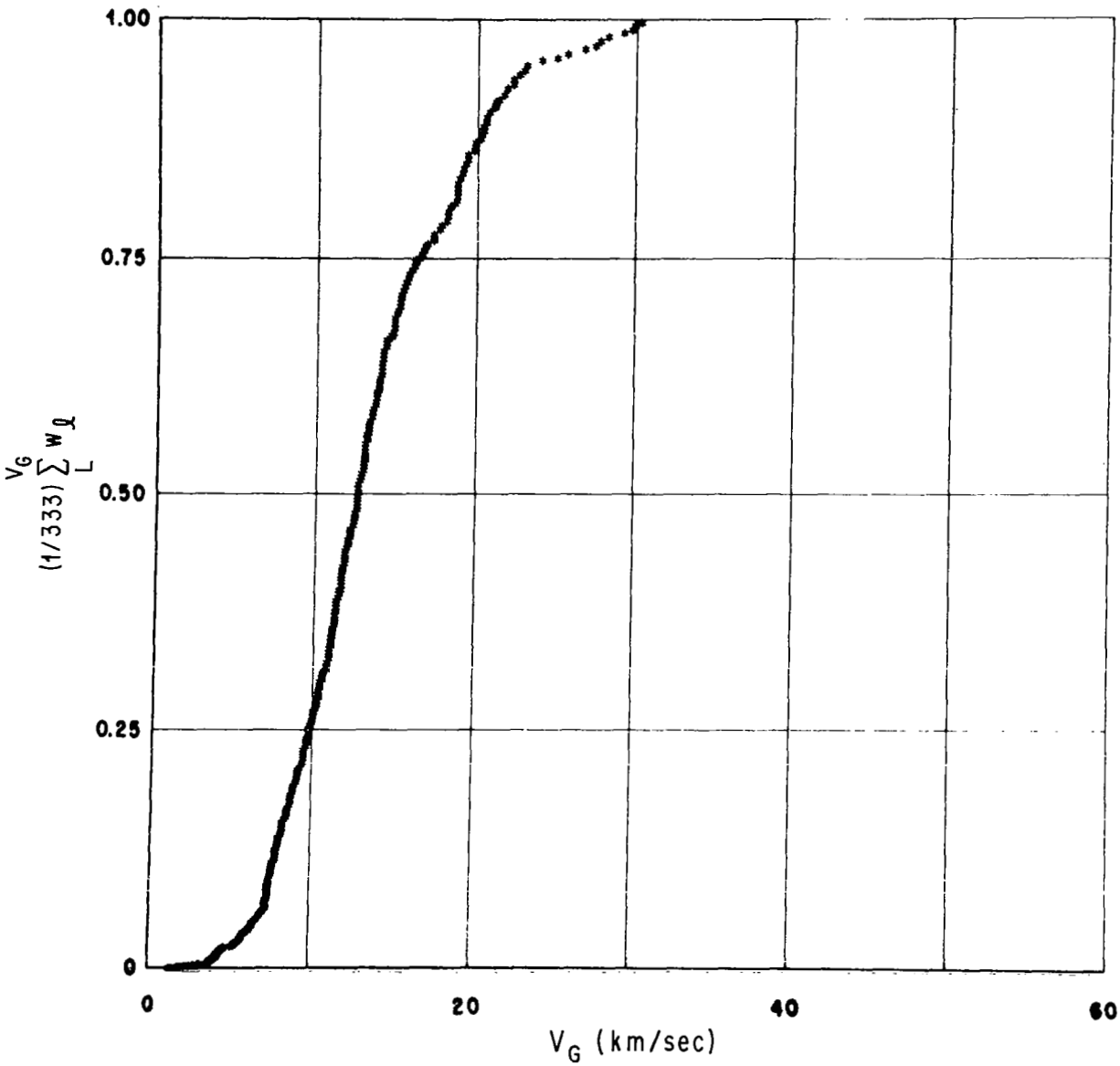

FIGURE 38a. DISTRIBUTION OF LUNAR-IMPACT VELOCITY, LUNAR WEIGHTING, SUB-SAMPLE "A"

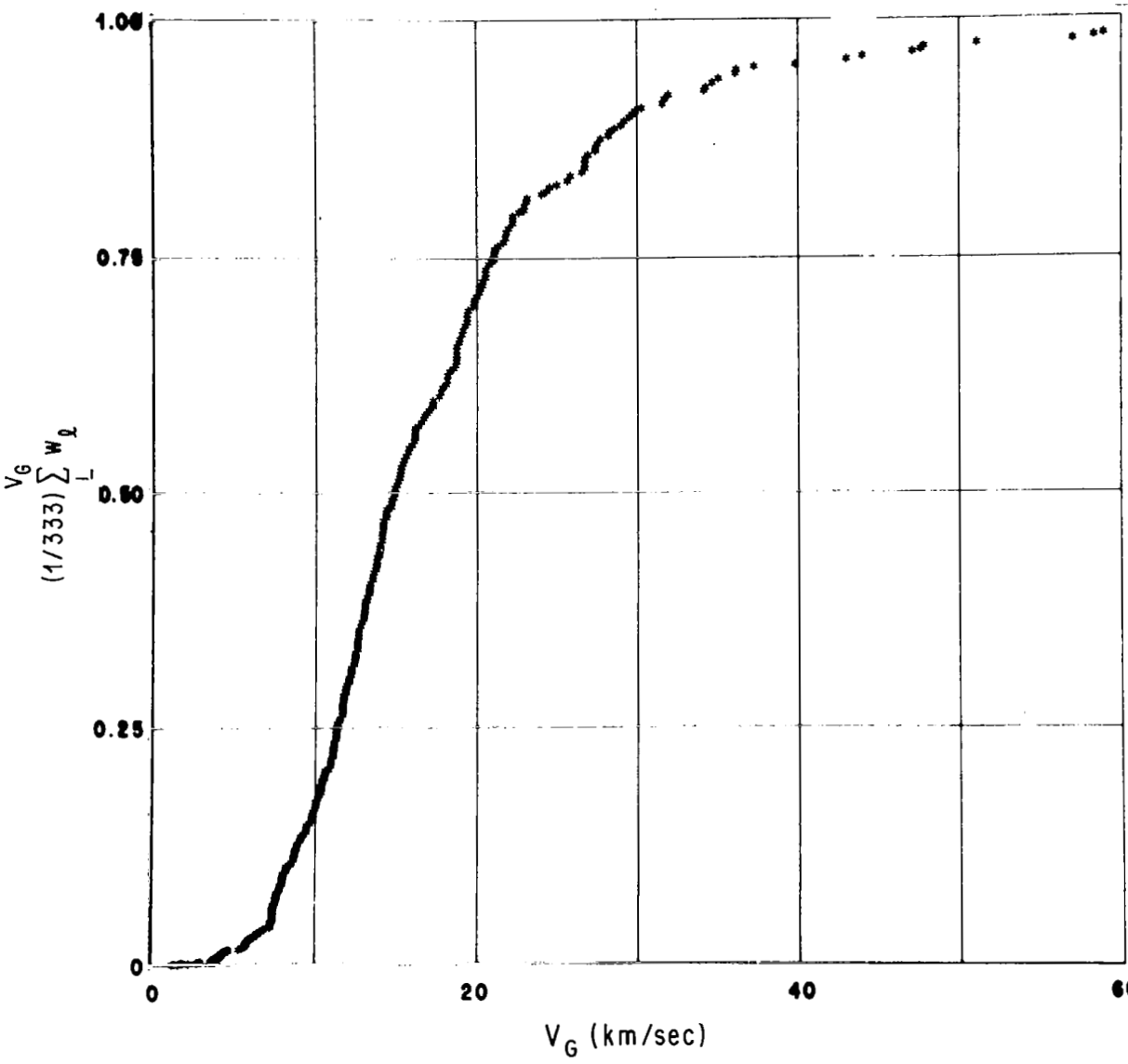

FIGURE 38b. DISTRIBUTION OF LUNAR-IMPACT VELOCITY, LUNAR WEIGHTING, SUB-SAMPLE "B"

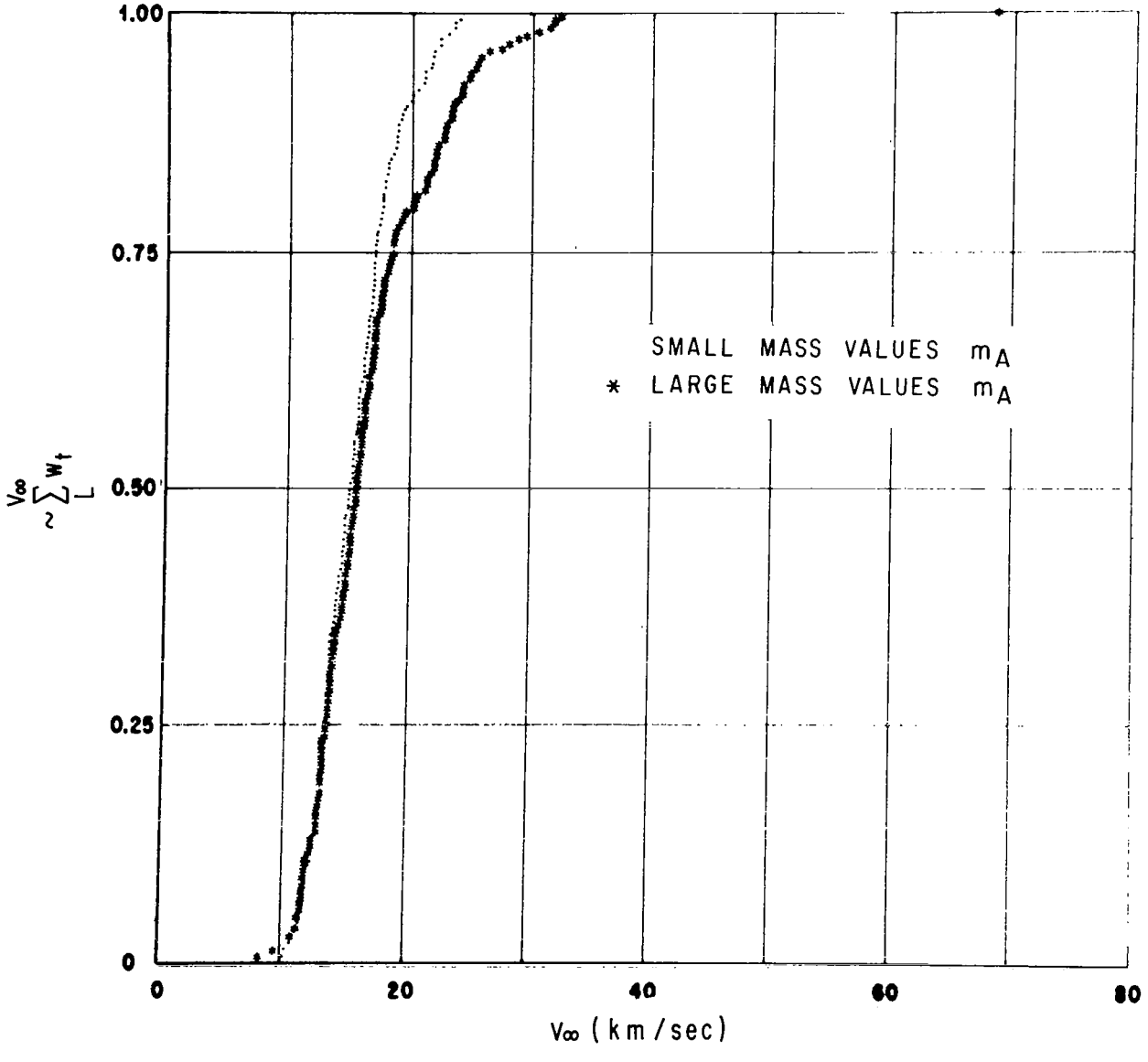

FIGURE 39a. DISTRIBUTION OF AIR-ENTRY VELOCITY FOR TWO MASS REGIMES, TERRESTRIAL WEIGHTING, SUB-SAMPLE "A"

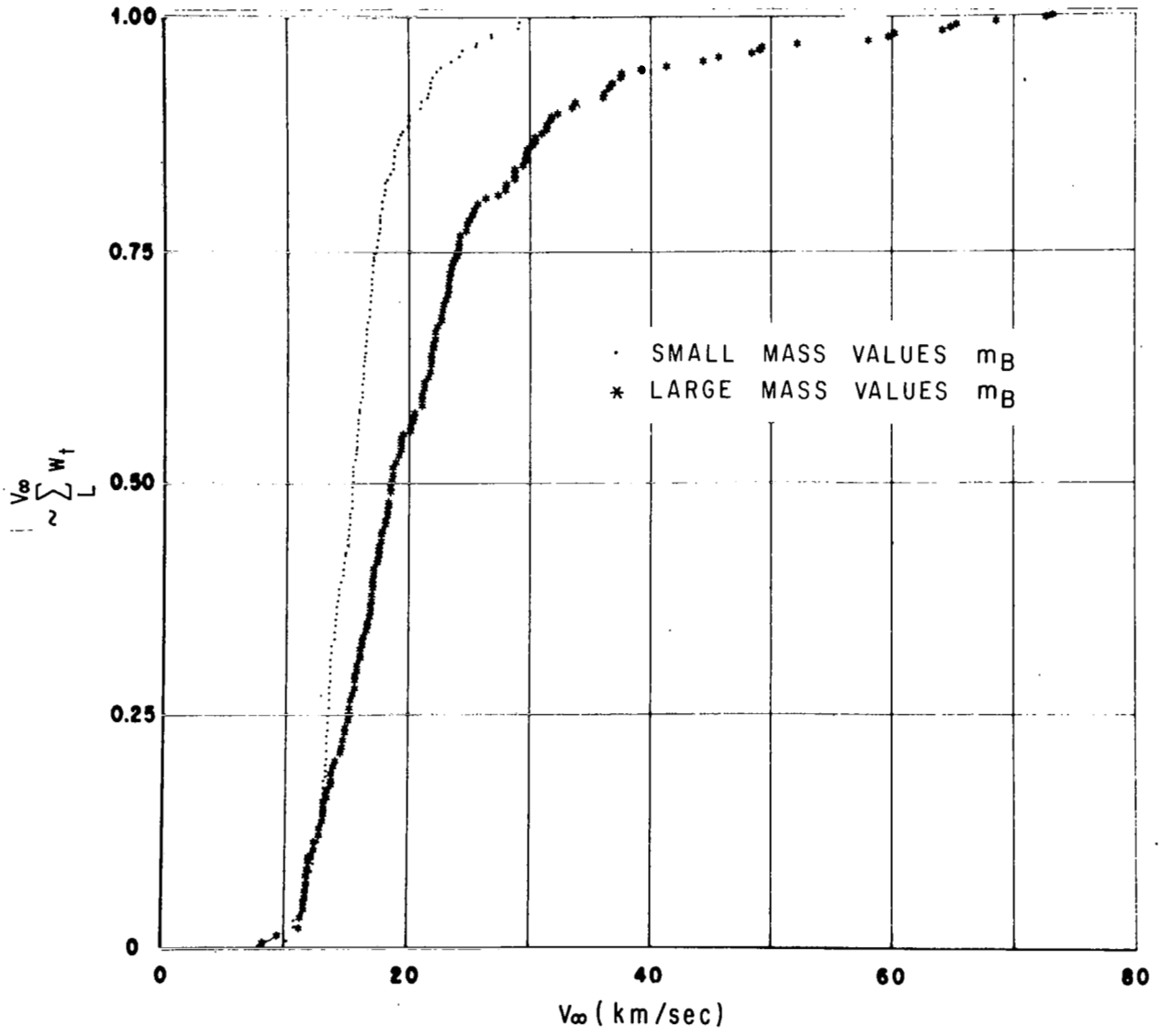

FIGURE 39b. DISTRIBUTION OF AIR-ENTRY VELOCITY FOR TWO MASS REGIMES, TERRESTRIAL WEIGHTING, SUB-SAMPLE "B"

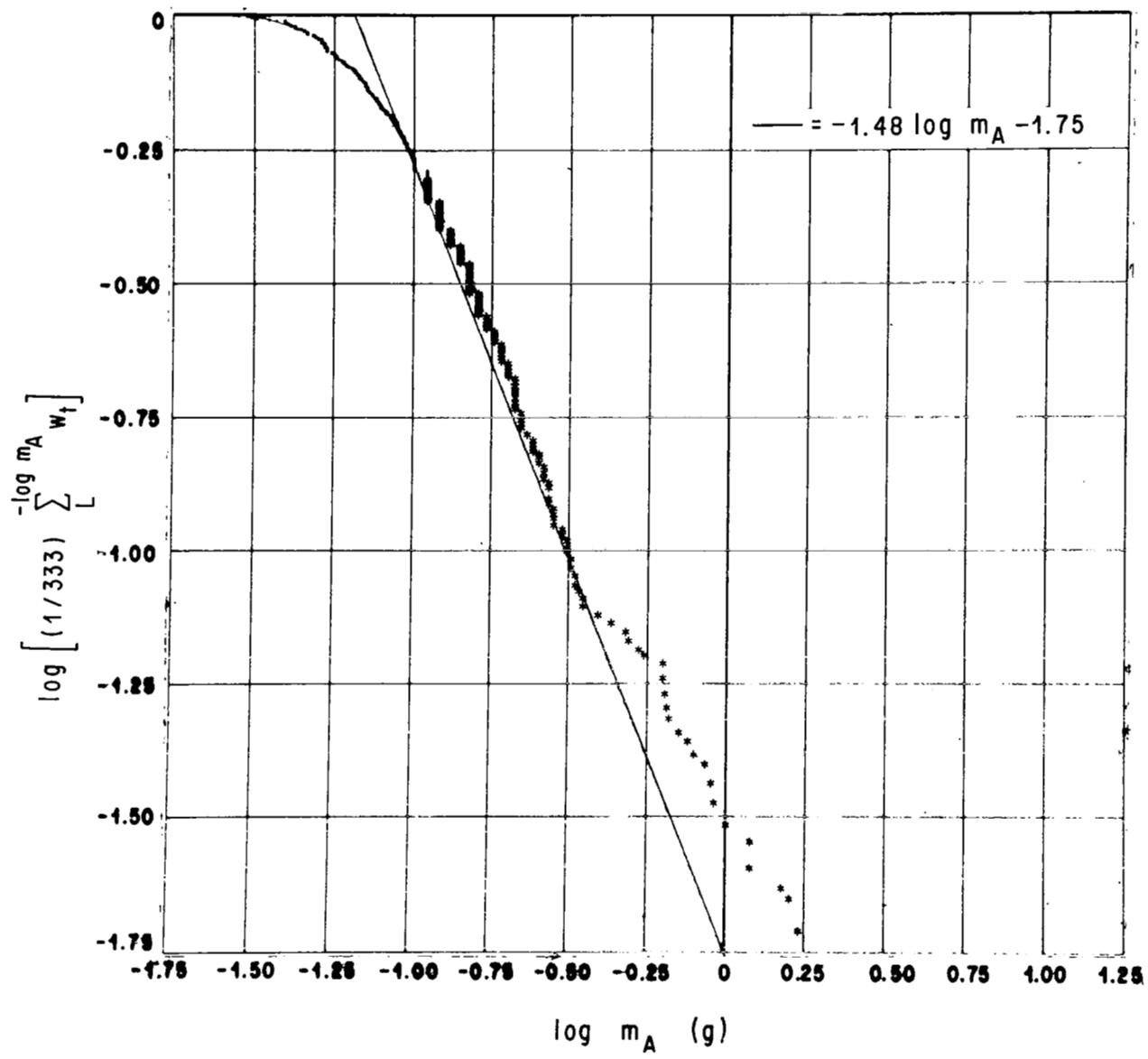

FIGURE 40a. DISTRIBUTION OF MASS, TERRESTRIAL WEIGHTING, SUB-SAMPLE "A"

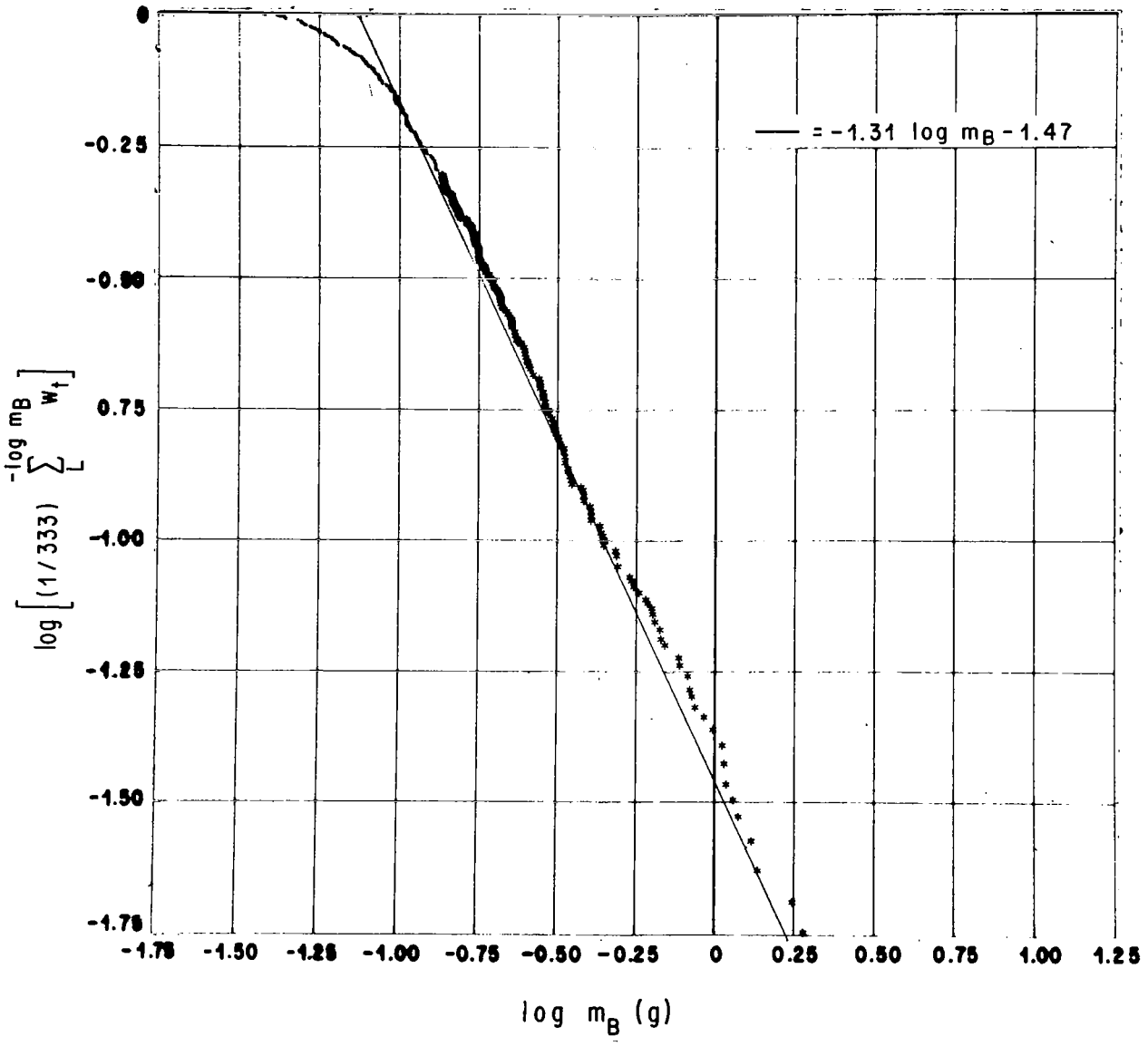

FIGURE 40b. DISTRIBUTION OF MASS, TERRESTRIAL WEIGHTING, SUB-SAMPLE "B"

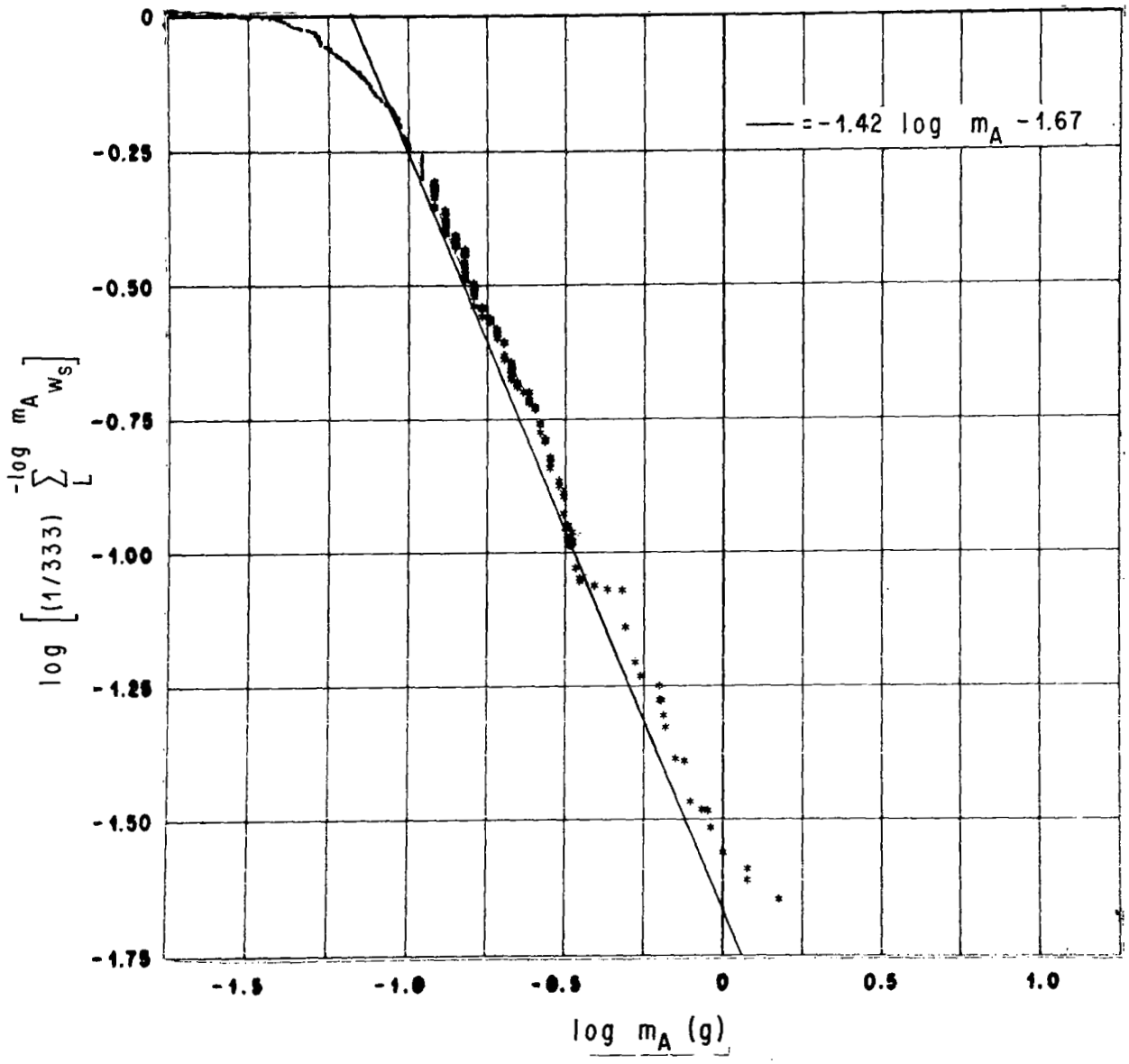

FIGURE 42a. DISTRIBUTION OF METEOROID MASS, SPATIAL WEIGHTING, SUB-SAMPLE "A"

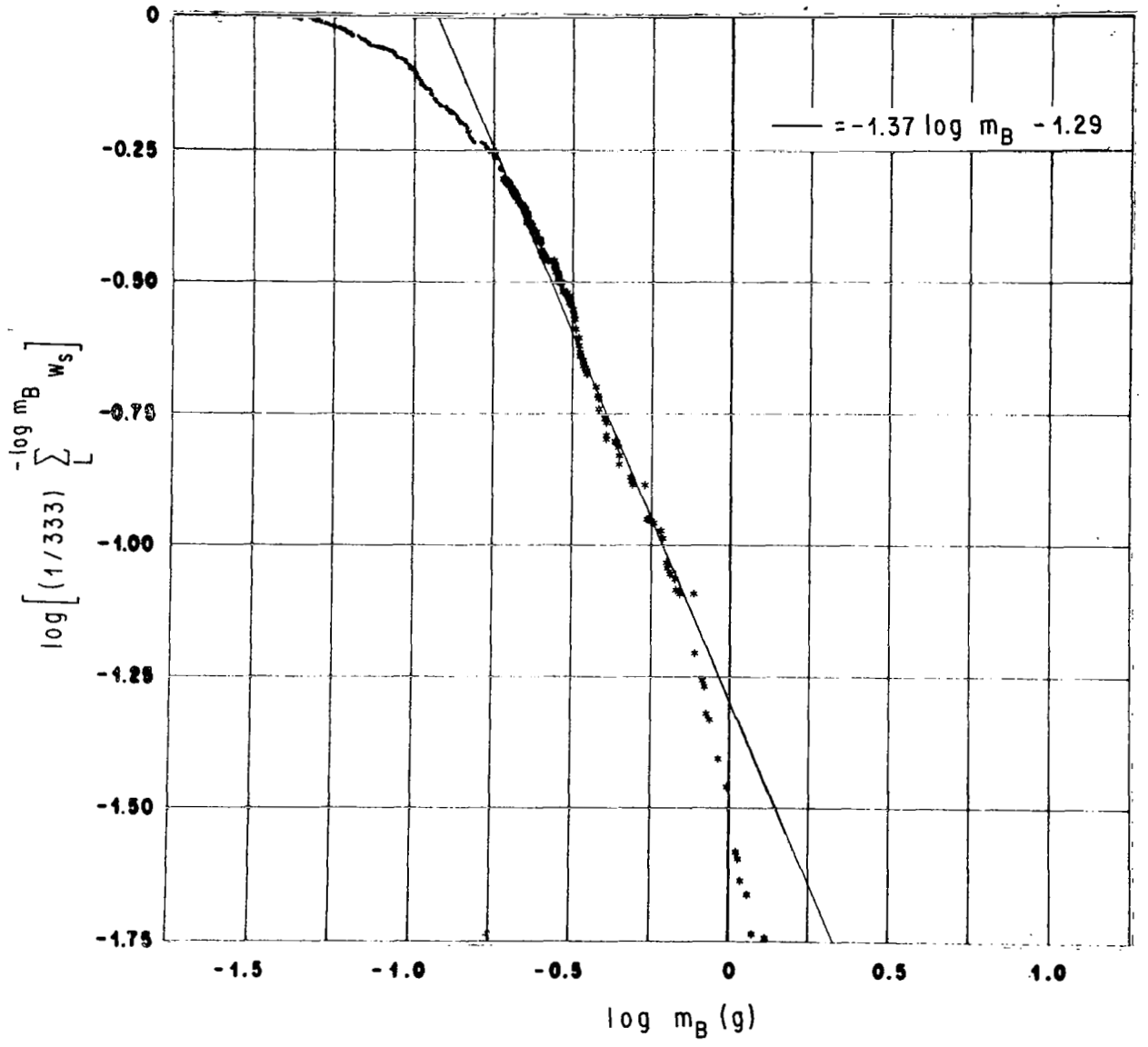

FIGURE 42b. DISTRIBUTION OF METEOROID MASS, SPATIAL WEIGHTING, SUB-SAMPLE "B"

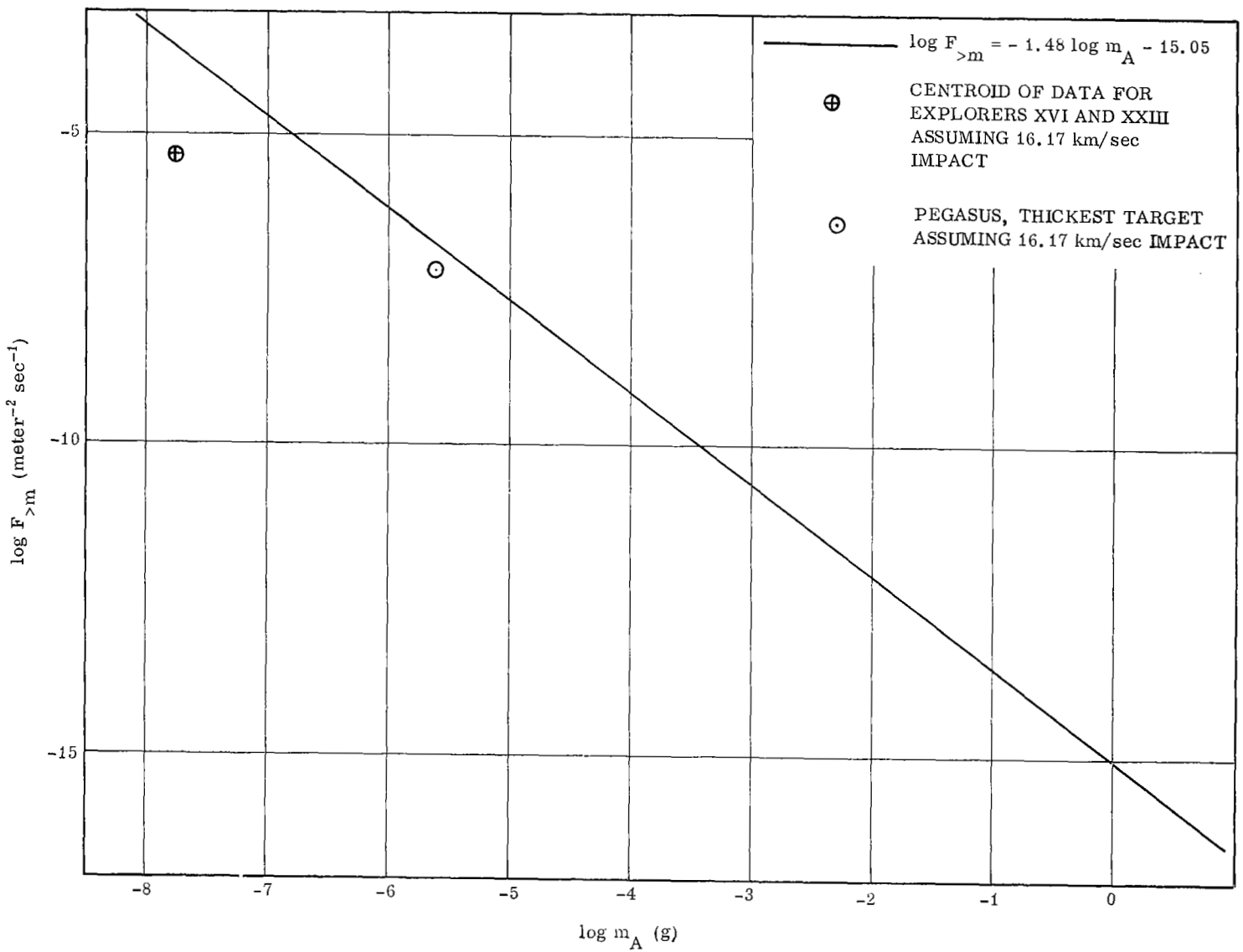

FIGURE 43a. MASS-CUMULATIVE INFLUX OF SATELLITE-PUNCTURING METEOROIDS PRESUPPOSING VELOCITY DISTRIBUTION FROM PHOTOGRAPHIC METEORS INVARIANT WITH RESPECT TO MASS, VERSUS EXTRAPOLATED METEOR MODEL, SUB-SAMPLE "A"

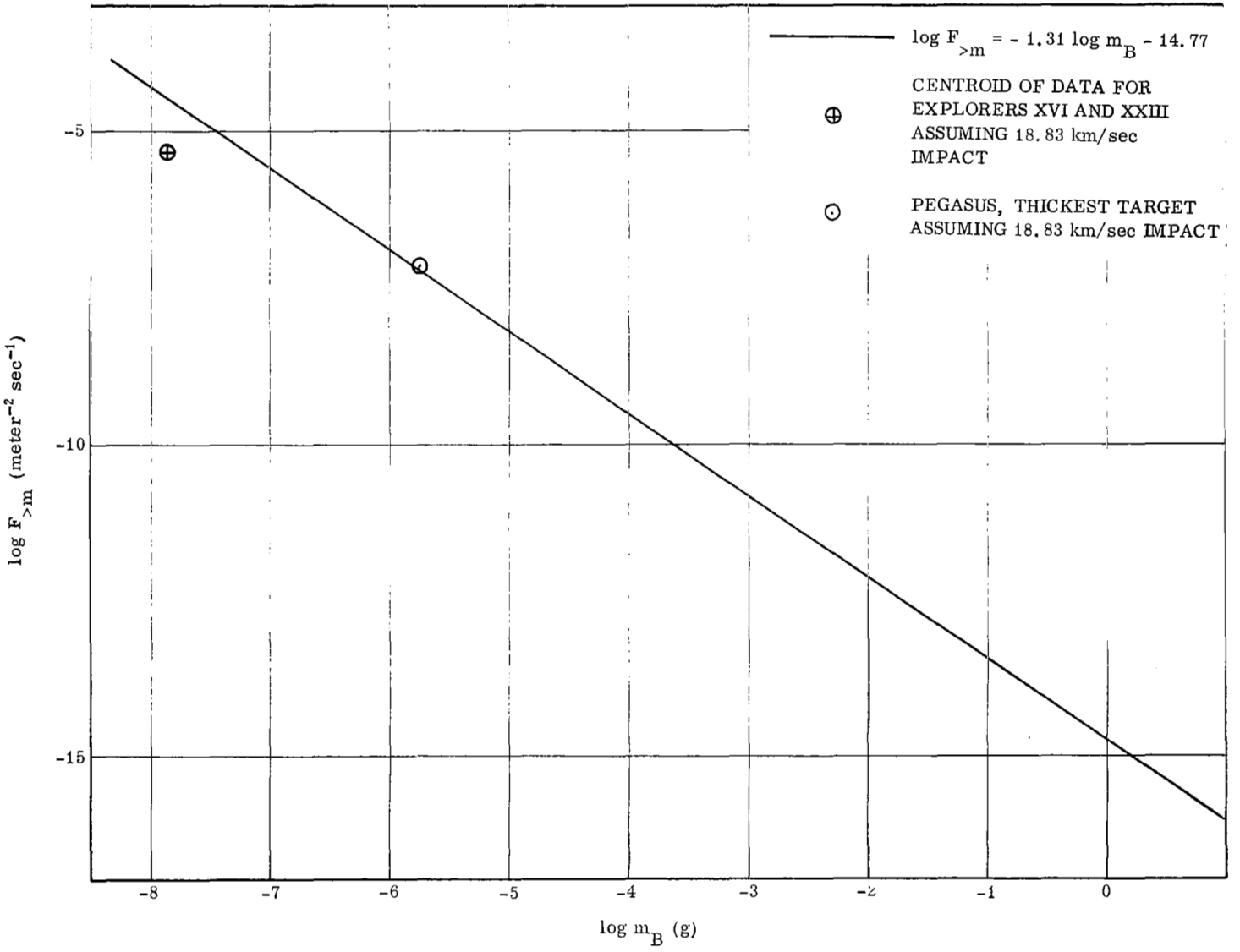

FIGURE 43b. MASS-CUMULATIVE INFLUX OF SATELLITE-PUNCTURING METEOROIDS PRESUPPOSING VELOCITY DISTRIBUTION FROM PHOTOGRAPHIC METEORS INVARIANT WITH RESPECT TO MASS, VERSUS EXTRAPOLATED METEOR MODEL, SUB-SAMPLE "B"

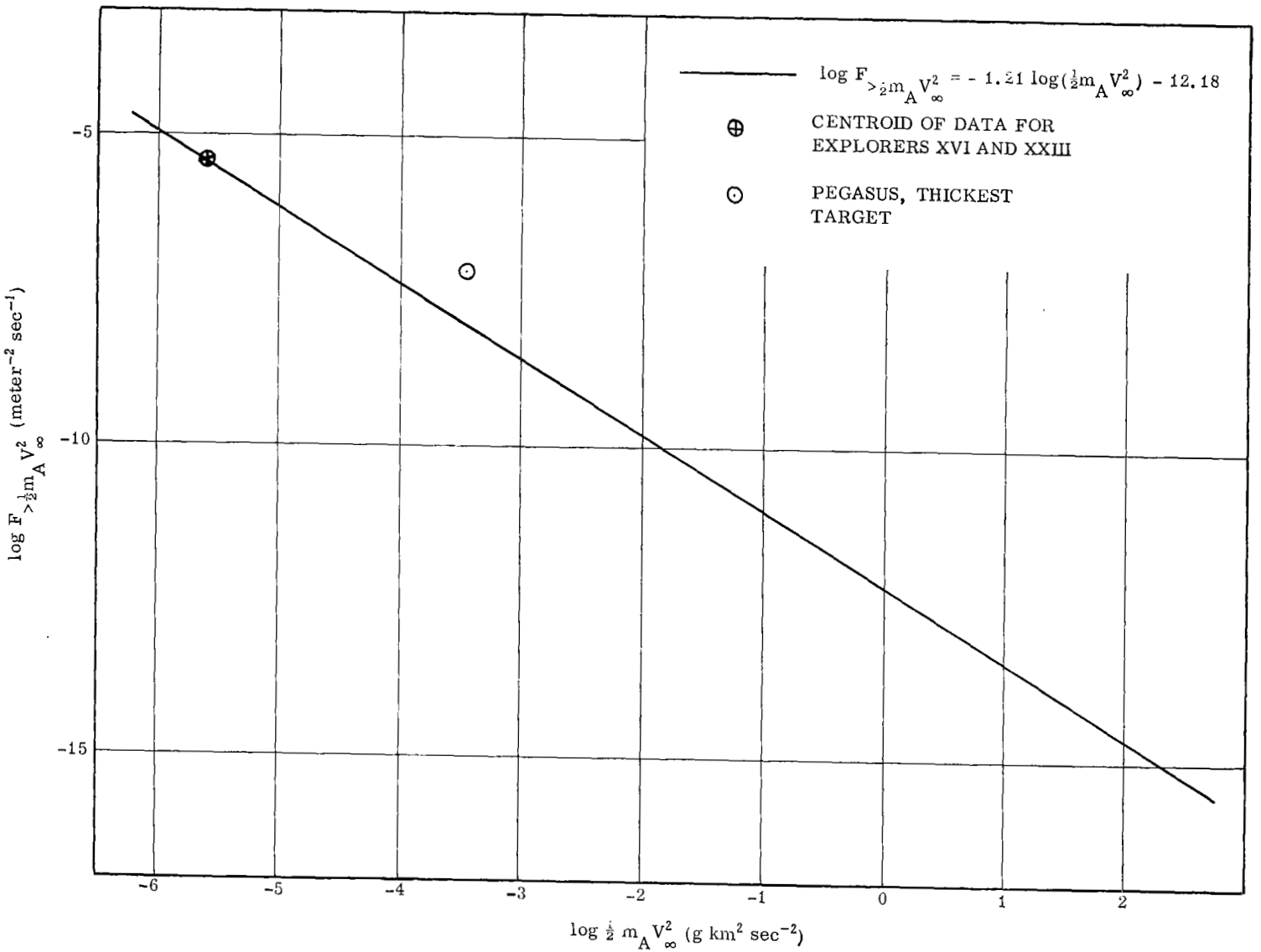

FIGURE 44a. ENERGY-CUMULATIVE INFLUX OF SATELLITE-PUNCTURING METEOROIDS VERSUS EXTRAPOLATED MODEL FROM PHOTOGRAPHIC METEORS, SUB-SAMPLE "A"

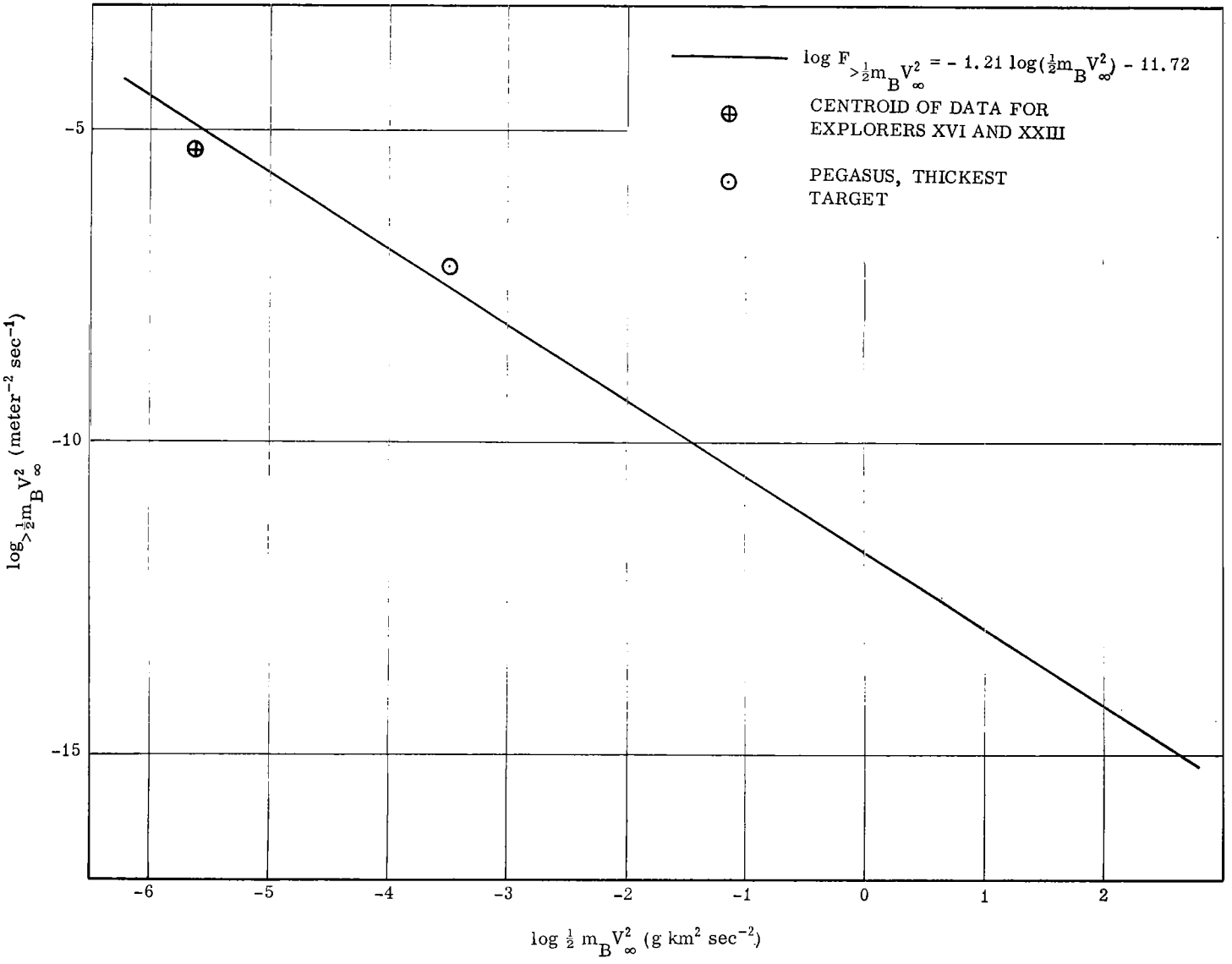

FIGURE 44b. ENERGY-CUMULATIVE INFLUX OF SATELLITE-PUNCTURING METEOROIDS VERSUS EXTRAPOLATED MODEL FROM PHOTOGRAPHIC METEORS, SUB-SAMPLE "B"

REFERENCES

1. Way, K., Gove, N. B., and van Lieshout, R.: Waiting for Scientific Information Tools We Could Have Now. Physics Today, Vol. 15, No. 2, February 1962, pp. 22-27.

2. Öpik, E. J.: Physics of Meteor Flight in the Atmosphere. Interscience Publishers, Inc., New York, 1958.

3. Levin, B. Yu.: The Physical Theory of Meteors, and Meteoric Matter in the Solar System. (Originally in Russian 1956), Translation of Chapters 1-3: ASTIA Document No. AD 110091.

4. Lovell, A. C. B.: Meteor Astronomy. Oxford University Press, London, 1954.

5. McKinley, D. W. R.: Meteor Science and Engineering. McGraw-Hill Book Co., Inc., New York, 1961.

6. Hawkins, G. S.: Meteors, Comets, and Meteorites. McGraw-Hill Book Co., New York, 1964.

7. Cosby, W. A., and Lyle, R. G.: The Meteoroid Environment and its Effects on Materials and Equipments. NASA Special Publication 78, 1965.

8. Vedder, J. F.: Minor Objects in the Solar System. Space Science Reviews, Vol. 6, No. 3, 1966, pp. 365-414.

9. Dalton, C. C.: Meteoroid Hazard to Space Vehicles in Orbit Near the Earth: A Functional Interpretation of the Information for Design and Operations Decisions. NASA Technical Memorandum X-789, December 1962.

10. Meteoroid Damage Working Group. Reviews of Selected Aspects of the Meteoroid Hazard. NASA-MSFC Rept. No. MDWG-63-1, February 15, 1963.

11. Meteoroid Damage Working Group. A Bibliography Concerning Aspects of the Meteoroid Hazard. NASA-MSFC Report No. MDWG-63-2, April 1, 1963.

12. Whipple, F. L., and Hawkins, G. S.: Meteors. In: Encyclopedia of Physics, S. Flugge, Ed., Astrophysics III: The Solar System, Vol. 52, Springer-Verlag, Berlin, 1959, pp. 519-564.

13. Öpik, E. J.: Problems in the Physics of Meteors. Am. J. Phys., Vol. 26, No. 2, February 1958, pp. 70-80.

14. Frost, V. C.: Aerospace Meteoroid Environment and Penetration Criterion. Aerospace Corp. Rept. TOR-269(4560-40)-2, Contract AF04-695-269, Air Force Station, Los Angeles, California, August 17, 1964.

15. Christman, D. R., and McMillan, A. R.: The Meteoroid Environment and its Consequences to Spacecraft Structures. Journal of Environmental Sciences, Vol. 9, No. 1, February 1966, pp. 14-18.

16. Dalton, C. C.: Near Earth and Interplanetary Meteoroid Flux and Puncture Models. Paper No. EN-14, American Astronautical Society 1967 National Symposium. Saturn V/Apollo and Beyond. Huntsville, Alabama. In: Vol. 1, pp. AAS 67-334 (EN-14-1) through AAS 67-334 (EN-14-21).

17. Katasev, L. A., and Kulikova, N. V.: Meteor Satellites of the Earth. Proceedings of the Seventh International Space Science Symposium (Vienna, 1966), Space Research VII, Vol. 2, North Holland Publishing Co., Amsterdam, 1967, pp. 1443-1450.

18. McCrosky, R. E., and Posen, A.: Orbital Elements of Photographic Meteors. Smithsonian Contributions to Astrophysics, Vol. 4, No. 2, Smithsonian Institution, Washington, D. C., 1961, pp. 15-84.

19. Öpik, E. J.: Atomic Collisions and Radiation of Meteors. Reprint No. 100, Harvard College Observatory, 1933.

20. Kresak, L.: A Relation Between the Orbits and Magnitude Distribution of Meteors. Bulletin of the Astronomical Institutes of Czechoslovakia, Vol. 15, No. 5, 1964, pp. 190-195.

21. Mood, A. McF.: Introduction to the Theory of Statistics. McGraw-Hill Book Co., Inc., New York, 1950.

22. Dalton, C. C.: Estimation of Tolerance Limits for Meteoroid Hazard to Space Vehicles 100-500 Kilometers Above the Surface of the Earth. NASA Technical Note D-1996, February 1964.

REFERENCES (Continued)

23. Lloyd, D. K., and Lipow, M.: Reliability: Management, Methods, and Mathematics. Prentice-Hall, Inc., Englewood Cliffs, N. J., 1962.

24. Hald, A.: Statistical Tables and Formulas. John Wiley and Sons, New York, N. Y., 1952.

25. Whipple, F. L.: Photographic Meteor Studies, I. Proceedings of the American Philosophical Society, Vol. 79, No. 4, November 1938, pp. 499-548.

26. Verniani, F.: On the Luminous Efficiency of Meteors. Smithsonian Contributions to Astrophysics, Vol. 8, No. 5, Smithsonian Institution, Washington, D.C., 1965, pp. 141-172.

27. Whipple, F. L.: Meteors and the Earth's Upper Atmosphere. Reviews of Modern Physics, Vol. 15, No. 4, October 1943, pp. 246-264.

28. Öpik, E. J.: Tables of Meteor Luminosities. The Irish Astron. J., Vol. 6, No. 1, March 1963, pp. 3-11.

29. Hawkins, G. S.: The Method of Reduction of Short-Trail Meteors. Smithsonian Contributions to Astrophysics, Vol. 1, No. 2, Smithsonian Institution, Washington, D. C., 1957, pp. 207-214.

30. Clough, N., and Lieblein, S.: Significance of Photographic Meteor Data in the Design of Meteoroid Protection for Large Space Vehicles. NASA Technical Note D-2958, August 1965.

31. Kallmann, H. K.: Quantitative Estimate of Frequency and Mass Distribution of Dust Particles Causing the Zodiacal Light. Memoires de la Societe Royal des Sciences de Liege, Vol. 15, Special Number (Symposium 1954), 1955, pp. 100-113.

32. Öpik, E. J.: The Masses of Meteors. Memoires de la Societe Royale des Sciences de Liege, 4th Series, No. 15, 1955, pp. 125-146.

33. Kallmann, H. K.: Relationship Between Masses and Visual Magnitudes of Meteors. In: Meteors. (A Symposium on Meteor Physics, 1954), T. R. Kaiser, Ed., Special Supplement (Vol. 2) to the Journal of Atmospheric and Terrestrial Physics, Pergamon Press Ltd., London, 1955, pp. 43-54.

34. Öpik, E. J.: The Masses and Structure of Meteors. In: Meteors. (A Symposium on Meteor Physics, 1954), T. R. Kaiser, Ed., Special Supplement (Vol. 2) to the Journal of Atmospheric and Terrestrial Physics, Pergamon Press Ltd., London, 1955, pp. 33-35.

35. Weiss, A. A.: The Incidence of Meteor Particles Upon the Earth. Australian J. Phys., Vol. 10, 1957, pp. 397-411.

36. Eshleman, V. R.: Book Review [of Ref. 2], Science, Vol. 129, May 15, 1959, p. 1354.

37. Dalton, C. C.: Effects of Recent NASA-ARC Hypervelocity Impact Results on Meteoroid Flux and Puncture Models. NASA Technical Memorandum X-53512, September 7, 1966.

38. Smith, H. J.: The Physical Theory of Meteors. V. The Masses of Meteor-Flare Fragments. Astrophys. J., Vol. 119, No. 2, March 1954, pp. 438-442.

39. Jacchia, L. G.: The Physical Theory of Meteors: VIII, Fragmentation as Cause of the Faint Meteor Anomaly. Astrophys. J., Vol. 121, 1954, pp. 521-527.

40. McCrosky, R. E.: Some Physical and Statistical Studies of Meteor Fragmentation: PhD Thesis, Harvard University, Cambridge, Massachusetts, 1955, (AD No. 93 444).

41. Whipple, F. L.: A Comet Model: III, The Zodiacal Light. Astrophys. J., Vol. 121, 1955, pp. 750-770.

42. Whipple, F. L.: Photographic Meteor Orbits and Their Distribution in Space. Astron. J., Vol. 59, No. 1218, July 1954, pp. 201-217.

REFERENCES (Continued)

43. Ceplecha, Z.: Dynamic and Photometric Mass of Meteors. Bulletin of the Astronomical Institutes of Czechoslovakia, Vol. 17, No. 6, 1966, pp. 347-354.

44. Ceplecha, Z.: Classification of Meteor Orbits. In: Meteor Orbits and Dust (Symposium in Cambridge 1965). Smithsonian Contributions to Astrophysics, Vol. 11, NASA Special Publication 135, 1967, pp. 35-60.

45. Ceplecha, Z.: Discrete Levels of Meteor Beginning Height. Special Report No. 279, Smithsonian Astrophysical Observatory, Cambridge, Massachusetts, June 7, 1968.

46. Allen, H. J., and Baldwin, B. S., Jr.: Frothing as an Explanation of the Acceleration Anomalies of Cometary Meteors. J. Geophys. Res., Vol. 72, No. 13, July 1, 1967, pp. 3483-3496.

47. Allen, H. J., Baldwin, B. S., Jr., and James, N. A.: Effect on Meteor Flight of Cooling by Radiation. NASA Technical Note D-2872, June 1965.

48. Lebedinets, V. N., and Portnyagin, Yu. I.: Fragmentation of Dense Meteoroids in the Atmosphere. Soviet Astron.-AJ, Vol. 11, No. 4, January-February 1968, pp. 700-711.

49. Dalton, C. C.: The Masses of Meteors and the Selection of a Representative Data Sample. In: Research Achievements Review, Vol. 2, Rept. No. 10. Terrestrial and Space Environment Research at MSFC. NASA Technical Memorandum X-53760, 1967, pp. 63-73.

50. Cook, A. F.: The Physical Theory of Meteors. Paper, Presented at Symposium on Physics and Dynamics of Meteors, International Astronomical Union, Tatranska Lomnica, September 4-9, 1967.

51. Dohnanyi, J. S.: Model Distribution of Photographic Meteors. Bellcomm, Inc., Technical Report 66-340-1, Contract NASw-417, March 29, 1966.

52. Miller, C. D.: Simultaneous Correction of Velocity and Mass Bias in Photography of Meteors. NASA Technical Report R-280, February 1968.

53. Hawkins, G. S., and Southworth, R. B.: The Statistics of Meteors in the Earth's Atmosphere. Smithsonian Contributions to Astrophysics, Vol. 2, No. 11, Smithsonian Institution, Washington, D. C., 1958, pp. 349-364.

54. Dalton, C. C.: Inferences from Photographic Meteors. In: Meteor Orbits and Dust (Symposium in Cambridge 1965), Smithsonian Contributions to Astrophysics, Vol. 11, NASA Special Publication 135, 1967, pp. 81-90.

55. Dalton, C. C.: Statistical Analysis of Photographic Meteor Data - Part I - Öpik's Luminous Efficiency and Supplemented Whipple Weighting. NASA Technical Memorandum X-53325, September 2, 1965.

56. Jacchia, L. G., Verniani, F., and Briggs, R. E.: An Analysis of the Atmospheric Trajectories of 413 Precisely Reduced Photographic Meteors. Smithsonian Contributions to Astrophysics, Vol. 10, No. 1, Smithsonian Institution, Washington, D. C., 1967, pp. 1-139.

57. Ericke, K. A.: Space Flight, Vol. 1: Environment and Celestial Mechanics. D. van Nostrand Co., Inc., New York, 1960.

58. Kells, L. M., Kern, W. F., and Bland, J. R.: Spherical Trigonometry with Naval and Military Applications. McGraw-Hill Book Co., Inc., New York, 1942.

59. Russell, H. N., Dugan, R. S., and Stewart, J. Q.: Astronomy, I. The Solar System. Ginn and Company, New York, 1945.

60. Davies, F. G., and Gill, F. C.: Radio Echo Measurements of the Orbits of Faint Sporadic Meteors. Monthly Notices, Royal Astronomical Society, Vol. 121, 1960, pp. 437-462.

61. Keay, C. S. L.: The Annual Variation in the Radiant Distribution of Sporadic Meteors. Journal of Atmospheric and Terrestrial Physics, Vol. 25, 1963, pp. 507-513.

62. McKinley, D. W. R.: Meteor Velocities Determined by Radio Observations. The Astrophys. J., Vol. 113, No. 2, March 1951, pp. 225-267.

REFERENCES (Continued)

63. Öpik, E. J.: The Distribution of Meteor Stream Intensity over the Celestial Sphere. Memories de la Societe Royale des Sciences des Liege, 4th Series, No. 15, 1955, p. 147.

64. Öpik, E. J.: Proceedings, Royal Irish Academy, Vol. 54, Sec. A, No. 12, 1951.

65. Beard, D. B.: Absence of Craters on the Far Side of the Moon. Nature, Vol. 184, Supp. No. 21, 1959, p. 1631.

66. Shoemaker, E. M., Hackman, R. J., and Eggleton, R. E.: Interplanetary Correlation of Geologic Time. Advances in the Astronautical Sciences, Vol. 8, Plenum Press, Inc., New York, 1962, pp. 70-89.

67. Hale, D. P., and Wright, J. J.: Meteoric Flux and Density Fields About a Finite Attractive Center Generated by a Stream Monoenergetic and Monodirectional at Infinity. J. Geophys. Res., Vol. 69, September 1, 1964.

68. Hartmann, W. K.: Terrestrial and Lunar Flux of Large Meteorites in the Last Two Billion Years. Icarus, Vol. 4, 1965, pp. 157-165.

69. Öpik, E. J.: The Lunar Surface as an Impact Counter. Royal Astronomical Society Monthly Notices, Vol. 120, No. 5, 1960, pp. 404-408.

70. Öpik, E. J.: Interaction of Meteoric Bodies with the Terrestrial Atmosphere. Irish Astron. J., Vol. 8, March-June 1967, pp. 53-62.

71. Fesenkov, V. G.: Meteoric Matter in Interplanetary Space. NASA Technical Translation F-378, November 1965.

72. Ingham, M. F.: Interplanetary Matter. Space Science Reviews, Vol. 1, March 1963, pp. 576-588.

73. Beard, D. B.: Comets and Cometary Debris in the Solar System. Reviews of Geophysics, Vol. 1, No. 2, May 1963, pp. 211-229.

74. Briggs, R. E.: Steady-State Space Distribution of Meteoric Particles under the Operation of the Poynting-Robertson Effect. Astron. J., Vol. 67, No. 10, December 1962, pp. 710-723.

75. Jacchia, L. G., and Whipple, F. L.: Precision Orbits of 413 Photographic Meteors. Smithsonian Contributions to Astrophysics, Vol. 4, No. 4, Smithsonian Institution, Washington, D.C., 1961, pp. 97-129.

76. Hawkins, G. S., and Southworth, R. B.: Orbital Elements of Meteors. Smithsonian Contributions to Astrophysics, Vol. 4, No. 3, Smithsonian Institution, Washington, D. C., 1961, pp. 85-95.

77. Dycus, R. D., and Bradford, D. C.: The Origin of Meteors Inferred from Orbital Elements. Icarus, Vol. 3, 1964, pp. 306-310.

78. Öpik, E. J.: The Starry Bodies in the Solar System. Part II. The Cometary Origin of Meteorites. In: Advances in Astronomy and Astrophysics. Vol. 4, Academic Press, New York, 1966, pp. 301-336.

79. Jacchia, L. G., Verniani, F., and Briggs, R. E.: Selected Results from Precision-Reduced Super-Schmidt Meteors. In: Meteor Orbits and Dust (Symposium in Cambridge 1965), Smithsonian Contributions to Astrophysics, Vol. 11, NASA Special Publication 135, 1967, pp. 1-7.

80. Babadzhanov, P. B., and Kramer, E. N.: Orbits of Bright Photographic Meteors. In: Meteor Orbits and Dust (Symposium in Cambridge 1965), Smithsonian Contributions to Astrophysics, Vol. 11, NASA Special Publication 135, 1967, pp. 67-79.

81. Hawkins, G. S., and Upton, E. K. L.: The Influx Rate of Meteors in the Earth's Atmosphere. Astrophys. J., Vol. 128, 1958, pp. 727-735.

82. Lindblad, B.-A.: Luminosity Function of Sporadic Meteors and Extrapolation of Influx Rate to Micrometeorite Region. In: Meteor Orbits and Dust (Symposium in Cambridge 1965), Smithsonian Contributions to Astrophysics, Vol. 11, NASA Special Publication 135, 1967, pp. 171-180.

REFERENCES (Continued)

83. Watson, F. G.: Between the Planets. Harvard University Press, Cambridge, 1956.

84. Lovell, A. C. B.: Geophysical Aspects of Meteors. In: Encyclopedia of Physics, Vol. XLVIII, Geophysics II, S. Flugge, Ed., Springer-Verlag, Berlin, 1957, pp. 427-454.

85. McCrosky, R. E.: Distributions of Large Meteoric Bodies. Special Report No. 280, Smithsonian Astrophysical Observatory, Cambridge, Massachusetts, June 14, 1968.

86. Whipple, F. L.: On Meteoroids and Penetration. The J. of the Astronautical Sciences, Vol. 10, No. 3, Fall 1963, pp. 92-94.

87. Dohnanyi, J. S.: Mass Distribution of Meteors. Astrophys. J., Vol. 149, No. 3, September 1967, pp. 735-737.

88. Erickson, J. E.: Velocity Distribution of Photographic Meteors. J. Geophys. Res., Vol. 73, No. 12, June 15, 1968, pp. 3721-3726.

89. Divari, N. B.: The Cosmic Dust Cloud Around the Earth. Soviet Astron.-AJ, Vol. 10, No. 6, May-June 1967, pp. 1017-1030.

90. Jacchia, L. G.: On the "Color-Index" of Meteors. Astron. J., Vol. 62, pp. 358-362.

91. Millman, P. M.: Meteor News. The Relative Number of Bright and Faint Meteors. Royal Astronomical Society (Canada) Journal, Vol. 51, No. 1, February 1957, pp. 113-115.

92. Fialko, E. I.: The Energy Distribution of Meteoric Bodies. Soviet Astron.-AJ, Vol. 9, No. 2, September-October 1965, pp. 322-326.

93. Dalton, C. C.: Statistical Analysis of Photographic Meteor Data, Part 2: Verniani's Luminous Efficiency and Supplemented Whipple Weighting. NASA Technical Memorandum X-53360, November 18, 1965.

94. Marcus, A. H.: Comments on Fialko's Paper, 'The Energy Distribution of Meteoroids.' Soviet Astron.-AJ, Vol. 11, No. 3, November-December 1967, pp. 537-538.

95. Fialko, E. I.: Comments on Marcus' Criticism of 'The Energy Distribution of Meteoroids.' Soviet Astron.-AJ, Vol. 11, No. 3, November-December 1967, pp. 539-540.

96. Fialko, E. I.: The True and Apparent Kinetic-Energy Distribution of Meteors. Soviet Astron.-AJ, Vol. 11, No. 4, January-February 1968, pp. 692-699.

97. Öpik, E. J.: Astronomical Aspects of the Exploration of Space. II. The Irish Astron. J., Vol. 6, No. 7, September 1964, pp. 260-272.

98. van de Hulst, H. C.: Zodiacal Light in the Solar Corona. Astrophys. J., Vol. 105, 1947, pp. 471-488.

99. Blackwell, D. E., Dewhirts, D. W., and Ingham, M. F.: The Zodiacal Light. In: Advances in Astronomy and Astrophysics, Vol. 5, Academic Press, New York, 1967, pp. 1-69.

100. Gurtler, C. A., and Grew, G. W.: Meteoroid Hazard Near Moon. Science, Vol. 161, No. 3840, 2 August 1968, pp. 462-464.

101. Nilsson, C.: Some Doubts About the Earth's Dust Cloud. Science, Vol. 153, No. 3741, 9 September 1966, pp. 1242-1246.

102. Dubin, M., and McCracken, C. W.: Measurements of Distributions of Interplanetary Dust. Astron. J., Vol. 67, No. 5, June 1962, pp. 248-256.

103. Alexander, W. M., McCracken, C. W., Secretan, L., and Berg, O.E.: Review of Direct Measurements of Interplanetary Dust from Satellites and Probes. In: Space Research, III. W. Preister, Ed., North-Holland Publishing Co., Amsterdam, 1963, pp. 891-917.

104. Konstantinov, B. P., Bredov, M. M., Mazets, R. P.: Experimental Data as Evidence Against the Hypothesis on the Earth's Dust Cloud. NASA CR-93742, 1968. (Translated from the Russian Dokl. A.N.S.S.R. Geofizika, tom 174, no. 3, 1957, pp. 580-582).

REFERENCES (Continued)

105. Koptev, Y.: Is There a Dust Cloud. Spaceflight, Vol. 10, No. 6, June 1968, pp. 194-195.

106. Erickson, J. E.: Mass Influx and Penetration Rate of Meteor Streams. J. Geophysics Research, Vol. 74, No. 2, January 1969, pp. 576-585.

107. Anders, E., and Arnold, J. R.: Age of Craters on Mars. Science, Vol. 149, No. 3691, September 24, 1965, pp. 1494-1496.

108. Southworth, R. B.: Space Density of Radio Meteors. In: Studies in Interplanetary Particles. Smithsonian Astrophysical Observatory, Special Report 239, Cambridge, May 31, 1967, pp. 77-97.

109. Divari, N. B.: A Meteor Model for the Zodiacal Cloud. Soviet Physics-Astronomy, Vol. 11, No. 6, May-June 1968, pp. 1048-1052.

110. Abelson, P. H.: Mariner IV Mission. Science, Vol. 149, No. 3689, September 10, 1965, p. 1179.

111. Anderson, H. R.: Mariner IV Measurements Near Mars: Initial Results. Spacecraft Description and Encounter Sequence. Science, Vol. 149, No. 3689, September 10, 1965, pp. 1226-1228.

112. Alexander, W. M., McCracken, C. W., and Bohn, J. L.: Zodiacal Dust: Measurements by Mariner IV. Science, Vol. 149, No. 3689, September 10, 1965, pp. 1240-1241.

113. Dalton, C. C.: Theoretical Relationships for Meteoroid Puncture Experiments. NASA Technical Note D-3244, February 1966.

114. Greenhow, J. S.: Limitations of Radar Techniques for the Study of Meteors. In: Proceedings of the Symposium on the Astronomy and Physics of Meteors (Cambridge 1961), Smithsonian Contributions to Astrophysics, Vol. 7, Smithsonian Institution, Washington, D. C., 1963, pp. 5-17.

115. Whipple, F. L.: The Physical Theory of Meteors. VII. On Meteor Luminosity and Ionization. Astrophys. J., Vol. 121, No. 1, January 1955, pp. 241-249.

116. Furman, A. M.: Meteor Trail Ionization Theory. IV. Ionization Efficiency Through Collision of Vaporized Meteoroid Particles with Air Molecules. Soviet Astron.-AJ, Vol. 10, No. 5, March-April 1967, pp. 844-852.

117. Hawkins, G. S.: Meteor Ionization and its Dependence on Velocity. Astrophys. J., Vol. 124, 1956, pp. 311-313.

118. Millman, P. M., and McKinley, D. W. R.: Meteor Echo Durations and Visual Magnitudes. Can. J. Phys., No. 34, 1956, p. 50.

119. Delcourt, J.: Physics of Meteors. NASA Technical Translation F-8802, February 1964.

120. Derbeneva, A. D.: The Luminous Flux and Ionizing Power of Meteor Trails. Soviet Astron.-AJ, Vol. 11, No. 4, January-February 1968, pp. 688-691.

121. Slattery, J. C., and Friichtenicht, J. F.: Ionization Probability of Iron Particles at Meteoric Velocities. Astrophys. J., Vol. 147, No. 1, 1967, pp. 235-244.

122. McIntosch, B. A.: Radar Echo Duration as a Function of Meteoroid Mass. Can. J. Phys., Vol. 45, 1967, pp. 3419-3422.

123. Whipple, F. L., and Hughes, R. F.: On the Velocities and Orbits of Meteors, Fireballs, and Meteorites. In: Meteors (A Symposium on Meteor Physics, 1954), T. R. Kaiser, Ed., Special Supplement (Vol. 2) to the Journal of Atmospheric and Terrestrial Physics, Pergamon Press Ltd., London, 1955, pp. 149-156.

124. Whipple, F. L.: The Meteoritic Risk to Space Vehicles. Reprint 499-57 (Astronautical Congress in Barcelona, 1957), American Rocket Society, New York, 1957.

125. Whipple, F. L.: The Meteoritic Risk to Space Vehicles. In: Vistas in Astronautics (Astronautics Symposium in San Diego, 1957), Pergamon Press, New York, 1958, pp. 115-124.

REFERENCES (Continued)

126. Hawkins, G. S., Lindblad, B.-A., and Southworth, R. B.: The Velocity of Faint Meteors. Smithsonian Contributions to Astrophysics, Vol. 8, No. 4, Smithsonian Institution, Washington, D. C., 1964, pp. 133-139.

127. Baker, K.: Additional Data on the Velocity of Faint Meteors. NASA Research Report No. 4, Contract NASr-158, Harvard College Observatory and Smithsonian Astrophysical Observatory, Cambridge, December 1963.

128. Hawkins, G. S.: Interplanetary Debris Near the Earth. In: Annual Review of Astronomy and Astrophysics, Vol. 2, Annual Reviews, Inc., Palo Alto, California, 1964, pp. 149-164.

129. Eshleman, V. R., and Gallagher, P. B.: Radar Studies of 15th-Magnitude Meteors. Astron. J., Vol. 67, No. 5, June 1962, pp. 245-248.

130. Lebedinets, V. N., and Kashcheev, B. L.: Meteoric Matter Near the Earth's Orbit From Radio Meteor Observations. Soviet Astron.-AJ, Vol. 10, No. 4, January-February 1967, pp. 683-693.

131. Babadzhanov, P. B.: Determination of Atmospheric Temperature, Pressure, and Density from Photographic Observations of Meteors. *Geomagnetism and Aeronomy*, Vol. 6, No. 1, 1966, pp. 118-121.

132. Katasev, L. A.: Photographic Methods in Meteor Astronomy. NASA Technical Translation F-142, OTS 64-11021, 1964.

133. Kovshun, I. N.: New Determinations of Meteoroid Masses. Geomagnetism and Aeronomy, Vol. 6, 1966, pp. 548-555.

134. Levin, B. J.: The Distribution of True Radiants of Meteor Bodies Down to a Definite Limit of Mass. In: International Geophysical Year, 1957/1958, Annals, Vol. 11, 1961, pp. 187-193.

135. Verniani, F.: Meteor Masses and Luminosity. Smithsonian Contributions to Astrophysics, Vol. 10, No. 3, Smithsonian Institution, Washington, D. C., 1967, pp. 181-195.

136. Whipple, F. L.: On Meteoroids and Penetration. J. of Geophys. Res., Vol. 68, No. 17, September 1, 1963, pp. 4929-4939.

137. McCrosky, R. E., and Soberman, R. K.: Results from an Artificial Iron Meteoroid at 10 km/sec. Research Note 62-803, Air Force Cambridge Research Laboratories, Cambridge, Massachusetts, July 1962.

138. Cook, A. F., Jacchia, L. G., and McCrosky, R. E.: Luminous Efficiency of Iron and Stone Asteroidal Meteors. Smithsonian Contributions to Astrophysics, Vol. 7, Smithsonian Institution, Washington, D. C., 1963, pp. 209-220.

139. Baldwin, B. S., Jr., and Allen, H. J.: A Method for Computing Luminous Efficiencies from Meteor Data. NASA Technical Note D-4808, September 1968.

140. Utah Research and Development Co., Inc.: *A Program to Determine the Luminous* Coefficients of Artificial Meteors. Revised Final Report, Contract No. NAS 9-2833, NASA Manned Spacecraft Center, December 3, 1965.

141. Friichtenicht, J. C., Slattery, J. C., and Tagliaferri, E.: A Laboratory Measurement of Meteor Luminous Efficiency. The Astrophys. J., Vol. 151, No. 2, February 1968, pp. 747-758.

142. Levin, B. Yu.: Fragmentation of Meteor Bodies. Nature, Vol. 196, No. 4854, November 10, 1962, pp. 527-529.

143. Kruchinenko, V. G.: Meteoroid Disintegration. Geomagnetism and Aeronomy, Vol. 5, 1965, pp. 74-80.

144. Kramer, Ye. N.: Disintegration of Meteors. Geomagnetism and Aeronomy, Vol. 5, 1965, pp. 210-215.

REFERENCES (Concluded)

145. Hoffman, H. S., and Longmire, M. S.: Meteor Ion Spectra. Nature, Vol. 218, June 1, 1968, pp. 858-859.

146. Smirnov, V. A.: Identification of Spectral Lines in Meteors by Means of Laboratory Dispersion Standards. Soviet Physics-Astronomy, Vol. 11, No. 6, May-June 1968, pp. 1053-1058.

147. Jones, D.: Norman Pogson and the Definition of Stellar Magnitude. Leaflet No. 469, Astronomical Society for the Pacific, San Francisco, California, July 1968.

NASA-Langley, 1969 —— 30 M146

"The aeronautical and space activities of the United States shall be conducted so as to contribute . . . to the expansion of human knowledge of phenomena in the atmosphere and space. The Administration shall provide for the widest practicable and appropriate dissemination of information concerning its activities and the results thereof."

—NATIONAL AERONAUTICS AND SPACE ACT OF 1958

NASA SCIENTIFIC AND TECHNICAL PUBLICATIONS

TECHNICAL REPORTS: Scientific and technical information considered important, complete, and a lasting contribution to existing knowledge.

TECHNICAL NOTES: Information less broad in scope but nevertheless of importance as a contribution to existing knowledge.

TECHNICAL MEMORANDUMS: Information receiving limited distribution because of preliminary data, security classification, or other reasons.

CONTRACTOR REPORTS: Scientific and technical information generated under a NASA contract or grant and considered an important contribution to existing knowledge.

TECHNICAL TRANSLATIONS: Information published in a foreign language considered to merit NASA distribution in English.

SPECIAL PUBLICATIONS: Information derived from or of value to NASA activities. Publications include conference proceedings, monographs, data compilations, handbooks, sourcebooks, and special bibliographies.

TECHNOLOGY UTILIZATION PUBLICATIONS: Information on technology used by NASA that may be of particular interest in commercial and other non-aerospace applications. Publications include Tech Briefs, Technology Utilization Reports and Notes, and Technology Surveys.

Details on the availability of these publications may be obtained from:

SCIENTIFIC AND TECHNICAL INFORMATION DIVISION

NATIONAL AERONAUTICS AND SPACE ADMINISTRATION

Washington, D.C. 20546